UNIVERSITÉ DU QUÉBEC À MONTRÉAL

HOLOCENE RECONSTRUCTION OF SPRUCE BUDWORM-FIRE INTERACTIONS IN THE MIXED BOREAL FOREST OF QUÉBEC (CANADA)

THESIS

PRESENTED

AS A PARTIAL REQUIREMENT

TO THE PH.D IN BIOLOGY

BY

MARC-ANTOINE LECLERC

MAY 2024

UNIVERSITÉ DU QUÉBEC À MONTRÉAL

CHRONOLOGIE HOLOCÈNE DE L'INTERACTION ENTRE LA TORDEUSE DES BOURGEONS DE L'ÉPINETTE ET LES FEUX DANS LA FORÊT MIXTE DU QUÉBEC (CANADA)

THÈSE

PRÉSENTÉE

COMME EXIGENCE PARTIELLE

DU DOCTORAT EN BIOLOGIE

PAR

MARC-ANTOINE LECLERC

MAI 2024

ACKNOWLEDGEMENTS

I am forever grateful to Drs. Hubert Morin, Martin Simard, and Olivier Blarquez for their encouragement, patience, guidance, feedback, comments, thoughts and for providing lots of laughs. I could not have asked for a groovier bunch of supervisors. A big thank you to François Gionest for help in the field. Marika Tremblay, and Guillaume Vigneault thank you for your help in the lab and becoming scale counting wizards. A big thank you to my lab mates Dr. Audrey Lemay, Cassy Berguet, Dr. Maxence Martin, Dr. Valentina Buttò, Hugues Terreaux de Félice for support, insightful discussions, and help whenever I was jammed. A thank you to Dr. Cornelia Krause for some cross-dating breakthroughs and for great discussions. A huge thank you to Valérie Néron for keeping me entertained, and coming up with great StartUp ideas, your presence is sorely missed. Huge thank you to Claire Fournier and Mireille Boulianne for being the best lab technicians ever! Thank you to Anne-Élizabeth Harvey for teaching me 'the lepidopteran scale method'. To my 'thesis support group' Barbara Wong, Claudio Mura, Paola Ayala Borda, Sara Kurakawa, and Marie Frissard, thank you for putting up with my whining when I was blue. Thank you to the 'Chaire de recherche industrielle CRSNG sur la croissance de l'épinette noire et l'influence de la tordeuse des bourgeons de l'épinette sur la variabilité des paysages en zone boréale' for funding the project.

All the hugs, kisses, and thanks go out to Moman, Popa, and Marie-Eve. They have been there through thick and thin supporting me morally and financially: I cannot thank you enough and am forever in your debt. A thank you to Bill New for keeping in touch and always providing sage advice. To all my friends, teachers, professors, mentors, and influential acquaintances for somehow leading me to this point, thank you. I look forward to my next adventure, thank you all. And Lindsay Hill.

DEDICATION

À Moman et Popa

PREFACE

This dissertation was only possible with the collaboration of my supervisor Dr. Hubert Morin, co-supervisor Dr. Martin Simard, and former co-supervisor Dr. Olivier Blarquez. All three guided me through the development of my research questions for Chapters 2, 3, and 4. Dr. Olivier Blarquez provided guidance and key insights for the analysis used in Chapters 2 and 4. Dr. Martin Simard guided me through the aerial survey analysis in Chapter 2, and the dendrochronological analysis in Chapter 3. Finally, Dr. Hubert Morin provided thought provoking questions, discussions, and guidance when interpreting the results of Chapters 2, 3, and 4. Dr. Murray Hay provided suggestions and detailed edits for Chapters 2 and 3. Dr. Allan Carroll also provided suggestions to Chapter 2 that greatly improved the manuscript. Finally, I developed the research questions, methods, collected, prepared, analyzed all data, wrote the entire dissertation and anticipated publications coming from it. Chapter 2 was published in *The Holocene* under the title 'Lepidopteran scales in lake sediments as a reliable proxy for spruce budworm outbreak events in the boreal forest of Eastern Canada' with changes brought to the manuscript following suggestions from the anonymous reviewers. Chapters 3, and 4 are expected to be submitted for publication.

TABLE OF CONTENTS

LIST OF FIGURES

LIST OF TABLES

LIST OF ABREVIATIONS, AND ACRONYMS

^{210}Pb	Radioactive lead isotope
CRS	Constant Rate Supply
KOH	Potassium hydroxide
rpm	Revolutions per minute
C_{int}	Interpolated charcoal accumulation
C_{back}	Background charcoal accumulation
C_{peak}	High frequency signal leftover after removing background accumulations
C_{fire}	The disturbance event (wildfire or spruce budworm outbreak) signal
C_{noise}	Errors within the high frequency signal
O1	Spruce budworm outbreak from 1971–1985
O2	Spruce budworm outbreak from 1946–1959
O3	Spruce budworm outbreak from 1912–1929
OP	Present spruce budworm outbreak (2010-present)
TP	True positive
TN	True negative
FP	False positive
FN	False negative
MCC	Matthews correlation coefficient
EPS	Expressed population signal
GSI	Growth suppression index

GAM generalized additive model

RWI Ring-width index

A Agreement

D Disagreement

Pgl *Picea glauca*

Pma *Picea mariana*

^{14}C radiocarbon isotope

cal. yr. BP Calibrated years before present; present refers to the year 1950

BP Before present; present refers to the year 1950

EH Early Holocene

HTM Holocene Thermal Maximum

MCA Medieval Climate Anomaly

LIA Little Ice Age

NaOCl Bleach

LOWESS Locally weighted scatterplot smoothing

STARS Sequential T-test Analysis of Regime Shifts

IP4 Inverse Propotionality with 4 corrections

MCMC Markow Chain Monte Carlo

LIST OF SYMBOLS AND UNITS

m asl	meters above sea-level
ha	Hectare
˚N	Degrees North
˚W	Degrees West
psi	Pound per square inch
˚C	Degrees Celsius
cm^3	cubic centimeter
mL	millimeters
µL	microliters
m	meters
µm	micrometers
mm^2	Square millimeters
events*kyr^{-1}	Numver of events per 1000 years

RÉSUMÉ

Dans le contexte des changements climatiques, les reconstructions plurimillénaires sont fondamentales à notre compréhension de la variabilité des processus écosystémiques tels que les épidémies d'insectes et les feux de forêt. Les reconstitutions couvrant l'Holocène nous permettent d'observer comment ces perturbations naturelles se sont comportées et ont interagi au cours de différentes phases climatiques et ont le potentiel de fournir un cadre pour la gestion durable des forêts. Cependant, pour que notre compréhension à de vastes échelles temporelles soit robuste et précise, nous devons utiliser des proxys adéquats qui ont été validés et calibrés. J'utilise la forêt boréale mixte de l'est du Canada comme système modèle pour valider et calibrer l'utilisation d'un nouveau paléo-proxy, les écailles de papillon, afin de détecter les épidémies de tordeuse des bourgeons de l'épinette dans l'histoire récente et ensuite de reconstruire les événements liés à la tordeuse et aux feux de forêt au cours de l'Holocène. J'ai démontré que les accumulations d'écailles de papillon dans les sédiments de surface des lacs sont capables de détecter les épidémies locales de la tordeuse, car elles concordent bien avec les relevés aériens effectués à la fin du XXe siècle (1967-1986; 2010-présent) . En utilisant les mêmes carottes de sédiments de surface, j'ai ensuite évalué si les accumulations d'écailles de papillon interpolées annuellement et les cernes de croissance détectaient aussi bien les impacts locaux de la tordeuse des bourgeons de l'épinette, et si ces impacts enregistrés étaient synchrones. J'ai démontré que chaque proxy identifiait individuellement les impacts locaux de la tordeuse, coïncidant avec les intervalles des épidémies connues, et que, comparées l'une à l'autre, les deux approximations détectaient des périodicités d'épidémies similaires. De plus, j'ai démontré que les signaux enregistrés par les proxys étaient relativement synchrones. La relation entre les deux proxys suggère que les grandes accumulations d'écailles se traduisent par un plus grand pourcentage d'arbres affectés dans un peuplement, et par des cernes plus étroits. La validation et l'étalonnage de ce nouvel indicateur ont donc fourni une base plus solide et précise pour interpréter les accumulations d'écailles à des échelles de temps plurimillénaires. Enfin, j'ai reconstitué les événements liés à la tordeuse des bourgeons de l'épinette et aux feux de forêt dans la forêt boréale mixte au lac Buire tout au long de l'Holocène. J'ai observé une corrélation négative entre la fréquence des épidémies de la tordeuse et des feux de forêt pendant la majeure partie de l'Holocène, ce qui suggère une interaction liée aux échelles millénaire et locale/extra-locale, où une perturbation inhibe la présence de l'autre. Aussi, la fréquence des perturbations a oscillé au cours de l'Holocène suite à l'établissement postglaciaire du sapin baumier, et que la perturbation dominante semblait être déterminé par des évènements de changements climatique rapides et significatifs. Cette étude a permis de mieux comprendre la variabilité à long terme des principales perturbations de la forêt boréale mixte et leurs interactions. Les résultats de cette thèse contribuent à l'ensemble des connaissances sur l'écologie forestière et les interactions entre les perturbations et donnent un aperçu de cadres potentiels qui pourraient être utilisés dans la gestion durable des forêts.

Mots clés : *Choristoneura fumiferana*, feux, écailles de papillon, interactions entre perturbations, l'Holocène, forêt boréale mixte

ABSTRACT

Within the context of a changing climate, multi-millennial reconstructions are fundamental to our understanding of the range of variability in key ecosystem processes such as insect outbreaks and wildfires. Reconstructions spanning the Holocene allow us to observe how natural disturbances have behaved, and interacted in different climate phases and may provide a sustainable forest management framework going forward. However, for our understanding at vast temporal scales to be robust and accurate, we require the use of adequate proxies that have been validated and calibrated. I use the eastern Canadian mixed boreal forest as a model system to validate, and calibrate the use of a novel paleo-proxy, lepidopteran scales, to detect spruce budworm outbreaks in recent history, and then reconstruct spruce budworm, and wildfire events over the course of the Holocene. I demonstrated that lepidopteran scale accumulations in lake surface sediment are able to detect local spruce budworm outbreaks as these achieved high agreement with aerial surveys conducted in the late 20th century (1967-1986; 2010-present). Using the same surface sediment cores, I then assessed whether annually interpolated lepidopteran scale accumulations and tree-ring records both detected local spruce budworm impacts, and if the recorded impacts were synchronous. I demonstrated that each proxy individually identified local spruce budworm impacts at a periodicity of approximately 16 to 32 years coinciding with known outbreak return intervals, and that, when compared to each other, both proxies detected similar outbreak periodicities. Further, I demonstrated that the proxy record signals were relatively synchronous, and that the relationship between the two records suggests that large lepidopteran scale accumulations translate to a greater percentage of affected trees in a stand, and to greater recorded growth suppression i.e., narrower ring-widths. The validation and calibration of this novel proxy therefore provided a more robust and accurate foundation to interpret lepidopteran scale accumulations at multi-millennial time scales. Finally, I reconstructed spruce budworm and wildfire events in the mixed boreal forest at lake Buire throughout the Holocene. The frequency of spruce budworm and wildfire events exhibited a negative correlation for the majority of the Holocene suggesting a linked interaction at the millennial and local/extra-local scales where one disturbance inhibits the presence of the other. Further, disturbance event frequencies oscillated during the Holocene following the postglacial establishment of balsam fir, and the switch in the dominant disturbance tended to coincide with rapid significant climate change events. The present study advanced our understanding of the long-term range of variability of the main disturbances of the mixed boreal and their interactions. The results of this thesis contribute to the body of knowledge of forest ecology, and disturbance interactions and provide insight into potential frameworks that could be utilized in sustainable forest management.

Keywords : *Choristoneura fumiferana,* wildfire, lepidopteran scales, disturbance interactions, Holocene, mixed boreal fores*t*

CHAPTER 1
GENERAL INTRODUCTION

1.1 Climate change and disturbances

Climate is expected to become more variable (Easterling et al., 2000), and this increased variability is expected to lead to increased tree stress (Allen et al., 2010, 2015) along with more prevalent severe forest disturbances (Millar and Stephenson, 2015). Fire seasons are expected to become longer with the advent of warmer and drier conditions (Westerling et al., 2006, 2011; Flannigan et al., 2009, 2013). Further, warm, dry conditions will facilitate ignition and rate of spread as more fuel will be available to burn, likely leading to more frequent events, and events of greater intensity and/or severity (Woolford et al., 2014; Jolly et al., 2015; Wotton et al., 2010, 2017; Flannigan et al., 2009, 2013). Meanwhile for biotic forest disturbances such as insects, increased tree stress will likely exacerbate mortality resulting from outbreaks (e.g., Anderegg et al., 2015; De Grandpré et al., 2019). Additionally, the direct effects of warmer temperatures are expected to favour insect development, and survival (Ayres and Lombardo, 2000; Bale et al., 2002; Carroll et al., 2004; Berg et al., 2006; Bentz et al., 2010); it follows that outbreaks are therefore expected to be more severe due to larger populations (e.g., Ayres and Lombardo, 2000; Murdock et al., 2013; Weed et al., 2013). Further, due to their relatively short lifespan and generation time, insects are likely able to closely track climatic change (Parmesan, 2006) manifesting as distributional shifts to higher elevations and/or more northerly latitudes (Jepsen et al., 2008, 2011; Parmesan, 2006; Tai and Carroll, 2022), or move into historically novel habitats (e.g., Carroll et al., 2004) along with feed on historically novel host-trees (e.g., Cudmore et al., 2010; Cullingham et al., 2011; Erbilgin et al., 2014; Rosenberger et al., 2017). Similarly, with warmer temperatures, previously 'protected' hosts that exhibited phenological asynchrony may now face increased vulnerability to infestation (Régnière et al., 2012; Pureswaran et al., 2015, 2019). As such, variable climate appears to favour more 'mega-disturbances' (Millar and Stephenson, 2015; Allen et al., 2015; McDowell et al., 2020), and the future of the forested landscape appears quite bleak based on these predictions. However, it is important to consider a millennial or multi-millennial perspective, as past changes in climate and corresponding disturbance regime variability may elucidate how these regimes will behave given the current climate change context.

1.2 Climate variability during the Holocene

Climate did in fact vary over the course of the Holocene, a geological epoch lasting from around 11,700 BP (before present referring to the year 1950) to the present (just after the preindustrial era) that can be divided into 3 major climate periods (Wanner et al., 2008, 2011, 2015; Renssen et al., 2009; Walker et al., 2012; Shuman and Marsicek, 2016). The first period is known as the Early Holocene (EH) lasting from roughly 11,700-7000 BP and is believed to have started out quite cool but experienced very rapid warming early on followed by a slower rate of warming that culminated in the next period known as the Holocene Thermal Maximum (HTM; Wanner et al., 2015; Gajewski, 2015; Zhang et al., 2016, 2017; Neil and Gajewski, 2018). During the EH temperature has been modelled to have experienced a warming of 5°C in northern Canada relative to recording a warming of 1-2°C using pollen reconstructions (Gajewski, 2015; Zhang et al., 2017). The HTM, lasting from approximately 7000 BP-4200 BP, is described as a period of warm and relatively stable temperatures although cool incursions did occur (Mayewski et al., 2004). In Eastern North America, the HTM was slightly delayed due to the melting of the Laurentian Ice Sheet (Renssen et al., 2009, 2012; Marcott et al., 2013; Zhang et al., 2016, 2017), however, was quickly followed by postglacial vegetation recolonization (Blarquez and Aleman, 2016). Finally, the Holocene ends with the Neoglacial, a period generally described by a cooling trend associated with glacier advances (Wanner et al., 2008, 2011; Mann et al., 2009; Gajewski, 2015; Neil and Gajewski, 2018) despite this trend being recently contested (Marsicek et al., 2018). Within this general cooling, smaller climatic events have been identified (e.g., Mann et al., 2009). The first event is the Medieval Climate Anomaly (MCA) which occurred around 1000-700BP and was a short warm period with temperatures in North America exceeding the baseline period of 1961-1990 (Mann et al., 2009). The unusually warm event was shortly followed by a cold lapse known as the Little Ice Age (LIA) occurring from roughly 550-250 BP where temperatures were 0.24°C cooler relative to the MCA (Mann et al., 2009). The Neoglacial ends with the preindustrial era, a period that has experienced rapid warming (Wanner et al., 2011, 2015; Walker et al., 2012; Renssen et al., 2012).

1.3 Characterizing forest resilience using multiple proxies, and its implication for sustainable forest management

Adopting a long-term multi-millennial perspective will be key to understanding disturbance variability and, subsequently, successful forest management. The long-term perspective, using the different climate periods of the Holocene as a reference, would allow to observe the effects of these periods on disturbance characteristics such as frequency and severity (e.g., Ali et al., 2009, 2012; Blarquez et al., 2015; Navarro et al., 2018b). Additionally, the long-term perspective has the potential of revealing the range of change the

ecosystem can tolerate (i.e., resilience; Holling, 1973), along with potentially identifying tipping point conditions (e.g. Scheffer et al., 2001, 2003; Scheffer and Carpenter, 2003; Scheffer et al., 2012). More importantly the observed changes in variance that may occur during the different climate periods may provide a framework for sustainable forest management (e.g., Hennebelle et al., 2018) in an effort to best emulate the effects of the disturbance in question on forest ecosystems and encourage resilience. Although the information obtained from long-term multi-millennial reconstructions are too coarse in space and time to directly translate to stand-level management decisions such as silvicultural prescriptions (Swetnam et al., 1999; Keane et al., 2009), the range of historic variability of the ecosystem along with how landscape composition and structure have changed over time can be inferred (Landres et al., 1999). Describing the range of spatiotemporal variability in disturbance characteristics, such as frequency and/or severity, helps define the limits of an ecosystem, gain a better idea of historic landscape compositions and structures resulting from changes in climate, disturbance regimes, or both, and may identify the possible processes or successional pathways that brought an ecosystem to it's current state (Landres et al., 1999; Swetnam et al., 1999). Considering trade-offs between forest resilience and management objectives (e.g., Leclerc et al., 2021), the state of the forest may need to change and transform as a return to initial conditions may be maladaptive given the climatic context and defined objectives (Buma and Schultz, 2020).

In addition to adopting a long-term perspective to define disturbance regime variability, the use of multiple lines of evidence will play a major role in accurately identifying observed changes. Using multiple lines of evidence in the forms of different proxies allows for more accurate and interpretable disturbance regime reconstructions (e.g. Higuera et al., 2005; Higuera et al., 2011; Waito et al., 2018). As no proxy is a perfect recorder, different proxies have different advantages and drawbacks in terms of their spatiotemporal resolution, and so using a combination can provide a more accurate and robust understanding of the system or process under study.

An example of a proxy of insect presence that can have a relatively fine spatial and temporal resolution, while being able to cover large extents is remote sensing. In the form of satellites and aerial surveys, remote sensing can offer high spatial coverage and can, if desired, maintain relatively high spatial resolution (e.g. LiDAR vs. Landsat images; Zald et al., 2014; Senf et al., 2017; Zhang et al., 2022), and may maintain high temporal resolution ie. annual or seasonal changes (e.g., Khare et al., 2019) or assess long-term changes

using change detection (e.g., Cohen et al., 2010). This proxy's major constraint is that it is a relatively recent technology and so the temporal coverage is limited to the last 50 years or so. Further, satellites may not directly identify the damaging disturbance agent (i.e., burn vs. defoliation) since they assess resulting changes in reflectance of various wavelengths such as short-wave infrared, near infrared, and visible light (e.g., Leckie et al., 1988; Rullan-Silva et al., 2013), although the causative agent may be surmised based on ancillary data and information (Senf et al., 2017; Thapa et al., 2022; Stahl et al., 2023). For example, detecting defoliation using remote sensing is still difficult due to the subtle nature of the spectral change (Senf et al., 2017; Zhang et al., 2022; Thapa et al., 2022). Similarly, aerial surveys that visually map out defoliation can determine the spatial extent of the damage by assessing crown condition however, the causative agent is usually inferred based on the environmental context (i.e., species affected and/or time of year damage is observed, location, and, duration) and/or can fortunately be confirmed via field data.

Tree rings are another proxy that have high spatial and temporal resolution, and can cover time periods of about 300-400 years (e.g., Boulanger and Arseneault, 2004; Boulanger et al., 2012), although more recent work with subfossil trees may allow for millennial reconstructions (e.g. Simard et al. 2006, 2011; Gennaretti et al., 2014a,b). Very high temporal precision can be obtained with the annual formation of tree-rings. For example, fire seasonality can be gleaned based on the location of fire scars in the early- or latewood (e.g., Heyerdahl et al., 2001; Stephens et al., 2018; Rother et al., 2018). Further, fire severity can be inferred based on the presence/absence of fire scars and/or cohort establishment (e.g., Heyerdahl et al., 2001, 2007; Marcoux et al., 2013, 2015; Chavardès and Daniels, 2016). Even the spatial extent of burns can also be inferred from fire scars (Greene and Daniels, 2017). Tree-rings have also been a common proxy used to reconstruct spruce budworm (*Choristoneura fumiferana* Clem.) outbreak occurrence and even infer defoliation intensity (e.g., Blais, 1957, 1958, 1983; Morin and Laprise, 1990; Morin, 1994; Boulanger and Arseneault, 2004; Boulanger et al., 2012). Unfortunately, tree-rings are an indirect proxy and work from the assumption that growth reductions and their magnitude are due to a reduction in a tree's photosynthetic capacity caused by spruce budworm defoliation and not for some other reason (Ericsson et al., 1980; Swetnam et al., 1985). Interpretation, therefore typically involves a correction of some sort using a non-host species (Swetnam et al., 1985), and an awareness that there is a lag between the actual year of defoliation and when the tree records defoliation (Krause and Morin, 1995; Krause et al., 2012) as stored energy reserves will first be depleted in the tree before displaying signs of defoliation in its rings (Ericsson et al., 1980; Deslauriers et al., 2015).

In addition to the lag between the actual year of defoliation and that recorded by the tree, the ability to record defoliation events may even vary among tree species (e.g., Blais, 1957, 1962; Bouchard and Pothier, 2010). For example, white spruce [*Picea glauca* (Moench) Voss] is typically used in spruce budworm outbreak reconstructions because it is relative long-lived species, and is sensitive to spruce budworm defoliation (Bouchard et al., 2006; Bouchard and Pothier, 2010). Black spruce [*Picea mariana* (Mill.) Britton, Sterns & Poggenburg] has also been used in spruce budworm outbreak reconstructions (e.g., Tremblay et al., 2011; Krause et al., 2012), however due to its historical phenological asynchrony may have been less affected by defoliation (Nealis and Régnière, 2004), and likely a poorer recorder of defoliation events (Blais, 1957, 1962). Further, within a site and a species, individual tree reactions may vary potentially influencing a tree's ability to withstand and therefore record defoliation (e.g., Mageroy et al., 2014; Méndez-Espinoza et al., 2018).

Finally, tree-ring reconstructions work with surviving trees which may influence or bias the reconstruction and subsequent interpretation. The trees that are sampled are individuals that have survived previous outbreaks and as such the observed growth suppression may not reflect the true effects of the defoliation and subsequent tree mortality (Jardon et al., 2003; Bouchard et al., 2006; Pothier et al., 2012). Further, age of surviving trees can also influence their ability to record spruce budworm defoliation. Younger trees tend to experience less defoliation and be less affected by defoliation relative to more mature trees (MacLean, 1980, 1984; Krause et al. 2003), and even location in the canopy may influence experienced defoliation (Reams et al., 1988; Lavoie et al., 2019). This suggests that selection of individual trees becomes particularly important when constructing a tree-ring chronology. In addition to selecting the 'best' individuals, site history also becomes an important factor in determining which individuals are left onsite. For example, past fires and harvesting activities may alter species composition, and/or age distributions, potentially negatively affecting the ability to obtain an accurate spruce budworm reconstruction from a tree-ring chronology.

In contrast to tree-rings, lake sediment has a coarser spatial and temporal resolution, but has the advantage of covering thousands of years to view long-term patterns. From changes in the accumulation of paleo-proxies in lake sediment long-term changes in vegetation response to climate can be inferred (e.g., Richard,

1979; Richard et al., 1982; Richard, 1993, 1995), in addition to changes in disturbance regimes (e.g., Ali et al., 2009, 2012; Blarquez et al., 2015). The major advantage of paleo-proxies is their ability to reconstruct patterns, based on their changing accumulations, that may only be discernable over long periods of time. Thus, the fluctuation in paleo-proxy accumulation in response to slow changing variables such as climate provide insight into past variation and potential analogs to future conditions. However, as with the other mentioned proxies, use of paleo-proxies also requires careful interpretation. For example, sedimentary charcoal is presumed to be a direct proxy of a fire when reconstructing wildfire events at multi-millennial scales (e.g., Millspaugh and Whitlock, 1995; Clark et al., 1996; Long et al., 1998; Power et al., 2008; Whitlock et al., 2008). However, the presence of sedimentary charcoal does not necessarily imply fire occurrence around the lake as one must also consider the size of the charcoal particles. Small particles are believed to reflect 'background' accumulation coming from distant fires, reflecting regional burning, meanwhile large particles are presumed to result from local fires (Clark and Royall, 1995, 1996; Clark et al., 1998; Aleman et al., 2013).

Charcoal particles size, for the most part, is likely able to discriminate between local/extra-local and distant events, however, deposition and incorporation of charcoal is also very dependent on the weather conditions during the fire event (Oris et al., 2014). Similarly, larval head capsules and feces have been used to reconstruct large spruce budworm population events (Simard et al., 2002, 2006). However, interpretation of these proxies has been somewhat tricky suggesting that these proxies may not be reliable indicators of spruce budworm presence. Larval head capsules are well preserved but are not abundant along the sediment core profile (Simard et al., 2002) raising the question: does the absence of larval head capsules truly indicate an absence of the spruce budworm in the area? Conversely, feces produced by feeding spruce budworm larva are an abundant proxy, but these may degrade or decompose over time and therefore may not be found along the entire sediment core profile (Simard et al., 2002). Again, especially at greater depths, lack of feces may be due to absence of spruce budworm or may be the result of decomposition (Simard et al., 2002). As such, the vast temporal coverage offered by paleo-proxies to develop multi-millennial disturbance regime reconstructions must be coupled with careful interpretation.

1.4 The boreal forest and its main disturbances

The boreal zone is found across the Northern Hemisphere, covering large portions of Eurasia and North America consisting of wetland, open woodland, and closed forest ecosystems (Brandt et al., 2013; Price et al., 2013). Ecologically, the boreal zone and its ecosystems play a crucial role in nutrient cycling (Bhatti et al., 2000; Bonan, 2008; Kurz et al., 2013; Laroque et al., 2014), while its closed forest ecosystems are particularly important to the forest industry in terms of providing timber products and jobs (Brandt et al., 2013; Lemprière et al., 2013). The closed forest ecosystems are comprised of boreal black spruce forests generally made of pure stands of black spruce, and mixed boreal forests consisting of both deciduous and coniferous species (Bergeron, 2000; Brandt, 2009; Saucier et al., 2009). In North America, and more specifically in Québec, the mixed boreal forests are generally located between the black spruce forests to the north and the deciduous forests to the south (Bergeron, 2000; Brandt, 2009; Saucier et al., 2009). Acting somewhat as a transition zone between the deciduous and black spruce forests, the mixed boreal forest is home to a variety of deciduous and coniferous species such as trembling aspen [*Populus tremuloides* MIchx.], paper [*Betula papyrifera* Marshall] and yellow [*Betula* alleghaniensis Briit.] birches, balsam fir [*Abies balsamea* (L.) Mill], and white and black spruces (Bergeron, 2000; Brandt, 2009; Saucier et al., 2009). This relatively diverse forest experiences fairly complex regeneration patterns as disturbances leading to mortality and subsequent canopy gaps are variable due to heterogeneous species distributions and seed sources (Kneeshaw and Bergeron, 1996, 1998, 1999; Bergeron, 2000; Couillard et al., 2021).

The 2 main disturbances in the mixed boreal forest include the spruce budworm and wildfire. The spruce budworm is a native lepidopteran defoliator whose univoltine lifecycle consists of 6 larval, a pupal, and finally an adult moth stage (Royama, 1984; Royama et al., 2005, 2017; MacLean, 2016; Nealis, 2016). As a larva, the spruce budworm preferentially feeds on the current year's needles, and buds of balsam fir, while also consuming older foliage when necessary (Piene 1989), and feeding on white, black, and red spruce as secondary hosts (Hennigar et al., 2008). Three to four years of severe defoliation on balsam fir by the larvae often results in host-tree mortality (MacLean, 1980, 1984). Defoliation on the secondary hosts varies in severity with greater phenological synchrony in the case of white spruce resulting in greater severity, or lack of phenological synchrony in the case of black spruce resulting in less severe defoliation (Fuentealba et al., 2017; Pureswaran et al., 2018). Following feeding by the larvae, and formation of the pupa, adult moths emerge whereupon they are able to reproduce and disperse (Greenbank et al., 1980; Boulanger et al., 2017; Rhainds et al., 2021). The spruce budworm has historically exhibited widespread episodic outbreaks occurring every 30-40 years over the eastern Canadian boreal landscape in the 20th century (Blais, 1968,

1983, 1985a,b; Boulanger and Arseneault, 2004; Morin and Laprise, 1990; Morin, 1994; Boulanger et al., 2012). These outbreaks have varied in extent, severity, and duration (Candau et al., 1998; Gray et al., 2000; Jardon et al., 2003; Gray, 2008). Key to experiencing any outbreak is the presence of abundant host-trees at the stand and landscape scales (Su et al., 1996; Campbell et al., 2008; Colford-Gilks et al., 2012). Host-tree presence also creates the potential for the establishment of a positive feedback loop where defoliation by the budworm favours the regeneration and establishment of balsam fir in the canopy which then results in conditions prone to future outbreaks (Baskerville, 1975; Morin, 1994). Climatic conditions for this disturbance are likely to modulate severity and intensity of events by influencing insect survival and development (Ayres and Lombardo, 2000), and/or host-tree susceptibility (e.g., Anderegg et al., 2015; De Grandpré et al., 2019).

Wildfire is the other major disturbance in the mixed boreal forest (Johnson et al., 1998). As an abiotic disturbance, wildfire is dependent on physical conditions influencing ignition probability, and subsequent fire behaviour (Wotton et al., 2010; Macias Fauria et al., 2010; Woolford et al., 2014; Molinari et al., 2018). Climate and weather, in the forms of temperature, relative humidity, and precipitation are key influencers in an ecosystem's wildfire regime (Macias Fauria and Johnson, 2008; Macias Fauria et al., 2010). Over short time intervals, weather will affect fuel dryness and therefore fuel availability ultimately determining the probability of ignition, and subsequent fire spread (Van Wagner, 1967; Rothermel, 1983). Following ignition, wind will play a major role in dictating the extent of a fire and its rate of spread (Van Wagner, 1967; Rothermel, 1983). Although available fuel is determined by weather or climate, the horizontal and vertical distribution (i.e., the contiguity) of this fuel will greatly affect fire severity (Fulé et al., 1997; Falk et al., 2007). The presence of surface and ladder fuels can increase fire intensity facilitating the ground to crown transition (e.g., Byrom, 1959; Van Wagner, 1977), and relatively continuous crown cover can lead to high severity active crown fires as opposed to passive crown fires (i.e., torching; Cruz, 1999; Cruz et al., 2003, 2004, 2005). Over long time intervals, the climate of an area will directly act on wildfire via fire weather and indirectly influence vegetation composition, abundance and subsequent fuel structure and availability (Keeley et al., 2011; Littell et al., 2016; He and Lamont, 2018), which combined will dictate fire behaviour and the resulting wildfire regime (Blarquez et al., 2015; Dantas et al., 2016; Harrison et al., 2021). Such an interaction can result in a positive feedback loop, where burning of vegetation favours regeneration of particular fire-tolerant species, and the presence of such species can favour the occurrence of wildfire (Keeley et al., 2011; Rogers et al., 2015; Pausas, 2015; Lamont et al., 2020).

1.5 Disturbance interactions

At the stand and landscape scales disturbance agents interact with one another through forest legacies i.e., changes in forest structure and composition (Buma, 2015; Kleinman et al., 2019; Burton et al., 2020). Generally, disturbance interactions can be described as linked or compound (Simard et al., 2011; Buma, 2015). A linked disturbance interaction occurs when a preceding disturbance alters forest structure and/or composition in a way that influences the probability of occurrence, severity, intensity, extent, and/or frequency of a subsequent disturbance (Simard et al., 2011; Kleinman et al., 2019; Burton et al., 2020). Examples include the effects of defoliation on fire or vice versa, or the effects of bark beetle outbreaks on fuel distribution and load affecting fire behaviour (e.g., Hicke et al., 2012; Lynch and Moorcroft et al., 2008; Cohn et al., 2014; Meigs et al., 2011, 2015, 2016). A compound disturbance results from two disturbances occurring simultaneously or in quick succession where the sum of their effects is greater than the individual parts potentially yielding ecological surprises (Paine et al., 1998; Simard et al., 2011; Kleinman et al., 2019; Burton et al., 2020). Consider, for example, the tree mortality resulting from co-occurring drought and defoliation events compared to the sum of the mortality from only drought, and then only defoliation (e.g., De Grandpré et al., 2019), or similarly the mortality from co-occurring drought and bark beetle outbreaks (e.g., Hart et al., 2014, 2017).

The interaction between the major disturbances in the mixed boreal is nuanced and appears to depend on the temporal scale at which the interaction is assessed. Within about 10 years or less (short time scales), there appears to be a positive association between spruce budworm defoliation and fire occurrence particularly in host dominated stands (Fleming et al., 2002; James et al., 2017; Candau et al., 2018). The changes in the vertical fuel structure resulting from stand degradation following spruce budworm outbreaks result in increased contiguity and fuel hazard (Watt et al., 2018, 2020), and appear to be linked to the occurrence of more severe active crown fires (Stocks, 1987). However, over 10-100 years or at millennial and multi-millennial time scales there appears to be a negative association between the spruce budworm and wildfires where one disturbance inhibits the other (Sturtevant et al., 2012; Navarro et al., 2018b). Although the association between spruce budworm outbreaks and wildfires may vary over time, the fact that each disturbance appears to alter forest structure and/or composition in a way that affects probability of occurrence, frequency, severity, intensity, and/or extent suggests a linked interaction (Simard et al., 2011),

although this association has not yet been quantified in the mixed boreal forest at multi-millennial time scales.

1.6 Current state of knowledge and major contributions of this thesis

There is limited data on spruce budworm and wildfire dynamics in the mixed boreal forest at millennial and multi-millennial time-scales. For the most part, spruce budworm outbreak dynamics have been reconstructed with tree-rings via dendrochronological techniques. Although dendrochronology provides high spatiotemporal resolution, reconstructions have generally been limited to the past 300 to 400 years (Morin, 1994; Bergeron, 2000; Boulanger and Arseneault, 2004; Jardon et al., 2003; Bergeron et al., 2004; Boulanger et al., 2012), although the temporal coverage can be extended using subfossil trees (Simard et al., 2006). Historically, millennial and multi-millennial spruce budworm outbreak reconstructions have been done using larval head capsules (e.g., Jasinski and Payette, 2005; Lavoie et al., 2009), and in some cases using spruce budworm feces in combination with head capsules (Simard et al., 2002). Most recently through the use of a novel paleo-proxy, lepidopteran scales, a spruce budworm outbreak reconstruction was completed in the boreal black spruce forest (Navarro et al., 2018b). However, the interpretation of this novel paleo-proxy remains somewhat dubious as its use has not yet been validated or calibrated. Similarly, understanding multi-millennial wildfire dynamics in the mixed boreal forest is also limited (e.g., Jasinski and Payette, 2005; Lavoie et al., 2009; Colpron-Tremblay and Lavoie, 2010; Blarquez et al., 2015). Studies have mainly been done in high altitude forests or at high latitudes using soil charcoal (Couillard et al., 2012, 2013, 2021; Frégeau et al., 2015). Finally, until very recently, the interaction between the two disturbances at such vast temporal scales had not been described (e.g., Navarro et al., 2018b).

Given the current context of climate change and the potential for past climate variability to serve as starting points to develop appropriate silvicultural systems, the importance of understanding past disturbance regime variability cannot be understated. Both disturbances and climate play important roles in shaping ecosystems, and assessing disturbance behaviours over the course of different past climate phases has the potential of revealing how disturbances may react to current and perhaps future climate change. Silvicultural practices may be developed to best emulate disturbance regimes with the potential of meeting multiple objectives, such as maintain or increase biodiversity and maintain multiple ecosystem services (e.g., North and Keeton, 2008; Long 2009; Aszalos et al., 2022), but in order to do so forest managers will have to consider the long-

term variability in regime characteristics, not just mean frequency or mean severity (Bergeron et al., 2002; Hennebelle et al., 2018). Further, in order to maintain landscape and ecosystem resilience forest stewards will have to consider using multiple silvicultural techniques in conjunction with past disturbance variability (Bergeron et al., 2002).

Therefore, in an effort to gain a better understanding of past disturbance regime variability in the mixed boreal forest at millennial and multi-millennial time scales the goal (and corresponding hypotheses) of this doctoral thesis is threefold:

Objective 1: Validate the use of lepidopteran scales as a paleo-proxy by comparing their accumulation in lake sediments with aerial surveys during known documented outbreak periods

Lepidopteran scales are a novel microfossil paleo-proxy (Navarro et al., 2018a), that have been previously used to reconstruct large spruce budworm population events in the black spruce boreal forest (Navarro et al., 2018b). This proxy is particularly promising since the scales are abundant chitin containing structures that are well preserved in anaerobic environments such as lake sediments (Richards, 1947; Navarro et al. 2018a). Therefore, this proxy is more likely to be found over an entire sediment profile relative to other macrofossils (e.g. Simard et al., 2002, 2006), and an absence or a low accumulation of scales would likely suggest a small or endemic population. However, the use of this novel paleo-proxy has not been validated with modern spruce budworm proxies. The first objective of this dissertation is to determine whether lepidopteran scales are able to identify large spruce budworm populations events relative to those observed and recorded by aerial surveys, a modern proxy. If lepidopteran scales are an accurate measure of spruce budworm populations around a lake then large scale accumulations should coincide with known outbreak periods identified by aerial surveys because both proxies should identify the presence/absence of the defoliator. Lepidopteran scales are assumed to be a direct measure of the number of spruce budworm adult moths found around a lake, and so large scale accumulations should reflect a large number of moths while the aerial surveys, an indirect proxy of spruce budworm populations sizes but a direct measure of defoliation

and/or mortality, quantify the amount of stand-level defoliation caused by the insect, where greater defoliation should also correspond with larger spruce budworm populations.

Objective 2: Calibrate the use of lepidopteran scales against tree-rings, a known and commonly used proxy to reconstruct spruce budworm outbreaks, allowing for better interpretation of scale accumulations i.e., does a greater accumulation of scales reflect a more severe outbreak?

Assuming that lepidopteran scales are able to identify large spruce budworm population events, the next step in ameliorating interpretation is determining whether scale accumulation magnitude corresponds to the severity of an outbreak. The second objective of this dissertation is to compare the ability of the lepidopteran scales and tree-rings to record the effects of spruce budworm defoliation. If lepidopteran scales are an accurate measure of spruce budworm populations around a lake, then larger scale accumulations should correspond with larger growth suppression/greater number of trees affected because larger scale accumulations suggest larger spruce budworm adult moth populations meaning that the larvae have successfully fed on the host-tree's needles and molted into moths. Similarly, large adult spruce budworm moth populations would result from a large number of successfully feeding larvae corresponding to a reduction in foliage negatively affecting a tree's photosynthetic capacity and ability to produce photosynthates inhibiting tree growth resulting in the production of narrower tree-ring widths (Ericsson et al., 1980; Krause and Morin, 1995; Krause et al., 2012; Deslauriers et al., 2015). Additionally, the two signals (changes in both lepidopteran scale accumulations and tree-ring widths) are expected to be (relatively) synchronous because incorporation of lepidopteran scales into lake sediment is relatively quick (Tremblay, 2022), and the effects of spruce budworm defoliation manifested as a reduction in tree-ring widths typically becomes evident within 2-4 years of the actual event (Krause and Morin, 1995; Krause et al., 2012).

Objective 3: Reconstruct large spruce budworm population and wildfire events in the mixed boreal forest during the variable Holocene climate and in the context of changing vegetation

The final objective of the dissertation is to reconstruct large spruce budworm population and wildfire events in the mixed boreal forest over the course of the Holocene. This observational study utilizes the novel lepidopteran scale paleo-proxy in combination with sedimentary charcoal and arboreal pollen to determine changes in disturbance event frequencies, identify changes in relative tree species composition, and quantify the interaction between the two disturbances. Additionally, the effects of rapid significant climate change events on disturbance event frequencies was assessed. Following post-glacial vegetation recolonization in the mixed boreal forest, the spruce budworm is expected to be the preeminent disturbance given the abundance and near constant supply of balsam fir, its primary host-tree. Further, an abundance of host predisposes the mixed boreal forest to spruce budworm outbreaks, and the mortality resulting from budworm defoliation creates favourable conditions for balsam fir regeneration and establishment in the canopy (Kneeshaw and Bergeron, 1996, 1998, 1999; Bouchard et al., 2005, 2006, 2007); bringing about the establishment of a positive disturbance-vegetation feedback loop (Baskerville, 1975; Morin, 1994). Prior to the increase in abundance of balsam fir, the mixed boreal forest is expected to be dominated by wildfire, where vegetation was likely to be more fire-tolerant while also potentially promoting fire-prone conditions (Hély et al., 2000, 2010, 2020; Girardin et al., 2013; Blarquez et al., 2015; Blarquez and Aleman, 2016) permitting the establishment a positive wildfire disturbance-vegetation feedback loop. The large spruce budworm population and wildfire event frequencies are expected to exhibit an inverse relationship or negative correlation at millennial and multi-millennial scales (e.g., Navarro et al., 2018b) as both agents are 'competing' for a limiting and changing resource in the form of variable tree species biomass. Further, the greater frequency of a particular disturbance may be mediated by climate conditions. In Eastern North America, cool, dry conditions periodically occurring during the Holocene resulted in increased fire frequencies (Carcaillet et al., 2001a) where such conditions may simultaneously negatively affect spruce budworm survival and development (e.g., Ayres and Lombardo, 2000) resulting in fewer large population events.

The overall goal is to ameliorate our interpretation of the novel paleo-proxy of lepidopteran scales and then apply this understanding over the course of the Holocene within the ecosystem context of the mixed boreal forest potentially revealing any variability in the spruce budworm disturbance regime over time, and also how this regime interacted with wildfire. As such, gained knowledge in the variability of disturbance regime characteristics (i.e., disturbance event frequency) over time would ideally help develop sustainable forest

management practices that could be applied in an effort to mitigate the unwanted effects of climate change on the mixed boreal forest while still allowing timber harvesting.

1.7 Thesis structure overview

In chapter 2, I compare lepidopteran scale accumulations over the late 20th Century from 9 lakes to the corresponding observed defoliation around each lake as documented by aerial surveys.

In chapter 3, lepidopteran scale accumulations from the same 9 lakes in chapter 2 are compared to changes in tree-ring widths in order to determine whether both proxies are able to record the effects of spruce budworm defoliation in a stand and if both signals are synchronous.

In chapter 4, I reconstruct large spruce budworm population and wildfire events from a single lake and observe their interaction in the mixed boreal forest over the course of multiple rapid significant climate change events during the Holocene.

In chapter 5, I summarize the main results of this dissertation. I also briefly discuss implications of my results to the mixed boreal forest, and more importantly highlight potential future research avenues and needs.

CHAPTER 2
VALIDATION OF LEPIDOPTERAN SCALES AS A PROXY FOR EASTERN SPRUCE BUDWORM OUTBREAKS EVENTS

Marc-Antoine Leclerc, Olivier Blarquez, Martin Simard, and Hubert Morin

2.1 Abstract

Characterizing disturbance regimes over long time scales is paramount for describing and identifying their range of variability. The most important biotic disturbance in the eastern Canadian boreal forest is the eastern spruce budworm, a moth of the insect order Lepidoptera. Lepidopteran scales have recently been used to reconstruct spruce budworm population fluctuations throughout the Holocene. However, this novel proxy has yet to be validated by an independent proxy. This study aimed to determine whether lepidopteran scales found in the surface sediments of boreal lakes tracked large spruce budworm populations, i.e., outbreaks, using yearly aerial surveys (1967-present) of spruce budworm defoliation as an independent proxy. Scales were extracted (1 cm resolution) from the top 20 cm of ^{210}Pb-dated sediment cores recovered from nine lakes. To identify significant abundance peaks of scales in the time series, we removed background noise using a modified version of CharAnalysis. A 100-year smoothing window width combined with a 60th percentile threshold yielded the highest true positive and true negative occurrences, and the lowest false positive and false negative occurrences, with values of 0.69 and 0.70 for Cohen's Kappa and Matthews correlation coefficient, respectively. Our findings demonstrate that lepidopteran scales are a suitable proxy for identifying spruce budworm outbreaks in the sediment record.

2.2 Introduction

The ability to quantify forest disturbance regimes over long periods is essential for accurately identifying and describing their natural range of variability. A long-term perspective is particularly useful for capturing the evolution of a disturbance regime in response to changing climate and/or vegetation (e.g., Power et al., 2008; Ali et al., 2009, 2012; Blarquez et al., 2015). Moreover, looking into the past may hint at how current and future disturbance regimes may behave in a changing climate. Past observed long-term variability could serve as a useful framework for developing and applying sustainable forest management approaches (e.g.,

Hennebelle et al., 2018). For example, a long-term perspective obtained using sedimentary charcoal has allowed elucidating how fire frequencies and the amount of biomass burned have evolved in relation to various climate phases of the Holocene (e.g., Long et al., 1998; Ali et al., 2009, 2012; Blarquez et al., 2015). An accurate characterization of both abiotic and biotic disturbances over vast temporal scales improves our understanding of ecosystem functioning and favours the application of sensible forest management approaches (Landres et al., 1999; Swetnam et al., 1999; Keane et al., 2009).

Biotic disturbances, such as insect outbreaks, are key ecosystem processes affecting forest structure and composition (e.g., Cooke et al., 2007; Barbosa et al., 2012) and nutrient cycling (e.g., Mattson and Addy, 1975; Lovett et al., 2002). One of the most important disturbances in the eastern Canadian boreal forest is the eastern spruce budworm [*Choristoneura fumiferana* Clemens]. This native lepidopteran defoliator exhibits a univoltine lifecycle and cyclic population outbreaks (Royama, 1984; Jardon et al., 2003; Royama et al., 2005, 2017). The spruce budworm lifecycle consists of six larval stages, a pupal stage, and finally, an adult moth stage in which the insect disperses and reproduces (Nealis, 2016). In the larval stage, the spruce budworm feeds preferentially on the current year's needles, buds, and cones of mature balsam fir [*Abies balsamea* (L.) Mill]; however, this insect will also consume older needles and, to a lesser extent, feed on the needles of white spruce [*Picea glauca* (Moench) Voss] and black spruce [*Picea mariana* (Mill.) Britton, Sterns & Poggenburg] (Hennigar et al., 2008). Tree mortality in mature balsam fir typically occurs after 3 to 4 years of severe defoliation, and pure old stands tend to undergo greater defoliation than mixed stands (MacLean, 1980, 1984; Su et al., 1996; Campbell et al., 2008). Over the course of the 20th century, spruce budworm outbreaks in the boreal forest have tended to occur every 30 to 40 years at the landscape scale (Blais, 1983; Boulanger and Arseneault, 2004). These outbreaks have typically lasted 9 to 12 years (Nealis, 2016), although outbreak length can vary regionally (Gray et al., 2000). During an outbreak, spruce budworm populations increase rapidly to produce a massive number of adult moths (Cooke et al., 2007; Nealis, 2016).

Lepidopteran scales found in lake sediments have recently been used as a proxy to reconstruct spruce budworm population sizes over long timescales (e.g., Navarro et al., 2018b). This new paleo-proxy is particularly promising because the scales' chitinous structure is well preserved in anaerobic environments, such as lake sediments, and because scales are an abundant structure found on adult moths, produced in

enormous quantities during outbreaks (Ghiradella, 1998; Navarro et al., 2018a; Tremblay, 2022). Combined, the abundance of this microfossil and its durability has permitted the reconstruction of spruce budworm population fluctuations throughout the Holocene (Navarro et al., 2018b). However, as a novel paleo-indicator, its use has not yet been validated with an independent proxy, although outbreaks over the past 8000 years detected by the lepidopteran scales have been in agreement with other paleo-proxies such as spruce budworm larval head capsules, and feces (see Simard et al., 2002, 2006 for macrofossil reconstructions; Navarro et al., 2018b).

This study aims to determine whether lepidopteran scales could reliably identify local-scale periods of high spruce budworm populations, i.e., outbreaks, in the mixed boreal forests of Québec (Canada). We compare recent and known outbreak periods (1967-present) documented by aerial surveys to the accumulation of lepidopteran scales found in lake sediments. If lepidopteran scales provide an accurate proxy of spruce budworm population size, then large accumulations should coincide with known spruce budworm outbreak periods identified by aerial surveys, as both proxies indicate the presence or the absence of the defoliator.

2.3 Methods

2.3.1 Study area

Our sites were located between 47˚and 50˚N in the *Abies balsamea–Betula papyrifera* (Balsam fir–paper birch) and *Abies balsamea–Betula alleghaniensis* (Balsam fir–yellow birch) bioclimatic zones (Rowe, 1972; Saucier et al., 2009; Figure 2.1), and in areas having experienced varying levels of defoliation, as assessed on the ground in the sampling year (Table 2.1). All lakes were found at ≤ ca. 300 m asl and surrounded by flat or gently rolling terrain. The relative abundance of arboreal species varied across the region, although tree species composition remained similar, with stands typically comprising balsam fir, white spruce, black spruce, trembling aspen [*Populus tremuloides* Michx.], paper birch [*Betula papyrifera* Marshall], and yellow birch [*Betula alleghaniensis* Britt.], and jack pine [*Pinus banksiana* Lamb.] (Table 2.1).

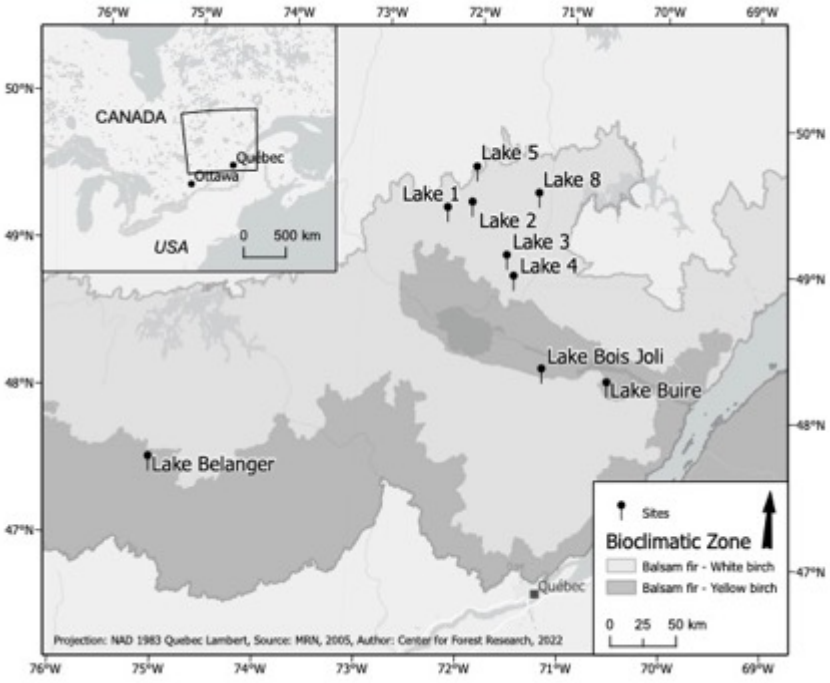

Figure 2.1: Location of the sampled lakes in central Québec, Canada.

Table 2.1: Site descriptions, associated lake characteristics, and the applied time-step used for interpolating each sediment core

Lake (North to South)	Coordinates (ºN, ºW)	Area (ha)	Depth of core extraction (m)	Year of sampling	Defoliation class	Tree species found in proximity of each lake	Interpolated time-step (years)
5	49.607, 71.998	3.91	9.7	2019	Severe	*Abies balsamea, Picea mariana, Populus tremuloides, Pinus banksiana*	5
8	49.445, 71.332	5.37	9.9	2019	Light	*Populus tremuloides, Abies balsamea, Picea mariana*	7
2	49.365, 72.030	4.11	8.5	2019	Severe	*Picea mariana, Pinus banksiana, Abies balsamea, Betula papyrifera, Populus tremuloides*	5
1	49.320, 72.286	1.20	5.5	2019	Severe	*Picea mariana, Pinus banksiana*	5
3	49.012, 71.646	2.62	8.3	2019	Moderate	*Betula papyrifera, Populus tremuloides, Abies balsamea, Picea mariana*	5
4	48.872, 71.566	0.94	5.2	2019	Light	*Picea mariana, Pinus banksiana, Populus tremuloides*	5
Bois Joli	48.245, 71.241	0.90	5.3	2019	Moderate	*Betula papyrifera, Populus tremuloides, Abies balsamea, Picea glauca*	8
Buire	48.165, 70.571	1.30	3.4	2018	Moderate	*Betula papyrifera, Populus tremuloides, Betula alleghaniensis, Abies balsamea, Picea mariana, Picea glauca*	6
Bélanger	47.477, 75.178	2.79	2.8	2017	None	*Betula alleghaniensis, Populus tremuloides, Abies balsamea, Picea glauca*	6

2.3.2 Lake sediment paleo-proxy: lepidopteran scales

2.3.2.1 Field sampling and subsampling preparation

We selected nine small (roughly ≤5 ha), deep lakes having little or no inflow or outflow (e.g., Millspaugh and Whitlock 1995; Ali et al., 2008). The lake–sediment interface and upper portion of the sediment record were collected using a gravity corer (Renberg, 1991; Renberg and Hansson, 2008). We subsampled the cores at a 1 cm resolution and removed 1 cm^3 from each subsample for use in lepidopteran scale analysis. Six subsamples from the upper portion of each core— 0–1, 2–3, 5–6, 9–10, 14–15, and 24–25 cm except for Lake 4 which required an extra sampling depth at 18–19 cm—were sent to Flett Research Ltd (Winnepeg, MB, Canada) to obtain measurements of ^{210}Pb activity. To convert ^{210}Pb activity into calendar years, we applied a constant rate of supply (CRS) model (Appleby and Oldfield, 1983; Binford, 1990; Appendix A).

Lepidopteran scales were extracted from the top 20 cm of each sediment core, corresponding to approximately the last 150 years, following a modified protocol initially developed by Navarro et al., (2018a). Briefly, each 1 cm^3 sediment subsample was deflocculated in 20% KOH at 17 psi and 121˚C for 30 minutes in a steam sterilizer (Amsco unit by Steris). The sediment was then wet-sieved at 53 µm, and the retained sediment was put into 50 mL centrifugation tubes. Twenty millilitres of sucrose solution (relative density = 1.24) was added to the tubes, which were then centrifuged at 4500 rpm for 20 minutes at 21˚C. The supernatant from each tube was removed, and 25 µL of 1% lactophenol cotton blue stain was added to the pellet to facilitate scale identification. The pellets were mounted on microscope slides and scales were identified and counted at 10x objective magnification (Tremblay, 2022).

2.3.2.2 Analysis

We identified peaks of lepidopteran scale abundance using a modified version of CharAnalysis, a procedure typically used to reconstruct paleo-fires from charcoal particles recovered from lake sediments (Higuera, 2009; Higuera et al., 2010; Appendix B). The short temporal scale (<200 years) and relatively small sample size of the scale series, however, precluded the use of the CharAnalysis program in its original design

(Higuera, 2009; Higuera et al., 2010). Therefore, we developed a simplified version of CharAnalysis in the R environment (R core team, 2021). For clarity, we use the same terminology as for the original program.

Raw sediment accumulation rates can vary downcore because of sediment compaction; thus, 1 cm thick samples in the upper portion represent a shorter time interval than those recovered at the bottom of the core. The subsequent analyses required implementing a constant time-step; therefore, we interpolated the raw accumulation rates to a constant time-step (C_{int}). From this, we could determine the background accumulation rate (C_{back}). Interpolation was performed by applying the best-fitting time step to the raw accumulations rates within each core with the *pretreatment* function in the *paleofire* R package (Blarquez et al., 2014; Table 2.1; Appendix B). We obtained background accumulation rates (C_{back}) using LOWESS, from the *locfit* package (Loader, 2020), running a smoothing window of 100 or 120 years corresponding to approximately three times the known spruce budworm outbreak return interval (30–40 years) in recent history (Blais, 1983; Morin, 1994; Boulanger and Arseneault, 2004; Boulanger et al., 2012). We selected this approach as an analogous procedure as for determining C_{back} for wildfires, which relies on a smoothing window approximately three times the mean fire return interval (Carcaillet et al., 2009; Blarquez et al., 2010). Peak scale accumulations (C_{peak}) were determined by subtracting C_{back} from the interpolated values to which a threshold *t* was applied to identify large spruce budworm populations, i.e., outbreaks (C_{fire}), and differentiate them from C_{noise}. The thresholds used to identify outbreaks were at the 40^{th}, 50^{th}, 60^{th}, 70^{th}, 80^{th}, 90^{th}, 95^{th}, and 99^{th} percentiles of C_{peak} and were applied globally, as each core had fewer than 30 samples (Higuera, 2009; Higuera et al., 2010).

We identified outbreak events as clusters of scale accumulations by applying a 20-year window (10 years pre-outbreak to 10 years post-outbreak) around the highest accumulation rate of a potential outbreak (C_{peak}) to reduce identifying false outbreaks. Any point falling within this window was considered to be part of the same outbreak event cluster. We selected this window length to encompass the 5- to 15-year period of severe defoliation when budworm populations are high (Blais, 1985b) and to encompass the variability in outbreak duration observed over the 20^{th} century (Gray et al., 2000).

2.3.3 Aerial surveys

Because lepidopteran scale accumulations within a small lake represent the local (approximately 200 m radius) spruce budworm population (Tremblay, 2022), we also estimated defoliation within a 200 m buffer around each lake. We performed this projection in ArcMap 10.4.1 (ESRI, 2015) using shapefiles of aerial surveys conducted from 1967 to present (MFFP, 2021a; Appendix C). We defined outbreak periods at each site as the first year of observed defoliation to the last year of observed defoliation within the buffer zone, even if within this period there were up to five consecutive years of no observed defoliation, a phenomenon that can sometimes occur locally (Gray, 2008). Furthermore, within the defined outbreak periods, at least 1 year of observed moderate or severe defoliation had to be recorded, as sedimentary lepidopteran scale accumulations cannot detect light defoliation events (Tremblay, 2022). If only light defoliation was observed in the outbreak period, this was not counted as an outbreak.

2.3.4 Outbreak period definition and detection

From the above criteria, we assessed outbreak detection (presence/absence) for the various smoothing windows and scale percentile thresholds using a confusion matrix, Cohen's Kappa, and Matthews correlation coefficient. We applied the CharAnalysis procedure over the entire time period covered by the sediment core (top 20 cm) to retain the variability in scale accumulations over the 20th century to most accurately identify large scale accumulations. However, the outbreak detection analysis was restrained to the latter portion of the 20th century, i.e., 1967-present, a period for which information was available for both proxies. During this period, two major outbreaks occurred in the province of Québec. Although they lasted 15 to 20 years at the regional scale (1967–1986 and 2010–present), defoliation rarely exceeded 10 to 15 years locally and showed variable temporal patterns (Gray et al., 2000). Therefore, we used site-scale defoliation patterns to determine the exact years of outbreak vs. non-outbreak periods for the confusion matrix. We defined the outbreak periods through aerial surveys by using the first and last year of detected defoliation across all sites within the study area spanning the years: 1971–1985 (O1; using the nomenclature in Jardon et al., 2003 and Boulanger et al., 2012), and 2010–present (OP; 'present outbreak', building off the previous nomenclature). Similarly, a non-outbreak period spanned from 1986 to 2009.

A 2 x 2 confusion matrix counted the number of occurrences—3 periods, i.e., 2 outbreaks and 1 non-outbreak x 9 lakes for a total of 27 observations—that both proxies agreed or disagreed (Table 2.2). The

matrix consisted of four cells: true positive (TP) where both proxies identified an outbreak; true negative (TN) where neither proxy detected an outbreak; false positive (FP), and false negative (FN; e.g., Chicco et al., 2021a,b,c) where proxies disagreed as one proxy identified an outbreak and the other did not.

Table 2.2: The generic confusion matrix used to assess the agreement between the lepidopteran scale accumulations and the aerial surveys. Observations where both proxies agree are counted in the 'outbreak–outbreak' or 'no outbreak–no outbreak' cells (TP: true positive and TN: true negative, respectively). Otherwise observations where the proxies disagree are counted in the 'outbreak–no outbreak' cells (FP: false positive, FN: false negative). The 'x' represents either the 100-year or the 120-year smoothing window.

		Aerial surveys	
		Outbreak	No outbreak
Lepidopteran scale smoothing 'x' year window width	Outbreak	True positive (TP)	False positive (FP)
	No outbreak	False negative (FN)	True negative (TN)

We assigned peak lepidopteran scale accumulations that surpassed the defined percentile threshold (C_{fire}), to the closest aerial survey-defined outbreak period (1971–1985; 2010–present) within 15 years. This window accounted for the variability resulting from ^{210}Pb measurements and subsequent age–depth estimates and was inspired by a similar method applied to assign sediment charcoal peaks based on fire scars (see Higuera et al., 2005). Cohen's Kappa, based on the 2 x 2 confusion matrix, served to quantify the agreement in outbreak detection between the two proxies (Cohen, 1960; Warrens, 2008, 2010; Chicco et al., 2021c). Cohen's Kappa typically ranges from –1 to 1, where values closer to 1 indicate agreement between the proxies, and values closer to 0 indicate that the agreement between the proxies occurs because of chance (Cohen 1960; Warrens 2014, 2015; Chicco et al., 2021c). Values closer to –1 indicate a disagreement between the proxy records (Chicco et al., 2021c).

In addition to Cohen's Kappa, we used the Matthews correlation coefficient (MCC) to quantify the agreement between the proxies as it may be more reliable and informative metric than Cohen's Kappa (Chicco et al., 2021a,b,c). The MCC is a performance metric assessing the association between variables

(Matthews, 1975) and is analogous to the ϕ (phi) coefficient in the case of a 2 x 2 matrix (Zysno, 1997; Baldi et al., 2000; Chicco and Jurman, 2020; Chicco et al., 2021a,b,c). Values range from –1 to 1, and these extremes indicate disagreement and agreement, respectively, whereas values of 0 indicate no relationship between the proxy records (Baldi et al., 2000; Chicco et al., 2021 a,b,c). The MCC generates a high value when both a majority of positive and negative instances are correctly classified (Chicco et al., 2021 a,b,c).

2.4 Results

Outbreak detection using the lepidopteran scales strongly agreed with the aerial surveys (23 true positive or negative vs. 4 false positive or negative; Table 2.3) producing a kappa of 0.69, and an MCC of 0.70 (Table 2.4). Successful detection generally increased when we lowered the percentile threshold, and we found greater accuracy when we applied a 100-year window width. The 100-year smoothing window generally had more true positive and fewer false negative detections relative to those of the 120-year window (Table 2.3). Maximum outbreak detection by the scales occurred at the 60th percentile threshold and was lowest at the 95th and 99th percentile thresholds regardless of the smoothing window size (Table 2.3). Generally, the number of false negatives increased with increasing percentile threshold (Table 2.3). A false positive for lake Bélanger (ca. 2005) occurred regardless of the threshold or smoothing window size, as the scale record had detected an outbreak, whereas none had been detected by aerial surveys (Table 2.3; Figure 2.2; Appendix C; Appendix D). Finally, an additional false positive occurred at the 40th or 50th percentile when applying the 100- and 120-year smoothing window, respectively (Table 2.3).

Table 2.3: Summary of the confusion matrix occurrences for the 100- and 120-year smoothing windows and percentile thresholds applied to the lepidopteran scale records from sediment cores collected from nine lakes. A higher number of true positives and negatives suggests greater agreement between the sedimentary

scale record and the aerial surveys, whereas a higher number of false positives and negatives suggests greater disagreement between both proxy records.

		Percentile threshold							
Smoothing window (years)		40	50	60	70	80	90	95	99
100	True positive	14	14	14	12	10	6	5	5
	False positive	2	1	1	1	1	1	1	1
	True negative	8	9	9	9	9	9	9	9
	False negative	3	3	3	5	7	11	12	12
120	True positive	14	14	13	11	9	6	5	5
	False positive	2	2	1	1	1	1	1	1
	True negative	8	8	9	9	9	9	9	9
	False negative	3	3	4	6	8	11	12	12

Table 2.4: The agreement in spruce budworm outbreak detection, expressed as Cohen's Kappa and Matthews correlation coefficient between lepidopteran scale accumulations and aerial surveys over the late 20th century (1967-present) using different window widths and percentile thresholds. Both Cohen's Kappa and Matthews correlation coefficient range from –1 to 1, where values close to –1 indicate disagreement, whereas values nearing 1 indicate strong agreement between the proxies. Values near 0 suggest no relationship or a chance agreement between the two proxies.

Smoothing window (years)	Percentile threshold (%)	Cohen's Kappa statistic (%)	Matthews correlation coefficient (%)
100	40	0.61	0.61
	50	0.69	0.70
	60	0.69	0.70
	70	0.56	0.59
	80	0.43	0.48
	90	0.21	0.28
	95	0.16	0.23
	99	0.16	0.23
120	40	0.61	0.61
	50	0.61	0.61
	60	0.63	0.64
	70	0.50	0.53
	80	0.38	0.43
	90	0.21	0.28
	95	0.16	0.23
	99	0.16	0.23

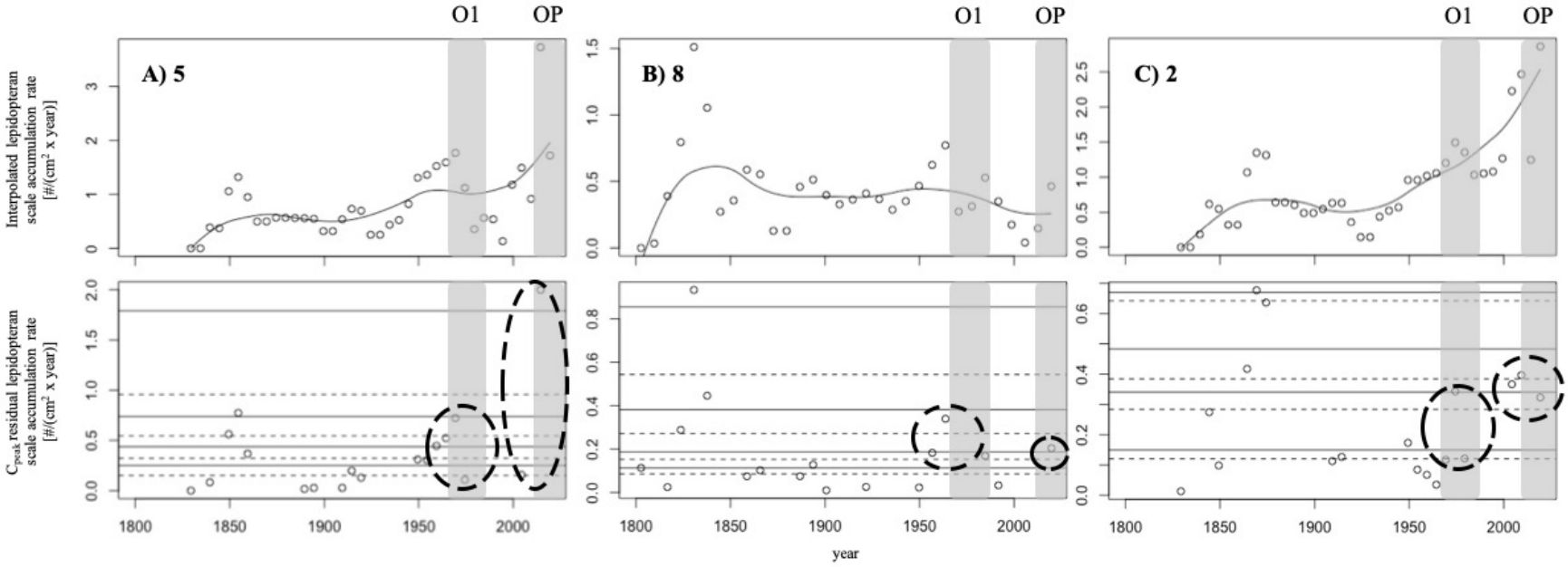
A) 5
B) 8
C) 2
O1
OP
Interpolated lepidopteran scale accumulation rate [#/(cm² x year)]
C_peak residual lepidopteran scale accumulation rate [#/(cm² x year)]
year
1800
1850
1900
1950
2000

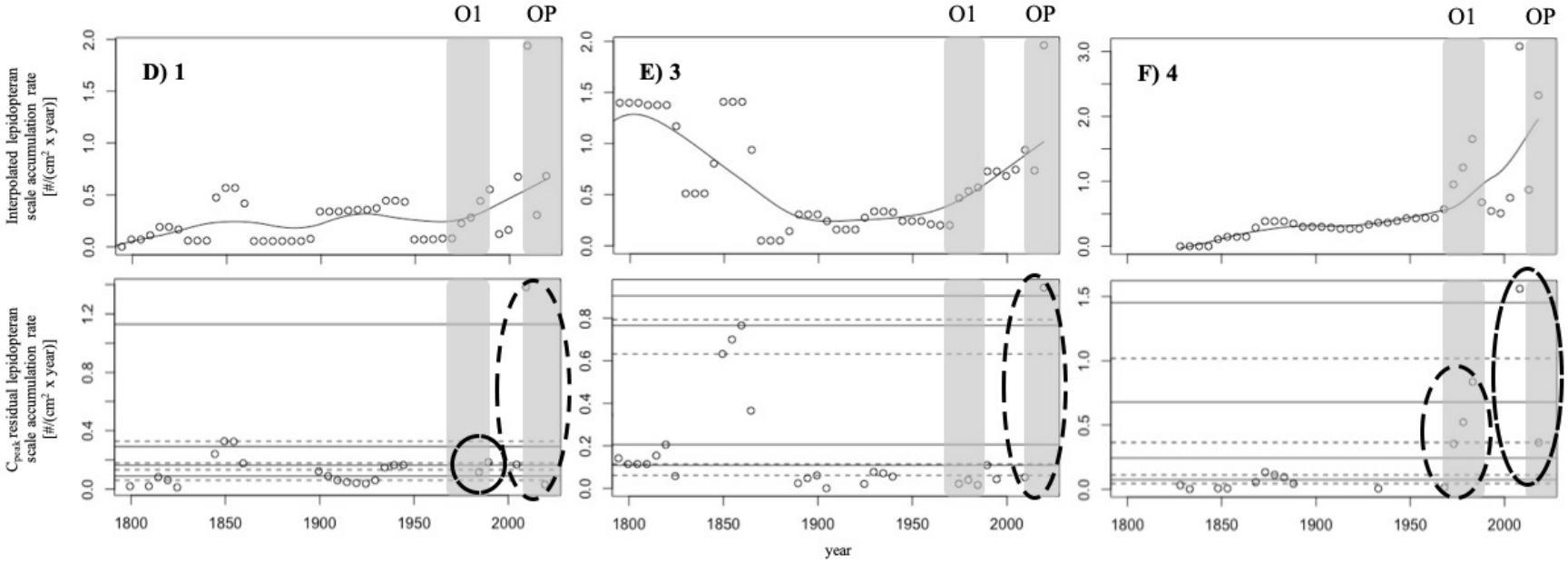
D) 1
E) 3
F) 4
O1
OP
Interpolated lepidopteran scale accumulation rate [#/(cm² x year)]
C_peak residual lepidopteran scale accumulation rate [#/(cm² x year)]
year
1800
1850
1900
1950
2000

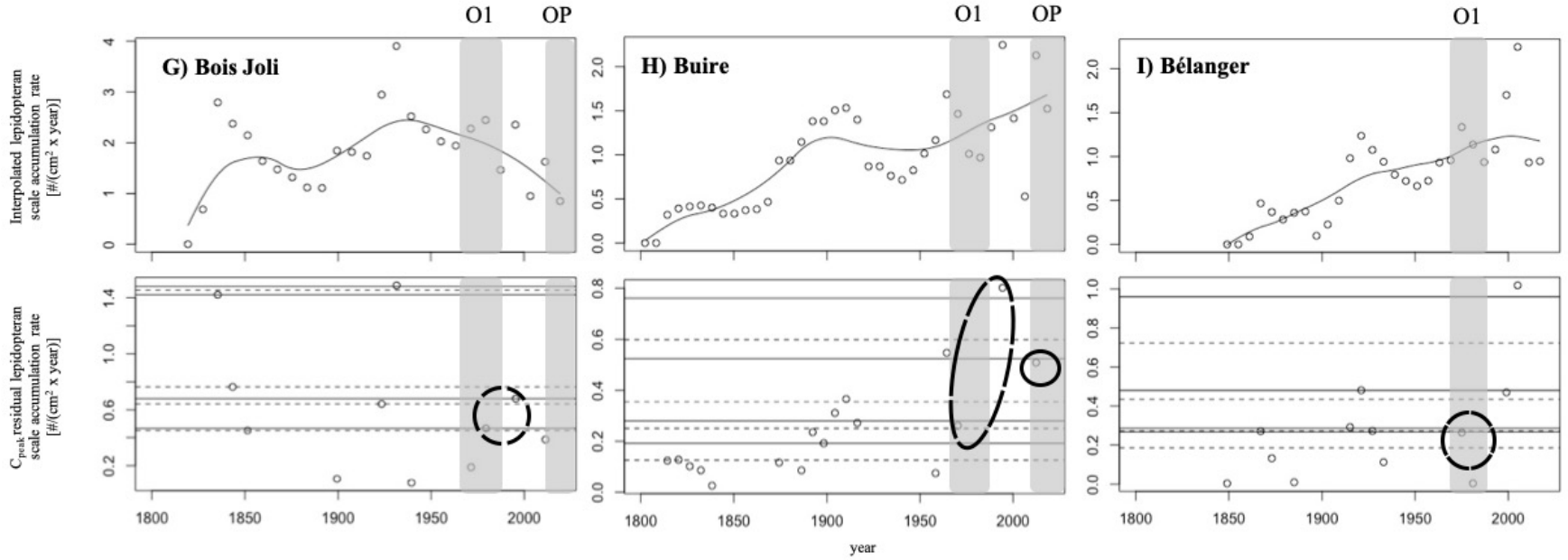

Figure 2.2: Interpolated lepidopteran scale accumulations and C_{peak} accumulations using the lepidopteran scale paleo-proxy for Lakes (a) 5, (b) 8, (c) 2, (d) 1, (e) 3, (f) 4, (g) Bois Joli, (h) Buire, (i) Bélanger. The grey boxes represent the detected and defined outbreak periods by the aerial surveys and are identified as O1 (1971–1985; 1980s outbreak), and OP (2010–present; current outbreak) using the nomenclature in Jardon et al., (2003), and Boulanger et al., (2012). The circles identify lepidopteran scale accumulation clusters representing potential outbreak events. Top panel: The solid smooth line represents the LOWESS with a 100-year smoothing window width used to determine the background accumulation rates (C_{back}), where everything above is considered a potential outbreak(C_{peak}). Bottom panel: The C_{peak} accumulations calculated as residuals along with the different percentile thresholds used. Dashed horizontal lines represent the 40^{th}, 60^{th}, 80^{th}, and 95^{th} percentile thresholds respectively, and the solid horizontal lines represent the 50^{th}, 70^{th}, 90^{th}, and 99^{th} percentile respectively above which the 'true' outbreak events (C_{fire}) were identified.

The threshold-smoothing combinations yielding the highest Cohen's Kappa (0.69) and MCC (0.70) were the 50th or 60th percentile thresholds applied using the 100-year smoothing window (Table 2.4). When using the 120-year smoothing window, we found the best agreement with the 60th percentile threshold, although this threshold yielded lower values for both statistics (0.06 less). For both smoothing window sizes, the poorest agreement was obtained with the 95th and 99th percentile thresholds (Table 2.4).

2.5 Discussion

Lepidopteran scales accurately identified outbreak periods. We observed a robust agreement in identifying outbreaks using both the sedimentary scale record and aerial surveys. The rate of agreement was slightly better when using a 100-year smoothing window to determine background accumulations than using a 120-year window. The 100-year window may be closer to three times the return interval typically used to estimate background accumulations (e.g., Blarquez et al., 2010) given the 30- to 40-year return interval of spruce budworm outbreaks over the 20th century (Blais, 1983; Morin, 1994; Boulanger and Arseneault, 2004; Boulanger et al., 2012). The larger 120-year window is at the upper end of the documented spruce budworm outbreak return interval and may be smoothing out too much variance (Appendix D); in certain cases, this causes some events to be categorized as background accumulations. Additionally, the highest agreement between both proxies, applying the 100-year smoothing window, was achieved using the 50th or 60th percentile thresholds. After removing background accumulations, C_{back}, the 50th and 60th percentiles appear to be optimal, as they are sufficiently high thresholds to distinguish C_{fire} from C_{noise}, but sufficiently low to retain scale accumulations that may represent smaller populations, i.e., potentially less severe outbreaks.

Although lepidopteran scales and aerial surveys are both indicators of the spruce budworm presence around a lake, they represent different measures of the local presence of this defoliator. Lepidopteran scales are a direct measure of the local insect biomass and physical presence of adult spruce budworm moths within a stand, whereas aerial surveys are an indirect measure of spruce budworm presence, as they document the impact of the defoliator via stand-level defoliation. Generally, agreement between proxies would be expected to be high because a large adult moth population requires the occurrence of intense defoliation by a large well-fed larval population. Thus, by focusing on outbreak detection, as we have done in this study,

the observed strong agreement between the proxy records was likely. However, focusing on outbreak severity could yield a different result, particularly at relatively fine spatial scales, such as for this study, because defoliated areas delineated by aerial surveys tend to be quite large, yet defoliation within these areas can be heterogeneous (Harris and Dawson, 1979; Kettela, 1982; MacLean and MacKinnon, 1996). Furthermore, the proportion of host trees in a given area becomes crucial as their abundance determines the area's defoliation class. For example, two areas may both be considered severely defoliated; however, the proportion of host trees in one area may only comprise 10% of the basal area whereas in the other area, host trees may occupy >75%. At small spatial scales, it is therefore possible that the defoliation class does not necessarily correspond to the adult moth population found around a lake. Hence, this explains why we opted to compare outbreak detection between the two proxies in the form of presence/absence rather than focusing on outbreak severity.

A possible explanation as to why outbreaks are recorded by lepidopteran scales at certain sites and not at others may be related to lake-level taphonomical processes and the size of the catchment basin. Lepidopteran scales are a fairly reliable indicator of annual moderate and severe spruce budworm defoliation in the forest surrounding a lake, as scales are deposited and incorporated relatively rapidly into the lake sediment (Tremblay, 2022). Nonetheless, sediment deposition and mixing is highly site-dependent (e.g., Conedera et al. 2009; Bennett and Buck, 2016) and may influence the vertical and horizontal distribution of the scales in the sediment column, thereby affecting analyses. An altered distribution of scales in the sedimentary record may result in an outbreak being spread over a greater downcore depth, creating a signal similar to background accumulation. Conversely, background accumulations can be concentrated within a relatively small depth to create a false outbreak signal as demonstrated potentially by the one observed false positive in our study. Such processes may be dictated by lake basin shape subsequently affecting sediment accumulation (Bennett and Buck, 2016). In this study, we attempted to control for such processes statistically through the use of the CharAnalysis procedure that utilizes interpolation, differentiating between background accumulations (C_{back}) and potential outbreak events (C_{peak}), and by applying a global threshold to further discriminate between potential outbreak and true outbreak events (C_{fire}), in addition to the use of outbreak clusters (see methods).

In addition to taphonomical processes, the dating of sediment is also associated with errors (e.g., Higuera et al., 2005), and age–depth models used to determine large lepidopteran scale accumulations may not be as precise as the aerial surveys which have an annual resolution (Appendix A, and Appendix B). Finally, the size of the catchment basin for lepidopteran scale input may influence outbreak detection. Tremblay (2022) found a strong correlation between the current year's lepidopteran scale accumulation and defoliation within a 200 m buffer around sampled lakes; however, scale catchment basins may be larger or smaller than initially thought potentially explaining possible outbreak identification mismatches between the proxies. The catchment basin size for lepidopteran scale input will require further investigation.

We demonstrated that lepidopteran scales are a reliable proxy for identifying spruce budworm outbreaks, as their abundance peaks in the sediment match observations via aerial surveys. Therefore using this novel microfossil to reconstruct large spruce budworm population events over longer time scales is warranted (e.g., Navarro et al., 2018b). We note that peaks found at greater sediment depths are likely to represent more than one outbreak period because of a loss of temporal precision with increasing sediment depth. These comparisons using recent historical and known events help calibrate the sediment proxy record, emphasizing the importance of a multi-proxy approach. Moreover, this calibration of proxies ensures more accurate results and improved interpretations at millennial and multi-millennial scales.

2.6 Acknowledgements

We thank Dr. Allan Carroll, and Dr. Murray Hay for constructive feedback on earlier versions of the manuscript. François Gionest for help in the field, and Marika Tremblay and Guillaume Vigneault for help in the laboratory.

2.7 Funding

The author(s) received funding from the 'Chaire de recherche industrielle CRSNG sur la croissance de l'épinette noire et l'influence de la tordeuse des bourgeons de l'épinette sur la variabilité des paysages en zone boréale'. ^{210}Pb age determination was funded by this.

CHAPTER 3
DETECTION OF SPRUCE BUDWORM IMPACTS BY LEPIDOPTERAN SCALES AND TREE RINGS ARE COMPLIMENTARY

Marc-Antoine Leclerc, Martin Simard, Olivier Blarquez, and Hubert Morin

3.1 Abstract

Applying a centennial or millennial perspective to disturbance regimes permits an understanding of how these events have varied in the past in relation to climate change. Correctly interpreting this variability is crucial when preparing sustainable forest management practices for future warming. The eastern spruce budworm (Lepidoptera) is the most important biotic disturbance in the eastern Canadian boreal forest. Adult moths are covered by chitinous scales, and lepidopteran scale records in lake sediments have been analyzed to reconstruct Holocene spruce budworm populations. However, the magnitude of these scale accumulations has yet to be calibrated using an independent proxy. Here, we determine whether the impacts of spruce budworm defoliation are recorded by both sedimentary lepidopteran scale accumulations and tree-ring widths. Cross-wavelet analysis revealed agreement between both records at five out of nine sites, with a stronger overlap between the scales and the proportion of affected trees than between the scales and a growth suppression index. Wavelet coherence revealed agreement and synchronous signals in six out of nine sites between scales and the growth suppression index, and agreement and synchronous signals in five out of nine sites between scales and the proportion of affected trees. A species-based composite chronology relying on *Picea glauca* produced the clearest outbreak record for both proxy records. Peak scale accumulations correlated well with smaller tree-ring widths, demonstrating that larger scale accumulations correspond to more severe defoliation events. Therefore, lepidopteran scales provide reliable records of spruce budworm abundance and can serve as a proxy record of these events at centennial and millennial time scales.

3.2 Introduction

Climate change is expected to favour more frequent and severe disturbance events (e.g., Millar and Stephenson, 2015; McDowell et al., 2020). In the boreal biome, these altered disturbance regimes include insect outbreaks, as insect survival, growth, and development are influenced directly or indirectly by a

changing climate. The projected climate-related consequences include the direct effects of temperature change (see, e.g., Berg et al., 2006; Bentz et al., 2010; Régnière et al., 2012), modified insect distributions (see, e.g., Jepsen et al., 2008, 2011), use of naïve host-tree species (see, e.g., Cullingham et al., 2011; Erbilgin et al., 2014; Rosenberger et al., 2017), and an altered insect-host tree phenology, possibly rendering less vulnerable hosts more vulnerable (Pureswaran et al., 2015, 2019; Fuentealba et al., 2017). Indirect climate effects, via drought and altered precipitation regimes, could result in greater host-tree mortality in conjunction with insect outbreaks (see, e.g., Allen et al,. 2010, 2015; Hart et al., 2014, 2017; De Grandpré et al., 2019), or a loss in outbreak regularity (Esper et al., 2007).

In the eastern Canadian boreal forest, the spruce budworm [*Choristoneura fumiferana* Clemens] is the main biotic disturbance (MacLean, 2016; Nealis, 2016). The spruce budworm is a native lepidopteran defoliator with a univoltine life cycle during which the insect begins as an egg, molts through six larval stages, forms a pupa, and emerges as an adult moth that can then reproduce and disperse (Royama, 1984; Royama et al., 2005; Régnière and Nealis, 2007; Nealis, 2016). Defoliation by larvae occurs preferentially on the current year needles of mature balsam fir [*Abies balsamea* (L.) Mill.], with older needles targeted at high populations densities (Piene, 1989; MacLean et al., 1996; Nealis, 2016). White [*Picea glauca* (Moench) Voss] and black spruce [*Picea mariana* (Mill.) Britton, Sterns & Poggenburg] are alternate budworm hosts (Hennigar et al., 2008). Defoliation by the larvae often results in growth reductions (Blais, 1957, 1958, 1962, 1983), and severe defoliation will result in tree mortality, particularly in the preferred host (MacLean, 1980, MacLean, 1984).

Twentieth-century outbreaks of this insect in eastern Canada have occurred roughly every 30 to 40 years (Blais, 1983; Boulanger and Arseneault, 2004; Volney and Fleming, 2007; Boulanger et al., 2012), producing important consequences for timber supply, and carbon cycling (Dymond et al., 2010). Outbreak duration is variable (5-20 years; Gray et al., 2000), and severity depends on stand composition with lower impacts in stands with a greater proportion of deciduous species (MacLean, 1980; Su et al., 1996; Colford-Gilks et al., 2012; Houndode et al., 2021). In recent outbreaks, black spruce stands have experienced lower levels of defoliation because of the phenological mismatch between bud burst and larval emergence (Nealis and Régnière, 2004); however, climate change may modify this relationship (Régnière et al., 2012; Pureswaran et al., 2015, 2018, 2019; Fuentealba et al., 2017).

Historically, spruce budworm outbreaks have been reconstructed using dendrochronology (e.g., Blais, 1958, 1962, 1983; Morin and Laprise, 1990; Morin, 1994), generally spanning the last 300 to 400 years (e.g., Boulanger and Arseneault, 2004; Boulanger et al., 2012). Outbreak detection and severity are identified using tree-ring widths (e.g., Blais, 1958, 1962, 1968, 1983; Morin and Laprise, 1990; Morin, 1994; Boulanger and Arseneault, 2004; Boulanger et al., 2012), with narrower ring widths representing a proxy of abundant spruce budworm and its feeding on needles, i.e., defoliation, once the background climate signal is removed from the record (Swetnam et al., 1985). Defoliation by budworm larvae reduces the photosynthetic capacity of the host trees, limiting available photosynthates to inhibit growth and produce narrower tree-rings (Ericsson et al., 1980; Deslaurier et al., 2015). A two-to-four-year lag may exist between the year of defoliation and subsequent production of narrow growth rings (Ericsson et al., 1980; Krause and Morin, 1995; Krause et al., 2012).

Although dendrochronological approaches have been extremely useful, interpreting these tree-ring records requires understanding how host-tree response, survivor bias, and the fading record combine to affect the tree-ring record. Most spruce budworm reconstructions rely on white spruce , as it is sensitive to defoliation, and is a relatively long-lived species (Blais, 1958, 1962; Bouchard and Pothier, 2010). Black spruce has also been used (e.g., Tremblay et al., 2011). However, outbreak records in black spruce may be harder to identify given the phenological mismatch between the defoliator and the host tree, possibly resulting in a less obvious growth reduction (Blais, 1957, 1962; Pothier et al., 2012; Krause et al., 2012).

Living trees included in dendrochronological reconstructions are survivors of past events, therefore, tree response and circumstances permitted their survival, raising questions regarding the observed growth suppression recorded in survivors as an accurate representation of a defoliation event (Jardon et al., 2003). Site history is also important, as disturbances such as wildfire and logging affect individual tree's ability to record events and influence which recorder trees are left on a site, affecting any reconstruction. Finally, dendrochronology is also limited by a tree's lifespan; black and white spruce can live up to 200 and 300 years, respectively (Burns and Honkala, 1990), and fewer older specimens result in a fading record and thus a biased reconstruction (e.g., Pothier et al., 2012; Duchesne et al. 2019).

Dendrochronological reconstructions of spruce budworm outbreaks at millennial or multi-millennial scales are relatively limited (e.g., Simard et al., 2011). Therefore, the use of other proxy records is required to extend the chronology. Previous paleoecological approaches to identify budworm outbreaks have included sediment records of budworm larval head capsules, and budworm feces (e.g., Simard et al., 2002, 2006). Such proxies have shortcomings, such as the small number of head capsules in the sediment and downcores feces degradation (Simard et al., 2002, 2006). More recently, chitinous lepidopteran scales, which cover adult moths, have proven to be an excellent proxy of spruce budworm populations (e.g., Navarro et al., 2018a,b). The abundance of scales in the sedimentary record—thousands cover a single adult budworm moth—and their long-term preservation in the lake sediment record related to their chitinous composition (Richards, 1947; Sturz and Robinson, 1986; Montoro Girona et al., 2018) improve on the former insect outbreak proxies. Moreover, the abundance of scales deposited into small lakes mirrors the local insect biomass, and lepidopteran scales are incorporated into the lacustrine sediment within the year (Tremblay, 2022). Finally, there is a high agreement between the photographic aerial survey record (1967-present) and the abundance peaks in the lepidopteran scale sedimentary record (Chapter 1).

Despite the potential of scales to track long-term spruce budworm abundance, further calibration remains. Here, we compare local dendrochronological records with the corresponding lepidopteran scale sedimentary records from a series of lakes. We aim to establish whether both proxy records record similar impacts of spruce budworm defoliation and, if so, assess signal synchronicity. We hypothesize that larger accumulations of lepidopteran scales in the sedimentary records match tree-rings records showing growth suppression/greater percentage of affected trees and that these two signals are synchronous. Greater scale accumulations in the sediment record should track larger adult spruce budworm moth populations around the lake (and more severe defoliation by larvae). The two signals are expected to be relatively synchronous as lepidopteran scale incorporation into the sediment is relatively quick (Tremblay, 2022), and the effects of defoliation as recorded by tree-ring widths become evident two to four years following a defoliation event (e.g., Krause and Morin, 1995; Krause et al., 2012).

3.3 Methods

3.3.1 Lepidopteran scales

3.3.1.1 Field sampling, subsample preparation, and identification

To obtain sedimentary lepidopteran scale records of outbreak, we selected nine deep and small (approximately ≤ 5 ha) lakes having little inflow or outflow located in areas that have recently sustained variable levels of defoliation (Figure 2.1; Table 3.1). We collected cores using a gravity corer to ensure recovery of the water-sediment interface (Renberg, 1991; Renberg and Hansson, 2008), and subsampled all cores at a 1 cm resolution. Subsample preparation for scale recovery and analysis is detailed in Chapter 1. Additionally, an age–depth model using the constant rate of supply model (Appleby and Oldfield, 1983; Binford, 1990) was produced relying on ^{210}Pb activity (analyses by Flett Research Ltd, Winnepeg, MB, Canada) measured at six depths along each core (0–1, 2–3, 5–6, 9–10, 14–15, 24–25 cm; and an additional depth for Lake 4 at 18–19 cm; Appendix A).

3.3.2 Tree-ring record

3.3.2.1 Field sampling, preparation, and identification

We produced local chronologies at each site by coring multiple trees (20–32 of the largest and oldest individuals) within a 200 m radius around each lake (from herein 'site' will refer to the sediment collected from lake and the cored trees) but up to an 800 m radius to sample enough individuals (Table 3.1). We extracted one to two cores from each tree at a height of approximately ≤30 cm above the ground surface, or in certain cases ≤70 cm above the ground surface depending on the presence of rot in the stem. Cores were prepared and mounted following standard dendrochronological procedures (Stokes and Smiley, 1968). Cores were scanned, and ring widths were measured using WinDendro software (Regent Instruments Inc. 2017; Guay et al., 1992). Samples were visually cross-dated using PAST5 software (SCIEM, 2015a) utilizing the Pearson correlation coefficient, threshold values of 60%–70% for the 'Gleichlauf test', and ≥4 for the Baillie/Pilcher and Hollstein t-tests to ensure correct dating (SCIEM, 2015b). The 'Gleichlauf test' calculates the percentage of overlapping years for two records having matching growth trends (SCIEM, 2015b). The Baillie/Pilcher and Hollstein tests are variations of the Student's t-test and assess the similarity between a pair of dendrochronological records (SCIEM, 2015b). The Baillie/Pilcher test obtains its t-statistic via a five-year moving average over a minimum series length of 25 years. In contrast, the Hollstein variation uses Hollstein Wuchswert detrending (SCIEM, 2015b). We subsequently verified cross-dated sample placement via COFECHA v.6.06 (Holmes, 1983) to confirm visual cross-dating. We then applied

the expressed population signal (EPS; Wigley et al., 1984; Buras, 2017) to obtain the most representative chronology for each site. Ring-width indices were obtained by detrending and standardizing the most representative chronologies for each site with a 60-year cubic spline using the R package *dplR* (Bunn, 2010). All subsequent analyses were performed in the R statistical environment (v.4.0.5; R Core Team, 2021). Details of the steps (settings, functions) are presented in Appendix E.

Defoliation events described by the mean growth suppression index (mean GSI), and percentage of defoliated trees (percent affected) for each site were obtained using the R package *dfoliatR* (Guiterman et al., 2020). We calculated each site's mean GSI and percent affected at an annual resolution (Guiterman et al., 2020). The tree-level growth suppression index (GSI) is calculated as (Swetnam et al., 1985; Swetnam and Lynch 1989; Guiterman et al., 2020):

$$GSI_i = H_i(NH_i - NH_m)\frac{\sigma_H}{\sigma_{NH}}$$

where GSI_i is the growth suppression index in year *i*, H and NH are the standardized host-tree and non-host ring-width series, respectively, NH_m is the mean non-host series' ring-width, and σ_H/σ_{NH} is the ratio between the standard deviation of the standardized host and non-host series (Guiterman et al., 2020). In this study, lack of local non-host individuals precluded the creation of a non-host series and use of a non-host correction such that the GSI_i simply became the standardized host-tree ring-width series.

3.3.3 Correlation and synchronicity between scale and tree-ring records

The correlation and synchronicity between lepidopteran scale and tree-ring records (mean GSI and percent affected) were assessed using wavelet analysis. First, lepidopteran scale accumulations over the entire sediment chronology for each lake were interpolated to an annual resolution using the *pretreatment* function from the *paleofire* R package (Blarquez et al., 2014) to retain the variability in these accumulations. The interpolation permitted directly comparing scale accumulation rate, mean GSI, and percent affected. Further, interpolation to a constant time step attempted to reduce potential effects of sediment compaction that could have occurred in the scale records. The signal of each variable for each site was modelled using generalized additive models (GAMs) with the *mgcv* package (Wood, 2017).

Lake 8 required removing and imputing a point (CE 1952) in the mean GSI data set to better model the mean GSI signal and ensure the constant time step required for wavelet analysis. The comparison between the original and altered data set is presented in Appendix F.

Table 3.1: Site history and current tree species composition within an approximately 200 m radius around each lake including tree species cored, expressed population signal (EPS), and the relationship, as determined by cross-wavelet and wavelet coherence analyses, between the lepidopteran scales and dendrochonological records (mean GSI and percent affected). All sediment cores were collected in 2019 except for Lakes 4, Buire, and Bélanger which were sampled in 2018, 2018, and 2017 respectively.

			Site and lake characteristics[2]								Wavelet analysis[5,6]															
											Cross-wavelet								Wavelet coherence							
			Species proportion in stand (%)				Past disturbance		Tree rings		Scales vs. GSI				Scales vs. %				Scales vs. GSI				Scales vs. %			
Lake[1]	Lat., Long.	Area (ha)	*Picea*	*Abies*	*Pinus*	decid	fire	harvest	spp.[3]	EPS[4]	All	O3	O2	O1	All	O3	O2	O1	All	O3	O2	O1	All	O3	O2	O1
5[S]	49.6070 −71.9980	3.91	17	51	2	12	1890	1996–1997, 2018	*Pma* (23/24)	0.931	A	A	D	D	D	A	D	D	A	A	A	A	A	D	A	A
8[L]	49.4454 −71.3322	5.37	3	39	–	45	–	Pre-1970, 1990	*Pma* (17/20)	0.75	D	A	D	D	A	A	A	A	D	D	D	D	D	D	D	D
2[S]	49.3648 −72.0296	4.11	34	2	3	18	–	Pre-1970, 1991, 1993, 2010	*Pma* (27/27)	–	A	D	–	D	A	D	–	A	A	A	A	A	A	A	A	A
1[S]	49.3200 −72.2860	1.20	58	–	9	–	1890, 1940	1995, 2016	*Pma* (24/28)	0.874	D	D	D	D	D	A	D	D	A	A	A	A	A	A	A	A
3[M]	49,0120 −71.6460	2.62	15	21	–	24	–	Pre-1970, 1982, 1993, 1997, 2014, 2017	*Pma* (27/28)	0.895	A	D	A	A	A	A	A	A	A	A	A	A	A	A	A	A
4[L]	48.8718 −71.5664	0.94	39	–	20	2	1951, 1985	Pre-1970	*Pma* (31/31)	–	A	–	A	A	A	–	A	A	D	–	–	D	D	–	A	D
Bois Joli[M]	48.2451 −71.2419	0.90	–	11	–	69	1900	Pre-1970, 1986, 1988, 2013	*Pgl* (27/32)	0.885	D	D	D	D	D	D	D	D	D	D	D	D	D	D	N/A	N/A
Buire[M]	48.1654 −70.5708	1.30	18	11	–	60	–	Pre-1970	*Pgl* (25/28)	0.861	D	D	A	D	D	D	A	D	A	D	A	A	D	D	D	D
Bélanger	47.4765 −75.1775	2.79	10	13	–	53	–	Pre-1970	*Pgl* (26/26)	–	A	A	D	D	A	A	D	A	A	A	A	A	A	A	D	A

[1]Defoliation classes observed: L, M, S, correspond to light, moderate, and severe, respectively. The lack of a superscript means no defoliation was observed

[2] Current species composition is derived from the information from the fourth forest inventory, and disturbance history includes years of recorded fire and harvesting events (MFFP 2021a,b). The first forest inventory did not provide exact dates, only that disturbance events occurred prior to year of survey (MFFP 2021a,b).

[3]*Pgl* and *Pma: Picea glauca* and *Picea mariana,* respectively. In parentheses is the maximum number of trees contributing to the chronology out of the total

[4]The expressed population signal (EPS) is used to obtain the most representative tree-ring chronology for a stand, and the typical cut-off applied is 0.85 (Wigley et al., 1984); '–' in this column indicates no change in EPS with the removal of any individual, therefore all individuals were retained.

[5]Circular mean quantified the relationship between proxy records: 'Agreement' (A; anti-phase between scales and mean GSI or in-phase between scales and percent defoliation) or 'disagreement' (D; in-phase between scales and mean GSI and anti-phase for scales and percent defoliation) for both cross-wavelet analysis and wavelet coherence.

[6]'All' is the circular mean of the entire calculated area; 'O3', 'O2', 'O1' correspond respectively to the 1912–1929, 1946–1959, and 1975–1992 outbreaks as determined by regional chronologies (Morin and Laprise, 1990; Boulanger and Arseneault, 2004; Boulanger et al., 2012). The '–' in these columns indicates that the circular mean could not be calculated for the particular outbreak, as it was not found in a statistically significant area, or in an area where $R^2 \geq 0.80$, or if one of the proxy records did not cover the period and thus analysis was limited to periods covered by both time series.

The correlation and synchronicity between the lepidopteran scale and mean GSI signals and between the scale and the percentage of affected trees (percent affected) signals were assessed using wavelets with the *biwavelet* R package (Gouhier et al., 2021) over the time period (1900-2019) common to both records as the trees cored were not old enough to go further back in time. The use of wavelets is particularly powerful for analyzing and comparing non-stationary signals through time (e.g., Torrence and Compo, 1998; Grinsted et al., 2004; Cazelles et al., 2008; Fernández-Macho, 2012, 2018). We applied a continuous Morlet wavelet transform to obtain the temporal trends for each variable rather than a discrete wavelet transform because the continuous wavelet transform is robust to noise, and this transform can extract phase interaction information between a pair time series (Mallat, 1998; Grinsted et al., 2004; Cazelles et al., 2008). Moreover, the Morlet wavelet offers a relatively good balance between time and frequency (Grinsted et al., 2004). For each site, we tested the strength of each variable's signal (significance in the power spectrum) against a background signal generated by an autoregressive process with a lag of 1, using a χ^2 test and an α value of 0.05 (Torrence and Compo, 1998; Gouhier et al., 2021).

Subsequently, we assessed any correlations between the scale and tree-ring records in the *biwavelet* R package via cross-wavelet analysis and wavelet coherence running 1000 Monte Carlo randomizations for the latter (Gouhier et al., 2021). Cross-wavelet analysis reveals points in time and return intervals (i.e., periodicities) where strong signals between the variables overlap, and which signal leads or lags (Grinsted et al., 2004; Labat, 2005). Wavelet coherence identifies correlations between a pair of measured series as a function of frequency, with the correlation ideally displaying a consistent relationship between the signals (phased-locked behaviour; Chatfield, 1989; Torrence and Compo 1998; Grinsted et al., 2004; Cazelles et al., 2008). The significance for both wavelet coherence and cross-wavelet analysis was tested against a background signal generated by an autoregressive process with a lag of 1, using a χ^2 test and an α value of 0.05.

Finally, we determined the nature of the interaction between the two proxies by determining the phasing of the signal pairs, that is, which signal was leading or lagging relative to the other (Grinsted et al., 2004; Cazelles et al., 2008). Phasing was represented graphically by arrows overlaid on wavelet power spectra with the arrowhead direction indicating the nature of the interaction. Arrows pointing to the right indicate that the two signals are in-phase when the peaks and troughs of both signals are synchronous. An arrow

pointing to the left indicates an anti-phase relationship when the peak of a signal lines up with the trough of the other signal (Grinsted et al., 2004). An upward arrow indicates that the scale record lags the dendrochronological record by π/2 (Grinsted et al., 2004), i.e., a peak/trough in lepidopteran scales occurs slightly after a peak/trough in either the mean GSI or percent affected. A downward arrow indicates that the scale record leads the tree-ring record by π/2 , i.e., a peak/trough in lepidopteran scales occurs slightly before a peak/trough in either the mean GSI or percent affected (Grinsted et al., 2004). We calculated the circular mean and standard deviation using the *circular* R package (Agostinelli and Lund, 2017) for the entire zone of significant high overlapping power and in zones of high correlation ($R^2 \geq 0.80$) over the entire study period (1900-2019) and for each known outbreak period (1912–1929, O3; 1946–1959, O2; and 1975–1992, O1; Morin and Laprise 1990; Boulanger and Arseneault, 2004; Boulanger et al., 2012) for each site.

Using the circular mean values and standard deviation, we described the signals as being in agreement (lepidopteran scale and mean GSI signals showing an anti-phase behaviour) or disagreement (in-phase behaviour represents disagreement. We expect that large spruce budworm impacts, related to large adult moth populations (abundant scale accumulations), will be reflected by a lower mean GSI (narrower tree-ring widths) because of greater larval defoliation. Conversely, lepidopteran scale and percent affected signals agree when these records exhibit in-phase behaviour and disagree when exhibiting anti-phase behaviour.

3.3.4 Composite chronologies

We created composite lepidopteran scale and tree-ring chronologies to determine whether a clearer signal could be obtained by combining sites and basing these composite records on tree species (three *P. glauca* and six *P. mariana* sites; Table 3.1). We combined standardized individual tree-level ring widths from the three *Picea glauca* sites to obtain the *P. glauca* composite. In contrast, the *Picea mariana* composite was built using the standardized individual tree-ring widths from the six *P. mariana* sites. The respective ring-width and percent affected composite records were developed using the *dplR* (Bunn, 2010), and *dfoliatR* (Guiterman et al., 2020) packages respectively. We combined the annually interpolated lepidopteran scale accumulations, obtained via the *pretreatment* function in the R *paleofire* package (Blarquez et al., 2014), from the respective *P. glauca* and *P. mariana* sites to obtain a composite mean lepidopteran scale accumulation for each tree taxa.

3.4 Results

3.4.1 Age-depth models, and lepidopteran scale and tree-ring proxy records

The age-depth models derived from ^{210}Pb measurements used to determine lepidopteran scale accumulations displayed similar shapes and low variability in date estimates over the study period (1900-2019; Appendix A). Lepidopteran scale accumulations, ring-width indices, and percent affected varied from site to site (Appendix G).

3.4.2 Wavelet analyses

The individual continuous Morlet wavelet transforms revealed strong significant return intervals (periodicities) in the scale and tree-ring records (Figure 3.1). Areas of significant high power in lepidopteran scale abundance had a periodicity of 8 to 32 years in seven out of nine sites from 1950-2019 (Figure 3.1). Areas of significant high power in the mean GSI, and percent affected also had a similar periodicity (8-32 years) for most of the study period (1900-2019) in seven of the nine sites (Figure 3.1). We observed areas of high power for mean GSI over the entire study period at all sites except Site 2 and high power for percent affected over the entire study period at all sites except Sites 1, and 2 (Figure 3.1).

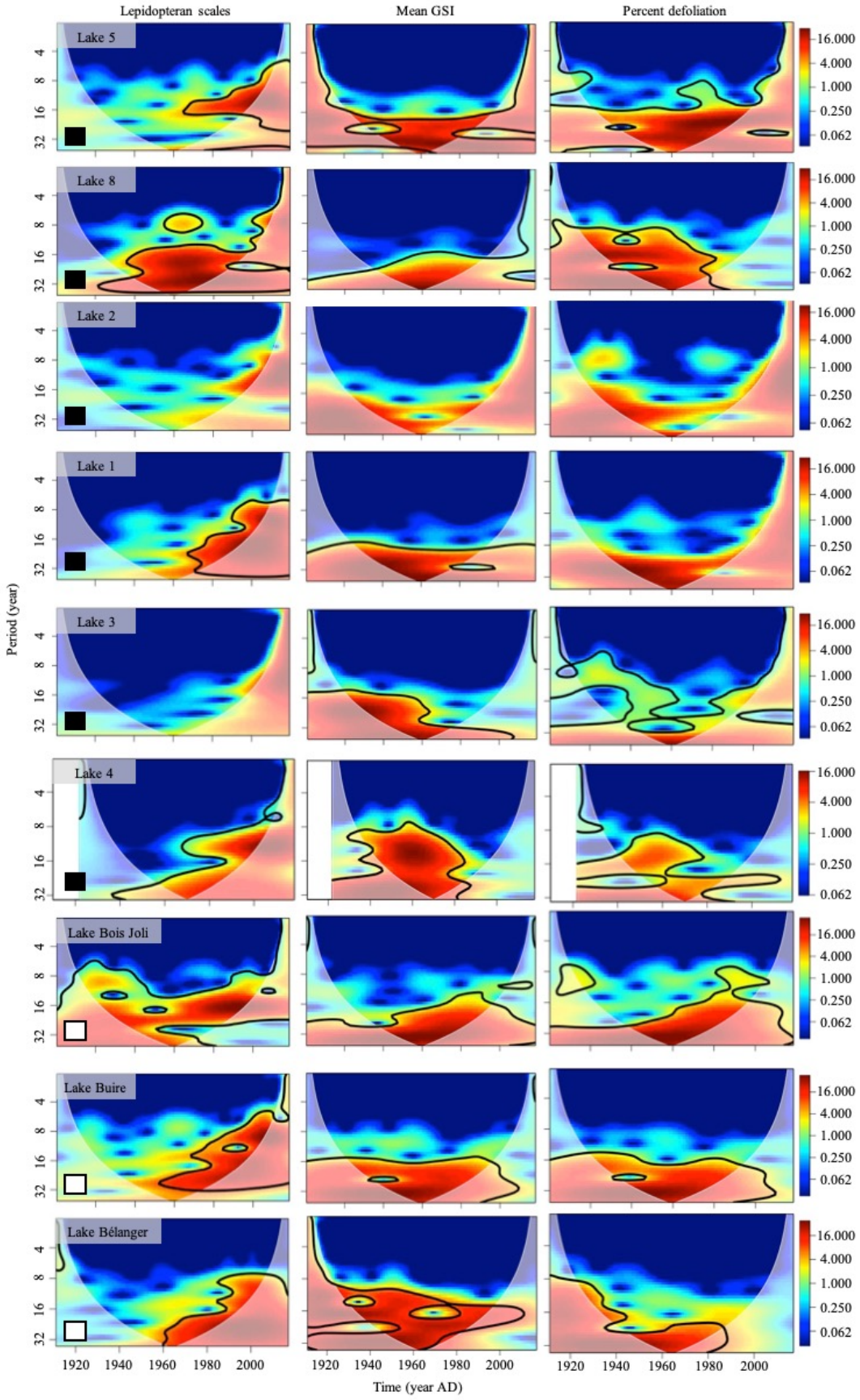
Lepidopteran scales
Mean GSI
Percent defoliation
Lake 5
Lake 8
Lake 2
Lake 1
Lake 3
Lake 4
Lake Bois Joli
Lake Buire
Lake Bélanger
Period (year)
4
8
16
32
16.000
4.000
1.000
0.250
0.062
1920
1940
1960
1980
2000
Time (year AD)

Figure 3.1: The power spectra of the paleo and tree-ring variables from 1900 to 2019. Warmer colours (*red, orange, yellow*) indicate high power relative to a background signal generated by an autoregressive process with a lag of 1, whereas cooler colours represent weaker power (Torrence and Compo, 1998). Statistically significant zones of power were determined using a χ^2 test ($p<0.05$) and are delineated by a thick black line (Torrence and Compo, 1998). The light grey shading delineates the recommended zone of interpretation, i.e., the cone of influence (Cazelles et al., 2008). Squares in the left hand corners of the spectra indicate the tree species cored; white, *Picea glauca*; black, *Picea mariana*.

The cross-wavelet analysis between both proxies revealed fairly consistent areas of overlapping power occurring at an 8-to-32-year periodicity of variable strength (Figure 3.2). Lepidopteran scales and mean GSI showed areas of significant overlapping low power at periodicities between 8 to 32 years over the complete period (1900-2019) (Figure 3.2). Phases did vary within the zones of significant overlapping power, and also among sites. However, the circular mean for the entire significant zone indicated agreement when greater scale accumulations corresponded to narrower ring widths at Sites 2, 3, 4, 5, and Bélanger (five of the nine sites; Table 3.1). For all sites, cross-wavelet analysis revealed areas of significant high power between lepidopteran scales and percent affected at periodicities of 8-to-32-years over the entire study period (Figure 3.2). Additionally, the phasing varied within the zones of high significant overlapping power; however, the circular mean calculated for the entire significant zone indicated agreement between the records, in which greater scale accumulations corresponded with a greater percentage of defoliated trees at Sites 2, 3, 4, 8, and Bélanger (five of the nine sites; Table 3.1).

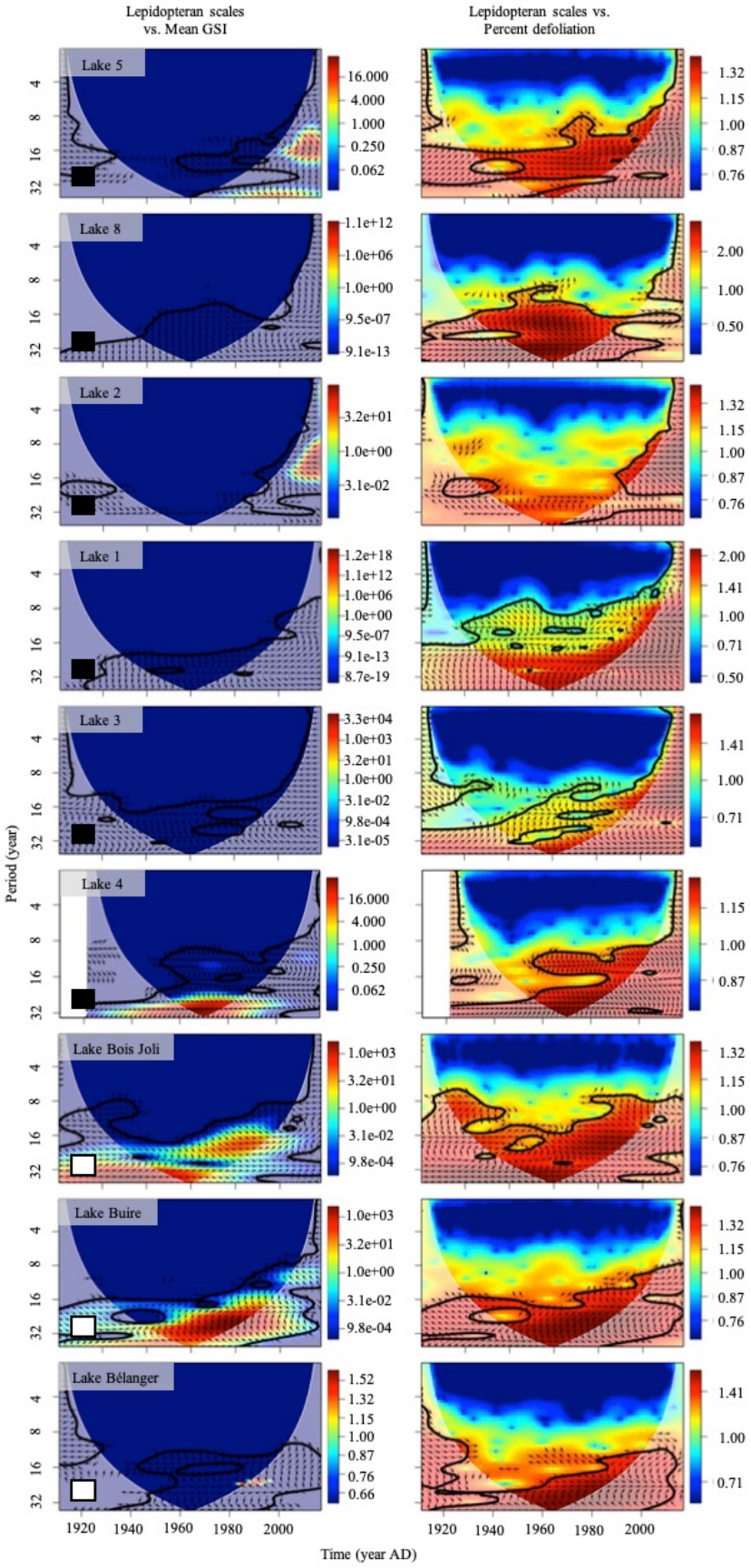
Lepidopteran scales vs. Mean GSI
Lepidopteran scales vs. Percent defoliation
Lake 5
Lake 8
Lake 2
Lake 1
Lake 3
Lake 4
Lake Bois Joli
Lake Buire
Lake Bélanger
Period (year)
4
8
16
32
16.000
4.000
1.000
0.250
0.062
1.1e+12
1.0e+06
1.0e+00
9.5e-07
9.1e-13
3.2e+01
3.1e-02
1.2e+18
1.1e+12
1.0e+06
1.0e+00
9.5e-07
9.1e-13
8.7e-19
3.3e+04
1.0e+03
3.2e+01
1.0e+00
3.1e-02
9.8e-04
3.1e-05
1.52
1.32
1.15
1.00
0.87
0.76
0.66
1.32
1.15
1.00
0.87
0.76
2.00
1.00
0.50
1.41
0.71
1920
1940
1960
1980
2000
Time (year AD)

Figure 3.2: The power spectra resulting from the cross-wavelet analysis applied to the paleo and dendrochronological records. Warmer colours (*red, orange, yellow*), indicate high common power relative to red noise, an autoregressive process with a lag of 1, whereas cooler colours represent weaker power (Torrence and Compo, 1998). Statistically significant zones of common power were determined using a χ^2 test ($p<0.05$) and are delineated by a thick black line (Torrence and Compo, 1998). The arrows in the areas of statistical significance help specify the type of association. Arrows pointing left indicate that the signals are anti-phase, where a peak of one signal lines up with a trough of the other signal. Arrows pointing right suggest that signals are in-phase, where peaks and troughs of both signals line up. Downward arrows indicate that the scale record leads the tree-ring record by $\pi/2$, whereas upward arrows indicate the opposite. The light grey shading delineates the recommended zone of interpretation, i.e., the cone of influence (Cazelles et al., 2008). Squares in the left-hand corners of the spectra indicate the tree species cored; white, *Picea glauca*; black, *Picea mariana*.

We observed a highly significant wavelet coherence between the scale and tree-ring records at a one-to-four-year periodicity over the study period (Figure 3.3). Significant correlations were observed at higher periodicities at Sites 2, 3, and 8 (Figure 3.3). The direction of the relationship between lepidopteran scales and mean GSI varied and depended on the site; however, the circular mean in the zones of high correlation ($R^2 \geq 0.80$) indicated agreement between the proxy records, in which greater scale accumulations coincided with narrower ring widths at Sites 1, 2, 3, 5, Buire, and Bélanger (six of the nine sites; Figure 3.3; Table 3.1). The circular mean in the zones of high correlation indicated an agreement between lepidopteran scales and the percent affected series at Sites 1, 2, 3, 5, and Bélanger (five out of the nine sites; Table 3.1). Phases did vary within the high correlation zones.

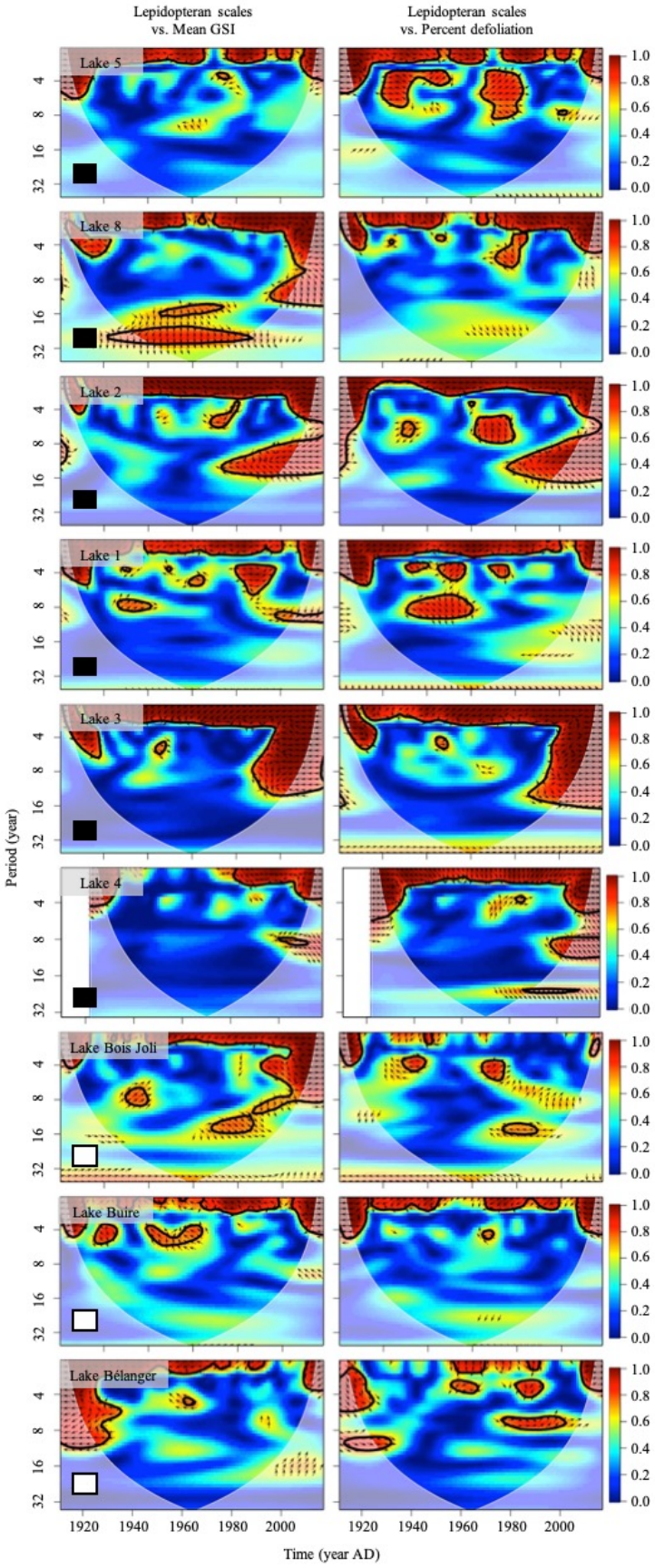
Lepidopteran scales
vs. Mean GSI
Lepidopteran scales
vs. Percent defoliation
Lake 5
Lake 8
Lake 2
Lake 1
Lake 3
Lake 4
Lake Bois Joli
Lake Buire
Lake Bélanger
Period (year)
4
8
16
32
1.0
0.8
0.6
0.4
0.2
0.0
1920
1940
1960
1980
2000
Time (year AD)

Figure 3.3: The power spectra of the wavelet coherence analysis applied to the paleo and dendrochronological records. Warmer colours (*red, orange, yellow*), indicate high common power relative to red noise, an autoregressive process with a lag of 1, whereas cooler colours represent weaker power (Torrence and Compo, 1998). Statistically significant zones of common power were determined using a χ^2 test ($p<0.05$) and are delineated by a thick black line (Torrence and Compo, 1998). The arrows in the areas of statistical significance help specify the type of association. Arrows pointing left indicate that the signals are anti-phase, where a peak of one signal lines up with a trough of the other signal. Arrows pointing right suggest that signals are in-phase, where peaks and troughs of both signals line up. Downward arrows indicate that the scale record leads the tree-ring record by $\pi/2$, whereas upward arrows indicate the opposite. The light grey shading delineates the recommended zone of interpretation, i.e., the cone of influence (Cazelles et al., 2008). Squares in the left-hand corners of the spectra indicate the tree species cored; white, *Picea glauca*; black, *Picea mariana*.

Agreement between both proxies at the individual outbreak level varied between site and depended on the applied analysis (Table 3.1). We observed a more consistent outcome for the wavelet coherence analysis (e.g., Sites 1, 2, 3, 8), although this consistency was site dependent. For example, we found consistent agreement in wavelet coherence between both proxies for all outbreaks at Sites 1, 2, and 3. In contrast, the wavelet coherence for Site 8 showed continual disagreement between both proxies for all outbreaks. Agreement for cross-wavelet analysis at the outbreak level was more variable, and only Lake Bois Joli displayed a constant disagreement between both proxies for all outbreaks (Table 3.1).

3.4.3 Composite chronologies

By creating species-specific composite chronologies, we obtained a clearer signal of spruce budworm impact for both proxies. The *Picea glauca* composite of lepidopteran scale accumulation revealed three relatively distinct peak scale accumulations corresponding to the three 20th century outbreaks (Figure 3.4). The ring-width index revealed three areas of growth suppression with three corresponding peaks in the proportion of defoliated trees. We did observe, however, a consistent 10-year lag between scale and tree-ring records. We only observed large lepidopteran scale accumulations in the *P. mariana* composite from ~2000 AD to 2019 (Figure 3.4). Similarly, the dendrochronological *P. mariana* composite revealed a major growth suppression and an increased percent affected from ~2000 AD to 2019 (Figure 3.4). The signal of the other outbreaks was less obvious for both proxy records (Figure 3.4).

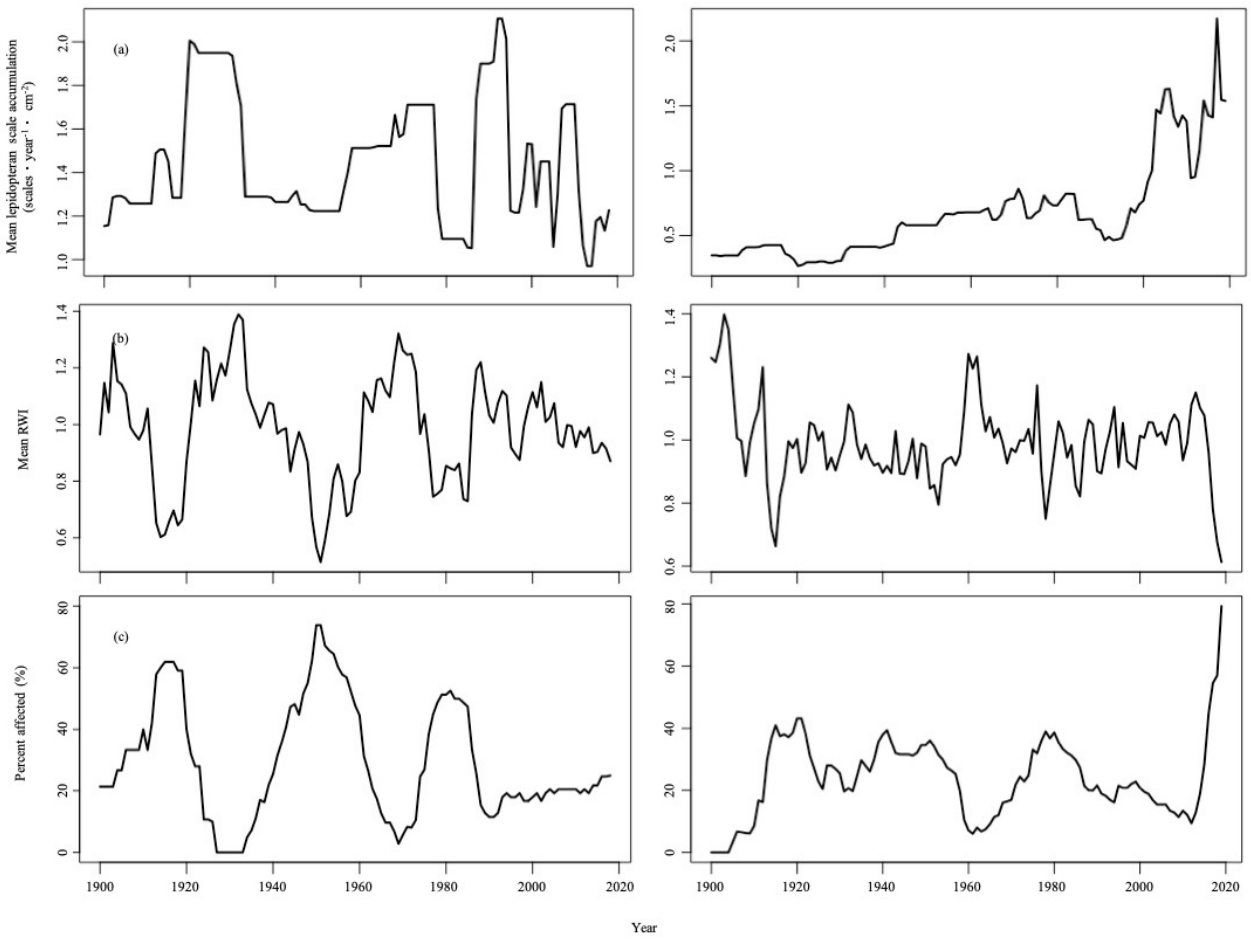

Figure 3.4: The *Picea glauca* and *Picea mariana* composite chronologies of the scale and tree-ring records. The *Picea glauca* (left column) and *Picea mariana* (right column) comprise (a) the mean lepidopteran scale accumulation, (b) the mean ring-width index (RWI), and (c) the proportion of affected trees (percent affected). The *P. glauca* composite incorporates data from three sites. The *P. mariana* composite incorporates data from six sites.

3.5 Discussion

Both the scale and tree-ring records record the impact of spruce budworm defoliation, and the signals are relatively synchronous, validating the use of lepidopteran scales for reconstructing centennial to multi-millennial spruce budworm population fluctuations. Lepidopteran scales are assumed to be a direct measure of the size of the adult moth spruce budworm population as their count represents the changing insect biomass around a lake over time (a stand-level phenomenon), with a greater count at a particular depth reflecting a larger budworm population. This assumption is based on prior knowledge of the insect's biology, including life cycle and development, feeding behaviour and impacts (e.g., Baskerville, 1975; Cooke et al.,

2007 Royama et al., 2005, 2017; Nealis, 2016), and the epidemiology of past outbreaks (e.g., Blais, 1983, 1985b; Morin, 1994; Jardon et al., 2003; Boulanger et al., 2012). In addition to representing changes in adult spruce budworm populations, lepidopteran scale accumulations are correlated with severe annual defoliation (Tremblay, 2022), indicating that greater accumulations may reflect more severe events. However, despite a relatively quick incorporation into the sediment record (Tremblay, 2022), the lepidopteran scale signal is affected by the rate of sediment deposition and mixing both highly variable among lakes, and even within a given lake (Bennett and Buck, 2016). There is also error associated with the dating of the sediment record (e.g., Higuera et al., 2005) producing artificial lags or asynchrony between the sediment record and the tree-ring record.

The tree-ring record, from which the mean GSI and percent affected variables are derived, is an indirect indicator of the spruce budworm presence. Specifically, mean GSI requires the growth records of several individual trees to obtain a mean stand-level growth pattern. An individual tree's reaction, i.e., the production of narrower growth rings, to a defoliation event is nonetheless unique in that multiple contributing factors, such as site conditions (e.g., MacKinnon and MacLean, 2003), species composition (e.g., Su et al., 1996; Campbell et al., 2008; Colford-Gilks et al., 2012; Chen et al., 2019), genetics (e.g., Mageroy et al., 2014; Méndez-Espinoza et al., 2018), age (MacLean, 1984; Krause et al., 2003), and tree height (Reams et al., 1988; Lavoie et al., 2019) can influence the extent, and speed that a tree exhibits growth suppression (e.g., Ericsson et al., 1980; Bauce et al., 1994; Houndode et al., 2021). The reaction and response time thus introduce variation in the mean stand growth to obscure the spruce budworm signal.

The percent affected metric, also based on tree ring widths, reflects the proportion of trees affected by the spruce budworm. More specifically, it is binary; depending on the applied defoliation threshold, a tree is counted as having been defoliated or not (Guiterman et al., 2020). Contrary to the mean GSI, which quantifies the change in the mean stand-level growth over time, percent affected is a coarser measure of the spruce budworm's impact on the stand because it testifies to changes in the proportion of trees considered as defoliated over time (Guiterman et al., 2020). However, both are based on the survivors of past outbreaks and other disturbances. Therefore, these survivors of past defoliation events may not necessarily reflect the true severity of the event (Jardon et al., 2003; Bouchard et al., 2006; Pothier et al., 2012). Moreover, harvesting and wildfires may remove trees that likely recorded a spruce budworm signal. Those remaining

trees tend to be younger and typically less affected by defoliation (MacLean, 1980, 1984; Krause et al., 2003). Finally, the tree species may influence the recorded spruce budworm signal. Defoliation on white spruce is reliably recorded (Blais, 1958, 1962, 1983; Bouchard and Pothier, 2010), whereas the defoliation signal in black spruce may not be as clear (Blais, 1957, 1962) despite their use in reconstructing outbreaks (e.g., Tremblay et al., 2011; Krause et al., 2012). Therefore, it is important to note that although the tree-ring record is more temporally precise than the paleo proxy, recorded annual changes in growth depend on survivors, and incorporate large amounts of variability such that annual changes in local defoliator populations cannot be directly inferred from this record (e.g., Swetnam and Lynch, 1993).

Both the scale and tree-ring records highlighted strong significant return intervals i.e., periodicities, in spruce budworm populations. The strong return interval signal identified by both proxies typically ranged from 16 to 32 years over the study period likely reflects the 20th century return interval of spruce budworm outbreaks that occurred every 30 to 40 years at the landscape scale (Blais, 1983, 1985a; Morin and Laprise, 1990; Jardon et al., 2003; Boulanger and Arseneault, 2004). The similar intervals identified indicate that both proxies detected spruce budworm impacts. A strong lepidopteran scale signal occurred in the latter half of the 20th century but was not observed in the first half. This pattern was evident at most sites, and may be due to little variability in scale accumulations from 1900-1950 which may have been amplified by the interpolation process making it difficult to distinguish peaks from background accumulations in combination with the shortening of the scale record to match the dendrochronological record (Appendix G). Conversely, we observed a strong signal in the dendrochronological data set over the entire study period (1900–2019) for both mean GSI and percent affected. However, the strength, return intervals, and time over which the signal was observed in both the scale and tree-ring records were site dependent. For example, at Site 4 a strong signal is observed in mean GSI and percent affected prior to 1950 but not after 1950, meanwhile we observed a strong signal the scale record after 1950. Conversely, Site Bois Joli displayed a strong signal in both proxy records throughout the study period.

The cross-wavelet analysis also identified zones of strong signal strength (high (significant) common power) at intervals of 16 to 32 years over the study period (1900-2019), suggesting that both proxy records, relative to one another, detect periods of high spruce budworm impact. However, we observed a difference in the strength of overlapping power when comparing lepidopteran scales to the mean GSI instead of percent

affected. Although significant, the weak overlap in power in the mean GSI signal relative to the percent affected signal may be because the accumulation of lepidopteran scales reflects the stand-level phenomenon of insect biomass around a lake. Mean GSI on the other hand, using the mean annual ring width of the stand (Swetnam et al., 1985; Swetnam and Lynch 1989; Guiterman et al., 2020), may introduce more tree-level variability. Although a general pattern may emerge, a fuzzier signal occurs in years when a single tree expresses good growth, and the majority do not. A coarser representation of the spruce budworm impact is derived from the percent affected variable, which relies on a binary approach (defoliated or not) on the basis of predetermined thresholds, to determine the proportion of defoliated trees in a stand (Guiterman et al., 2020). The percent affected variable represents better a stand-level phenomenon. The stronger overlap of high common power between lepidopteran scales and percent affected is therefore likely, as both variables measure the effects at similar spatial scales (i.e., the stand). In contrast, the mean GSI measures the tree-level effects and obtains an average outcome for the stand noting, however, that in this study a non-host correction could not be applied.

Wavelet coherence revealed a significant correlation over a short time period between the scale and tree-ring records, suggesting that the signals were synchronous. This correlation was typically observed at return intervals of four years or less, although the periodicity ranged from 0 to 16 years. Here, the return intervals can be interpreted as the time required for the proxies to record the spruce budworm signal. The zero-to-four-year return interval between the signals likely results from a combination of the time required for scale incorporation into the sediment, potential errors associated with the dating of the sediment core that carry over into the age–depth models for each core (e.g., Higuera et al., 2005), and the lag of two to four years after the onset of an outbreak for defoliation to become apparent in individual trees (Krause and Morin, 1995; Krause et al., 2012). However, we also recorded a significant correlation at longer intervals, and the implications of this remain unclear. A significant correlation at a interval ≥16 years was present in the latter half of the 20th century for sites 2, 3, 4, and 8. These zones of high correlation may result from chance, producing a spurious correlation between the proxy records at longer intervals. Timber harvesting occurred regularly around lakes 2, 3 and 8 in the latter half of the 20th century (Table 3.1 and Appendix G), likely altering host-tree proportion and dictating which individual trees remained onsite creating monotonous signals in both proxies resulting in spurious correlations. For example, the effect of past and current harvesting is well demonstrated within Site 2, as neither individual proxy exhibits a strong signal (zones of significant power). Curiously, the proxies at Site 2 still exhibit a significantly strong correlation, most likely spurious. The correlations of greater than four years observed at Site 4 may stem from the fires within the

site in 1951 and 1985 to produce spurious correlations at these longer periodicities. Therefore, site history can influence the spruce budworm signal recorded by the lepidopteran scales and tree rings to potentially produce variable areas of high power, dampen one or both signals, and ultimately affect detected correlations. Finally noting that strong signals at other return intervals may also be the result of mathematical artifacts such that multiples of a particular return interval may be highlighted. In this case, the biologically relevant 32-year interval would be identified along with the mathematically, but not, biologically relevant intervals of 8 or 16 years.

Wavelet analysis revealed that sedimentary lepidopteran scale and tree-ring records identify spruce budworm outbreaks (both individually and when compared with each other), and their signals are synchronous. The early part of the statement is supported by the presence of areas of high power (red zones; Figures 3.1, and 3.2) that may be significant (thick black line; Figure 3.1, and 3.2) in the individual and cross-wavelet spectra coinciding with the approximately 30-year spruce budworm outbreak cycle (30-year period along the y-axis; Figures 3.1, and 3.2). The latter part of the statement is supported by the presence of areas of high significant power within one to four years in the wavelet coherence spectra (Figure 3.3). The final piece of interpretation involves assessing the phases (arrows in the cross-wavelet and coherence figures; Figures 3.2 , and 3.3 the relationship summarized in Table 3.1) to characterize the relationship between the two proxies. The average directionality of the arrows indicates that both proxy records agree when large lepidopteran scales accumulation coincides with narrow tree rings or when large lepidopteran scale accumulation coincides with a large proportion of affected trees (Table 3.1). However, this agreement between proxies at the outbreak level was highly variable suggesting a complex relationship (Table 3.1).

The signal obtained from the composite chronologies was species-dependent. We observed a clear signal in the *P. glauca* composite with distinct periods of high lepidopteran scale accumulations, growth suppression, and large proportions of defoliated trees. This finding agrees with previous studies that demonstrated white spruce to be a good recorder of spruce budworm outbreak events (e.g., Blais, 1958, 1962; Bouchard and Pothier, 2010), and our recorded periods coincide very well with known outbreak periods of 1912–1929, 1949–1959, 1975–1992 (e.g., Morin and Laprise, 1990; Morin, 1994; Boulanger and Arseneault, 2004; Boulanger et al., 2012). However, there was a consistent 10-year lag between the lepidopteran scale accumulations and the dendrochronological variables, which is likely an artifact of sediment dating errors

(see Higuera et al,. 2005), and possibly also owe to the process of incorporation of lepidopteran scales into lake sediments including bioturbation, erosion redeposition and subaqueous slumping as observed in sedimentary charcoal (see Conedera et al., 2009).

In contrast, the *P. mariana* composite record was not as clear as that for *P. glauca*. We recorded periods of growth suppression around 1915, 1950, and 1980, although the latter two low-growth periods were not very evident. The current outbreak was clear in the composite record. The latter peak coincides with a peak of lepidopteran scale accumulations ca. 2000 to 2019 likely reflecting the current outbreak. Composite chronologies are therefore the most accurate method when interpreting lepidopteran scales at a regional scale because they reduce variability associated with site history and lake-level taphonomical processes and help circumvent the inability of every lake to record every outbreak, as outbreak severity is autocorrelated temporally (Jardon et al., 2003; Bouchard et al., 2006). This is especially important as there does not appear to be a particular suite of site properties, based on the current data used in this study, that govern precise and accurate spruce budworm event reconstructions (Table 3.1).

Our study demonstrated that lepidopteran scales and tree ring-derived variables recorded the impact of 20th-century spruce budworm outbreaks equally well and that the signals obtained from these proxies were (relatively) synchronous. A key takeaway from this study is that using a multi-proxy approach is essential for reconstructing past disturbances. Comparison of proxy records can determine whether events are equally well recorded in time and help better interpret the magnitude of a given event. More importantly, multiple lines of evidence provide a more robust interpretation of past disturbance events because differential recording abilities of the archives and the varying degree of influence by site history. Both lepidopteran scales and tree-ring widths performed equally well in recording the impacts of the spruce budworm, indicating that both proxies are reliable for longer-term reconstructions. As more lakes are sampled and long-term spruce budworm chronologies are obtained from lepidopteran scales, composite scale-tree-ring chronologies offer the best means of assessing the regional impact of the spruce budworm at centennial and millennial scales. Finally, given the current sample size and site information, it is difficult to determine which site properties favour the most precise and accurate reconstructions of spruce budworm populations and thus requires further study.

3.6 Acknowledgements

We thank Dr. Murray Hay for constructive feedback on earlier versions of the manuscript. François Gionest for help in the field, and Marika Tremblay and Guillaume Vigneault for help in the laboratory.

3.7 Funding

The author(s) received funding from the 'Chaire de recherche industrielle CRSNG sur la croissance de l'épinette noire et l'influence de la tordeuse des bourgeons de l'épinette sur la variabilité des paysages en zone boréale'. ^{210}Pb age determination was funded by this.

CHAPTER 4
HOLOCENE RECONSTRUCTION OF THE TWO MAJOR DISTURBANCES IN THE MIXED BOREAL FOREST SUGGESTS A LONG-TERM NEGATIVE INTERACTION

4.1 Abstract

Characterizing millennial and multi-millennial variability in disturbance regimes will be crucial in improving knowledge within the context of a changing climate and the development of sustainable forest management practices in the eastern Canadian mixed boreal forest. The major biotic and abiotic disturbances in the mixed boreal forest are the spruce budworm, and wildfire, respectively. The ability to reconstruct the variability of these disturbance agents under different climate conditions over long time periods will help elucidate the interaction between the agents and their dynamics in the mixed boreal forest. The objective of this observational study was to reconstruct the frequency of large spruce budworm population (LSBP) and wildfire disturbance events, and describe their interaction in the mixed boreal forest over the course of the Holocene within the context of changing vegetation and climatic conditions. Lepidopteran scales and sedimentary charcoal were used to reconstruct the local/extra-local disturbance history from lake sediment along with pollen to reconstruct changes in tree species composition (*Abies:Picea* ratio). Spruce budworm and wildfire disturbance events were determined using the CharAnalysis software. Regime shifts in disturbance event frequencies along with changes in tree composition were detected using Sequential T-test Analysis of Regime Shifts (STARS). Spearman's correlation was used to determine the type of relationship between spruce budworm and wildfire event frequencies. Over the course of the Holocene, 57 LSBP events and 76 wildfire events were detected with event frequencies ranging between 0.75-6.30 events*kyr^{-1} and 1.71-10.5 events*kyr^{-1} respectively. Nine and seven regime shifts in LSBP and wildfire event frequencies were detected respectively, along with two shifts in the *Abies:Picea* ratio. A significant negative correlation was observed between LSBP and wildfire event frequencies at the millennial scale over the course of the entire Holocene except from 1196-196 BP which exhibited a significant positive correlation. The first local lake sediment multi-millennial disturbance regime reconstruction comprising both spruce budworm and wildfire in the mixed forest revealed the potential existence of two disturbance-vegetation feedback loops, and a particular climate-fire-budworm interaction. The significant negative correlation observed between wildfire and LSBP event frequencies suggests a linked disturbance interaction where each disturbance establishes a positive disturbance-vegetation feedback loop that favours itself and inhibits the occurrence of the other. Further, rapid climate change events may act as a key trigger in establishing the respective disturbance-vegetation feedback loops.

4.2 Introduction

Within the context of increasing variability in temperature and precipitation (Easterling et al., 2000), the effects of forest disturbances are expected to be exacerbated (Dymond et al., 2010; Millar and Stephenson, 2015; McDowell et al., 2020). Greater tree mortality is likely to result from forest disturbances acting synergistically with other drivers (Allen et al., 2010, 2015; Hart et al., 2014, 2017; De Grandpré et al., 2019). Warming temperatures may create conditions favourable to more frequent fire by increasing ignition rates through greater fuel availability which is expected to result in more intense and/or severe fires (Westerling et al., 2003, 2006, 2011; Flannigan et al., 2009, 2013). Similarly, warming temperatures have the potential of favouring insect development and overwintering survival (Ayres and Lombardo, 2000; Berg et al., 2006; Bentz et al., 2010), resulting in larger populations and more severe insect outbreaks (Murdock et al., 2013; Weed et al., 2013), noting however, that during diapause prolonged periods of warm temperatures may negatively affect survival (Régnière et al., 2012). Moreover, in response to such changes in temperatures, distribution of insect outbreaks may shift into historically novel habitats in response to a changing climate (Jepsen et al., 2008, 2011; Régnière et al., 2012; Erbilgin et al., 2014), and/or result in feeding on host species that were formerly protected due to phenological asynchronies (Pureswaran et al., 2015, 2019; Fuentealba et al., 2017). Given the uncertainty surrounding disturbance regime behaviour under current climatic variability, potential analogs may be found by looking to past climate shifts and their effects on disturbance regimes.

The Holocene is a geological epoch that spans from roughly 11,700 years ago to the present (just after the preindustrial era) that experienced 3 major climate periods: the Early Holocene (EH; 11,700 BP-7000 BP; before present, present refers to the year 1950), the Holocene Thermal Maximum (HTM; 7000-4200 BP), and the Neoglacial (4200 BP- present) (Walker et al., 2012; Wanner et al., 2015; Shuman and Marsicek, 2016). Pre-7000 BP conditions were generally dry (Lavoie and Richard, 2000; Muller et al., 2003; Shuman and Marsicek 2016), and temperatures rapidly increased (Wanner et al., 2015; Zhang et al., 2016., 2017; Neil and Gajewski 2018). Following the collapse of the Laurentian Ice Sheet (Renssen et al., 2009; Marcott et al., 2013), and despite moisture variability (Lavoie and Richard 2000; Muller et al., 2003; Viau and Gajewski, 2009), the warm stable temperatures of the HTM (Viau and Gajewski, 2009; Shuman and Marsicek 2016; Neil and Gajewski 2018), favoured prompt postglacial vegetation recolonization (Blarquez and Aleman 2016). The last period was generally humid (Lavoie and Richard, 2000; Muller et al., 2003;

Shuman and Marsicek 2016) and underwent cooling (Wanner et al., 2008, 2011; Marsicek et al., 2018) but encompassed a brief dry period of warming (Medieval Climate Anomaly 1000-700 BP; MCA) and cooling (Little Ice Age 550-250 BP; LIA; Mann et al., 2009; Viau et al., 2012; Lafontaine- Boyer and Gajewski, 2014) ending with a rapid rate of warming (Renssen et al., 2012). Within these major climate periods, punctual rapid significant climate change events occurred (Mayewski et al., 2004; Wanner et al., 2011), associated with ice raft debris events (Bond et al. 1997, 2001; outbursts of freshwater), that likely affected changes in oceanic (Broecker, 1997, 2003; Törnqvist and Hijma 2012) and atmospheric circulatory patterns (Smith et al., 2016; Deininger et al., 2017) likely altering climate conditions in Europe and eastern North America affecting vegetation (Viau et al., 2002, 2006; Pàl et al., 2018) and wildfire (Florescu et al., 2019). The Holocene, given its past climate variability, therefore, is an appropriate period to study potential changes in disturbance regime behaviour.

Currently, the mixed boreal forest of Québec is dominated by two major forest disturbances: the spruce budworm and wildfire. The spruce budworm [*Choristoneura fumiferana* Clemens] is a native lepidopteran defoliator and is the major biotic disturbance in the mixed boreal forest (MacLean, 2016; Nealis, 2016; Pureswaran et al., 2016). As a larva, the spruce budworm preferentially feeds on current year's needles of mature balsam fir [*Abies balsamea* (L.) Mill], its primary host, also feeding on older needles when necessary (Piene, 1989) along with the needles of secondary hosts (Hennigar et al. 2008). Severe defoliation can result in tree mortality especially in balsam fir (MacLean, 1980, 1984; MacLean and Ostaff 1989), resulting in the formation of canopy gaps favouring the regeneration of balsam fir (Kneeshaw and Bergeron, 1996, 1998, 1999), along with its establishment in the canopy from preestablished seedlings and/or saplings (Bouchard et al., 2005, 2006, 2007). Incidentally, a greater proportion of balsam fir in a stand will also engender a greater probability of spruce budworm outbreaks, thereby establishing a positive disturbance-vegetation feedback loop (Baskerville, 1975; Morin, 1994) leading to episodic outbreaks (Cooke et al., 2007; Nealis 2016). This feedback loop has likely existed since the postglacial recolonization of the landscape by balsam fir (Simard et al., 2002, 2006, 2011; Navarro et al., 2018b).

Wildfire is the major abiotic disturbance in the mixed boreal forest. Climate and fuels play a substantial role in modulating wildfire disturbance regimes (Macias Fauria et al., 2010; Ali et al., 2012; Blarquez et al., 2015). Climate is described as a top-down control affecting ignition, fire spread, and intensity by influencing

fuel combustibility through temperature and humidity (Wotton et al., 2010; Woolford et al., 2014; Molinari et al., 2018). Long-term climate will influence fuel availability in the form of biomass, where in drier areas there is less vegetation and thus less fuel to burn, while in moister, more productive areas there is the possibility of greater fuel accumulation (Littell et al., 2016; He and Lamont, 2018; McLauchlan et al., 2020). Further, climate will influence the species composition (i.e., proportion of coniferous and deciduous trees) of an area which can in turn affect subsequent burning (Hély et al., 2000, 2020; Girardin et al., 2013; Blarquez et al., 2015), while burn frequency and severity can also dictate which plant species will be present due to differential species regeneration strategies and requirements (Burns and Honkala, 1990; Keeley et al., 2011; Pausas, 2015). Therefore, there is the potential for the establishment of a positive feedback loop; fire-tolerant species may facilitate fuel structures that favour fire in the stand (e.g., lodgepole pine or black spruce; Rogers et al., 2015; Lamont et al., 2020), and the act of burning at particular frequencies then favours the establishment and propagation of the fire-tolerant species (Dantas et al., 2016; Harrison et al., 2021). In the mixed boreal forest, stand composition will generally be dominated by deciduous species following wildfire (Bergeron, 2000; Couillard et al., 2021), however this is dependent on wildfire event frequency or time since last fire, along with the surrounding composition.

In addition to potentially forming their own disturbance-vegetation feedback loops, these two major forest disturbances are able to interact with one another through forest legacies such as changes in forest composition and structure (Buma and Wessman, 2011, 2012, 2013; Buma 2015). Generally, disturbance interactions can be categorized as being linked or compound (Simard et al., 2011; Kleinman et al., 2019; Burton et al., 2020). A linked disturbance interaction implies that the preceding disturbance alters stand structure and/or composition in such a way that the occurrence, extent, frequency and/or severity of the subsequent disturbance is affected (Simard et al., 2011). For example, the fuel structure and ensuing fire severity of a bark beetle infested stand is modulated by the time since the outbreak (Page and Jenkins, 2007a,b; Simard et al., 2011; Hicke et al., 2012). Similarly, insect defoliation occurring in dry coniferous forests limits available fuel and will reduce fire severity (Lynch and Moorcroft, 2008; Cohn et al., 2014). Alternatively, a compound disturbance interaction generally involves two disturbances occurring simultaneously or in quick succession having a greater effect together than each disturbance acting on its own (Paine et al., 1998; Simard et al., 2011). A clear example is the tree mortality resulting from a drought shortly followed by an insect outbreak (Hart et al., 2014, 2017; De Grandpré et al., 2019), or the severity of a fire preceded by a drought (Flannigan et al., 2013; Jolly et al., 2015; Millar and Stephenson, 2015). In the mixed boreal forest, the spruce budworm and wildfire appear to exhibit a linked disturbance interaction.

Over short time-scales, defoliation alters fuel structure in a manner increasing fire hazard (Stocks, 1987; Watt et al., 2018, 2020), fire occurrence (Fleming et al., 2002; Candau et al., 2018), and fire risk (James et al., 2017), meanwhile over decades to centuries, the relationship appears to be antagonistic by decreasing the availability of live ladder fuels (Sturtevant et al., 2012). Similarly over millennia, the interaction also appears to be negative, where one disturbance would inhibit the other (Navarro et al., 2018b) although the mechanisms behind the interactions have not yet been investigated.

Understanding past variability in disturbance regimes and their interactions given different climate phases and events during the Holocene will be key in elucidating the past disturbance dynamics of the mixed boreal forest ecosystem. For example, wildfire or spruce budworm events may predominately affect the mixed boreal forest under certain climate and/or vegetation conditions revealing information about possible system thresholds (Scheffer et al., 2001; Scheffer et al., 2012). Identifying such thresholds help characterize the forest's ecosystem state landscape (Scheffer and Carpenter, 2003) and potentially reveal factors that may move the ecosystem within this landscape and/or shape this state landscape (Scheffer et al., 2003; Van Nes et al., 2007; Scheffer and Van Nes, 2007). Furthermore, rapid significant climate change events such as Bond Events (Bond et al., 1997, 2001; Mayewski et al., 2004) may modulate disturbance regimes as observed in changes in sedimentary charcoal accumulations and fire frequency in Europe (Florescu et al., 2019), or alter vegetation (Pàl et al., 2018) with the potential of changing the interaction between disturbances. Therefore, the long-term reconstruction of past disturbance regime variability may provide insights and reveal conditions that could serve as potential analogs helping guide current and future forest management decisions and practices (Swetnam et al., 1999; Landres et al., 1999; Hennebelle et al., 2018).

The purpose of this observational study is to reconstruct the variability in frequency of wildfire and large spruce budworm population (LSBP) disturbance events in the mixed boreal forest over the course of the Holocene, and to characterize the long-term interaction between the two agents within the context of potentially changing vegetation and incursions of rapid significant climate change events. In the mixed boreal forest, following postglacial recolonization by balsam fir, it is expected that the spruce budworm will be the dominant disturbance due to the near constant availability of host-trees, and the subsequent implementation of a positive feedback between the insect and its host; presence of host-trees favour spruce budworm outbreaks, and spruce budworm outbreaks create favourable conditions for host-tree regeneration

and establishment in the canopy. However, prior to the arrival of balsam fir, wildfire is expected to be the dominant disturbance in the mixed boreal forest; tree species composition prior to the establishment of balsam fir is expected to be more fire-tolerant (Blarquez et al., 2015; Blarquez and Aleman, 2016), and therefore promote more fire-prone conditions (Hély et al., 2000, 2010, 2020; Girardin et al., 2013). Further, cooler and drier conditions are expected to favour the implementation of the wildfire disturbance-vegetation feedback loop as such conditions have led to greater fire frequency during the Holocene (Carcaillet et al., 2001a) while likely negatively affecting insect development and survival (Ayres and Lombardo, 2000; Bentz et al., 2010) reducing LSBP events. Finally, an inverse relationship, or negative correlation between the two disturbance agents at millennial and multi-millennial time-scales is expected (e.g., Navarro et al., 2018b) due to 'competition' for a limited and changing resource i.e., tree species biomass will vary through time.

4.3 Methods

4.3.1 Site description and field sampling

Lake Buire (48.16540°N, -70.57077 °W) is a small lake 1.3 ha in size, ca. 3.4 m deep with limited inflow and outflow. It is found in the *Abies balsamea-Betula papyrifer*a bioclimatic zone (Rowe, 1972; Saucier et al., 1998; Saucier et al., 2009) at 244 m asl, surrounded by rolling terrain, and is in an area that has sustained heavy spruce budworm defoliation (≥75%) from 1974–1984 and from 2016 to the time of sediment sampling (fall 2018; MFFP 2021a). The stand composition around the lake at the time of sampling, in decreasing order of relative abundance, consisted of: trembling aspen [*Populus tremuloides* Michx.], paper birch [*Betula papyrifera* Marshall], balsam fir [*Abies balsamea* (L.) Mill], black spruce [*Picea mariana* (Mill.) Britton, Sterns & Poggenburg], white spruce [*Picea glauca* (Moench) Voss], and yellow birch [*Betula alleghaniensis* Britt.] (MFFP 2021b). The sediment column of lake Buire was sampled by using a gravity corer (Renberg, 1991; Renberg and Hansson, 2008), and a modified Livingstone corer (Wright Jr. et al., 1984) to obtain, respectively, the lake-sediment interface, and the remainder of the column as overlapping 1 m segments. The latter were wrapped in Saran Wrap™ and placed in ABS plumbing tubes for transport and storage. Sediment from both core types were sampled at a 1 cm resolution. This was done in the field for the gravity corer segments while the Livingstone segments were divided in the laboratory. All samples were stored at 4°C until they were ready for processing.

4.3.2 Sediment core chronology, composition, and forest composition

The chronological framework of the sediment core was determined using a combination of ^{210}Pb and radiocarbon (^{14}C) dates to most accurately reconstruct the recent (last 150 years or so) and deep site history (thousands of years), respectively. ^{210}Pb activity measurements at 6 depths (0-1, 2-3, 5-6, 9-10, 14-15, and 24-25 cm) in the top 25 cm, of the gravity core was obtained by Flett Research Ltd (Winnepeg, MN, Canada) from which an age-depth model was derived using the Constant Rate Supply model (Appleby and Oldfield, 1983; Binford, 1990). Macrofossils (leaves, needles, and seeds of terrestrial vegetation) were extracted at 50 cm intervals along the entire sediment profile and sent to the Radiocarbon Laboratory of the André E. Lalonde AMS Laboratory at the University of Ottawa (Ottawa, ON, Canada) to obtain ^{14}C dates. Radiocarbon dates and ^{210}Pb dates were combined in the *rbacon* package (Blaauw and Christen, 2011; Blaauw et al., 2021) in the R environment (R core Team, 2021) to derive an age-depth model for the core.

In addition to establishing a chronological framework, core composition along with the successional context of the forest surrounding the lake was determined. Magnetic susceptibility of the sediment along the entire core profile was conducted using the Bartington MS2 System (Dearing, 1999). Magnetic susceptibility helps distinguish between organic and inorganic matter aiding in the identification of any run-off, erosion, flooding or sediment mixing events (Thompson et al,. 1975; Dearing and Flower, 1982; Da Silva et al., 2015). Values will typically fluctuate between 1 and -1 (SI units) where higher positive values indicate a higher proportion of inorganic material present in the sediment while slightly negative values or those occurring around 0 suggests that the core is composed of organic matter (Dearing, 1999). The successional context of the forest was determined by extracting and identifying arboreal pollen found in 1 cm^3 from the 1 cm core slices corresponding to an approximately 100-year sampling interval (Appendix H). Pollen extraction and identification was done using standard procedures (Faegri and Iversen, 1989) at l'Université de Montréal Palynology service laboratory. The ratio between the percent of *A. balsamea* pollen and *P. mariana* pollen was calculated at each corresponding 100-year interval. Both the magnetic susceptibility and pollen extraction and identification were done in an effort to better interpret the potential changes in disturbance regimes and their interactions through time.

4.3.3 Charcoal and lepidopteran scale sample preparation and processing

Two 1 cm^3 punches ('subsamples' from herein) were extracted from each 1 cm slice along the core profile for lepidopteran scale, and charcoal analysis. Charcoal subsamples were placed in bleach (10% NaOCl) for a period of at least 24 hours to deflocculate the sediment and to facilitate charcoal particle identification relative to organic matter (Blarquez et al., 2010). The subsamples were sieved using a 150 µm mesh, attempting to retain charcoal remains from local fires (Clark and Royall, 1995; Clark et al., 1996, 1998; Carcaillet et al., 2001b; Higuera et al., 2007). The retained charcoal remains were identified under a dissecting microscope coupled with a camera. The charcoal surface area (mm^2) in each subsample was quantified in the WinSEEDLE software (Regent Instruments Canada Inc. 2019).

Lepidopteran scale sample preparation followed a modified protocol from Navarro et al., (2018a). The subsamples were deflocculated in 20% KOH at 17 psi and 121°C for 30 minutes in a steam sterilizer (Amsco unit by Steris), wet sieved using a 53 µm mesh and the retained sediment put into 50 mL centrifugation tubes. Twenty millilitres of sucrose solution (relative density: 1.24) was added to the tubes, and these were centrifuged at 4500 rpm for 20 minutes at 21°C. The supernatant from each tube was removed and discarded while 25µL of 1% lactophenol cotton blue stain was added to the pellet in order to facilitate scale identification before being mounted on microscope slides for subsequent counting of the scales at 10X objective magnification (Tremblay, 2022).

4.3.4 Charcoal and lepidopteran scale event identification

The CharAnalysis software and procedure (Higuera, 2009; Higuera et al., 2010) was used to reconstruct periods of large adult spruce budworm populations and wildfire history over the course of the Holocene. The raw accumulation rates were interpolated to a constant time-step using the median sampling resolution (C_{int}). From the interpolated accumulation rates (C_{int}) the background accumulation rates (C_{back}) were determined using a LOWESS robust to outliers with a 500-year smoothing window to differentiate between the low and high frequency signals. The high frequency signal (C_{peak}) was isolated by subtracting the background accumulation rates (C_{back}) from the interpolated accumulation rates (C_{int}). Noise (C_{noise}) found within the high frequency signal was estimated using a Gaussian mixture model (Gavin et al., 2006; Higuera et al., 2010), and in an effort to remove this leftover noise that could result from sediment mixing (C_{noise}), a local threshold, within a 500-year window and using the 99^{th} percentile, was applied to identify lepidopteran

scale and charcoal peak events (C_{fire}). The peak events (C_{fire}) were subjected to a 'minimum count criterion' (Higuera et al. 2010), which determined whether two peaks were in fact two individual events, or if the two peaks originated from the same event. Finally, spruce budworm and wildfire peak event frequencies (number of events/1000 years) were calculated and then smoothed using a LOWESS with a 500-year window.

The 500-year smoothing window used to determine background accumulation rates, local thresholds, and smoothing of peak frequency was applied to both disturbances for comparability between disturbances and among studies. Background accumulation rates have typically been estimated using roughly 3 times the disturbance's return interval (Carcaillet et al., 2009; Blarquez et al., 2010). The spruce budworm outbreak return interval in recent history has been 30 to 40 years in the mixed boreal forest (Blais, 1983, 1985a; Morin and Laprise, 1990; Boulanger and Arseneault, 2004) which would result in an approximately 100-year smoothing window, while the fire return interval in *Abies balsamea-Betula papyrifera* type ecosystems appears to be around 300 years based on the estimates of Frégeau et al., (2015), Couillard et al., (2013), and Couillard et al., (2021) which would yield a smoothing window of approximately 900 years. However, to apply a robust local threshold to estimate spruce budworm events, a window of around 400 years would have been required to include at least 30 samples (Higuera et al., 2010). Finally, preliminary analyses revealed that the 500-year window-width yielded the highest Signal-to-Noise Ratio and Goodness of Fit values where shorter or longer widths yielded less conservative or more conservative event estimates respectively. Therefore, the 500-year window-width used in this study is a trade-off between biological and statistical considerations, and allows for a comparison with the results obtained by Navarro et al., (2018b).

4.3.5 Charcoal and lepidopteran scale regime shift analysis

Sequential T-test Analysis of Regime Shifts (STARS; Rodionov, 2004; Rodionov and Overland, 2005; Rodionov, 2006) was used to detect any changes in the observed disturbance event frequencies and vegetation composition over the course of the Holocene in the R environment (R core team, 2021). Prior to this analysis peak spruce budworm and wildfire event frequencies were estimated using a Gaussian kernel density function, that was bootstrapped with 1000 replicates, with a 200-year window width while applying a correction for edge bias (Mann, 2004; also see Mann, 2008) with the *kdffreq* function in the *paleofire* R package (Blarquez et al., 2014), based on the events identified by CharAnalysis. The 200-year window was

selected as it was the best compromise between retention of variance and number of samples used to calculate the frequencies within the window (Appendix I). A 200-year cut-off was applied at the beginning and the end of the chronology in order to remove any edge effects that could affect subsequent analysis.

The STARS method was used to identify change points in the respective disturbance event frequency and pollen accumulation time series over the course of the Holocene by comparing each observation to the previous observations and determining whether a regime shift has occurred (Rodionov, 2004; Stirnimann et al., 2019; details in Appendix J). This analysis was done using a running window of specified width, *l*, within which a Student's t-test was performed determining whether the new observation was part of a new regime or not (Rodionov, 2004; Stirnimann et al., 2019). A potential change point, *c*, was identified when the mean value of the new regime exceeded the range established by the old regime (Rodionov, 2004; Rodionov and Overland, 2005). If the cumulative sum of the normalized deviations, the Regime Shift Index (RSI), at each potential change point remained positive then a regime shift was detected, and the opposite was true if the RSI became negative (Rodionov 2004; Rodionov and Overland 2005).

The *rstars* function (Stirnimann et al., 2019) was applied to each disturbance regime peak frequency time series along with the ratio between balsam fir and black spruce pollen accumulations (*Abies:Picea* ratio) using a window-width representing 1001 and 1000 years respectively. The window-width was selected to be large enough to encompass successional turnover based on the lifespan of the trees found in the mixed boreal forest, typically living no longer than approximately 300 years in the case of balsam fir and black spruce (Burns and Honkala, 1990; Bergeron, 2000), while also remaining short enough to fit within the main known climate periods of the Holocene i.e., the EH, HTM, and Neoglacial which encompassed the MCA, and the LIA, and pre-industrial era (Walker et al., 2012). Neither of the disturbance event peak frequencies nor the *Abies:Picea* ratio time series were prewhitened as the disturbance series were obtained from the rigorous procedure applied in CharAnalysis, while for the pollen series, using the Inverse Proportionality with 4 corrections (IP4 method) yielded exactly the same result as an analysis without prewhitening (Appendix K). The significance level (α) used to test the RSI was 0.05, and Huber's weight parameter was in all time series was set to 1.

Finally, Spearman correlations between spruce budworm and wildfire event frequencies smoothed with a 200-year window were conducted to quantify the interaction between the two disturbances over the course of the Holocene. These correlations were conducted in 1000-year blocks as opposed to a running window to remain consistent with the above-mentioned analyses. Additionally, the 1000-year blocks allowed to indirectly observe the effects of the different climate periods on disturbance interactions. Significant correlations were determine using a significance level of 0.05

4.4 Results

4.4.1 General core characteristics and CharAnaysis output

The Buire sediment core was 762 cm in length dating to just over 8600 cal yr BP (Figure 4.1). Analysis was restrained to the top 751 cm (340-1080 cm) due to the inversion at the bottom of the core (Table 4.1; Figure 4.1). Sediment accumulation rate was relatively constant at approximately 10 $yr*cm^{-1}$, and consisted of homogeneous gyttja (organic sediment); magnetic susceptibility values oscillated around 0 except at ~1010 cm at a somewhat gradual gyttja-clay transition where values were greater than 1.

Table 4.1: The sampling interval and associated dates (cal. year BP ± standard deviation) used to construct the age-depth model for Lake Buire

Lab ID	Depths (cm)	Dated material	^{210}Pb cal. year BP/ ^{14}C yr BP	±	cal. BP (associated probability)
^{210}Pb	340-341	Bulk sediment	-68	3	-
^{210}Pb	359-360	Bulk sediment	151	12	-
UOC-8707	407-413	Organic macrofossils	528	20	610-621 (5.4%) 515-555 (90.0%)
UOC-8708	498-502	Organic macrofossils	998	21	905-961 (85.1%) 830-855 (9.1%) 804-809 (1.2%)
UOC-8709	585-595	Organic macrofossils	2519	28	2679-2742 (29.3%) 2608-2641-(15.0%) 2492-2600 (51.1%)
UOC-8710	678-682	Organic macrofossils	3126	23	3324-3397 (72.4%) 3252-3295 (23.0%)
UOC-8711	766-774	Organic macrofossils	3794	25	4117-4146 (8.0%) 3975-4097 (87.4%)
UOC-8712	858-862	Organic macrofossils	4590	27	5401-5448 (28.1% 5389-5392 (0.2%) 5282-5328 (57.0%) 5137-5162 (5.7%)
UOC-8713	948-952	Organic macrofossils	5685	27	6405-6535 (95.4%)
UOC-8714	1036-1044	Organic macrofossils	7467	44	8191-8375 (95.4%)
UOC-8715	1095-1102	Organic macrofossils	4978	28	5829-5856 (4.6%) 5642-5750 (88.6%) 5614-5630 (2.2%)

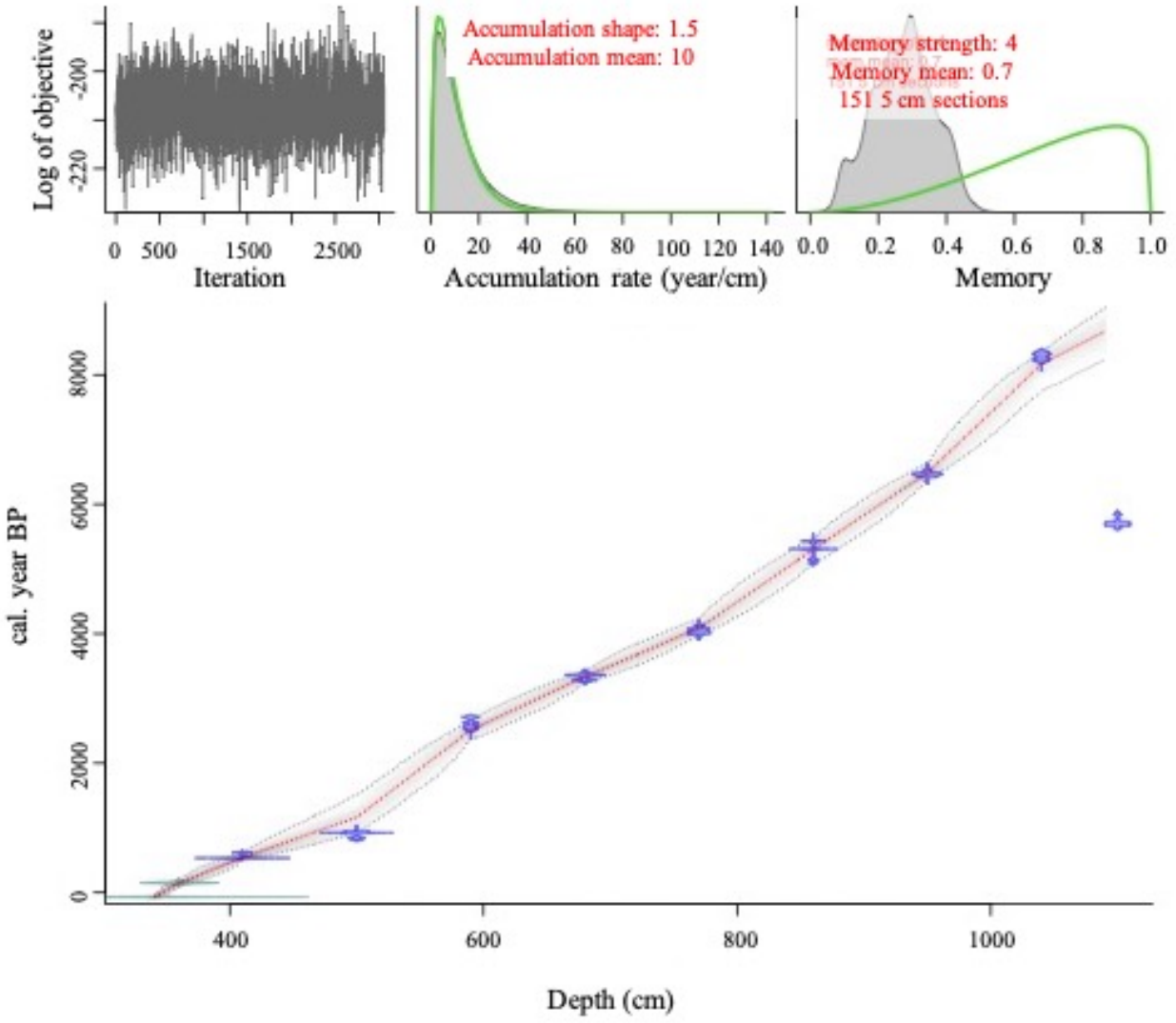

Figure 4.1: The age-depth model (*red line*) with 95% confidence interval (*grey shading*) and associated characteristics for Lake Buire obtained from the *rbacon* package (Blaauw et al. 2021). The estimated age-depth model (*main panel*) where the green and blue points indicate the sampling locations of the ^{210}Pb and radiocarbon dates, respectively, along with their associated estimated errors. Marko Chain Monte Carlo (MCMC) simulations (*upper left panel*) are shown where no visible trend in the distribution is ideal. Accumulation shape (*top centre panel*) takes on a gamma distribution (*green line*) with the shaded portion depicting the modelled accumulation of the core. Memory (*top right panel*), determines the autocorrelation between depths using a beta distribution (*green line*) where a lower memory suggests a more variable accumulation rate over time (Blaauw and Christen 2011).

The CharAnalysis procedure detected 57 lepidopteran scale events over the course of the study period (Figure 4.2), however one outlying observation in this time series was removed prior to the analysis as it was an abnormally high accumulation (Appendix L). The frequency of lepidopteran scale events varied

between 0.75 events*kyr^{-1} and 6.30 events*kyr^{-1} occurring at 7225 BP and 4706 BP, respectively. A total of 76 fire events were detected using the CharAnalysis procedure (Figure 4.2). The frequency of charcoal events varied between 10.5 events*kyr^{-1} and 1.71 events*kyr^{-1} occurring at 8655 BP and 7841 BP, respectively. Prior to approximately 6000 BP wildfire event frequency was generally greater than lepidopteran scale event frequency, however, after this date an oscillation between the disturbance event frequencies is observed (Figure 4.2).

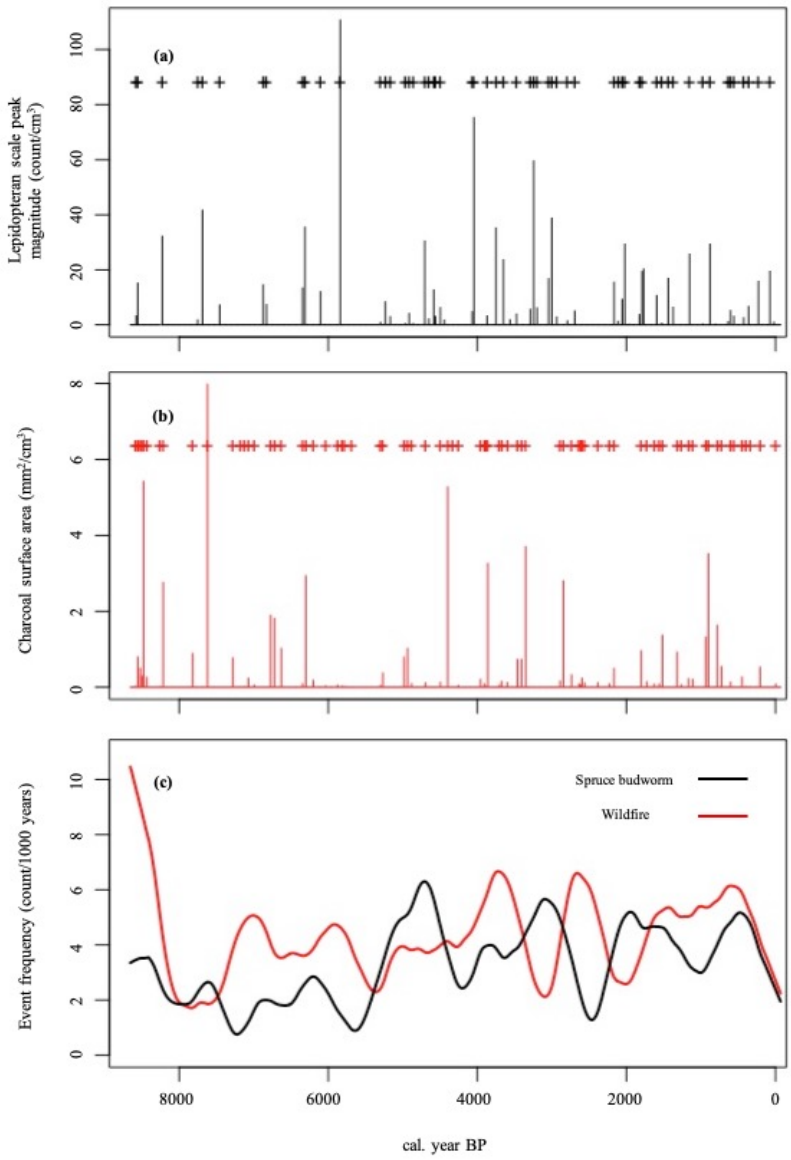

Figure 4.2: Disturbance event magnitude and frequency obtained from CharAnalysis using a 500-year smoothing window. Each identified peak (+; diamonds above the respective accumulations) exceeded the low frequency signal (C_{back}) and the 99th percentile local threshold applied to the high frequency signal

(C_{peak}). (a) Spruce budworm event peak magnitude; (b) wildfire event peak magnitude; (c) disturbance event frequencies.

4.4.2 Detected regime shifts and the interaction between the spruce budworm and wildfire

Multiple regime shifts (i.e., changes in mean) were detected in spruce budworm and wildfire event frequencies along with the *Abies:Picea* ratio over the course of the Holocene. Nine shifts in mean spruce budworm event frequency were detected, while seven shifts in mean wildfire event frequency were detected (Figure 4.3). Finally, two regime shifts were detected in the *Abies:Picea* ratio (Figure 4.3). One occurred at approximately 6000 BP where there was an increase in the mean ratio, and another shift occurred at around 3500 BP with a decrease in the mean ratio. Further, the regime shift in the *Abies:Picea* ratio at roughly 6000 BP roughly coincides with particularly large shift in spruce budworm event frequency (Figure 4.3).

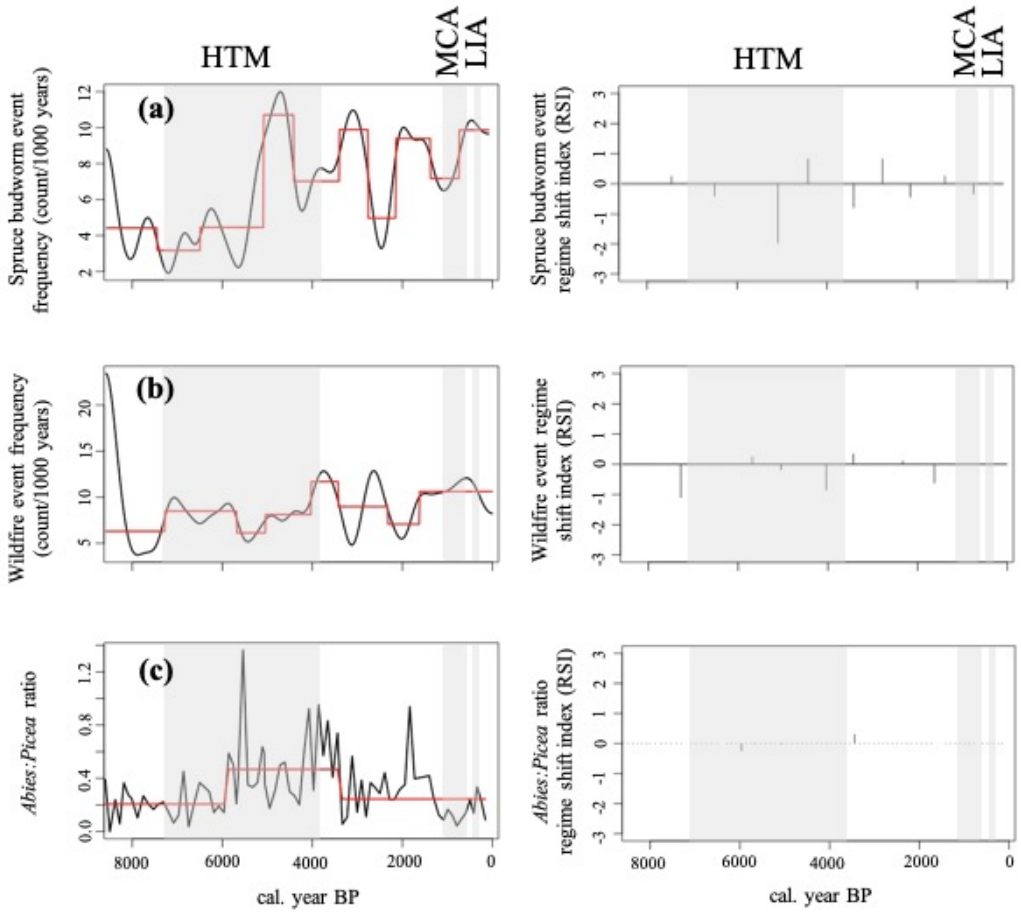

Figure 4.3: The Sequential T-Test Analysis of Regime Shifts (STARS) output for Lake Buire's spruce budworm event and wildfire event frequencies, and *Abies:Picea* ratio over the course of the Holocene. The

reconstructed disturbance event frequency (*black line*) and mean (*red line*) with corresponding Regime Shift Index and regime shifts (*bars*) for (a) the reconstructed spruce budworm event frequency, (b) the reconstructed wildfire event frequency, and (c) the *Abies:Picea* ratio. Some of the known climatic phases are identified: the Holocene Thermal Maximum (HTM), Medieval Climate Anomaly (MCA), and the Little Ice Age (LIA).

A significant negative correlation was identified between spruce budworm and wildfire event frequencies over the majority of the Holocene (Table 4.2; Figure 4.4). A significant positive correlation (Table 4.2) was observed between the two disturbances in the most recent portion of the chronology from 1196-196 BP where both disturbance event frequencies displayed similar trends (Figure 4.4). The remainder of the Holocene exhibited a negative correlation with the most negative correlation occurring from 3196-1196 BP and the least negative correlation occurring in 6196-5196 BP (Table 4.2).

Table 4.2: Spearman correlations conducted at a 1000-year interval between the spruce budworm and wildfire event frequencies for Lake Buire from 8186-196 cal. year BP. Correlations in italics indicate a significant correlation using an alpha value of 0.05

Period (cal. year BP)	Spearman's correlation (rho)	p-value
1196-196	*0.43*	<0.0001
2196-1196	*-0.73*	<0.0001
3196-2196	*-0.73*	<0.0001
4196-3196	*-0.23*	0.0271
5196-4196	*-0.54*	<0.0001
6196-5196	*-0.21*	0.0476
7196-6196	*-0.48*	<0.0001
8196-7196	*-0.68*	<0.0001

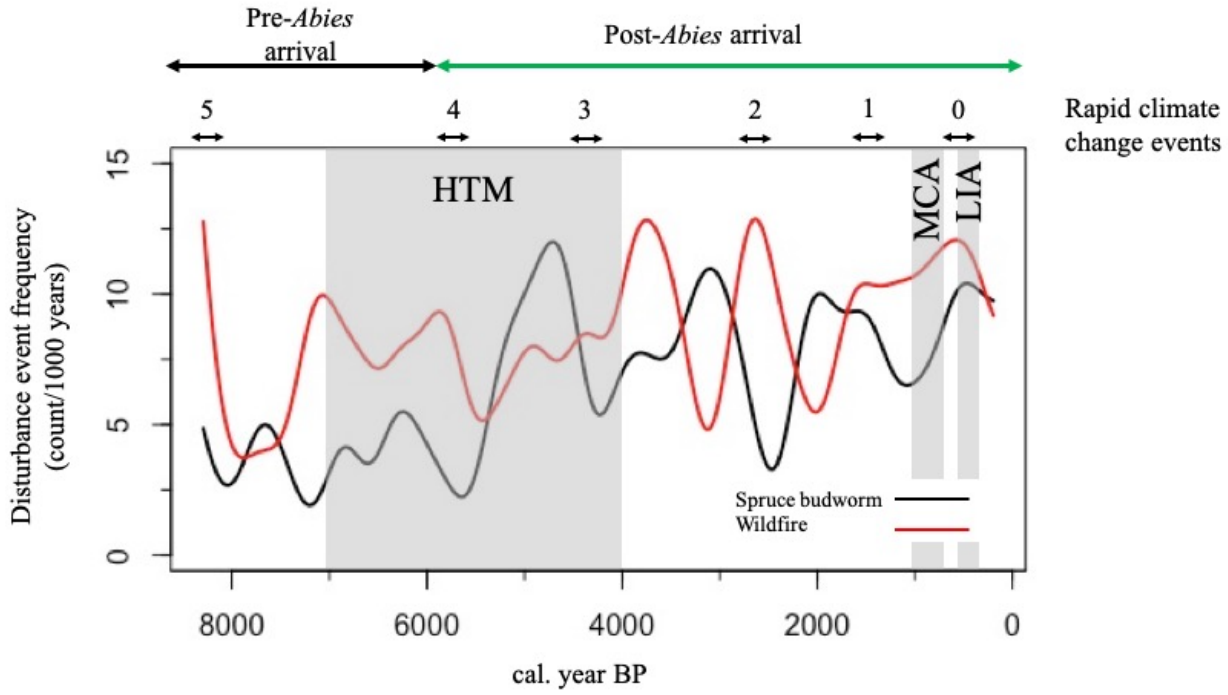

Figure 4.4: Variability in disturbance event frequencies over the course of the Holocene. Some known climatic phases are identified: The Holocene Thermal Maximum (HTM), Medieval Climate Anomaly (MCA), and the Little Ice Age (LIA). Further, the approximate timing of the postglacial recolonization arrival of *Abies balsamea* is identified along with approximate periods of inferred rapid significant climate change events.

4.5 Discussion

To the authors' knowledge, this is the first local multi-millennial spruce budworm and wildfire event reconstruction observing their long-term interaction in the mixed boreal forest of central Québec, Canada spanning the different climate phases of the Holocene using lepidopteran scales and sedimentary charcoal. The mixed boreal forest around Lake Buire appears to exhibit two distinct regimes: a wildfire or spruce budworm dominated regime. These can be visually represented by an ecosystem state landscape (see Scheffer and Carpenter, 2003) where the ecosystem, Lake Buire is depicted as a ball, that sits in one of two valleys or basins of attraction corresponding to an ecosystem dominated by a wildfire disturbance regime or as an ecosystem dominated by a spruce budworm disturbance regime (Figure 4.5). The hypothesis that the mixed boreal forest shifted from being wildfire dominated to dominated by the spruce budworm following the increase in abundance of balsam fir on the landscape around 6000 BP was not supported (Figure 4.5). Instead, following the increased balsam fir abundance, the ecosystem around Lake Buire oscillated between the two aforementioned basins, a phenomenon that has not been previously observed in

other ecosystems such as the boreal black spruce forest (Navarro et al., 2018b). The oscillatory behaviour is best illustrated by the change in disturbance frequencies throughout the Holocene and the many detected regime shifts (Figure 4.3; Figure 4.4; Figure 4.5).

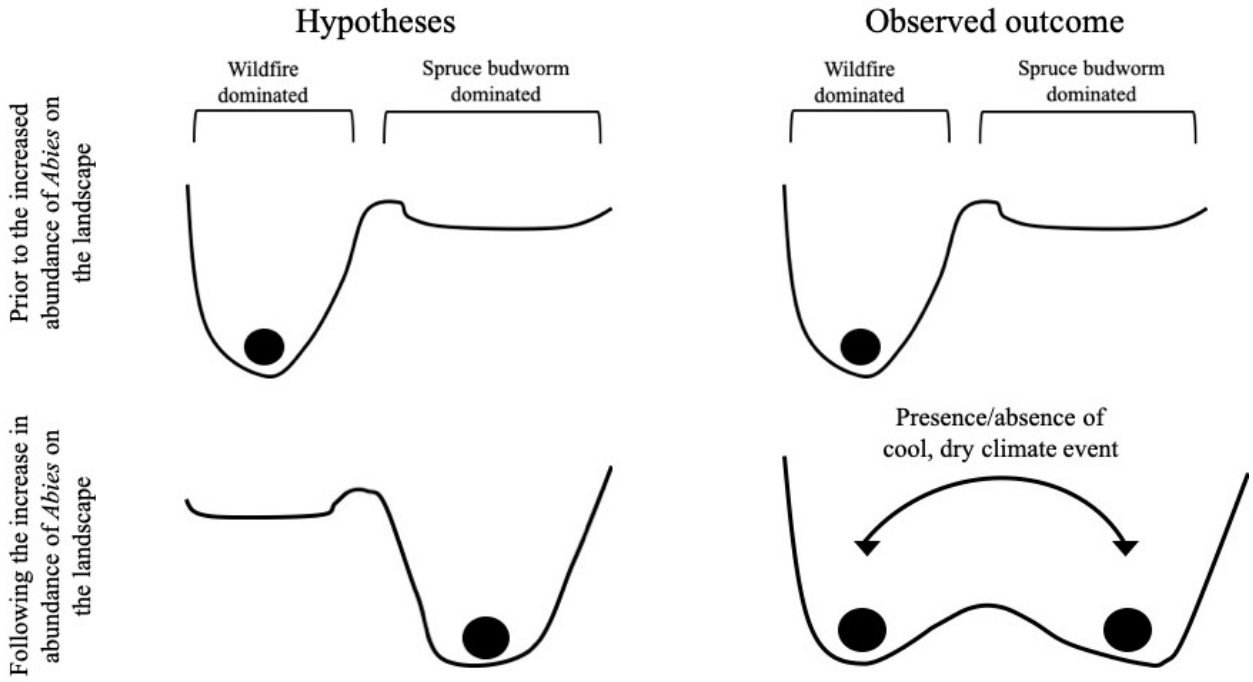

Figure 4.5: Summary of the mixed boreal forest ecosystem's position (*ball*) and ecosystem state landscape (*cup*) prior and after the postglacial recolonization by balsam fir around Lake Buire and the effect of cold, dry conditions on the ecosystem in eastern North America.

The observed oscillation between the abiotic and biotic disturbance frequencies may result from changes in forest composition around the lake that altered the ecosystem state landscape by creating basins of attraction of similar dimensions (Figure 4.5). Pre-8000 BP, wildfire tends to dominate which also coincides with a low mean *Abies:Picea* ratio suggesting a greater abundance of black spruce around the lake relative to fir resulting in an ecosystem state landscape favourable to wildfire. The mean ratio then increases as the warm conditions during the Holocene Thermal Maximum (HTM) allows for postglacial recolonization and increased abundance of balsam fir around the lake at roughly 6000 BP (Blarquez and Aleman, 2016) setting the stage for more frequent large spruce budworm population events (Figure 4.3) due to basins probably becoming of equal depth and size (Figure 4.5). Following the arrival of balsam fir and around 3500 BP there is a decrease in the *Abies:Picea* ratio due to an increased proportion of black spruce around the lake. This drop in the ratio also coincides with the establishment of an oscillation between the spruce budworm and

wildfire event frequencies as quantified by multiple regime shifts (Figure 4.3; Figure 4.4), suggesting movement of the ecosystem between the disturbance basins contrary to our initial hypothesis (Figure 4.5). Therefore, the changes in relative arboreal species abundance, as measured by the *Abies:Picea* ratio, likely altered the basin shapes of the ecosystem state landscape facilitating the movement of the ecosystem from one basin to the other given an appropriate trigger, which may be suggestive of a particular interaction between the disturbance agents.

The oscillating disturbance frequencies revealed an inverse relationship or negative interaction between the two disturbance agents in the mixed boreal forest at a 1000-year interval at Lake Buire and could be interpreted as competition for a limited resource. Generally, a strong negative correlation between disturbance frequencies was observed, confirming the relationship described by Navarro et al., (2018b) in the boreal black spruce forest, and is suggestive of a linked disturbance interaction (Simard et al., 2011; Kleinman et al., 2019), at local or extra-local (roughly 1km-10km area around a lake), and at millennial or multi-millennial scales. Further, this interaction could be viewed as a trophic interaction where disturbances are 'organisms' competing for a food resource (vegetation) while also creating conditions that favour their own survival (Pausas and Bond, 2020a, 2020b, 2022). Wildfire is an ancient process (He and Lamont, 2018), that is part of the ecosystem (Pausas and Bond, 2018; McLauchlan et al., 2020; Harrison et al., 2021), and as an 'organism' is an herbivore generalist (McCullough et al., 1998), with the ability of consuming all available fuel (Bond and Keeley, 2005; Pausas and Bond, 2018; Pausas and Bond, 2020a) that competes with the spruce budworm, an herbivore specialist (Hennigar et al., 2008; Nealis, 2016). Wildfire would negatively affect spruce budworm host-tree abundance by consuming the budworm's preferred food source along with all other vegetation (McCullough et al., 1998) resulting in food scarcity limiting LSBPs. Further, over long time periods wildfire may create more fire-prone conditions by favouring growth of fire-tolerant species (Rogers et al., 2015) that more easily re-establish post-fire via semi-serotinous cones, or sprouting (see Burns and Honkala, 1990; Bergeron, 2000). Conversely, through differential canopy host-tree mortality (Martin et al., 2019, 2020) creating variable canopy gap sizes resulting in complex regeneration patterns (Kneeshaw and Bergeron, 1998, 1999; D'Aoust et al., 2004; Couillard et al., 2021), LSBP events appear to favour the regeneration and establishment of balsam fir in the canopy subsequently predisposing the forest to further spruce budworm events (Baskerville, 1975; Morin, 1994; Bouchard et al., 2005, 2006, 2007). As such, transitioning from a spruce budworm or wildfire disturbance-vegetation feedback loop would likely require some sort of external forcing, such as a rapid climate change event.

The initiation and establishment of the above mentioned positive disturbance-vegetation feedback loops likely depend on a key trigger: appropriate climatic conditions. It is possible that the alternating disturbance frequencies may be influenced by the periodic occurrence of punctual rapid climate change events (Bond et al., 1997, 2001; Mayewski et al., 2004) that appear to coincide with the switch in the dominant disturbance by moving the ecosystem into the different basins of attraction (Figure 4.4; Figure 4.5). Such rapid climate change events have been associated with ice-raft debris events that altered oceanic thermohaline circulatory (Broecker 1997, 2003; Alley and Agustsdottír, 2005; Törnqvist and Hijma, 2012) and atmospheric circulatory patterns (Smith et al., 2016; Deninger et al., 2017) resulting in cool, dry conditions (Willard et al., 2005; Li et al., 2007; Springer et al., 2008; Orme et al., 2020), which during the Holocene have been correlated with changes in sedimentary charcoal accumulations in Europe (Florescu et al., 2019), and have resulted in higher wildfire frequencies in eastern North America (Carcaillet et al., 2001a). Simultaneously, cooler conditions are likely to have had a negative effect on insect development and survival (Ayres and Lombardo, 2000; Bentz et al., 2010; Pureswaran et al., 2018) resulting in fewer LSBP events. It is possible that the presence/absence of such rapid climate change events may: primarily influence the presence/absence of wildfire events, or primarily influence the presence/absence of the spruce budworm or influence both event types simultaneously. Further, the absence of one disturbance-vegetation feedback loop may allow for the establishment of the competing feedback loop or the climate-disturbance interaction may be much more complex than suggested here (see Kefi et al., 2016). The influence of rapid climate change events mediating the interaction between the two disturbance agents is a hypothesis that the authors would like to put forward for further testing based on their observations.

Around Lake Buire the spruce budworm and wildfire have been key ecosystem processes in the mixed boreal forest of central Québec over the past roughly 8000 years. Over the course of the Holocene, the two disturbances appear to exhibit an inverse relationship and have varied in frequency. Similar to the black spruce forest, an inverse relationship between disturbance frequencies was observed, however, the reccurring oscillation between disturbance frequencies at Lake Buire was not (Navarro et al., 2018b). At Lake Buire, host-tree availability and abundance appears to be the primary determinant of spruce budworm population fluctuations, while climate effects may play a more secondary role, although it is difficult to pinpoint the more influential factor since they are not mutually exclusive (Buma et al., 2019). Conversely, wildfire as an herbivore generalist and a more stochastic physical process appears to be primarily driven by

climate (Bessie and Johnson, 1995; Riley et al., 2019; Halofsky et al., 2020), and subsequently modulated by the vegetation present on the landscape (Hély et al., 2000, 2010, 2020; Girardin et al., 2013; Blarquez et al., 2015). Therefore, the peculiar oscillatory pattern between disturbance event frequencies may be the result of the punctual rapid significant climate change events, in combination with the change in arboreal species composition abundance.

Since this is the first reconstruction of its kind using lepidopteran scales and charcoal to reconstruct local Holocene disturbance frequencies and their interaction in the mixed boreal forest, the observed interaction needs to be confirmed to determine whether the observed pattern is due to site-level effects or may reflect a more general long-term regional behaviour. With a greater number of sediment profiles analyzing both spruce budworm population fluctuations and wildfire during the Holocene in the mixed boreal forest, a more accurate and precise picture of site-level variability of these disturbances can be attained which may elucidate the role of local and extra-local species composition on disturbance event frequency. Additionally, as more and more sediment profiles are analyzed there is also the opportunity to disentangle the effects of climate and/or vegetation composition on disturbance regimes. Finally, by combining multiple sediment profiles, a regional composite may be created to gain a broader and more general picture of spruce budworm and wildfire variability through time along with potential changes in their interactions.

4.6 Acknowledgements

Thank you to Marika Tremblay and Guillaume Vigneault for help in the laboratory, and Hugues Terreaux de Félice and Cassy Berguet for help in the field. Big thank you to Claire Fournier and Mireille Boulianne for lending equipment and preparing sucrose solution.

4.7 Funding

The author(s) received funding from the ‘Chaire de recherche industrielle CRSNG sur la croissance de l’épinette noire et l’influence de la tordeuse des bourgeons de l’épinette sur la variabilité des paysages en zone boréale’. ^{210}Pb age determination and radiocarbon dates were funded by this.

CHAPTER 5
GENERAL CONCLUSIONS

5.1 Key findings of the thesis

The key findings of this doctoral thesis relate to three main topics. First, lepidopteran scales are a good paleo-proxy that can be used to reconstruct long-term spruce budworm population fluctuations from lake sediments. Second, the use of a multi-proxy approach is fundamental to describing disturbance regimes as it allows for more accurate and robust interpretations. Finally, the spruce budworm and wildfire have coevolved in the mixed boreal forest as demonstrated by variability in their respective frequencies over the past 8000 years. The disturbances exhibited a significant negative correlation suggesting an inverse relationship and that they are mutually exclusive at local spatial and multi-millennial time scales. Further, presence or absence of rapid significant climate change events may influence and allow for the establishment of particular disturbance-vegetation feedback loops.

5.1.1 The primary objectives: validation and calibration of a novel paleo-proxy

The ability to reconstruct spruce budworm population fluctuations over long time intervals has been done using lepidopteran scales (e.g., Navarro et al., 2018a,b), however it was only assumed that this novel paleo-proxy was appropriate for such purposes. The primary objective of this thesis was to determine whether this novel paleo-proxy accurately captured spruce budworm population fluctuations. This was done by using known outbreaks of the late 20th century identified by aerial surveys and comparing these to spruce budworm population fluctuations inferred by the lepidopteran scales. High agreement between both proxies was obtained, suggesting that lepidopteran scales are able to detect periods of large spruce budworm populations. In addition to this, scale accumulations were then compared to tree-ring widths, a common and well-established spruce budworm proxy (e.g., Blais, 1968, 1983; Morin and Laprise, 1990; Morin, 1994; Boulanger and Arseneault, 2004; Boulanger et al., 2012) in an effort to gain insight into whether large scale accumulations corresponded with more severe defoliation events. Although the exact relationship was dependent on lake-level taphonomy, site history and conditions, along with tree-level characteristics, and tree species, a generally strong correlation was observed between both proxies where greater scale accumulations were associated with narrower ring-widths, and more particularly a greater proportion of defoliated trees. This can be interpreted as greater scale accumulations do tend to reflect more severe defoliation events.

The multi-proxy approach via the use of multiple lines of evidence validated the use of lepidopteran scales confirming their ability to identify outbreaks, and also helped improve scale peak accumulation interpretation. Utilizing multiple lines of evidence therefore is essential for disturbance reconstructions as use of different proxies can overcome and compensate the shortcomings of individual proxies, and more importantly when combined, paint a clearer picture of the observed disturbance regimes. For example, as done in this thesis, combining the use of remote sensing (aerial surveys) and a paleo-proxy (lepidopteran scales) confirmed the latter's ability to identify periods of large populations, meaning that the identification of such events via scale accumulations over much longer time intervals is valid. The comparison with tree-ring widths added another dimension to the interpretation of lepidopteran scale accumulations; larger accumulations coincided with smaller ring-widths or a greater percentage of affected trees suggesting that more severe events were reflected by greater scale accumulations. Combined, the evidence suggests that lepidopteran scales can identify periods of large populations, and that larger accumulations reflect more severe defoliation events laying the ground work for interpretation of scale accumulations over millennial and multi-millennial time-scales.

As such, the use of current known events to validate and calibrate past disturbance events will help in identifying and/or describing current potential mechanisms helping interpret and better understand past disturbance variability (Buma et al., 2019; Buma, 2021). Neo-ecological methodology, the ability to study and elucidate mechanisms that currently explain disturbance characteristics (frequency, severity, extent, etc.), can be combined with paleoecological methodology to help explain past variation (Buma et al., 2019). Conversely, the past variation over vast time periods encompassed by paleoecological studies can be combined with modern understanding of systems to forecast and set in place ecological and socioeconomic frameworks that may be adaptive in the face of climate change (Buma et al., 2019; Buma and Schultz, 2020). Future research in disturbance ecology should therefore, where possible, employ a multi-proxy and combined methodological approach to gain a better understanding of disturbance regimes.

5.1.2 Final objective: application of the novel paleo-proxy by reconstructing long-term variability in the two major disturbance regimes of the mixed boreal forest

After establishing that lepidopteran scales are an appropriate proxy to reconstruct long-term spruce budworm population fluctuations, the final objective of this doctoral thesis was to reconstruct the long-term

variability in the two major disturbance regimes of the mixed boreal forest. The multi-millennial reconstruction of both large spruce budworm population and wildfire events revealed that their frequencies were variable through time. An increase in the frequency of large spruce budworm population events coincided with an increase in the *Abies:Picea* ratio around 6000 BP suggesting that the increase in abundance of the budworm's primary host created conditions that favoured outbreaks. Conversely, prior to 6000 BP, wildfire fire event frequency was greater than spruce budworm event frequency. From 6000 BP onward, a peculiar oscillation between the disturbances' frequencies is observed, where one peaks in a period where the other troughs. The inverse relationship between spruce budworm and wildfire event frequencies observed by Navarro et al., (2018b) was also observed at Lake Buire in the mixed boreal forest, however the degree of oscillation between disturbance peak frequencies were not the same. The peculiar, and consistent oscillation is hypothesized to result from punctual rapid significant climate change events related to ice raft debris events (Bond et al., 1997, 2001), determining which disturbance-vegetation feedback loop is allowed to establish. These events in eastern North America are believed to have brought about cool, dry conditions (Mayeski et al., 2004; Willard et al., 2005; Smith et al., 2016; Deninger et al., 2017; Orme et al., 2020) which were favourable to wildfire during the Holocene (Carcaillet et al., 2001a), while simultaneously creating unfavourable conditions for insect development and survival (e.g., Ayres and Lombardo, 2000; Bentz et al., 2010; Pureswaran et al., 2018), resulting in fewer outbreaks, and potentially less severe outbreaks too. At Lake Buire, the occurrence of these rapid climate change events coincided with periods of high wildfire, and low spruce budworm event frequencies suggesting that climate may serve as an external trigger affecting the disturbance frequencies. Therefore, during such an event, the spruce budworm-vegetation feedback loop is prevented from establishing or limited in its influence. Normally, during warmer conditions the spruce budworm defoliates balsam fir in such a way that creates gaps favouring the regeneration, and establishment of balsam fir in the canopy, then favouring subsequent outbreaks due to abundant host (Baskerville, 1975; Morin, 1994). Conversely during this cool and dry period, conditions become favourable to wildfire, allowing for the establishment of the wildfire-vegetation feedback loop or at least permitting it to become more influential. Under the cool and dry conditions, wildfire frequency is expected to increase (Carcaillet et al., 2001a), favouring regeneration of tree species with particular adaptations such as semi-serotinous cones, allowing for relatively rapid recolonization, and coincidently such species tend to be more likely to burn (e.g. Rogers et al., 2015; Lamont et al., 2020).

The establishment of disturbance-vegetation feedback loops may facilitate the transition of a landscape from one that is susceptible to the spruce budworm to one that is susceptible to wildfire by way of the wildfire

return interval and its ability to influence the composition and structure of this landscape. For example, the proportion of balsam fir within a stand is, in part, determined by the time since last fire where shorter return intervals tend to limit and inhibit balsam fir establishment, while long return intervals allow the conifer to establish (Bergeron 2000; Ali et al., 2008; Couillard et al., 2021). As a shade-tolerant species, balsam fir seedling and/or saplings are able to grow underneath a canopy, and can eventually replace this canopy, but this requires a long fire-free period (Burns and Honkala, 1990; Bergeron, 2000). Meanwhile, shorter wildfire return intervals tend to inhibit the establishment of balsam fir (Ali et al., 2008; Asselin et al., 2016; Couillard et al. 2021) and will favour species that regenerate well following fire such as black spruce, trembling aspen and/or paper birch (Burns and Honkala 1990). At a broader scale, landscape composition is determined by the composition of the individual stands making up the landscape. If the majority of stands have a high proportion of balsam fir, the landscape is likely to be highly susceptible to the spruce budworm, and could have developed as a result of long wildfire return intervals. Additionally, spruce budworm outbreaks would also produce landscapes susceptible to further outbreaks, as at the stand-level, structure and composition is altered in a manner to favour the regeneration and establishment of balsam fir in the canopy (Baskerville 1975; Morin 1994). Conversely, a landscape with a low proportion of balsam fir would suggest that most stands tend to experience relatively short wildfire return intervals (Ali et al., 2008; Couillard et al., 2021). The wildfire return interval, in turn, is largely dependent on the coinciding of temperature, humidity, and wind conditions favourable to ignition and fire spread along with the occurrence of ignitions (Macias Faurai and Johnson 2008; Macias Fauria et al., 2010). These conditions are determined by climate over long time intervals, and weather over short time intervals. Once ignited, the fire behaviour depends on weather conditions (temperature, humidity, and wind), topography, and the vertical and horizontal distribution of fuels (Van Wagner 1967, 1977; Rothermel 1983; Fulé et al., 1997; Falk et al., 2007). As such the wildfire return interval may alter the abundance and spatial distribution of tree species over a landscape in a manner that shifts its susceptibility from the budworm to wildfire and vice versa.

Of note is the frequency of wildfire events corresponding to an approximately 83-200 year fire return interval (12-5 events per thousand years, respectively) at Lake Buire which was found to be higher than those observed in other studies but falls within the range of calculated frequencies over the course of the Holocene within the province of Québec. For example, Couillard et al., (2021) in mixed boreal forest sites located in northern Québec, found an average fire return interval of 280 to 340 years. Similarly, Couillard et al. (2013), in the mixed boreal forest found considerably longer return intervals from 9600 to 250 cal. yr BP. However, at sites where charcoal was found at the soil surface from 250 cal. yr BP to present, Couillard

et al. (2013) observed fire intervals ranging from 70-250 years, similar to the intervals calculated by Carcaillet et al. (2001a) over the course of the Holocene. Further, other studies conducted in the mixed coniferous boreal forest have found return intervals in central Québec ranging from 69-273 years in recent history (Bergeron et al. 2001), and a mean regional fire interval of 170±124 years over the past 5000 years (Frégeau et al. 2015). In the black spruce boreal forest, regional fire return interval was found to vary from 83-167 years (Ali et al., 2012), although some sites exhibited a fire return interval of up to 500 years (Ali et al., 2008). The major difference between the wildfire return interval observed at Lake Buire relative to other studies appears to be the generally greater fire frequency, and the consistent oscillation in wildfire frequency, where other studies obtained lower variability. This greater fire frequency, however falls within the frequencies observed by other studies, and as noted by Couillard et al., (2021) the persistence of balsam fir–paper birch forests is still possible with a 200-year fire return interval. Meanwhile, the consistent oscillation in wildfire frequency may be a result of site-level varability as the studies cited above were able to calculate a mean regional change in wildfire frequency, which was not possible for Lake Buire as it is a single site.

At local/extra-local and multi-millennial time-scales the observed disturbance interaction appear to be a linked interaction (Simard et al., 2011; Kleinman et al., 2019) displaying an inverse relationship, where wildfire excludes spruce budworm and vice versa. This suggests that although both entomologists and wildfire ecologists are predicting more frequent and severe outbreaks and fires given future climate change (e.g. Ayres and Lombardo, 2000; Flannigan et al., 2009, 2013; Millar and Stephenson, 2015; Anderegg et al., 2015), the results of this thesis suggest a potentially more nuanced outcome. The inverse relationship best demonstrated by the peculiar oscillation in disturbance frequencies suggests that both entomologists and wildfire ecologists may be correct in their predictions, with a caveat. Both are correct in that there may be periods of higher event frequencies and severities for each particular disturbance, but these periods may not occur at the same time, at least not at the local/extra-local spatial and multi-millennial time scale. Additionally, the major disturbances of the mixed boreal forest appear to be influenced by different drivers affecting how these regimes will manifest given different climate conditions. For example, presence of abundant susceptible host-trees is necessary for spruce budworm outbreaks to occur, otherwise at low abundances the insect would likely remain at endemic levels (Cooke et al., 2007; MacLean, 2016; Nealis, 2016). As such, without available host-trees, climate conditions favourable to insect development and survival are unlikely to result in outbreaks due to low food availability i.e., host-tree biomass. Conversely, wildfire can burn any type of vegetation (McCullough et al., 1998; Bond and Keeley, 2005; Pausas and Bond, 2018; Pausas and Bond, 2020a), although coniferous species tend to burn better than deciduous ones

(Hély et al. 2000, 2010; Girardin et al., 2013), and appears to be dependent on suitable climatic conditions that will favour fuel availability, fire ignition, and spread (e.g., Wotton et al., 2010; Macias Fauria et al., 2010; Woolford et al., 2014; Molinari et al., 2018) while vegetation type subsequently modulates fire behaviour (Girardin et al., 2013; Blarquez et al., 2015; Hély et al., 2000, 2020). Therefore, both disturbance agents may experience more frequent and severe events (e.g., Ayres and Lombardo, 2000; Dale et al., 2001; Flannigan et al., 2009, 2013; Millar and Stephenson, 2015; Allen et al., 2015), however, these may not, over long time intervals, occur simultaneously likely excluding the possibility of compound disturbance interactions (Paine et al., 1998), since the relationship between the spruce budworm and wildfire appears to be a negative linked disturbance interaction. Further, the establishment of one disturbance-vegetation feedback loop relative to the other likely depends on the vegetation and/or climate context. The hurdle facing forest managers is therefore adopting and/or adapting silvicultural strategies to best reflect the stand characteristics resulting from each disturbance under the right conditions.

5.2 Implications for forest management

Within the context of a changing climate, forest management strategies will have to adapt. Establishing a management framework will help managers better determine which strategies need to be applied. However, upon which reference or baseline would such a management framework be based on? The Holocene (~11,700 BP- present; Walker et al., 2012) could serve as a long-term reference as through this period climate, vegetation, and disturbance regimes have varied (e.g., Renssen et al., 2009; Wanner et al., 2012; Mayewski et al., 2004; Ali et al., 2012; Blarquez et al., 2015; Navarro et al., 2018b). The observed changes in the past have the potential to serve as analogs for future climate or at least may provide a sense of the experienced variability acting as a starting point for forest managers to implement sustainable practices (e.g., Swetnam et al., 1999; Landres et al., 1999; Keane et al., 2009; Hennebelle et al., 2018). For example, managers could use an observed range (minimum and maximum values) of disturbance frequencies to delineate boundaries within which this metric would ideally fall along with the overall trend to determine whether a system has exceeded its historical resilience (Landres et al., 1999). Furthermore the emulation of disturbance regimes could act as a coarse-filter ecosystem management method that may allow for the meeting of multiple forest management objectives including maintaining biodiversity, and ecosystem services (e.g., North and Keeton, 2008; Long, 2009; Oliver et al., 2015; Aszalos et al., 2022). Therefore, it becomes exceedingly important to know how disturbance regimes have varied in the past during different climate phases and within and across different ecosystems. This understanding allows for gaining a better understanding of a system's resilience, along with the identification of potential tipping points.

The proxies used in this thesis provide a spatial and temporal resolution that is too coarse for the development of particular stand-level silvilcultural prescriptions, but give forest managers a better understanding of the mixed boreal forest's response to change along with the dynamics of its two major disturbances. Thus the implications for forest management that can be extracted from this Holocene reconstruction will likely relate to landscape composition and structure as the paleo-proxies used do not allow for finer resolution applications or interpretations (Landres et al., 1999; Swetnam et al., 1999). The variable Holocene climate, and the mixed boreal forest's and disturbance agents' responses to this variability may serve as potential analogs for future climate conditions. Based on this, potential climate scenarios may include the following type of conditions: warm and dry, cool and dry, warm and humid, and/or cool and humid. Under warm, dry conditions forest fires are likely to be more frequent (Wooldford et al., 2014; Jolly et al., 2015; Molinari et al., 2018), as well as be more intense and severe (Flannigan et al., 2009, 2013; Millar and Stephenson, 2015) due to a greater proportion of available fuel (Byrom 1959; Van Wagner 1967, 1977; Rothermel 1983). Favourable conditions to wildfire would likely result in a landscape composition and structure with a lower proportion of balsam fir due to shorter wildfire return intervals (Ali et al., 2008; Asselin et al., 2016; Couillard et al., 2021), ultimately limiting spruce budworm populations given the lower proportion of available host-trees. A similar outcome may result from cool, dry conditions, as these conditions have resulted in greater fire frequency during the Holocene (Carcaillet et al. 2001a). Further, cool conditions are likely to negatively affect insect survival and development (Bale et al., 2002), probably resulting in fewer outbreaks as budworm populations will be less able to escape population control factors (Berryman, 1987; Ayres and Lombardo, 2000). Managing a landscape susceptible to wildfire will likely involve focusing on creating a heteroegenous fuel distribution across the landscape by incorporating fuel breaks (natural and/or anthropogenic), prescribed burns (Wotton et al., 2017), and perhaps favouring a larger proportion of deciduous species on the landscape (Hély et al., 2000, 2010; Girardin et al., 2013). Finally, the development of annual allowable cuts that account for more frequent fires and greater areas burned (i.e., a reduction in annual allowable cut), may allow for maintaining a more continuous forest cover likely resulting in a more fire-resilient landscape along with a more stable long-term timber supply (Drapeau et al., 2024).

Conversely, warm, humid conditions are likely to produce a landscape composition and structure that will be favourable to the spruce budworm with the establishment and proliferation of balsam fir. The greater

humidity would increase fuel moisture reducing the chance of ignition along with limiting available fuel to burn (Bessie and Johnson 1995; Macias Fauria and Johnson 2008; Macias Fauria et al., 2010). This potential reduction in possible ignitions and subsequent burning would increase the wildfire return interval enabling a large proportion of stands to reach late successional stages where balsam fir can occupy the canopy and successfully establish in the understory (Bergeron 2000; Ali et al., 2008; Couillard et al., 2021). The greater proportion of fir on the landscape has the potential of allowing the establishment of a spruce budworm-vegetation feedback loop (Baskerville, 1975; Morin, 1994) and the occurrence of more intense and severe outbreaks (Murdock et al., 2013; Weed et al., 2013). The key to managing the spruce budworm susceptible landscape will be the identification and harvesting of mature forest stands which would reduce the landscape's susceptibility to the defoliator while also providing an economic benefit. Simlarly, under cool, humid conditions the frequency of both disturbances are expected to be attenuated due to limited available fuels and fewer ignitions along with poor insect survival and development restraining budworm population growth. The possibility of prolonged absence of disturbance on the landscape would allow the forest to mature and reach late successional stages resulting in an increase in the proportion of balsam fir, ultimately creating a landscape composition and structure that would be susceptible to the spruce budworm.

The development of appropriate silvicultural prescriptions applied at the stand-level (i.e., types of cut utilized, harvesting intervals, which species to harvest, which species to replant and at what density) must rely on more contemporary studies that have quantified changes in stand composition and structure following wildfire or LSBP events. For example, uneven-aged type cuts, such as patch cuts of variable sizes, used in tandem with single-tree selection would likely better reflect the heterogeneous mortality that occurs during a spruce budworm outbreak (Martin et al., 2019, 2020). Further, frequent entries in a single stand would be necessary to reflect the temporal heterogeneity of the tree mortality during an outbreak. The broader spatial and temporal perspective obtained from paleo-reconstructions offers a framework for managing landscape composition and structure within which contemporary quantification of stand compositional and structural changes could be placed to influence cross-scale drivers that affect both wildfire and spruce budworm events. The subtlety will be in understanding when and if it will be best for the ecosystem, which is managed in a way to fulfill our needs, to return to a similar state i.e., a resilient ecosystem (Holling, 1973), or if it will be best for the ecosystem to adapt and/or transform in a fashion that would ultimately maintain high species diversity and function even though it may not resemble its initial state (Oliver et al., 2015).

Not only will the development of appropriate forest management be important but the accurate detection of epidemic spruce budworm populations will be key in effectively managing our forests. Currently, in Québec aerial surveys are used to estimate the amount of defoliation occurring in forest stands in conjunction with insect traps to infer outbreaks, i.e., large spruce budworm populations. However, defoliation observed by aerial surveys may not necessarily reflect an epidemic spruce budworm population in the area in question. First, in a polygon composed of host and non-host tree species defoliation severity is based on defoliation of the host species (M. Simard, personal communication, email August 12 2021). Therefore, a severely defoliated polygon could either be a polygon with 10% basal area comprised of host-trees or a polygon of 90% basal area comprised of defoliated host-trees. Severe defoliation in the polygon with a low basal area may be an inaccurate reflection of the population in the stand as the defoliation may simply be due to the endemic population present in the stand just as it could result from a large population. The degree of defoliation could be weighted by the proportion of host-trees present in the polygon since defoliation is known to be lower in mixed and those stands dominated by deciduous species (Su et al., 1996; Cappucino et al., 1998). Thus, inferring an epidemic population solely based on defoliation intensity may be misleading at the individual polygon level noting however, that the landscape within which such a polygon is found is taken into account. Secondly, aerial surveys may in fact fail detect to defoliation events below a certain threshold relative to other proxies such as tree-ring widths as observed in the western spruce budworm (Campbell et al., 2006; Alfaro et al., 2018; Tai and Carroll, 2022). However, tree-ring widths are unable to quantify current outbreaks or spruce budworm population sizes, and so aerial surveys in combination with other lines of evidence will prove critical in accurately determining the current stage of the population cycle. Thus, a multi-proxy approach may prove to be useful in attaining an adequate detection of defoliation events, and this may be of particular concern when attempting to manage damage done by the insect on the timber supply.

Additionally, gaining a better understanding of adult moth migration events will also be key in effectively managing our forests. Unfortunately, despite lepidopteran scales being a direct measure of the local insect biomass, the temporal resolution typically obtained from lake sediment cores do not allow for assessing within-outbreak spruce budworm movements. Scale accumulations most likely provide a single snapshot of local budworm populations over an entire outbreak period. In an effort to obtain a more accurate representation of the regional budworm population, the creation of a composite chronology, i.e., averaging

scale accumulations from multiple sediment cores, may help reduce the individual site-level variability but this does not change the fact that large accumulations likely still only represent the cumulative budworm population size over the course of an entire outbreak, and going further back in time, large accumulations may represent multiple outbreak periods. As such, modern studies will need to be used to gain a better knowledge of causes of within-outbreak adult moth movements (Régnière and Nealis, 2019; Rhainds et al., 2021), factors influencing their movements (Régnière et al., 2019 a,b) along with their quantification (Greenbank et al. 1980; Boulanger et al., 2017; Larroque et al., 2020).

5.3 Future research

Given that lepidopteran scales are a novel paleo-proxy, there are many potential avenues to explore and future research needs to be met. Potential avenues of research may include but are not limited to: utilization of the technique in other ecosystems to reconstruct past lepidopteran outbreaks around the globe, and developing methodological approaches that may facilitate analysis. A key research need will involve sampling and analyzing multiple lakes within a given ecosystem allowing for the creation of composite chronologies to infer more general and regional disturbance agent behaviour and interactions while simultaneously elucidating disturbance regimes and interactions at local/extra-local spatial scales.

At a global level, the use of the novel lepidopteran scale paleo-proxy may be warranted and utilized for multi-millennial reconstructions in other systems. Long-term reconstructions could be done across the globe for a variety of different defoliating insects, if certain criteria are met. The first being that the disturbance agent in question must be of the order Lepidoptera which will ensure the presence of scales in the sediment. Secondly, the sampled lakes must be relatively small, deep with little to no inflow-outflow helping to ensure relatively low sediment disturbance (e.g., Millspaugh and Whitlock, 1995; Ali et al,. 2008), and ideally, situated in an area that has recently undergone known defoliation. This last requirement helps ensure the detection of the insect (i.e., that one find scales in the sediment), lack of scales in the upper sediment layers in areas of known defoliation may suggest that the selected lake is a poor recorder. Finally, the fluctuation in lepidopteran scale accumulation should be paired with other proxies (e.g., dendrochronology) for validation and calibration. As such long-term reconstructions, for example, are possible for the pine processionary moth (e.g., Camarero et al., 2022), winter moth (e.g., Tikkanen and Roininen, 2001; Simmons et al., 2014), and larch budmoth (e.g., Esper et al., 2007), or even defoliating species in South America (e.g.,

Paritsis and Veblen, 2011). Closer to home in North America, potential millennial or multi-millennial reconstructions could be done for the western spruce budworm [*Choristoneura freemani* Razowski, 2008].

Lepidopteran scale identification and counting is slow and labour-intensive, and any method that could speed up the process would be beneficial. During sample processing the ability to create a pellet that consists only of scales would facilitate count. Currently 'impure' pellets are a mixture of fine sediment, lepidopteran scales, and other chitinous and vegetative structures. Methods that could 'purify' the subsample or pellet would greatly speed up the identification and counting process. Discriminating the material in the 'impure' pellet using mass and/or surface area in a manner similar to gel electrophoresis may be a potential avenue of research (H. Morin, personal communication, in-person conversation). Lepidopteran scales would be expected to be quite light, have a relatively large surface area, and therefore would be expected to travel further than the other material. A secondary step would be necessary, however, in order to discriminate between the scales and other chitinous material found in the pellets.

There is also discussion of utilizing Artificial Intelligence or Machine Learning in an effort to automate the counting and identification process of the lepidopteran scales (O. Blarquez, personal communication, in-person conversation). This automation would be incredibly beneficial in speeding up analysis, however, developing the proper algorithm to identify lepidopteran scales may be difficult. Currently, the scales are in 'impure' pellets and once placed on microscope slides can be sometimes rolled up, folded, and sometimes partially obscured by sediment or the other chitinous material retained in the pellet. The ability to identify the scales in this situation would likely require a particularly complex algorithm, considering that lepidopteran scale identification can take around three months to learn in humans (personal observation). Even in a purified pellet containing only scales, these may be folded, rolled, or even obscured by other scales again likely creating a need for a complex algorithm for count accuracy.

An increase in the number of long-term reconstructions of spruce budworm population fluctuations would allow for the creation of composite sediment chronologies providing a clearer picture of changes at the regional, ecosystem, and/or landscape level over vast periods of time. A larger number of available

chronologies to create a composite chronology would help remove any site-level variability and provide a more robust picture of the disturbance over broader spatiotemporal scales. Conversely, looking at multiple individual chronologies retains, and reveals site-level variability with the potential to identify factors that may influence the observed variability. In a broader context, the greater number of sediment chronologies, as composites or kept as individual chronologies, may reveal differences in spruce budworm population fluctuations in different forest types. Increased sampling should be done in both black spruce, and mixed boreal forests to compare the variability in spruce budworm population fluctuations within and between the forest types. Sampling in these ecosystems may provide insight as to how the disturbance regime is affected by a changing climate. At the moment, there is uncertainty regarding the insect moving North and being able to feed on black spruce, since historically, phenological asynchrony between this secondary host and larval development typically restricted defoliation intensity, but with projected warming trends, budburst and larval emergence will likely be synchronous (Régnière et al., 2012; Pureswaran et al., 2015, 2019; Fuentealba et al., 2017) potentially resulting in outbreak dynamics that may not have been observed in the 20th century. As such, past long-term spruce budworm outbreak variability in the black spruce forest could provide a clearer picture of potential future behaviour. Similarly, observing the long-term spruce budworm outbreak variability in the mixed boreal forest would be an interesting exercise as this forest falls within the core of the insect's historic distribution. Long-term reconstructions in the mixed boreal forest may or may not reveal changes in outbreak frequency and/or magnitude with changes in climate.

Finally, pairing long-term spruce budworm and wildfire reconstructions in the mixed boreal forest would additionally provide a more complete picture of the evolution of the ecosystem through time. Long-term wildfire reconstructions using lake sediment in the mixed boreal forest have been very limited (e.g., Blarquez et al., 2015), although reconstructions have been done using soil charcoal in either high-altitude mixed forests or in mixed stands at higher latitudes (e.g., Couillard et al., 2013, 2021). However generally speaking, long-term wildfire variability in the mixed boreal forest is not particularly well described. Therefore, analyzing sediment chronologies for both large spruce budworm population and wildfire events would provide insights on particular individual disturbance regimes, their interactions, and reference periods that could be used as a framework to improve current silvicultural practices.

APPENDIX A

LAKE-LEVEL AGE-DEPTH MODELS

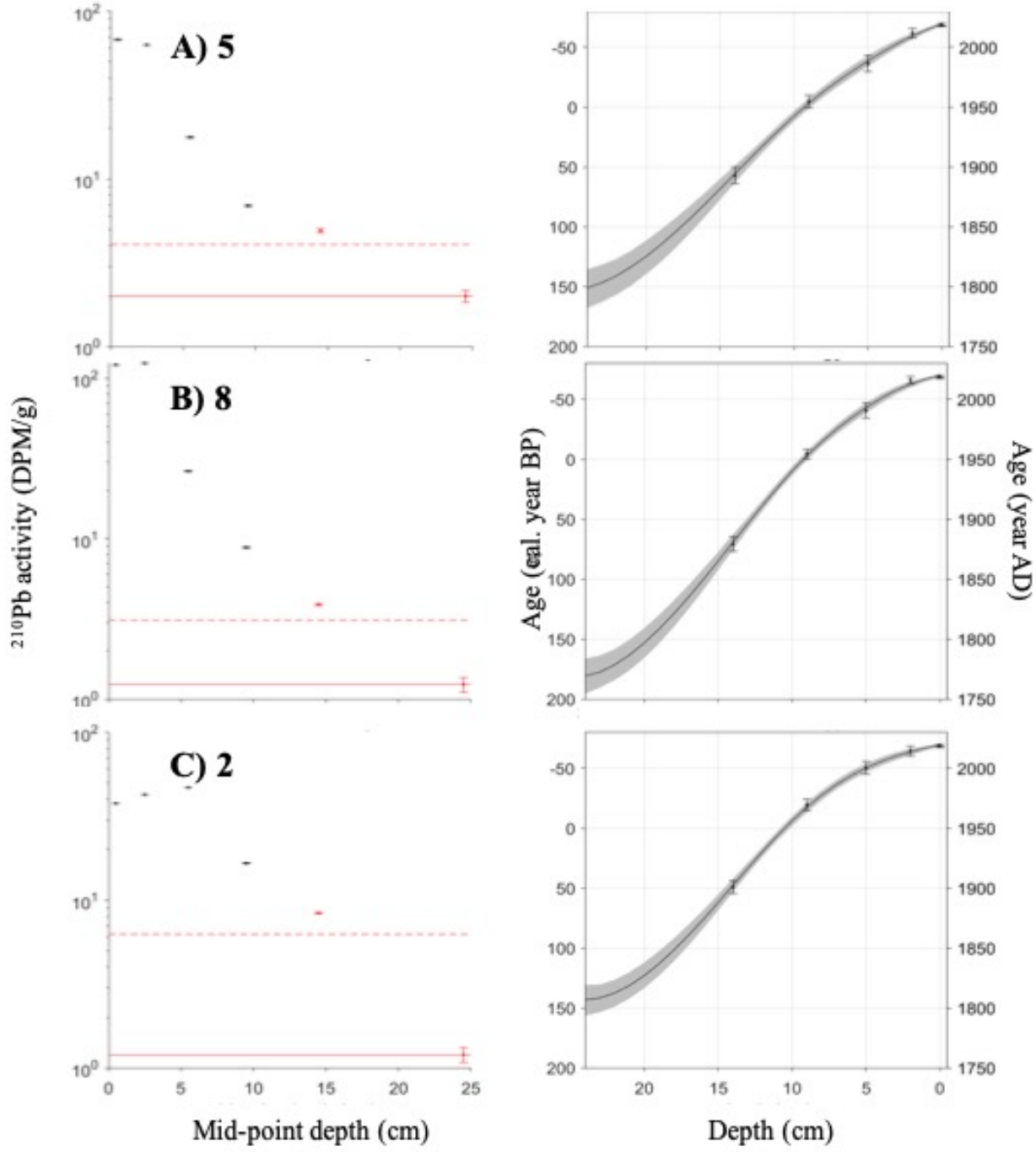

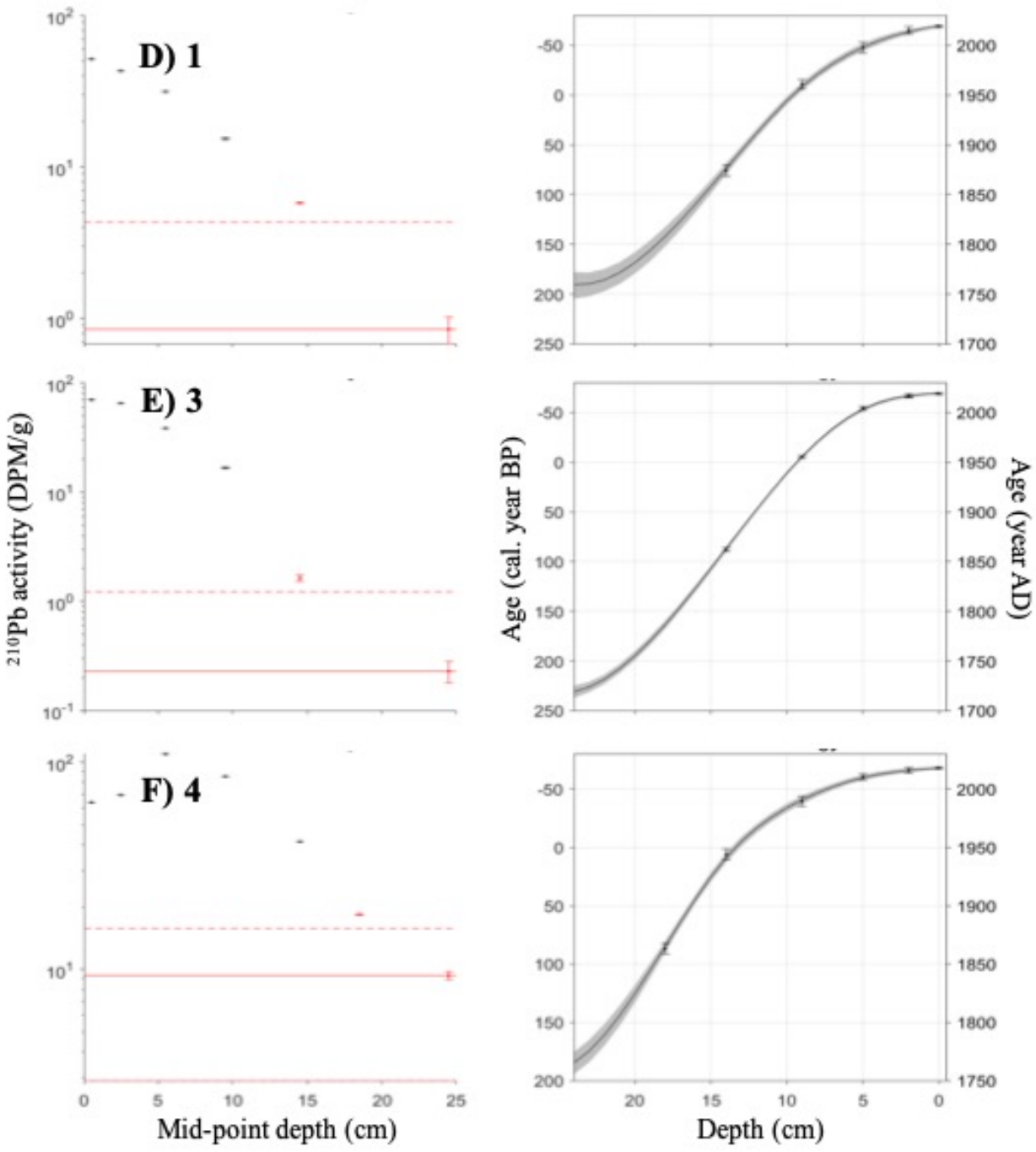
D) 1
E) 3
F) 4
^{210}Pb activity (DPM/g)
Mid-point depth (cm)
Age (cal. year BP)
Age (year AD)
Depth (cm)

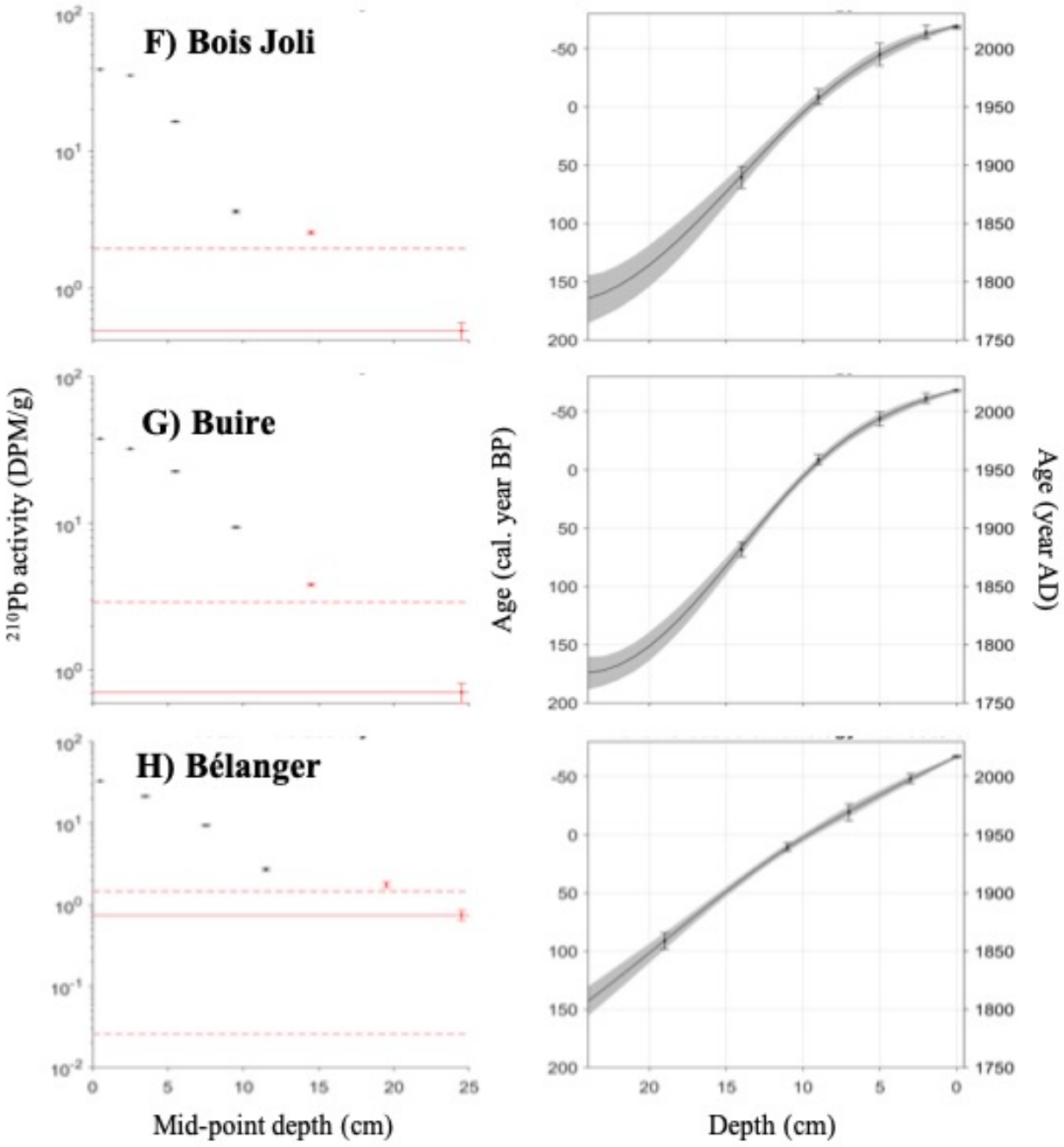

Figure A.1: Individual lake ^{210}Pb total activity and age-depth models for Lakes (a) 5, (b) 8, (c) 2, (d) 1, (e) 3, (f) 4, (g) Bois Joli, (h) Buire, and (i) Bélanger. Left panel: Total ^{210}Pb activity for the sampled depths (with error bars) and estimated background rate (*red line*) with error (*dashed red line*). Right panel: ^{210}Pb Constant Rate Supply age-depth model with dates and error bars and cubic smoothing spline with 95% confidence interval (*grey shaded area*).

APPENDIX B
CHARANALYSIS WORKFLOW AND LEPIDOPTERAN SCALE ACCUMULATIONS WITH INTERPOLATED TIME-STEP

A simplified CharAnalysis method was employed to identify periods of large spruce budworm population, i.e., outbreaks. The original CharAnalysis program could not be used because of the nature of the samples: a relatively short time interval and small sample size. The simplified CharAnalysis method however followed the same steps as the original program and used similar terminology (Figure B.1; Table B.1); and was performed in the R statistical environment (R Core Team, 2021). Various smoothing windows were implemented following the interpolation to a constant time step and prior to determining C_{back} (Figure B.1; 'user-determined smoothing function' step). To clarify, depending on the age-depth model, the interpolation to a constant time step can result in the imputation of scale accumulations between the ^{210}Pb-dated years. This means that although each core initially had 20 lepidopteran scale samples, interpolation to a specified constant time step often results in additional scale accumulation points in the chronology to maintain this constant time step (Figure B.2). After determining C_{back}, a global threshold, *t* (Table B.1), was applied in the form of the 40th, 50th, 60th, 70th, 80th, 90th, 95th, and 99th percentiles to C_{peak} for each lake in an effort to isolate spruce budworm outbreak events (Figure B.1; 'application of global threshold' step). Moreover, applying a 20-year window centred around the highest scale accumulation resulted in the formation of scale accumulation clusters to identify outbreaks that helped reduce the chance of identifying false outbreaks.

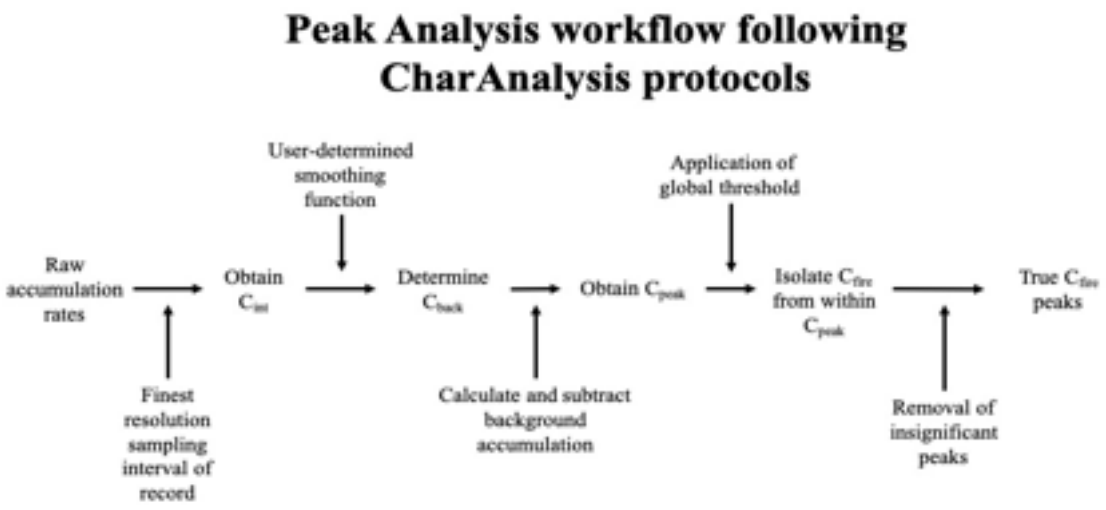

Figure B.1: The workflow of the analysis used to identify lepidopteran scale peaks (outbreaks) in the surface sediment. Based on Higuera, (2009).

Table B.1: The terminology used in CharAnalysis to define the state of the samples over he course of the analysis. Although the terms here refer to wildfire events, the terminology was adopted to describe the evolution of samples to identify spruce budworm outbreaks. Modified from Higuera, (2009).

Term	Description
C_{int}	Interpolated accumulation rate
C_{back}	The background accumulation rate or trend
C_{peak}	Signal remaining after removing the background accumulation rate; the high frequency trends
C_{noise}	A component of C_{peak}; portion of the high frequency trend likely related to sediment mixing and other errors
C_{fire}	The other component of C_{peak}; the fire signal
t	Specific threshold value used to differentiate C_{noise} from C_{fire}

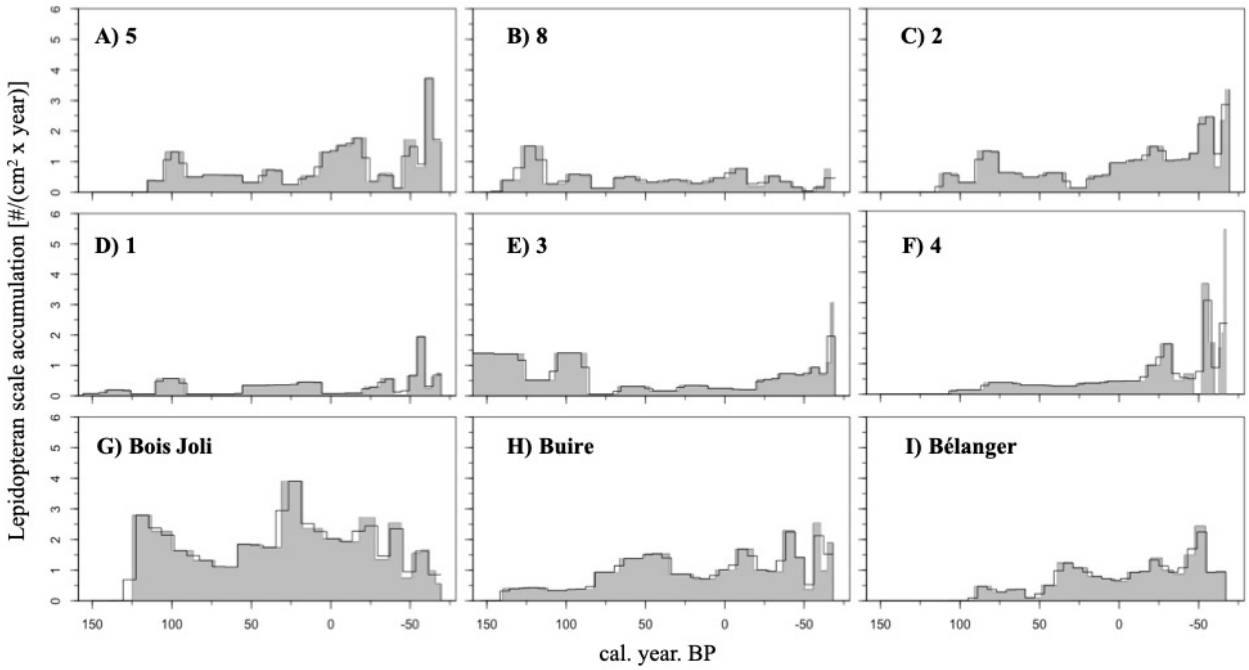

Figure B.2: Lake-level lepidopteran scale accumulations (*grey bars*) and corresponding finest best fitting interpolation time step (*thin black line*) for Lakes (a) 5, (b) 8,(c) 2, (d) 1, (e) 3, (f) 4, (g) Bois Joli, (h) Buire, (i) Bélanger. The constant time step applied to Lakes 1, 2, 3, 4, 5 was 5 years, while a constant time step of 6 years was applied to Lakes Buire and Bélanger and finally a constant time step of 7, and 8 years were applied to Lakes 8, and Bois Joli respectively.

APPENDIX C

AERIAL SURVEY DATA DESCRIBING SITE-LEVEL DEFOLIATION WITHIN THE 200 M BUFFER AROUND EACH LAKE

Table C.1: Site-level defoliation within the 200 m buffer of each sampled lake according to the aerial surveys conducted 1967 to 1991, and 2007 to the present. Defoliation classes of 0, 1, 2, 3 correspond to no defoliation, light, moderate, and severe defoliation respectively (MFFP, 2021a).

Lake	Year	Maximum observed defoliation class
5	1974	3
	1975	3
	1976	3
	1977	3
	1978	3
	1985	3
	2015	3
	2016	2
	2017	2
	2018	3
	2019	3
8	1974	3
	1975	3

Lake	Year	Maximum observed defoliation class
	1977	3
	1980	3
	1981	3
	1984	1
	2015	2
	2016	2
	2017	2
	2018	3
	2019	3
	1974	2
	1975	3
	1976	3
	1977	3
2	1978	3
	1983	2
	2010	3
	2011	3

Lake	Year	Maximum observed defoliation class
	2012	3
	2013	3
	2014	3
	2015	3
	2016	3
	1974	1
	1977	3
	1978	3
	1983	2
	1984	1
1	2011	3
	2012	3
	2013	3
	2014	3
	2015	3
	2016	3
3	1974	3

Lake	Year	Maximum observed defoliation class
	1975	3
	1976	3
	1977	3
	1978	3
	1979	3
	1980	3
	1981	3
	1982	3
	1983	3
	1984	3
	1985	3
	2010	2
	2011	2
	2012	3
	2013	3
	2014	3
	2015	3

Lake	Year	Maximum observed defoliation class
	2016	3
Bois Joli	1973	1
	1974	2
	1975	3
	1976	3
	1977	3
	1978	3
	1980	1
	1981	3
	1982	3
	1983	3
	1984	2
	1985	1
	2013	1
	2014	1
	2015	2
	2016	2

Lake	Year	Maximum observed defoliation class
	2017	1
	2018	2
	2019	2
	1974	3
	1976	3
	1977	3
	1978	3
	1979	3
	1980	3
	1981	3
4	1982	3
	1983	3
	1984	3
	1985	3
	2012	2
	2013	3
	2015	3

Lake	Year	Maximum observed defoliation class
	2016	3
Buire	1974	3
	1975	3
	1976	3
	1977	3
	1978	3
	1979	2
	1980	2
	1981	3
	1983	3
	1984	2
	1985	1
	2015	1
	2016	3
	2017	3
	2018	3
Bélanger	1971	1

Lake	Year	Maximum observed defoliation class
	1972	3
	1973	2
	1974	3
	1975	3
	1976	3
	1977	3
	1978	3
	1979	3
	1980	3
	1981	3
	1982	0

APPENDIX D

LEPIDOPTERAN SCALE SPRUCE BUDWORM OUTBREAK DETECTION USING A 120-YEAR SMOOTHING WINDOW

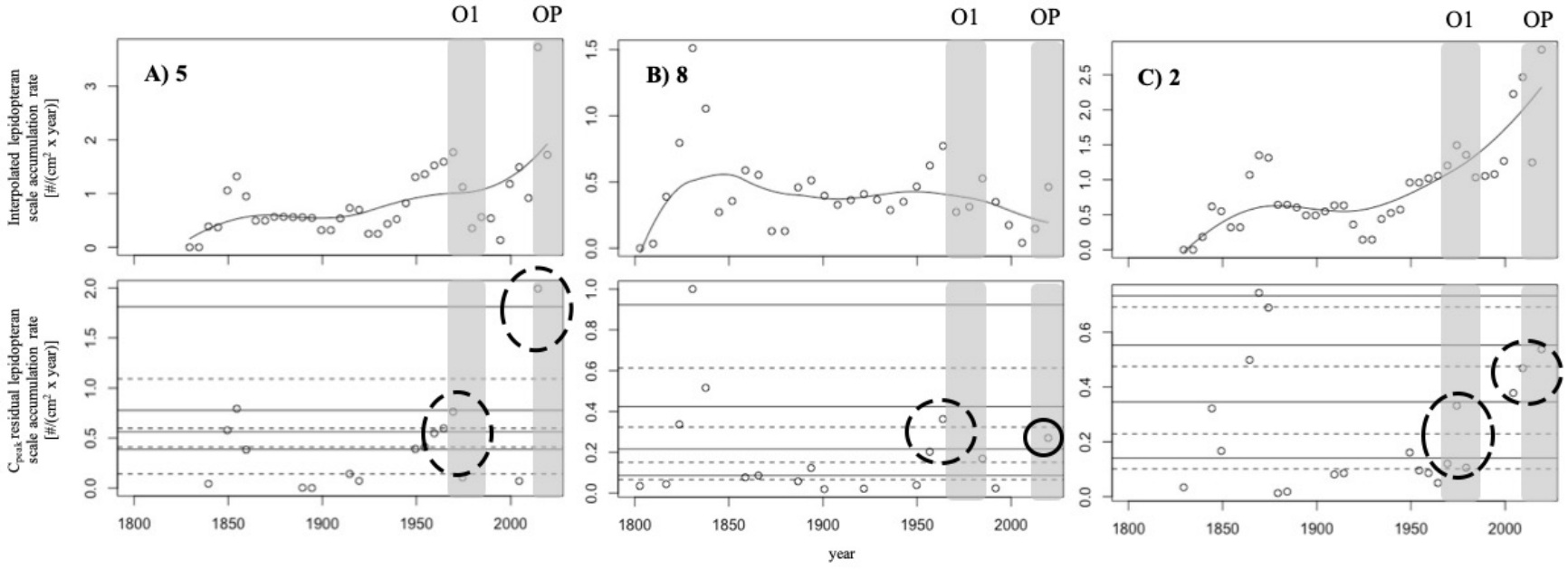

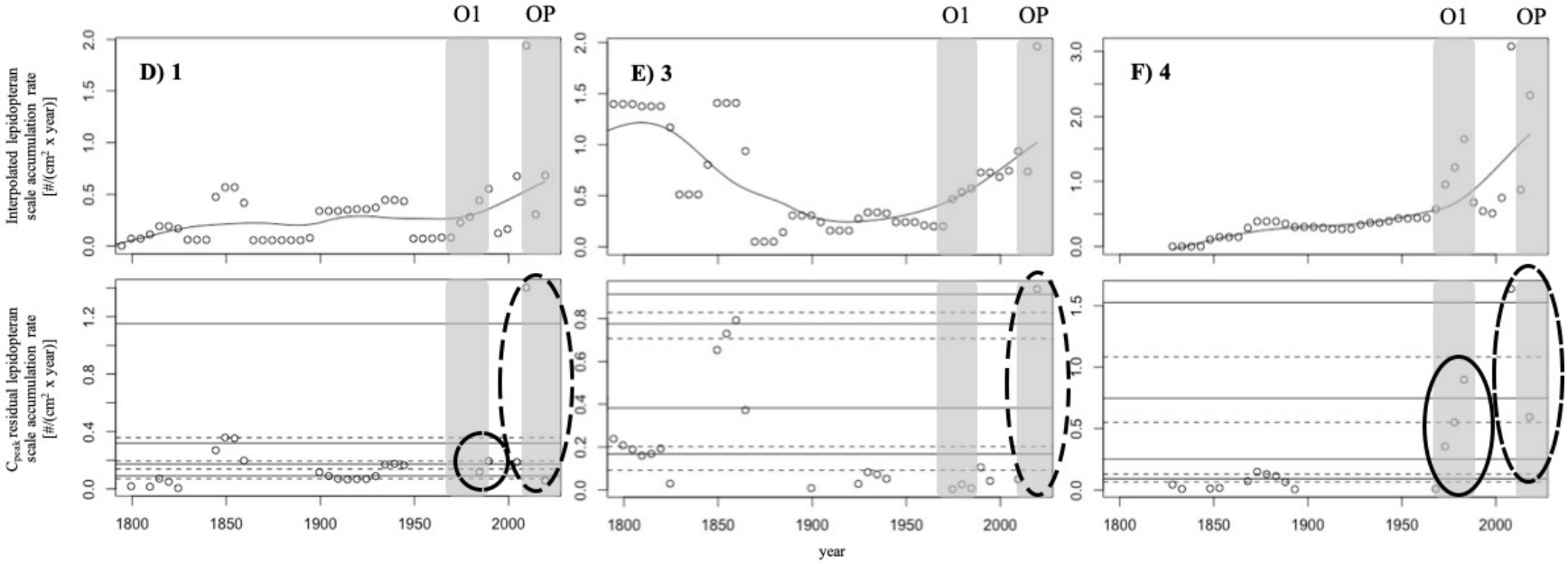
D) 1
E) 3
F) 4
O1
OP
Interpolated lepidopteran scale accumulation rate [#/(cm² x year)]
C_peak residual lepidopteran scale accumulation rate [#/(cm² x year)]
year

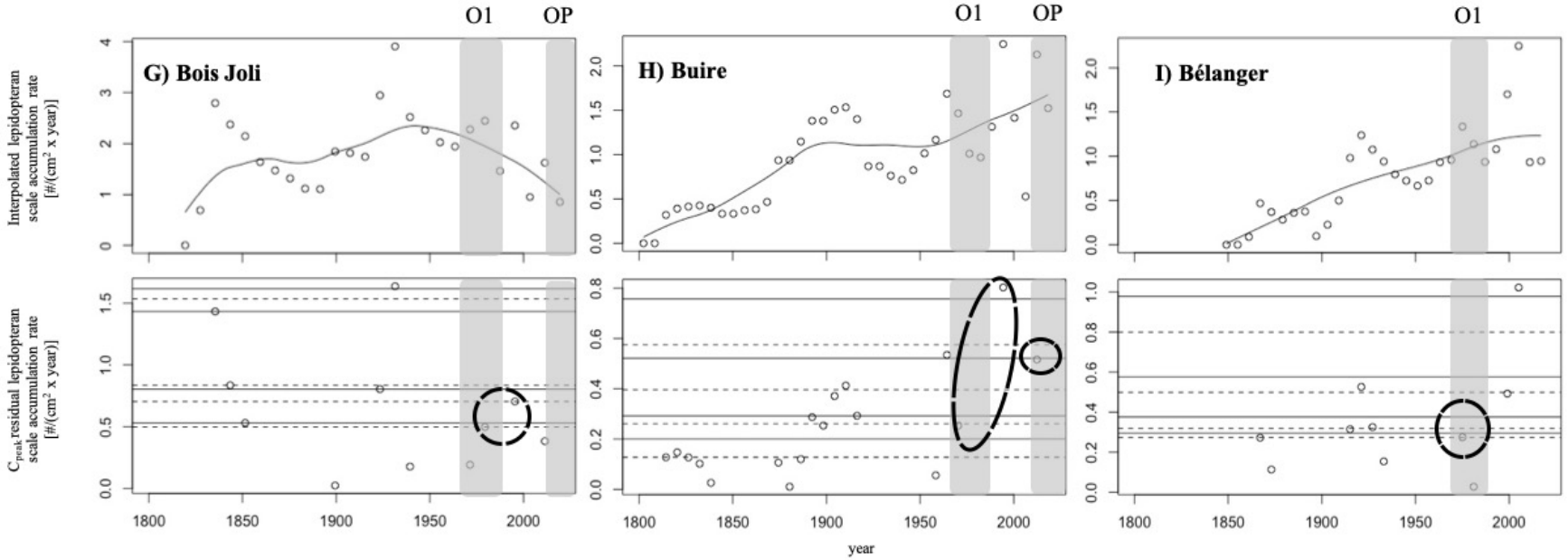

Figure D.1: Interpolated lepidopteran scale accumulations and C_{peak} accumulations using the lepidopteran scale paleo-proxy for Lakes (a) 5, (b) 8, (c) 2, (d) 1, (e) 3, (f) 4, (g) Bois Joli, (h) Buire, (i) Bélanger. The grey boxes represent the detected and defined outbreak periods by the aerial surveys and are identified as O1 (1971–1985; 1980s outbreak), and OP (2010–present; current outbreak) using the nomenclature used in Jardon et al., (2003), and Boulanger et al., (2012). The circles identify lepidopteran scale accumulation clusters representing potential outbreak events. Top panel: The solid smooth line represents the LOWESS with a 120-year smoothing window width used to determine the background accumulation rates (C_{back}), where everything above is considered a potential outbreak (C_{peak}). Bottom panel: The C_{peak} accumulations calculated as residuals along with the different percentile thresholds used. Dashed horizontal lines represent the 40^{th}, 60^{th}, 80^{th}, and 95^{th} percentile thresholds respectively, and the solid horizontal lines represent the 50^{th}, 70^{th}, 90^{th}, and 99^{th} percentile thresholds respectively above which the 'true' outbreak events (C_{fire}) were identified.

APPENDIX E
MEAN GSI AND WAVELET METHODOLOGICAL DETAILS

The mean growth suppression index (mean GSI) and the proportion of defoliated trees ('percent affected') for each site were obtained using the R package *dfoliatR* (Guiterman et al., 2020) to describe defoliation events. As non-host chronologies for the sites were unavailable, we determined tree-level defoliation events running the *defoliate_trees* function without a non-host chronology at a standard deviation threshold value of −1.28 and a minimum length of time of eight years (Swetnam and Lynch, 1989; Lynch, 2012; Guiterman et al., 2020). Both the *bridging events* and *series-end events* parameters were set as 'TRUE'. The former command eliminated multiple defoliation events that were most likely the same defoliation event over the course of the outbreaks. The latter detected the outbreak that was currently underway in the region. With the *outbreak* function set using the default settings, we calculated the mean GSI, and percent affected for each site at an annual resolution (Guiterman et al., 2020). The tree-level growth suppression index (GSI) is calculated as (Guiterman et al., 2020):

$$GSI_i = H_i - (NH_i - NH_m)\frac{\sigma_H}{\sigma_{NH}}$$

where GSI_i is the growth suppression index in year *i*, H and NH are the standardized host-tree and non-host ring-width series, respectively, NH_m is the mean non-host series' ring width, and σ_H/σ_{NH} is the ratio between the standard deviation of the standardized host and non-host series (Guiterman et al., 2020). In the absence of a non-host series, the GSI simply becomes the standardized host-tree ring-width series.

The correlation and synchronicity between the lepidopteran scale and tree-ring records (mean GSI and percent affected) were assessed using wavelet analysis. First, lepidopteran scale accumulations for each lake were interpolated to an annual resolution over the entire sediment chronology using the *pretreatment* function from the *paleofire* R package (Blarquez et al., 2014), permitting direct comparison between the scale and tree-ring records. The signal of each variable for each site was modeled using generalized additive models (GAMs) with a penalized cubic regression spline in the *gam* function from the *mgcv* R package (Wood, 2017). The number of knots was determined on the basis of model fit to the data and use of the *gam.check* function, which assessed the distribution of the residuals (visually and with a statistical test), the relationship between the measured and predicted variable, and normality (Wood, 2017). Wavelet analysis

was conducted in the *biwavelet* R package using the *wt* function with default settings to obtain temporal trends for each variable, and then the *xwt*, *wtc* functions (Gouhier et al., 2021) to determine correlation between the scale and tree-ring records. Finally, we determined the nature of the interaction between the two proxies by calculating the phase of the signal pairs which serves to reveal the nature of the interaction of the two records (Grinsted et al., 2004; Cazelles et al., 2008). We calculated the circular mean and standard deviation using the *circular* R package (Agostinelli and Lund, 2017) for the entire zone of significant high overlapping power and zones of high correlation ($R^2 \geq 0.80$) over the entire study period and for each individual known outbreak period (1912–1929, O3; 1946–1959, O2; and 1975–1992, O1; Morin and Laprise, 1990; Boulanger and Arseneault, 2004; Boulanger et al., 2012) for each site. Further, using the circular mean values and standard deviation, we described the signals as being in agreement or disagreement.

APPENDIX F

EFFECTS OF THE REMOVAL AND REPLACEMENT OF THE OUTLYING DATA POINT IN THE SITE 8 MEAN GSI SERIES

We removed and replaced an outlier from the mean GSI series, as it blurred the observed signal with downstream effects in wavelet analysis. We applied an identical procedure with the outlier and the imputed data point that replaced the outlier as described in the methods section. Retention of the outlying point for the year 1952 resulted in a linear mean GSI signal, when the mean GSI signal was not linear and actually decreased—presumably because of defoliation over the course of the ca. 1950 spruce budworm outbreak — as observed in other dendrochronological studies (Figure F.1a; Boulanger et al., 2012.). To obtain a more representative signal, we removed this outlier. However, to conduct wavelet analysis, a constant time-step is required; therefore, we interpolated a data point to replace the outlier. We believe that the resulting modeled signal better reflected the trend in mean GSI (Figure F.1b).

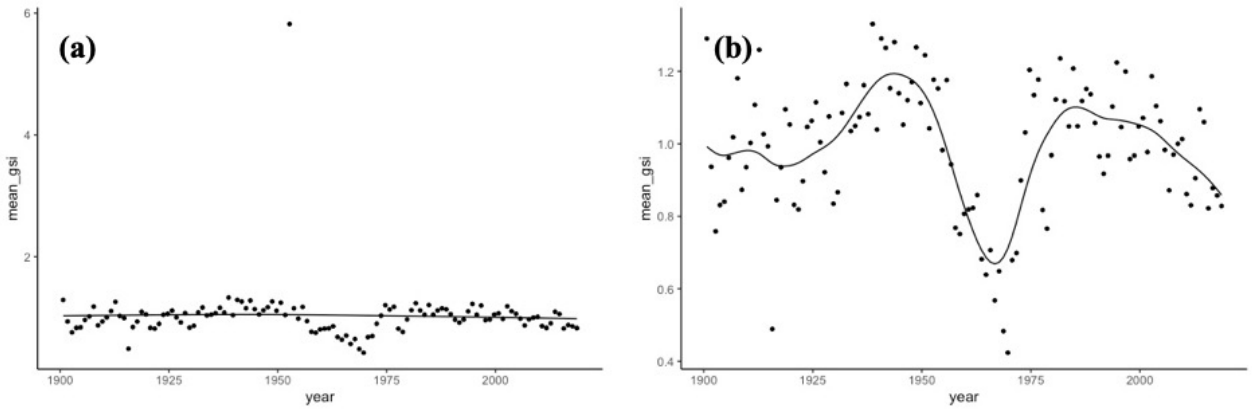

Figure F.1: The fitted GAM to the mean GSI of Site 8 (a) with the outlier and (b) with the interpolated data point.

The retention or replacement of the outlier subsequently affected the wavelet analysis conducted on the scale and tree-ring records. The power spectra of the mean GSI differed markedly (Figure F.2). The power spectrum with the retained outlier failed to detect any signal relative to red noise (Figure F.2a), whereas the power spectrum of the mean GSI with the imputed data point produced an area of significant power at a periodicity of about 32 years over the course of the middle to latter portion of the 20th century (Figure F.2b). Similarly, the effect of the retained outlier cascaded into the cross-wavelet and wavelet coherence analyses. The influence of the retained outlier did not markedly change the outcome of the cross-wavelet analysis in

terms of strength of areas of common power. Nonetheless, the zones of statistical significance did in fact vary as did the associated phases (Figure F.3). The differences in wavelet coherence analysis were less subtle. as different areas of significantly high correlation were identified, depending on whether we retained or replaced the outlier (Figure F.4). Furthermore, the associated phases in these areas of significant high correlation also differed (Figure F.4). We believe that the model using the replaced data point in the mean GSI is more representative of the data, and thus used this imputed data point for our analyses.

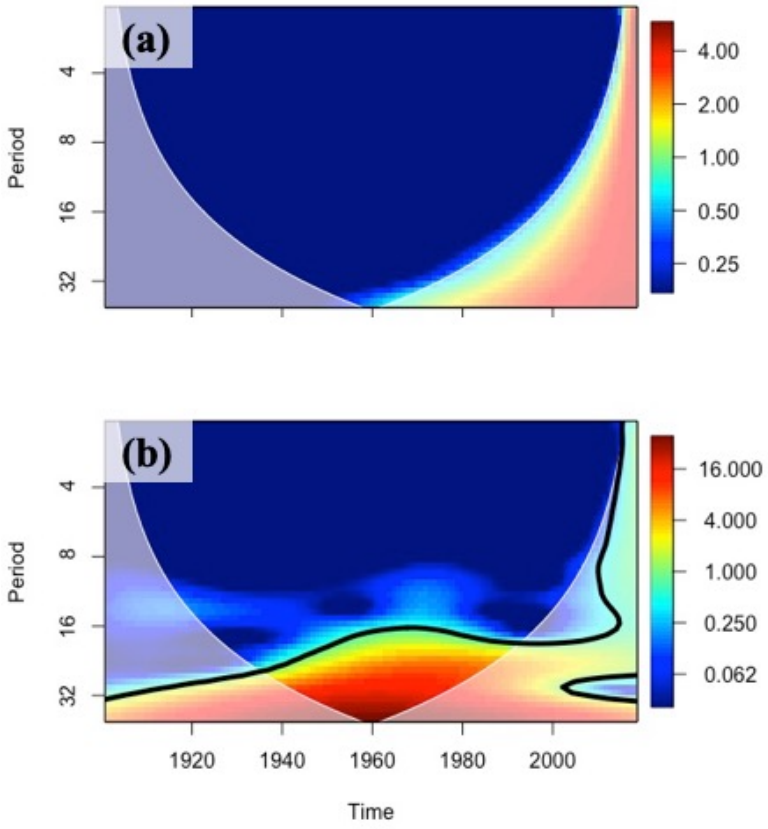

Figure F.2: Site 8's power spectra resulting from the applied continuous Morlet wavelet transform to the mean GSI series (a) with the outlier and (b) with the interpolated data point. Warmer colours (*red, orange, yellow*) indicate high power relative to red noise, an autoregressive process with lag 1, whereas cooler colours suggest weaker power (Torrence and Compo, 1998). Statistically significant zones of power were determined using a χ^2 test ($p<0.05$) and are delineated by a thick black line (Torrence and Compo, 1998). The light grey shading delineates the recommended zone of interpretation, i.e., 'cone of influence' (Cazelles et al., 2008).

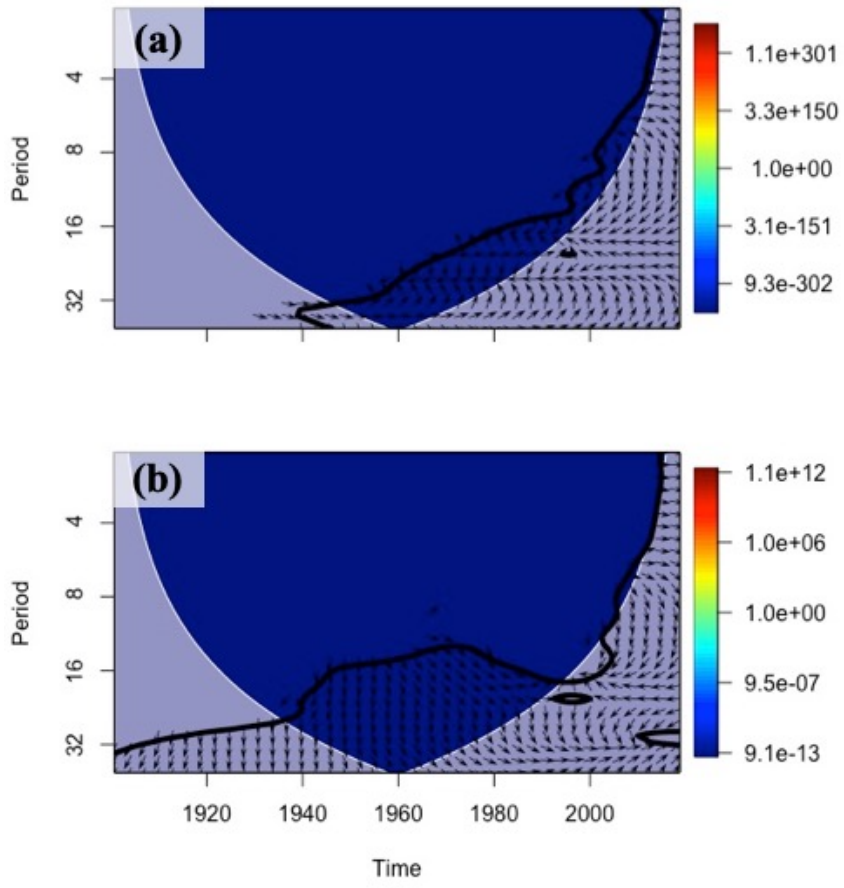

Figure F.3: The cross-wavelet analysis between the lepidopteran scale and mean GSI series applied to Site 8 (a) with the outlier, and (b) with the interpolated data point. Warmer colours (*red, orange, yellow*) indicate high overlapping power relative to red noise, an autoregressive process with lag 1, whereas cooler colours suggest weaker overlapping power (Torrence and Compo, 1998). Statistically significant zones of power were determined using a χ^2 test ($p<0.05$) and are delineated by a thick black line (Torrence and Compo, 1998). The arrows in the areas of statistical significance specify the type of association. Arrows pointing left indicate the signals are anti-phase, where a peak of one signal lines up with a trough of the other signal. Arrows pointing right suggest signals are in-phase, where peaks and troughs of both signals line up. Downward arrows indicate that the scale record leads the tree-ring record by $\pi/2$, whereas upward arrows indicate the opposite. The light grey shading delineates the recommended zone of interpretation, i.e., 'cone of influence' (Cazelles et al., 2008).

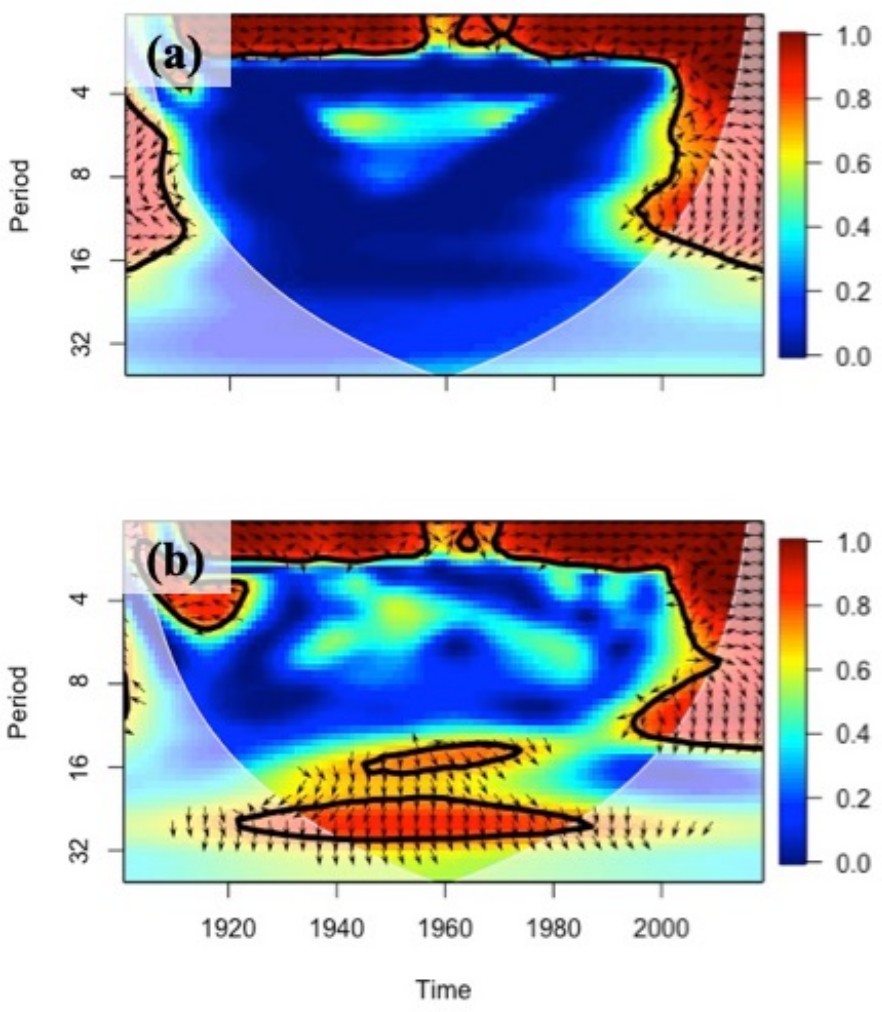

Figure F.4: The wavelet coherence analysis between the lepidopteran scale and mean GSI series applied to Site 8 (a) with the outlier, and (b) with the interpolated data point. Warmer colours (*red, orange, yellow*) indicate high correlation, relative to red noise, autogressive process of lag 1, whereas cooler colours represent weaker correlations (Torrence and Compo, 1998). Statistically significant zones were determined using a χ^2 test ($p<0.05$) and are delineated by a thick black line (Torrence and Compo, 1998). The arrows in areas of statistical significance specify the type of association. Arrows pointing left indicate the signals are anti-phase, where a peak of one signal lines up with a trough of the other signal. Arrows pointing right suggest signals are in-phase, where peaks and troughs of both signals line up. Downward arrows indicate that the scale record leads the tree-ring record by $\pi/2$, whereas upward arrows indicate the opposite. The light grey shading delineates the recommended zone of interpretation, i.e., 'cone of influence' (Cazelles et al., 2008).

APPENDIX G

LEPIDOPTERAN SCALE AND TREE-RING CHRONOLOGIES USED FOR WAVELET ANALYSIS

The full surface sediment chronologies for the lakes of all sites is presented (Figure G.1) along with the corresponding sediment and tree-ring chronologies used for the wavelet analysis for each individual site (Figures G.2–G.10). The temporal interval of lepidopteran scale accumulation analysis was 1900 AD-2019 AD (Figure G.1) to match the time interval covered by the tree-ring chronologies.

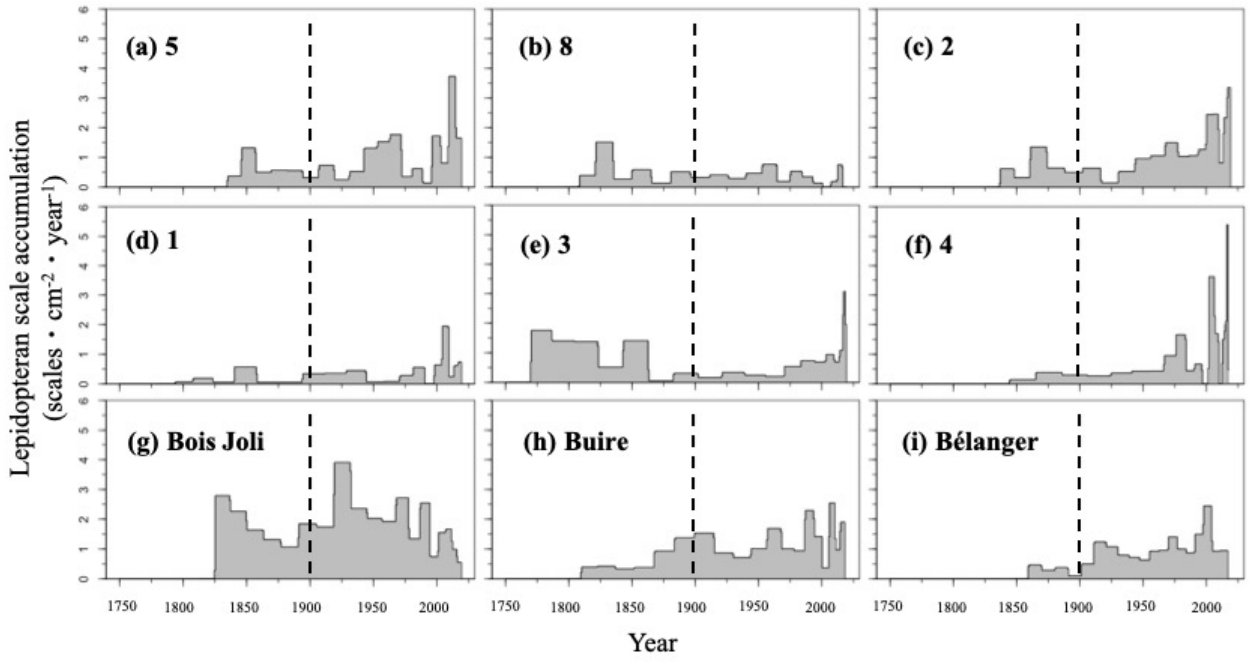

Figure G.1: The lepidopteran scale accumulation rate (*grey bars*) and annually interpolated lepidopteran scale accumulations (*thin continuous black line delineating grey bars*) for (a) Lake 5, (b) Lake 8, (c) Lake 2, (d) Lake 1, (e) Lake 3, (f) Lake 4, (g) Lake Bois Joli, (h) Lake Buire, and (i) Lake Bélanger. Accumulation records to the right of the vertical dotted line (1900 AD) were analyzed in the study, whereas scale accumulation before 1900 AD was not. The grey bars represent the lepidopteran scale accumulations for each lake; the continuous black line represents the respective annually interpolated accumulation rates.

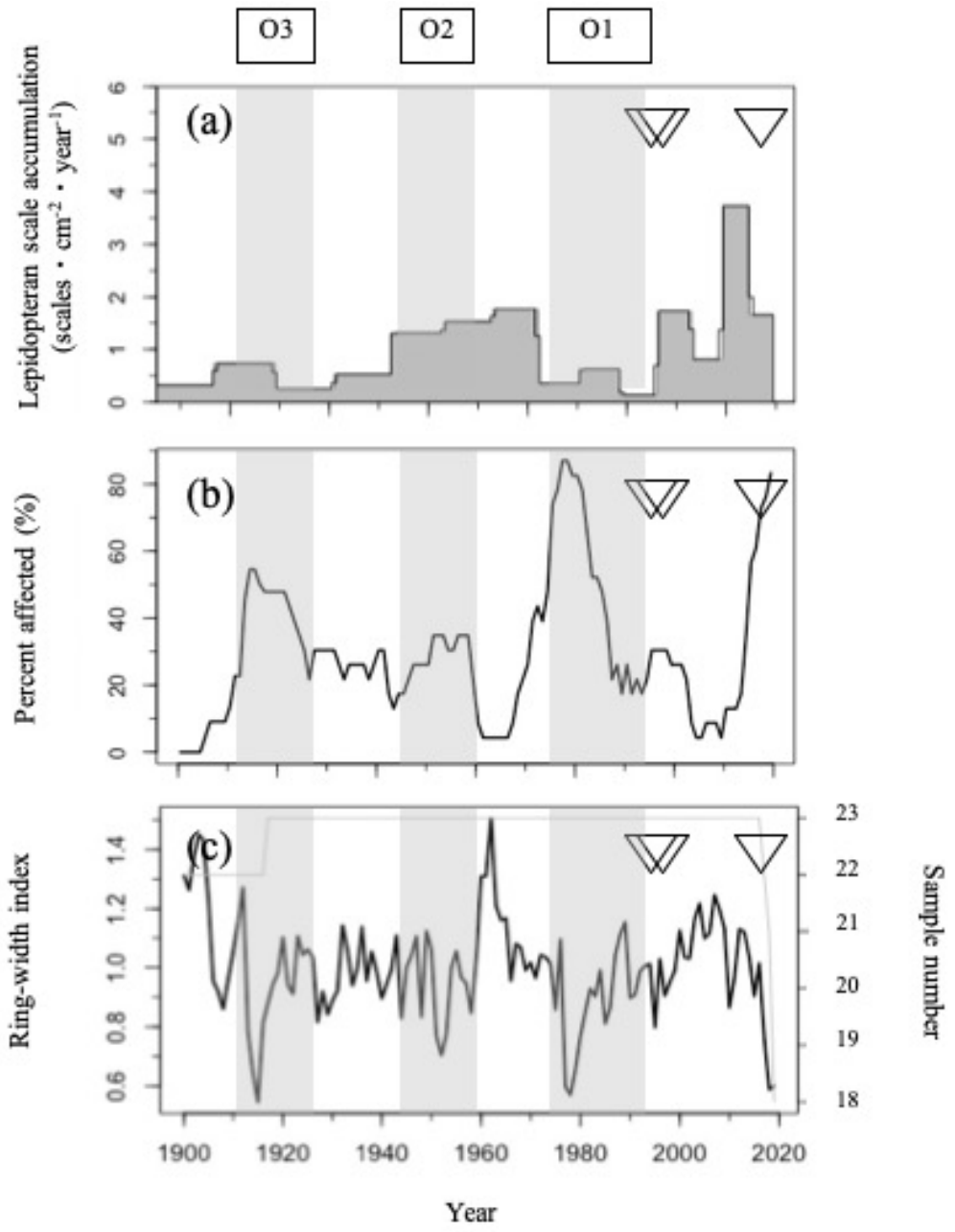

Figure G.2: The lepidopteran and tree-ring width indices recording the impacts of the spruce budworm for Site 5. The (a) lepidopteran scale accumulation rate (*dark grey bars*) and annually interpolated accumulation rate (*black line delineating grey bars*), (b) the proportion of affected trees, and (c) ring-width index (*black line*), and sample number (*grey line*) for the expressed population signal (EPS) chronology from 1900-2019. The white triangles represent the approximate dates of known recorded timber harvesting events within a 200 m radius around the lake on the basis of available forest inventory data. O3, O2, and O1 delineate the periods of known spruce budworm outbreaks in the 20th century corresponding to 1912-1929, 1946-1959, and 1975-1992 respectively (Morin and Laprise, 1990; Boulanger and Arseneault, 2004; Boulanger et al., 2012).

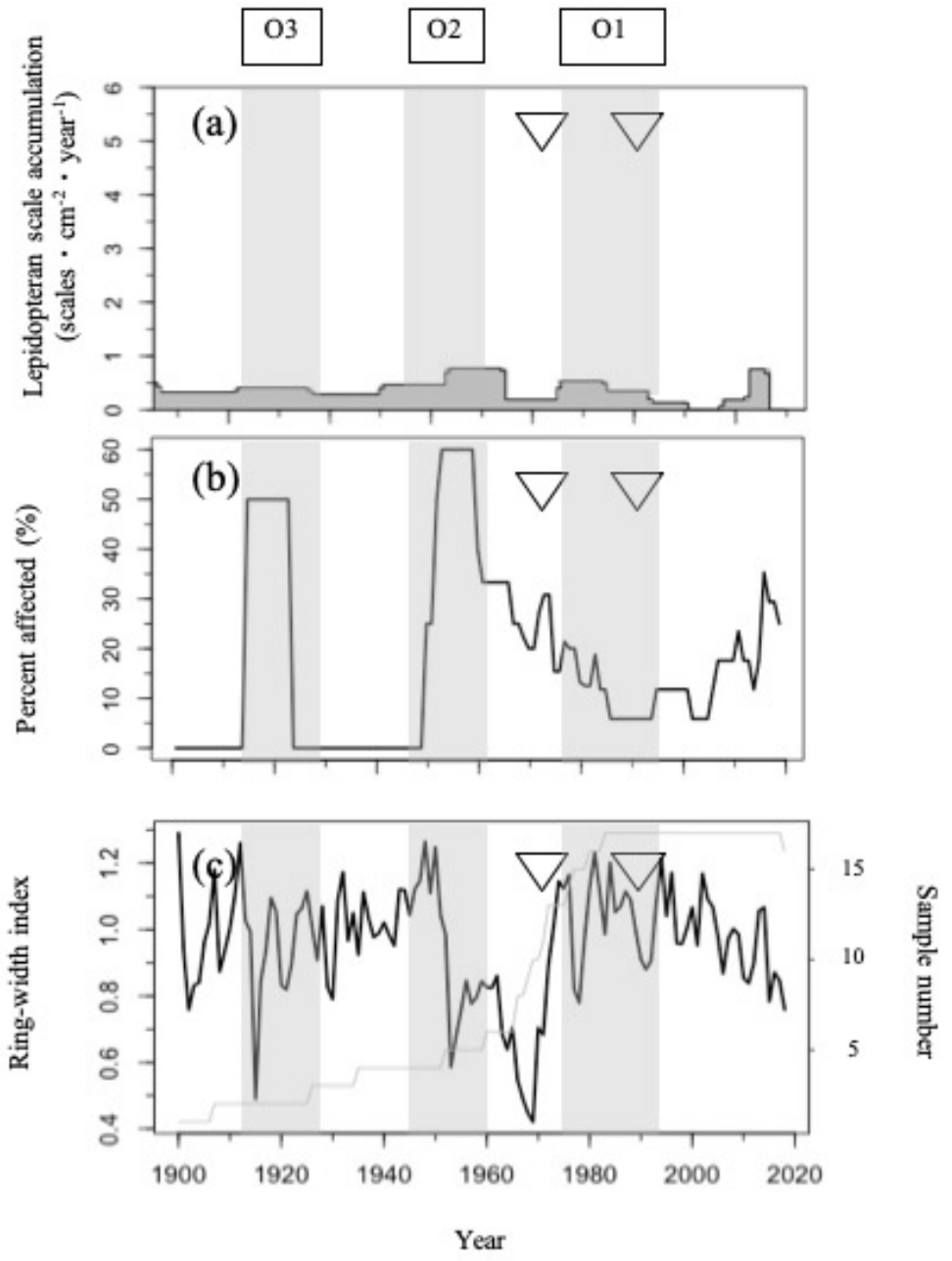

Figure G.3: The lepidopteran and tree-ring width indices recording the impacts of the spruce budworm for Site 8. The (a) lepidopteran scale accumulation rate (*dark grey bars*) and annually interpolated accumulation rate (*black line delineating grey bars*), (b) the proportion of affected trees, and (c) ring-width index (*black line*), and sample number (grey line) for the expressed population signal (EPS) chronology from 1900-2019. The white triangles represent the approximate dates of known recorded timber harvesting events within a 200 m radius around the lake on the basis of available forest inventory data. O3, O2, and O1 delineate the periods of known spruce budworm outbreaks in the 20th century corresponding to 1912-1929, 1946-1959, and 1975-1992 respectively (Morin and Laprise, 1990; Boulanger and Arseneault, 2004; Boulanger et al., 2012).

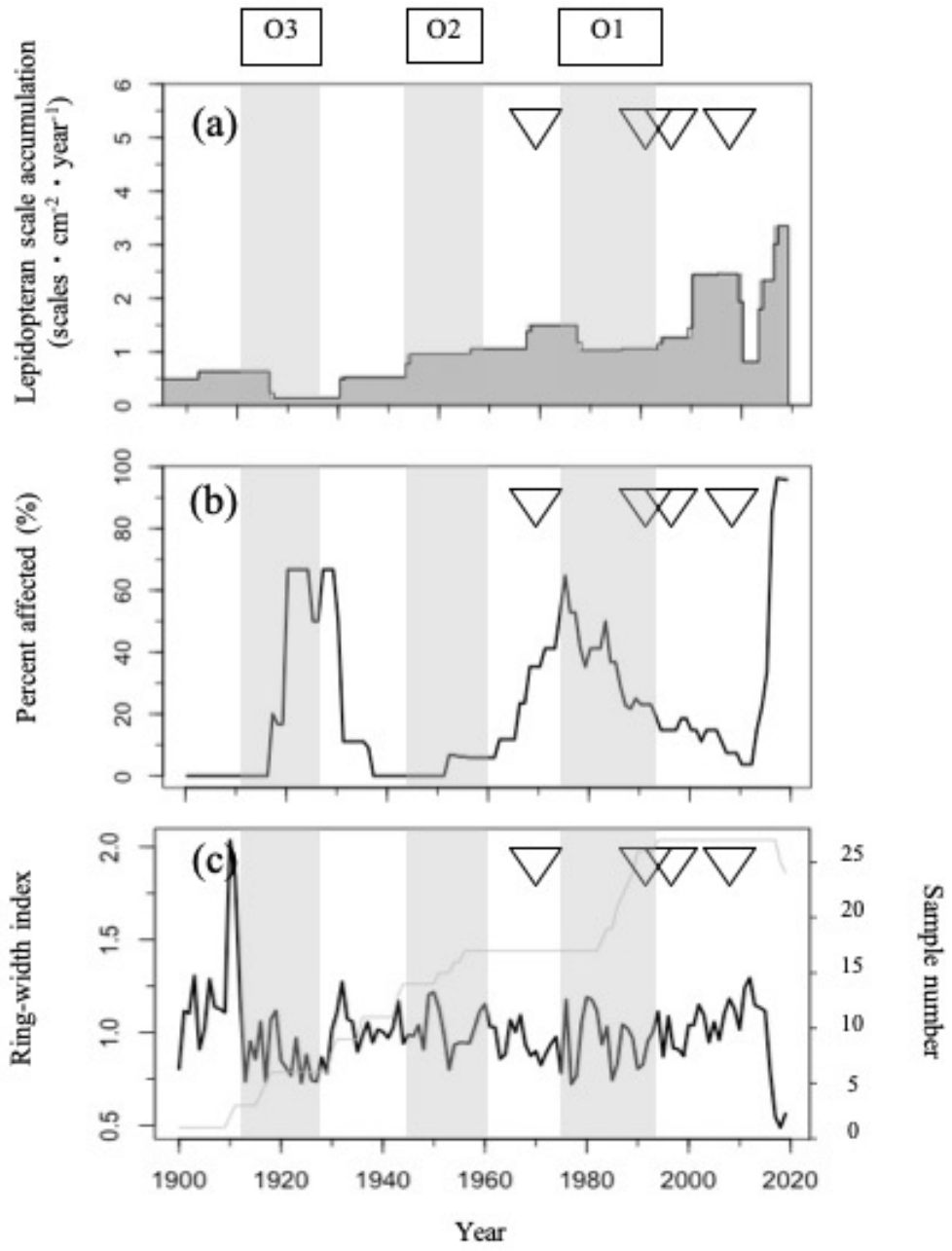

Figure G.4: The lepidopteran and tree-ring width indices recording the impacts of the spruce budworm for Site 2. The (a) lepidopteran scale accumulation rate (*dark grey bars*) and annually interpolated accumulation rate (*black line delineating grey bars*), (b) the proportion of affected trees, and (c) ring-width index (*black line*), and sample number (*grey line*) for the expressed population signal (EPS) chronology from 1900-2019. The white triangles represent the approximate dates of known recorded timber harvesting events within a 200 m radius around the lake on the basis of available forest inventory data. O3, O2, and O1 delineate the periods of known spruce budworm outbreaks in the 20th century corresponding to 1912-1929, 1946-1959, and 1975-1992 respectively (Morin and Laprise, 1990; Boulanger and Arseneault, 2004; Boulanger et al., 2012).

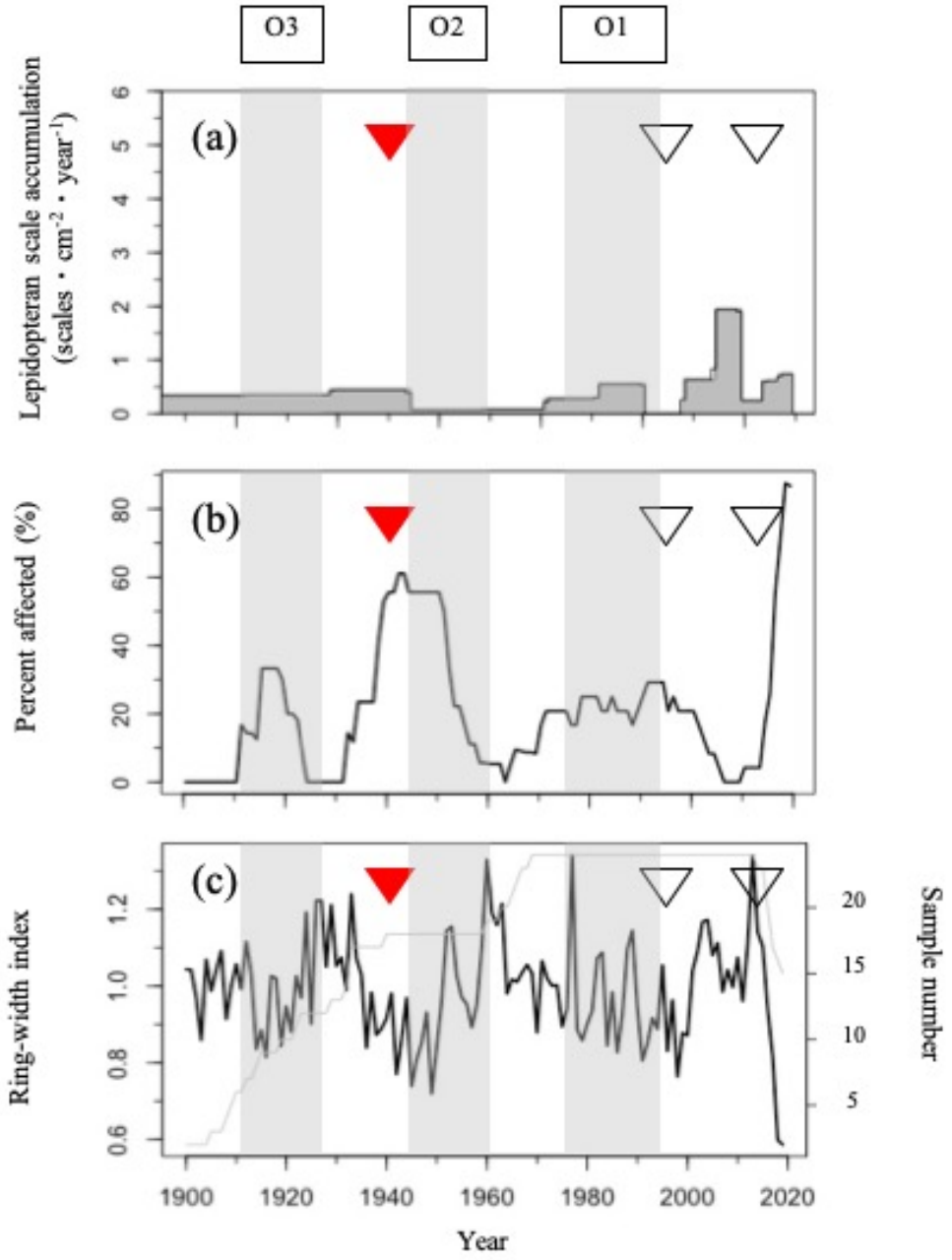

Figure G.5: The lepidopteran and tree-ring width indices recording the impacts of the spruce budworm for Site 1. The (a) lepidopteran scale accumulation rate (*dark grey bars*) and annually interpolated accumulation rate (*black line delineating grey bars*), (b) the proportion of affected trees, and (c) ring-width index (*black line*), and sample number (*grey line*) for the expressed population signal (EPS) chronology from 1900-2019. The white and red triangles represent the approximate dates of known recorded timber harvesting, and wildfire events, respectively, within a 200 m radius around the lake on the basis of available forest inventory data. O3, O2, and O1 delineate the periods of known spruce budworm outbreaks in the 20th century corresponding to 1912-1929, 1946-1959, and 1975-1992 respectively (Morin and Laprise, 1990; Boulanger and Arseneault, 2004; Boulanger et al., 2012).

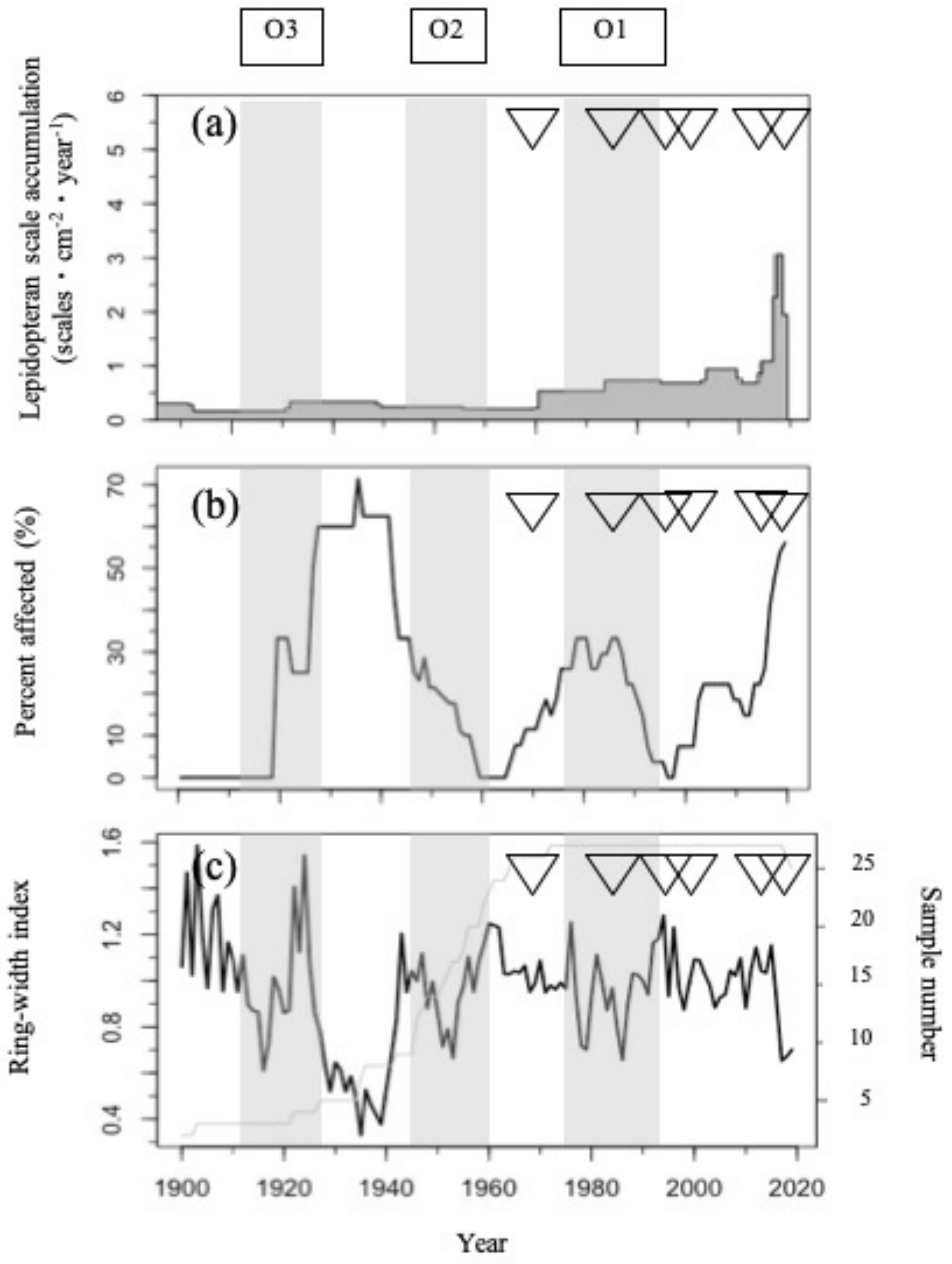

Figure G.6: The lepidopteran and tree-ring width indices recording the impacts of the spruce budworm for Site 3. The (a) lepidopteran scale accumulation rate (*dark grey bars*) and annually interpolated accumulation rate (*black line delineating grey bars*), (b) the proportion of affected trees, and (c) ring-width index (*black line*), and sample number (*grey line*) for the expressed population signal (EPS) chronology from 1900-2019. The white triangles represent the approximate dates of known recorded timber harvesting events within a 200 m radius around the lake on the basis of available forest inventory data. O3, O2, and O1 delineate the periods of known spruce budworm outbreaks in the 20th century corresponding to 1912-1929, 1946-1959, and 1975-1992 respectively (Morin and Laprise, 1990; Boulanger and Arseneault, 2004; Boulanger et al., 2012).

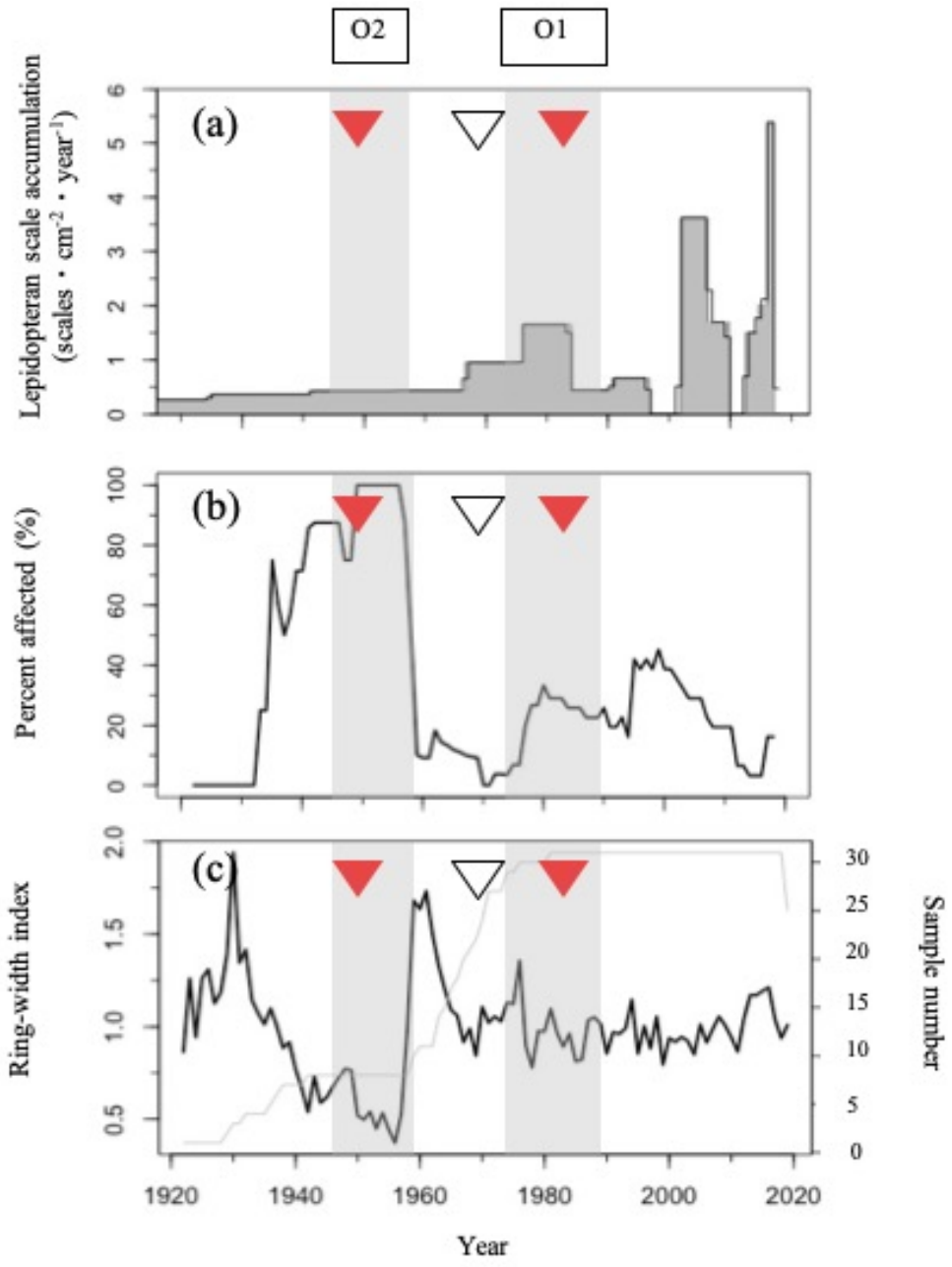

Figure G.7: The lepidopteran and tree-ring width indices recording the impacts of the spruce budworm for Site 4. The (a) lepidopteran scale accumulation rate (*dark grey bars*) and annually interpolated accumulation rate (*black line delineating grey bars*), (b) the proportion of affected trees, and (c) ring-width index (*black line*), and sample number (*grey line*) for the expressed population signal (EPS) chronology from 1900-2019. The white and red triangles represent the approximate dates of known recorded timber harvesting, and wildfire events, respectively, within a 200 m radius around the lake on the basis of available forest inventory data. O3, O2, and O1 delineate the periods of known spruce budworm outbreaks in the 20th century corresponding to 1912-1929, 1946-1959, and 1975-1992 respectively (Morin and Laprise, 1990; Boulanger and Arseneault, 2004; Boulanger et al., 2012).

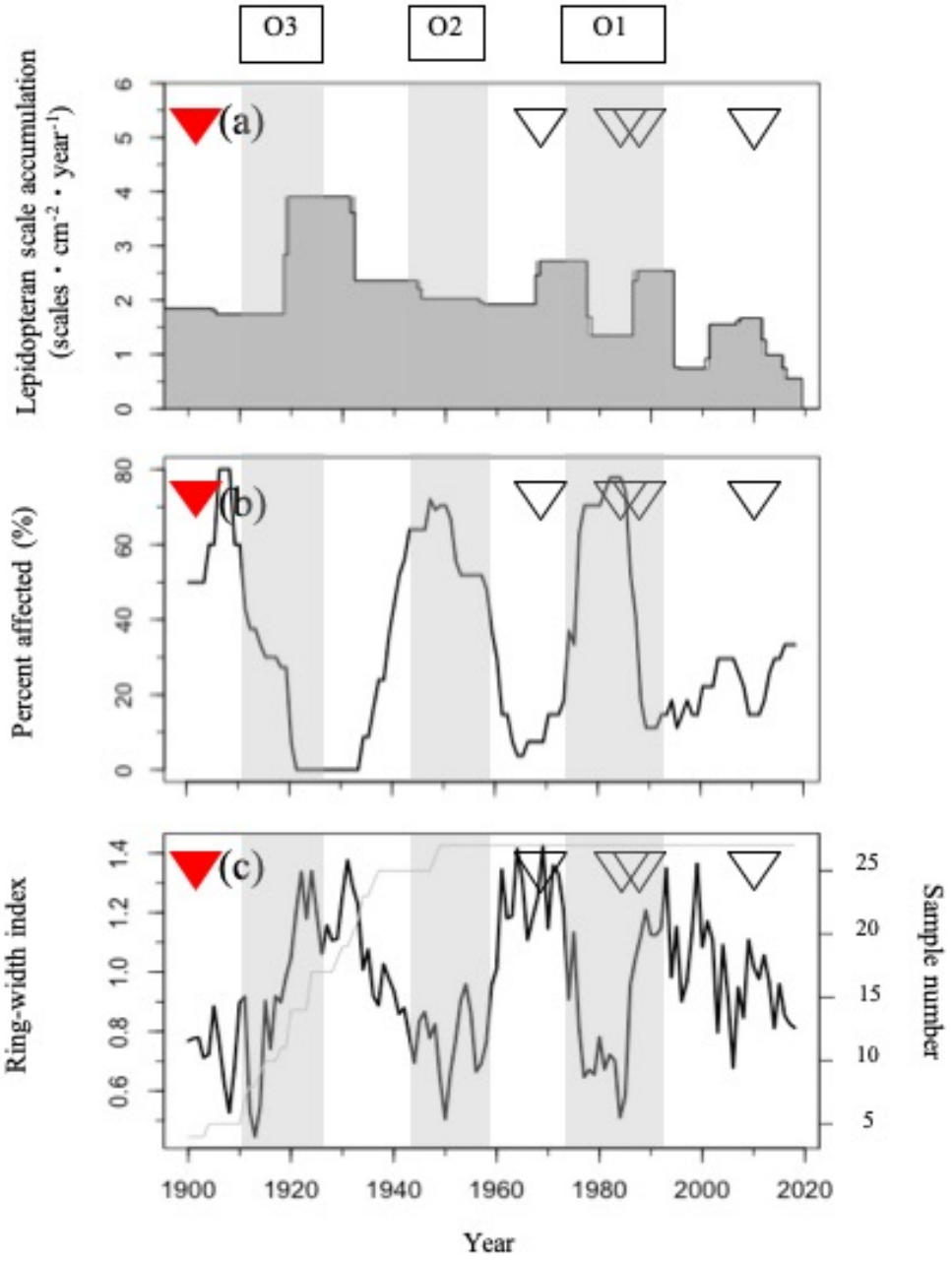

Figure G.8: The lepidopteran and tree-ring width indices recording the impacts of the spruce budworm for Site Bois Joli. The (a) lepidopteran scale accumulation rate (*dark grey bars*) and annually interpolated accumulation rate (*black line delineating grey bars*), (b) the proportion of affected trees, and (c) ring-width index (*black line*), and sample number (*grey line*) for the expressed population signal (EPS) chronology from 1900-2019. The white and red triangles represent the approximate dates of known recorded timber harvesting, and wildfire events, respectively, within a 200 m radius around the lake on the basis of available forest inventory data. O3, O2, and O1 delineate the periods of known spruce budworm outbreaks in the 20th century corresponding to 1912-1929, 1946-1959, and 1975-1992 respectively (Morin and Laprise, 1990; Boulanger and Arseneault, 2004; Boulanger et al., 2012).

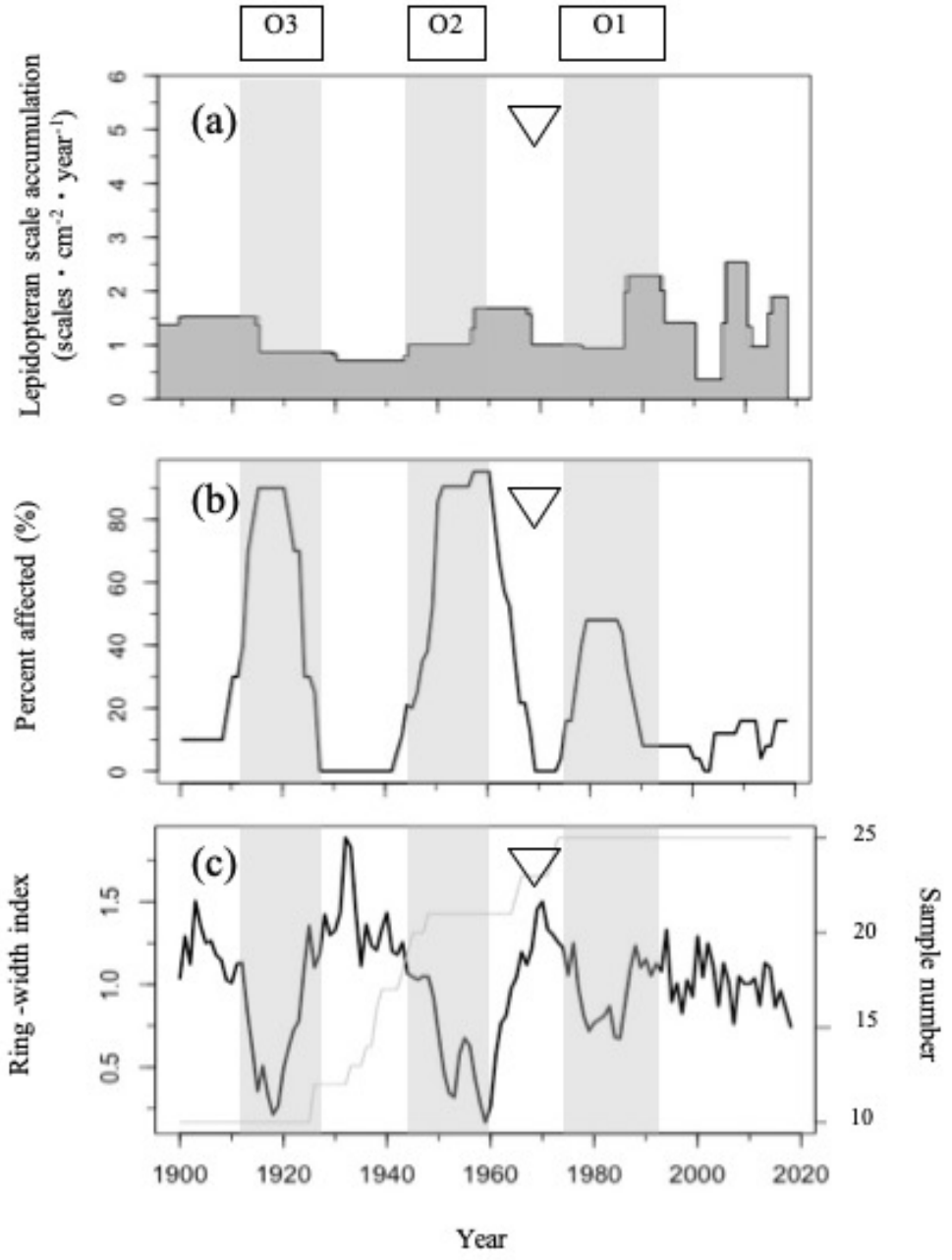

Figure G.9: The lepidopteran and tree-ring width indices recording the impacts of the spruce budworm for Site Buire. The (a) lepidopteran scale accumulation rate (*dark grey bars*) and annually interpolated accumulation rate (*black line delineating grey bars*), (b) the proportion of affected trees, and (c) ring-width index (*black line*), and sample number (*grey line*) for the expressed population signal (EPS) chronology from 1900-2019. The white triangles represent the approximate dates of known recorded timber harvesting events within a 200 m radius around the lake on the basis of available forest inventory data. O3, O2, and O1 delineate the periods of known spruce budworm outbreaks in the 20th century corresponding to 1912-1929, 1946-1959, and 1975-1992 respectively (Morin and Laprise, 1990; Boulanger and Arseneault, 2004; Boulanger et al., 2012).

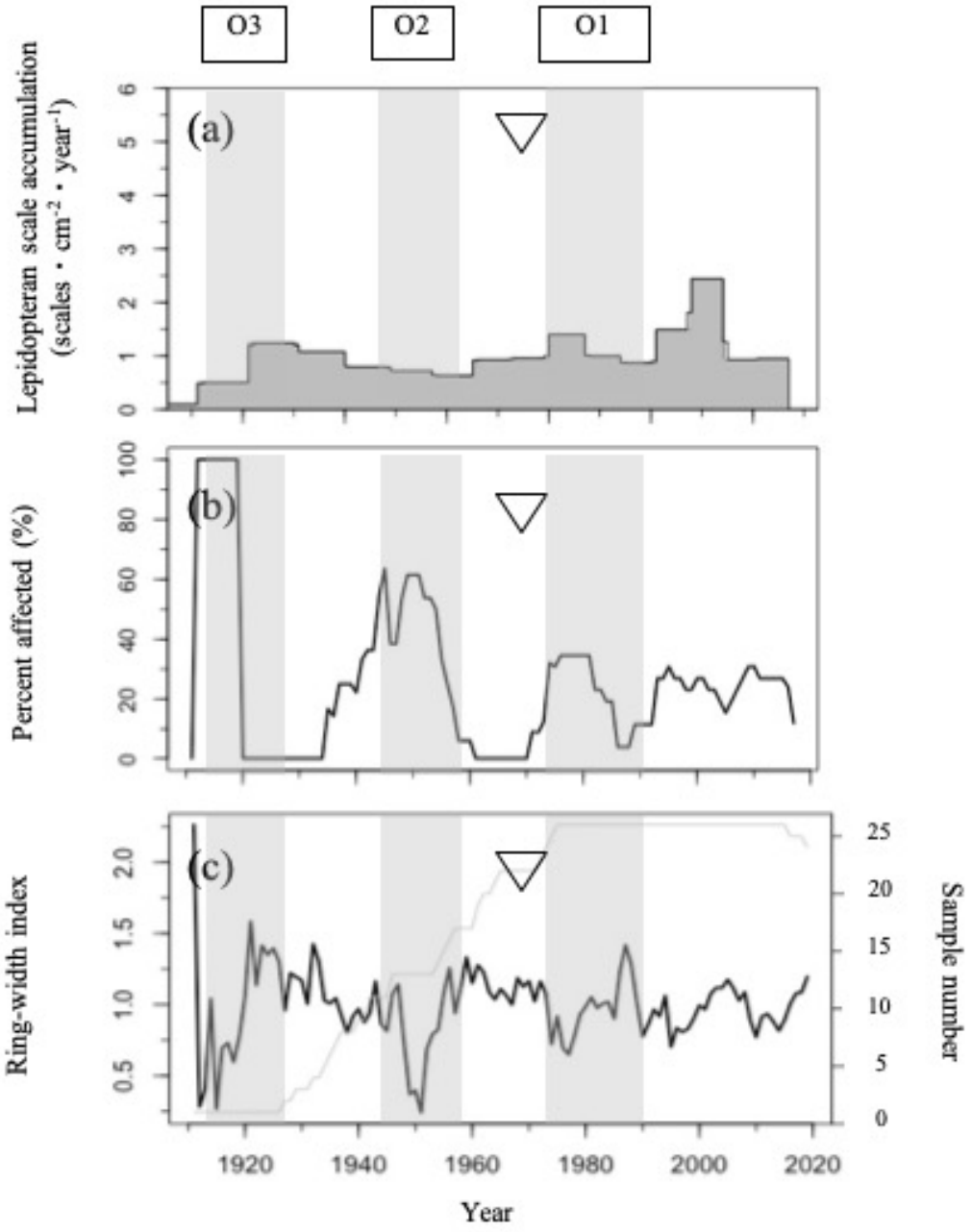

Figure G.10: The lepidopteran and tree-ring width indices recording the impacts of the spruce budworm for Site Bélanger. The (a) lepidopteran scale accumulation rate (*dark grey bars*) and annually interpolated accumulation rate (*black line delineating grey bars*), (b) the proportion of affected trees, and (c) ring-width index (*black line*), and sample number (*grey line*) for the expressed population signal (EPS) chronology from 1900-2019. The white triangles represent the approximate dates of known recorded timber harvesting events within a 200 m radius around the lake on the basis of available forest inventory data. O3, O2, and O1 delineate the periods of known spruce budworm outbreaks in the 20th century corresponding to 1912-1929, 1946-1959, and 1975-1992 respectively (Morin and Laprise, 1990; Boulanger and Arseneault, 2004; Boulanger et al., 2012).

APPENDIX H
POLLEN DIAGRAMS

Pollen counts of the major arboreal species in the mixed boreal forest were conducted over the entire length of the Lake Buire sediment column at an approximate 100-year interval to obtain the changes in forest composition over time. Specifically, species typically associated with wildfire presence and absence such as *Picea cf mariana*, and *Betula spp* and *Abies balsamea*, and *Pinus strobus* respectively, were retained and assessed. Percentage of each species over time was derived from the pollen influx (Figure H.1). The *Abies:Picea* ratio was obtained by dividing the percentage of *A. balsamea* pollen present relative to the percentage of *P. cf. mariana* pollen present at each corresponding depth. Therefore, an increase in the ratio suggests a greater proportion of *A. balsamea* present relative to *P. cf. mariana* or a decrease in the proportion of *P. cf. mariana* present relative to *A. balsamea*. Conversely, a decrease in the ratio may suggest either an increase in *P. cf. mariana* relative to *A. balsamea* or a decrease in *A. balsamea* pollen relative to *P. cf. mariana*. The pollen graph was created using the *rioja* package (Juggens, 2020) with the R statistical software (R Core Team, 2021).

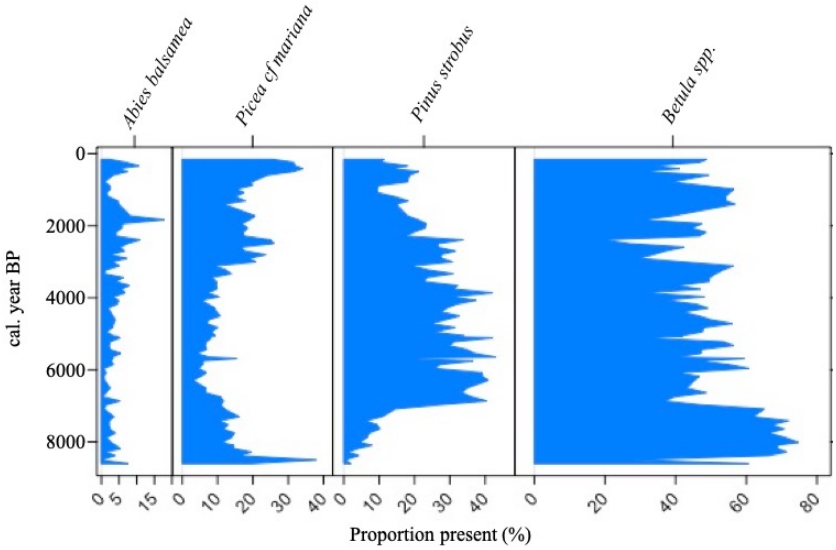

Figure H.1: The percentage of pollen of the major arboreal species present over time at Lake Buire.

APPENDIX I
DISTURBANCE EVENT FREQUENCY SMOOTHING WINDOW WIDTHS

In order to determine the optimal smoothing window width, percent change in the variability of disturbance event frequency was calculated using the following:

$$\%\ change = \frac{(reference\ value - new\ value)}{reference\ value}$$

where *reference value* was the variance in event frequency captured with the smallest useable window width (100 years in this case); *new value* was the variance in event frequency captured by a window-width of 200, 300, 400, 500, 1000 years, or a window width determined by unbiased cross-validation ('BW.UCV'; Blarquez et al. 2014; Figure I.1). A negative value in the *% change* metric suggests a loss in variance. In an effort to strike a balance between retaining as much variability as possible and maintain an adequate sample size, the 200-year window was selected to calculate the event frequencies for both the spruce budworm and wildfires (Figure I.2).

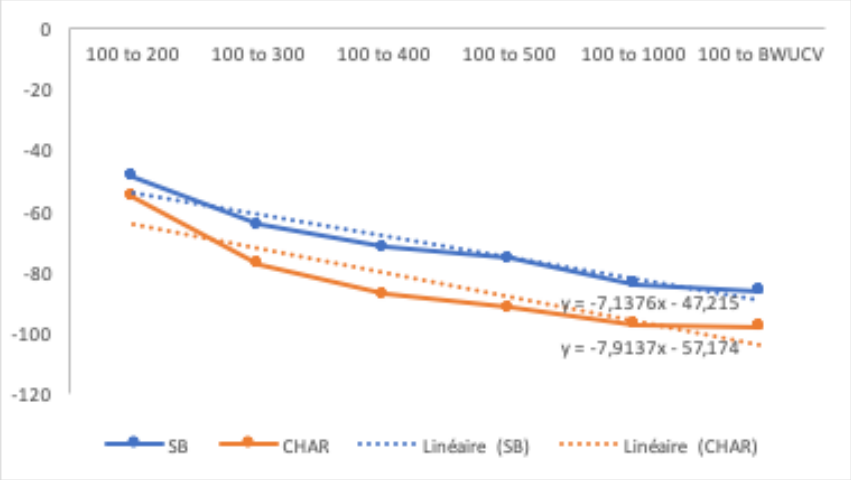

Figure I.1: The percent change in the variance when using different smoothing window widths for lepidopteran scale (*SB; blue points and lines*) and charcoal accumulations (*CHAR; orange points and line*).

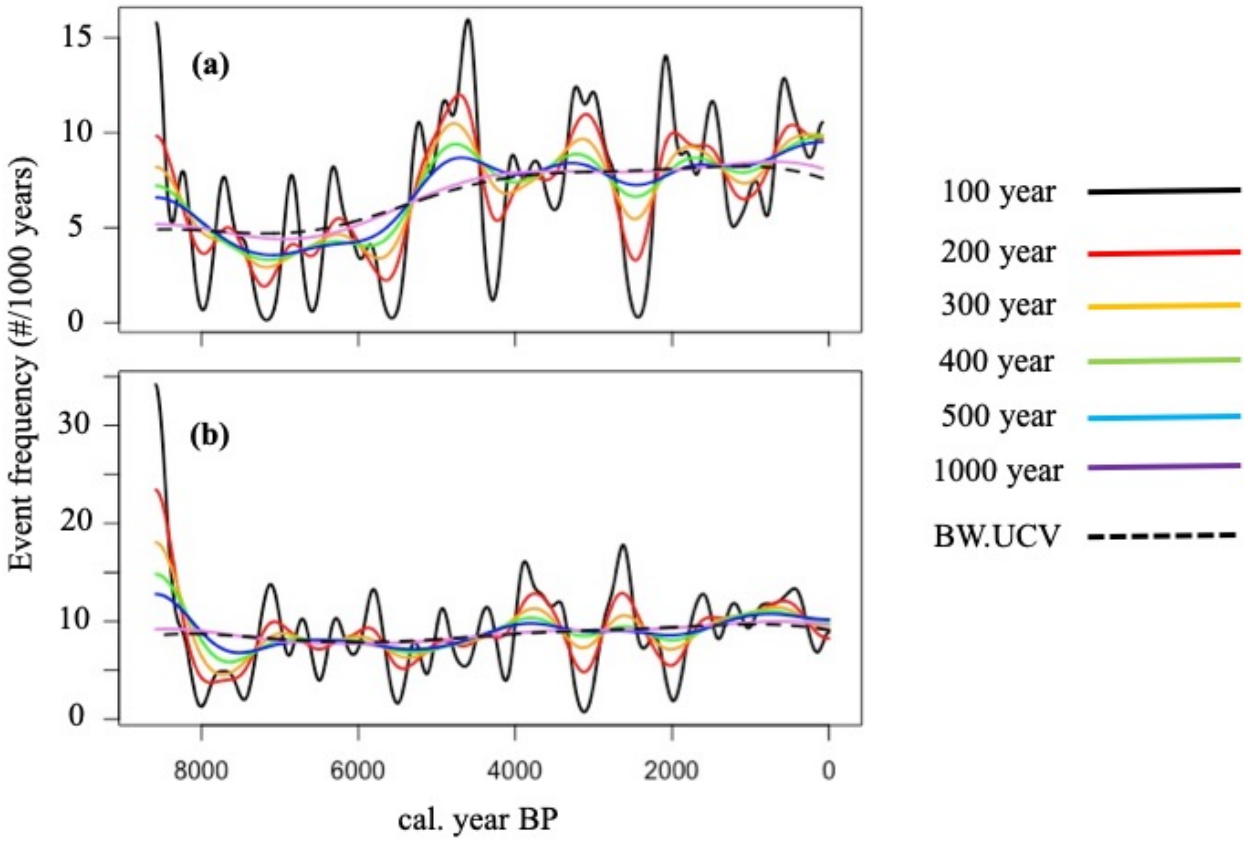

Figure I.2: The disturbance event frequencies as calculated by different smoothing window widths with the *kdffreq* function (Blarquez et al., 2014) for (a) the large spruce budworm population and (b) wildfire events.

APPENDIX J
STARS METHODOLOGICAL DETAILS

The STARS method is used to identify change points in a time series (i.e. changes in spruce budworm and wildfire event frequencies over the course of the Holocene) by comparing each observation to the previous observations and determining whether a regime shift has occurred (Rodionov, 2004; Stirnimann et al., 2019). This is done using a running window of specified width, *l*, within which a Student's t-test is performed determining whether the new observation rejects or fails to reject the null hypothesis i.e., is there the presence of a regime shift? (Rodionov, 2004; Stirnimann et al., 2019). A potential change point is identified when the mean value of the new regime exceeds the range established by the old regime (Rodionov, 2004; Rodionov and Overland, 2005):

$$\overline{x_{new}} = \overline{x_{cur}} \pm t\sqrt{2\sigma_l^2/_l}$$

where $\overline{x_{new}}$ is the mean for the new regime; $\overline{x_{cur}}$ is the mean for the current regime; *t* is the value obtained from the t-distribution with degrees of freedom of 2*l*-2 at probability level *p* (Rodionov 2004); σ_l^2 is the average variance of the *l*-year intervals in the time series; *l* is the window width specified by the user. The Regime Shift Index (RSI) is calculated at each potential change point, *c*, and is used to reject (or fail to reject) the null hypothesis (Rodionov 2004; Rodionov and Overland 2005):

$$RSI_c = \sum_{i=c}^{c+m} \frac{x_i^*}{l\sigma_l}$$

where RSI_c is the cumulative sum of normalized deviations, x_i^*, of the new potential mean with $x_i^* = \overline{x_{new}} - x_i$ indicating a downward shift and $x_i^* = \overline{x_{new}} - x_i$ indicating an upward shift (Rodionov, 2004; Stirnimann et al., 2019); *c* is the potential change point; *m* is the number of observations since starting the new regime and ranges from 0 to *l*-1; *l* is the user-specified window width; and σ_l is the mean standard deviation of all the intervals in the time-series of width *l* (Rodionov and Overland, 2005). A new regime is identified at *c* when the RSI sum maintains a positive value over the length of *l*-1; otherwise, if the sum becomes negative, the test has failed at the chosen level of significance, *p*, and RSI is assigned a value of 0 (Rodionov, 2004; Rodionov and Overland, 2005).

Prior to conducting STARS certain considerations must be taken into account such as prewhitening the data, selecting an appropriate window width, and weighing of observations. In this case, none of the time series were prewhitened prior to conducting STARS. The disturbance event peak frequencies were derived from output of the CharAnalysis program. The identified events are what are leftover following the application of multiple and rigorous thresholds (Higuera, 2009; Higuera et al., 2010). The *Abies:Picea* ratio time series did not undergo this process, however, prewhitening of this series by applying the Inverse Proportionality with 4 corrections (IP4 method) yielded exactly the same result as an analysis without prewhitening (Appendix K). The specified window width should be chosen based on the units of the time series and the phenomenon one is investigating (Stirnimann et al., 2019), noting that smaller window width can result in an increase of detected regime shifts (Rodionov, 2004; Rodionov and Overland, 2005). Finally, outlying observations can be weighed using Huber's weight parameter to reduce their effect on calculated regime means thereby avoiding faulty regime shift detections (Rodionov, 2006; Stirnimann et al., 2019). Huber's weight parameter in a sense determines the cut-off range for outlying values i.e., a Huber's weight parameter of 1 considers that values falling beyond 1 standard deviation from the mean are outliers. If the observation value is less than or equal to the Huber's weight parameter value it is then given a value of 1 (not an outlier), otherwise applied weights will be inversely proportional to its distance from the new regime's mean value (Rodionov, 2006; Stirnimann et al., 2019).

APPENDIX K
ABIES:PICEA RATIO RAW VS. PREWHITENING

The pollen influx, and subsequent *Abies:Picea* ratio did not undergo the CharAnalysis procedure and may have warranted prewhitening of the observations to remove any background noise. Prewhitening using the IP4 method (Rodionov, 2006) in the *rstars* function (Stirniman et al., 2019) was done on the ratio and compared to the unprewhitened data (Figure K.1). No differences were found between the two analyses (Table K.1), and therefore, the raw data was used.

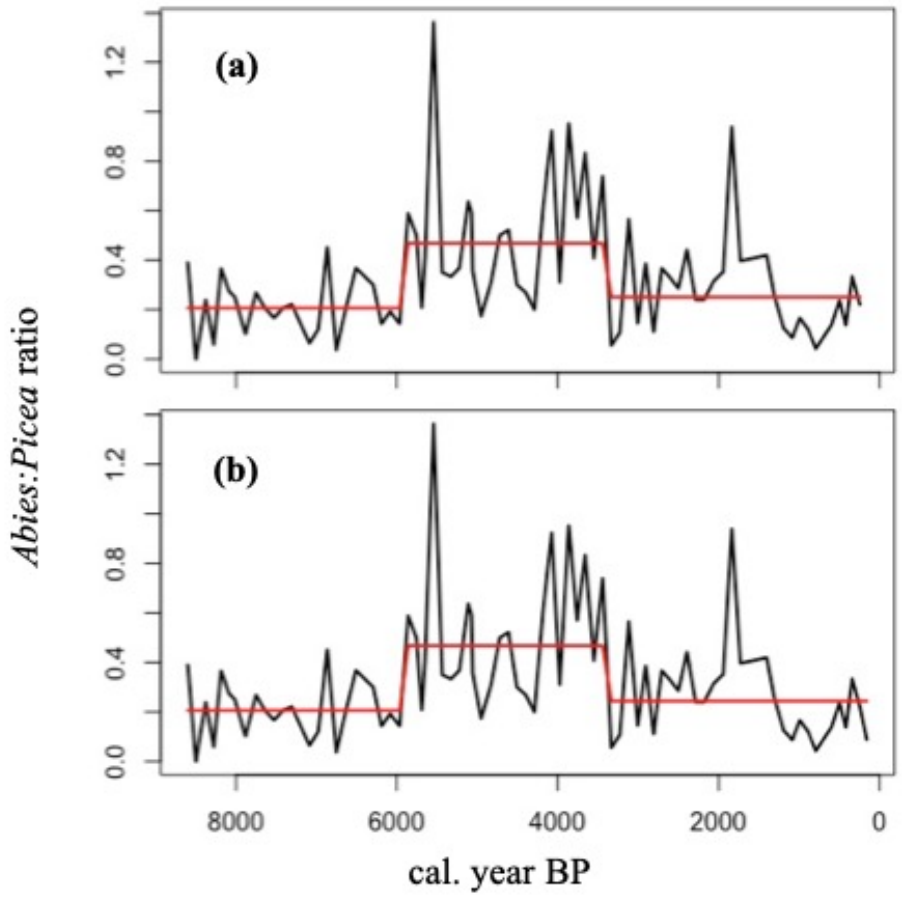

Figure K.1: The *Abies:Picea* ratio (*black line*) and mean ratio (*red line*) for Lake Buire over the course of the Holocene (a) with prewhitened observations using the IP4 method and (b) without any prewhitening.

Table K.1: Comparison of the STARS conducted on the raw and prewhitened *Abies:Picea* ratio

Observations	Number of detected shifts	Shift occurrence (cal. year BP)	Calculated means
Raw	2	5962, 3441	0.207, 0.468, 0.244
IP4 method	2	5962, 3441	0.207, 0.468, 0.250

APPENDIX L

RAW HOLOCENE LEPIDOPTERAN SCALE COUNTS AT LAKE BUIRE

Table L.1: Raw lepidopteran scale count at the various depths of the Lake Buire sediment column. The outlier is located at the 1048-1049 cm depth.

Depth (cm)	Lepidopteran scale count	Depth (cm)	Lepidopteran scale count
349-350	7	364-365	6
350-351	4	365-366	5
351-352	12	366-367	6
352-353	2	367-368	5
353-354	9	368-369	7
354-355	17	369-370	11
355-356	8	370-371	17
356-357	10	371-372	13
357-358	19	372-373	29
358-359	13	373-374	11
359-360	10	374-375	2
360-361	13	375-376	3
361-362	24	376-377	1
362-363	22	377-378	2
363-364	15	378-379	4

Depth (cm)	Lepidopteran scale count	Depth (cm)	Lepidopteran scale count
379-380	4	399-400	7
380-381	4	400-401	1
381-382	7	401-402	4
382-383	5	402-403	15
383-384	1	403-404	2
384-385	7	404-405	18
385-386	8	405-406	19
386-387	6	406-407	5
387-388	4	407-408	9
388-389	12	408-409	12
389-390	4	409-410	13
390-391	4	410-411	11
391-392	13	411-412	18
392-393	4	412-413	9
393-394	11	413-414	24
394-395	6	414-415	19
395-396	12	415-416	13
396-397	17	416-417	12
397-398	3	417-418	18
398-399	3	418-419	4

Depth (cm)	Lepidopteran scale count	Depth (cm)	Lepidopteran scale count
419-420	14	439-440	10
420-421	36	440-441	3
421-422	9	441-442	15
422-423	13	442-443	11
423-424	6	443-444	16
424-425	23	444-445	12
425-426	25	445-446	12
426-427	11	446-447	20
427-428	22	447-448	17
428-429	7	448-449	23
429-430	14	449-450	11
430-431	15	450-451	21
431-432	4	451-452	9
432-433	6	452-453	11
433-434	4	453-454	10
434-435	10	454-455	14
435-436	7	455-456	19
436-437	12	456-457	25
437-438	6	457-458	25
438-439	8	458-459	31

Depth (cm)	Lepidopteran scale count	Depth (cm)	Lepidopteran scale count
459-460	24	479-480	10
460-461	11	480-481	12
461-462	16	481-482	12
462-463	16	482-483	16
463-464	16	483-484	10
464-465	11	484-485	10
465-466	15	485-486	3
466-467	10	486-487	12
467-468	19	487-488	9
468-469	10	488-489	7
469-470	9	489-490	7
470-471	13	490-491	14
471-472	10	491-492	16
472-473	16	492-493	3
473-474	21	493-494	9
474-475	13	494-495	10
475-476	14	495-496	16
476-477	5	496-497	12
477-478	9	497-498	13
478-479	10	498-499	17

Depth (cm)	Lepidopteran scale count	Depth (cm)	Lepidopteran scale count
499-500	32	519-520	19
500-501	12	520-521	12
501-502	22	521-522	12
502-503	16	522-523	9
503-504	6	523-524	14
504-505	5	524-525	21
505-506	11	525-526	13
506-507	11	526-527	10
507-508	11	527-528	12
508-509	20	528-529	23
509-510	15	529-530	26
510-511	8	530-531	5
511-512	17	531-532	14
512-513	14	532-533	12
513-514	16	533-534	9
514-515	31	534-535	13
515-516	8	535-536	12
516-517	11	536-537	16
517-518	13	537-538	14
518-519	37	538-539	15

Depth (cm)	Lepidopteran scale count	Depth (cm)	Lepidopteran scale count
539-540	31	559-560	36
540-541	29	560-561	11
541-542	18	561-562	13
542-543	46	562-563	4
543-544	11	563-564	26
544-545	25	564-565	14
545-546	10	565-566	19
546-547	8	566-567	39
547-548	12	567-568	30
548-549	9	568-569	16
549-550	14	569-570	12
550-551	9	570-571	16
551-552	9	571-572	13
552-553	17	572-573	22
553-554	23	573-574	21
554-555	16	574-575	11
555-556	31	575-576	22
556-557	35	576-577	32
557-558	24	577-578	16
558-559	16	578-579	28

Depth (cm)	Lepidopteran scale count	Depth (cm)	Lepidopteran scale count
579-580	32	599-600	32
580-581	13	600-601	30
581-582	24	601-602	36
582-583	14	602-603	24
583-584	18	603-604	19
584-585	25	604-605	40
585-586	20	605-606	34
586-587	26	606-607	24
587-588	41	607-608	21
588-589	28	608-609	40
589-590	6	609-610	29
590-591	10	610-611	54
591-592	24	611-612	21
592-593	23	612-613	27
593-594	14	613-614	36
594-595	23	614-615	51
595-596	27	615-616	28
596-597	24	616-617	39
597-598	30	617-618	21
598-599	36	618-619	19

Depth (cm)	Lepidopteran scale count	Depth (cm)	Lepidopteran scale count
619-620	13	639-640	18
620-621	34	640-641	24
621-622	40	641-642	43
622-623	26	642-643	55
623-624	11	643-644	43
624-625	12	644-645	38
625-626	9	645-646	16
626-627	17	646-647	26
627-628	32	647-648	29
628-629	31	648-649	64
629-630	37	649-650	29
630-631	17	650-651	38
631-632	14	651-652	22
632-633	16	652-653	39
633-634	13	653-654	15
634-635	15	654-655	26
635-636	8	655-656	20
636-637	43	656-657	17
637-638	23	657-658	24
638-639	18	658-659	32

Depth (cm)	Lepidopteran scale count	Depth (cm)	Lepidopteran scale count
659-660	24	679-680	17
660-661	12	680-681	12
661-662	30	681-682	34
662-663	44	682-683	27
663-664	29	683-684	18
664-665	20	684-685	24
665-666	49	685-686	9
666-667	24	686-687	11
667-668	31	687-688	24
668-669	83	688-689	15
669-670	47	689-690	8
670-671	38	690-691	10
671-672	30	691-692	8
672-673	26	692-693	15
673-674	19	693-694	9
674-675	24	694-695	9
675-676	45	695-696	28
676-677	21	696-697	34
677-678	34	697-698	45
678-679	23	698-699	23

Depth (cm)	Lepidopteran scale count	Depth (cm)	Lepidopteran scale count
699-700	22	719-720	34
700-701	14	720-721	22
701-702	18	721-722	14
702-703	22	722-723	16
703-704	21	723-724	30
704-705	26	724-725	18
705-706	23	725-726	24
706-707	18	726-727	31
707-708	31	727-728	36
708-709	45	728-729	26
709-710	33	729-730	75
710-711	27	730-731	49
711-712	34	731-732	22
712-713	41	732-733	40
713-714	28	733-734	17
714-715	27	734-735	35
715-716	33	735-736	10
716-717	28	736-737	15
717-718	53	737-738	15
718-719	54	738-739	11

Depth (cm)	Lepidopteran scale count	Depth (cm)	Lepidopteran scale count
739-740	25	759-760	20
740-741	24	760-761	24
741-742	28	761-762	20
742-743	23	762-763	24
743-744	24	763-764	82
744-745	47	764-765	34
745-746	20	765-766	53
746-747	35	766-767	13
747-748	32	767-768	41
748-749	28	768-769	31
749-750	15	769-770	25
750-751	11	770-771	9
751-752	5	771-772	6
752-753	11	772-773	18
753-754	10	773-774	33
754-755	5	774-775	32
755-756	19	775-776	13
756-757	16	776-777	22
757-758	8	777-778	24
758-759	34	778-779	14

Depth (cm)	Lepidopteran scale count	Depth (cm)	Lepidopteran scale count
779-780	31	799-800	23
780-781	41	800-801	42
781-782	32	801-802	24
782-783	24	802-803	17
783-784	40	803-804	17
784-785	23	804-805	15
785-786	29	805-806	40
786-787	19	806-807	21
787-788	30	807-808	44
788-789	15	808-809	25
789-790	33	809-810	10
790-791	23	810-811	29
791-792	22	811-812	19
792-793	15	812-813	32
793-794	23	813-814	15
794-795	22	814-815	25
795-796	19	815-816	45
796-797	39	816-817	35
797-798	23	817-818	27
798-799	24	818-819	11

Depth (cm)	Lepidopteran scale count	Depth (cm)	Lepidopteran scale count
819-820	21	839-840	20
820-821	11	840-841	15
821-822	12	841-842	21
822-823	5	842-843	26
823-824	24	843-844	20
824-825	19	844-845	25
825-826	9	845-846	22
826-827	12	846-847	27
827-828	33	847-848	20
828-829	18	848-849	16
829-830	16	849-850	22
830-831	16	850-851	38
831-832	38	851-852	20
832-833	26	852-853	15
833-834	12	853-854	29
834-835	22	854-855	33
835-836	31	855-856	35
836-837	28	856-857	30
837-838	18	857-858	18
838-839	10	858-859	24

Depth (cm)	Lepidopteran scale count	Depth (cm)	Lepidopteran scale count
859-860	22	879-880	38
860-861	32	880-881	34
861-862	10	881-882	47
862-863	17	882-883	23
863-864	11	883-884	25
864-865	14	884-885	22
865-866	14	885-886	17
866-867	20	886-887	43
867-868	17	887-888	14
868-869	19	888-889	26
869-870	16	889-890	20
870-871	24	890-891	31
871-872	35	891-892	68
872-873	28	892-893	8
873-874	37	893-894	22
874-875	14	894-895	43
875-876	40	895-896	35
876-877	20	896-897	39
877-878	31	897-898	39
878-879	40	898-899	46

Depth (cm)	Lepidopteran scale count	Depth (cm)	Lepidopteran scale count
899-900	36	919-920	37
900-901	177	920-921	74
901-902	27	921-922	43
902-903	19	922-923	24
903-904	52	923-924	38
904-905	29	924-925	46
905-906	26	925-926	44
906-907	34	926-927	42
907-908	45	927-928	28
908-909	39	928-929	23
909-910	33	929-930	19
910-911	42	930-931	23
911-912	49	931-932	29
912-913	36	932-933	39
913-914	39	933-934	32
914-915	35	934-935	30
915-916	41	935-936	33
916-917	30	936-937	88
917-918	30	937-938	39
918-919	28	938-939	48

Depth (cm)	Lepidopteran scale count	Depth (cm)	Lepidopteran scale count
939-940	66	959-960	41
940-941	23	960-961	45
941-942	17	961-962	36
942-943	46	962-963	53
943-944	38	963-964	51
944-945	31	964-965	36
945-946	13	965-966	35
946-947	31	966-967	40
947-948	33	967-968	27
948-949	41	968-969	54
949-950	20	969-970	32
950-951	54	970-971	58
951-952	32	971-972	18
952-953	54	972-973	8
953-954	31	973-974	25
954-955	24	974-975	8
955-956	30	975-976	5
956-957	19	976-977	13
957-958	28	977-978	4
958-959	45	978-979	10

Depth (cm)	Lepidopteran scale count	Depth (cm)	Lepidopteran scale count
979-980	12	999-1000	27
980-981	12	1000-1001	36
981-982	5	1001-1002	45
982-983	14	1002-1003	46
983-984	5	1003-1004	37
984-985	10	1004-1005	33
985-986	2	1005-1006	38
986-987	18	1006-1007	16
987-988	21	1007-1008	22
988-989	20	1008-1009	22
989-990	15	1009-1010	17
990-991	10	1010-1011	31
991-992	14	1011-1012	16
992-993	13	1012-1013	34
993-994	16	1013-1014	80
994-995	17	1014-1015	52
995-996	28	1015-1016	41
996-997	23	1016-1017	34
997-998	12	1017-1018	49
998-999	25	1018-1019	50

Depth (cm)	Lepidopteran scale count	Depth (cm)	Lepidopteran scale count
1019-1020	22	1039-1040	39
1020-1021	21	1040-1041	29
1021-1022	44	1041-1042	40
1022-1023	21	1042-1043	18
1023-1024	32	1043-1044	14
1024-1025	38	1044-1045	19
1025-1026	19	1045-1046	47
1026-1027	50	1046-1047	74
1027-1028	35	1047-1048	36
1028-1029	20	1048-1049	1513
1029-1030	15	1049-1050	38
1030-1031	11	1050-1051	29
1031-1032	24	1051-1052	34
1032-1033	42	1052-1053	27
1033-1034	60	1053-1054	18
1034-1035	22	1054-1055	13
1035-1036	23	1055-1056	9
1036-1037	57	1056-1057	10
1037-1038	25	1057-1058	11
1038-1039	25	1058-1059	13

Depth (cm)	Lepidopteran scale count	Depth (cm)	Lepidopteran scale count
1059-1060	17	1079-1080	18
1060-1061	15	1080-1081	6
1061-1062	8	1081-1082	25
1062-1063	8	1082-1083	11
1063-1064	5	1083-1084	2
1064-1065	2	1084-1085	3
1065-1066	13	1085-1086	1
1066-1067	6	1086-1087	3
1067-1068	11	1087-1088	6
1068-1069	17	1088-1089	1
1069-1070	9		
1070-1071	7		
1071-1072	22		
1072-1073	14		
1073-1074	5		
1074-1075	19		
1075-1076	15		
1076-1077	21		
1077-1078	31		
1078-1079	21		

REFERENCES

Agostinelli, C., and Lund, U. (2017). *R package 'circular': Circular Statistics* (version 0.4-93). https://r-forge.r-project.org/projects/circular/

Aleman, J.C., Blarquez, O., Bentaleb, I., Bonté, P., Brossier, B., Carcaillet, C., Gond, V., Gourlet-Fleury, S., Kpolita, A., Lefèvre, I., Oslisly, R., Power, MJ., Yongo, O., Bremond, L., and Favier, C. (2013). Tracking land-cover changes with sedimentary charcoal in the Afrotropics. *The Holocene 23* (12), 1853-1862. https://doi.org/10.1177/0959683613508159

Alfaro, R., vanAkker, L., Berg, J., Van Hezewijk, B., Zhang, Q-B., Hebda, R., Smith, D., and Axelson, J. (2018). Change in the periodicity of a cyclical forest defoliator: an indicator of ecosystem alteration in Western Canada. *Forest Ecology and Management 430*, 117-125. https://doi.org/10.1016/j.foreco.2018.07.060

Ali, A.A., Asselin, H., Larouche, A.C., Bergeron, Y., Carcaillet, C., and Richard, P.J.H. (2008). Changes in fire regime explain the Holocene rise and fall of Abies balsamea in the coniferous forests of western Québec. *The Holocene 18*, 693-703. https://doi.org/10.1177/0959683608091780

Ali, A.A., Carcaillet, C., and Bergeron, Y. (2009). Long-term fire frequency variability in the eastern Canadian boreal forest: the influences of climate vs. local factors. *Global Change Biology 15*, 1230-1241. https://doi.org/10.1111/j.1365-2486.2009.01842.x

Ali, A.A., Blarquez, O., Girardin, M.P., Hély, C., Tinquaut, F., El Guellab, A., Valsecchi, V., Terrier, A., Bremond, L., Genries, A., Gauthier, S., and Bergeron, Y. (2012). Control of the multimillennial wildfire size in boreal North America by spring climatic conditions. *Proceedings of the National Academy of Sciences of the United States of America 109*, 20966-20970. https://doi.org/10.1073/pnas.1203467109

Allen, C.D., Macalady, A.K., Chenchouni, H., Bachelet, D., McDowell, N., Vennetier, M., Kitzberger, T., Rigling, A., Breshears, B.D. Hogg, E.H., Gonzalez, P., Fensham, R., Zhang, Z., Castro, J., Demidova, N., Lim, J-H., Allard, G., Running, S.W., Smerci, A., and Cobb, N. (2010). A global overview of drought and heat-induced tree mortality reveals emerging climate change risks for forests. *Forest Ecology and Management 259*, 660-684. https://doi.org/10.1016/j.foreco.2009.09.001

Allen, C.D., Breshears, D.D., and McDowell, N.G. (2015). On underestimation of global vulnerability to tree mortality and forest die-off from hotter drought in the Anthropocene. *Ecosphere 6* (8), 129. https://doi.org/10.1890/ES15-00203.1

Alley, R.B., and Agustsdottír, A.M. (2005). The 8k event: cause and consequences of a major Holocene abrupt climate change. *Quaternary Science Reviews 24*, 1123-1149. https://doi.org/10.1016/j.quascirev.2004.12.004

Anderegg, W.R.L., Hicke, J.A., Fisher, R.A., Allen, C.D., Aukema, J., Bentz, B., Hood, S., Lichstein, J.W., Macalady, A.K., McDowell, N. Pan, Y., Raffa, K., Sala, A., Shaw, J.D., Stephenson, N.L., Tague, C., and Zeppel, M. (2015). Tree mortality from drought, insects, and their interactions in a changing climate. *New Phytologist 208* (3), 674-683. https://doi.org/10.1111/nph.13477

Appleby, P.G., and Oldfield, F. (1983). The assessment of 210Pb data from sites with varying sediment accumulation rates. *Hydrobiologia 103*, 29-35. https://doi.org/10.1007/BF00028424

Asselin, M., Grondin, P., Lavoie, M., and Fréchette F. (2016). Fires of the last millennium led to landscapes dominated by early successional species in Québec's clay belt boreal forest, Canada. *Forests 7* (205), 1-18. https://doi.org/10.3390/f7090205

Aszalos, R. Thom, D., Aakala, T., Angelstam, P., Brumelis, G., Galhidy, L., Gratzer, G., Hlasny, T., Katzensteiner, K., Kovacs, B., Knoke, T., Larrieu, L., Motta, R., Muller, J., Odor, P., Rozenbergar, D., Paillet, Y., Pitar, D., Standovar, T., Svoboda, M., Szwagrzyk, J., Toscani, P., and Keeton, W.S. (2022). Natural disturbance regimes as a guide for sustainable forest management in Europe. *Ecological Applications 32*, e2596. https://doi.org/10.1002/eap.2596

Ayres, M.P., and Lombardo, M.J. (2000). Assessing the consequences of global change for forest disturbance from herbivores and pathogens. *The Science of the Total Environment 262*, 263-286. https://doi.org/10.1016/S0048-9697(00)00528-3

Baldi, P., Brunak, S., Chauvin, Y., Andersen, C.A.F., and Nielsen, H. (2000). Assessing the accuracy of prediction algorithms for classification: An overview. *Bioinformatics 16*, 412-424. https://doi.org/10.1093/bioinformatics/16.5.412

Bale, J.S., Masters, G.J., Hodkinson, I.D., Awmack, C., Bezemer, T.M., Brown, V.K., Butterfield, J., Buse, A., Coulson, J.C., Farrar, J., Good, J.E.G., Harrington, R., Hartley, S., Hefin Jones, T., Lindroth, R.L., Press, M.C., Symrnioudis, I., Watt, A.D., and Whittaker, J.B. (2002). Herbivory in global climate change research: direct effects of rising temperature on insect herbivores. *Global Change Biology 8* (1), 1-16. https://doi.org/10.1046/j.1365-2486.2002.00451.x

Barbosa, P., Letourneau, D.K., and Agrawal, A.A. (dir). (2012). *Insect outbreaks revisited*. Wiley-Blackwell.

Baskerville, G.L. (1975). Spruce budworm- Super silviculturist. *The Forestry Chronicle 51* (4), 138-140

Bauce, É., Crépin, M., and Carisey, N. 1994. Spruce budworm growth, development and food utilization on young and old balsam fir trees. *Oecologia 97*, 499-507. https://doi.org/10.1007/BF00325888

Bennett, K.D., and Buck, C.E. 2016. Interpretation of lake sediment accumulation rates. *The Holocene 26* (7), 1092-1102. https://doi.org/10.1177/0959683616632880

Bentz, B.J., Régnière, J., Fettig, C.J., Hansen, E.M., Hayes, J.L., Hicke, J.A., Kelsey, R.G., Negrón, J.F., and Seybold, S.J. (2010). Climate change and bark beetles of the western United States and Canada: Direct and indirect effects. *BioScience 60* (8), 602-613. https://doi.org/10.1525/bio.2010.60.8.6

Berg, E.E., Henry, J.D., Fastie, C.L., De Volder, A.D., and Matsuoka, S.M. (2006). Spruce beetle outbreaks on the Kenai Peninsula, Alaska, and Kluane National Park and Reserve, Yukon Territory: Relationship to summer temperatures and regional differences in disturbance regimes. *Forest Ecology and Management 227* (3), 291-232. https://doi.org/10.1016/j.foreco.2006.02.038

Bergeron, Y. (2000). Species and stand dynamics in the mixed woods of Quebec's southern boreal forest. *Ecology 81* (6), 1500-1516. https://doi.org/10.1890/0012-9658(2000)081[1500:SASDIT]2.0.CO;2

Bergeron, Y., Gauthier, S., Kafka, V., Lefort, P., and Lesieur, D. (2001). Natural fire frequency for the eastern Canadian boreal forest: consequences for sustainable forestry. *Canadian Journal of Forest research 31* (3), 384-391. https://doi.org/10.1139/x00-178

Bergeron, Y., Leduc, A., Harvey, B.D., and Gauthier, S. (2002). Natural fire regime: a guide for sustainable management of the Canadian boreal forest. *Silva Fennica 36* (1), 81-95. https://doi.org/10.14214/sf.553

Bergeron, Y., Gauthier, S., Flannigan, M., and Kafka, V. (2004). Fire regimes at the transition between mixedwood and coniferous boreal forest in northwestern Quebec. *Ecology 85* (7), 1916-1932. https://doi.org/10.1890/02-0716

Berryman, A., A. (1987). The theory and classification of outbreaks. In P., Barbosa, and J.C., Schultz, (Eds.), *Insect Outbreaks* (pp. 3-30). Academic Press, Inc.

Bessie, W.C., and Johnson, E.A. (1995). The relative importance of fuels and weather on fire behavior in subalpine forests. *Ecology 76* (3), 747-762. https://doi.org/10.2307/1939341

Bhatti, J.S., and Apps, M.J. (dir). (2000). *Carbon and nitrogen storage in upland boreal forests*. In *Global climate change and cold regions ecosystems*. CRC Press

Binford, M.W. (1990). Calculation and uncertainty analysis of ^{210}Pb dates for PIRLA project lake sediment cores. *Journal of Paleolimnology 3*, 253-267. https://doi.org/10.1007/BF00219461

Blaauw, M., and Christen, A. (2011). Flexible paleoclimate age-depth models using an autoregressive gamma process. *Bayesian Analysis 6* (3), 457-474. https://doi.org/10.1214/11-BA618

Blaauw, M., Christen, A., and Aquino Lopez, M.A. (2021). *rbacon: Age-depth modelling using Bayesian statistics*. R package version 2.5.7. https://CRAN.R-project.org/package=rbacon

Blais, J.R. (1957). Some relationships of the spruce budworm, Choristoneura fumiferana (Clem.) to black spruce Picea mariana (Moench) Voss. *The Forestry Chronicle 33* (4): 364-372. https://doi.org/10.5558/tfc33364-4

Blais, J.R. (1958). Effects of defoliation by spruce budworm (*Choristoneura fumiferana* Clem.) on radial growth at breast height of balsam fir (*Abies blasamea* (L.) Mill.) and white spruce (*Picea glauca* (Moench) Voss.). *The Forestry Chronicle 34* (1), 39-47. https://doi.org/10.5558/tfc34039-1

Blais, J.R. (1962). Collection and analysis of radial-growth data from trees for evidence of past spruce budworm outbreaks. *The Forestry Chronicle 38* (4), 474-484. https://doi.org/10.5558/tfc38474-4

Blais, J.R. (1968). Regional variation in susceptibility of eastern North American forests to budworm attack based on history outbreaks. *The Forestry Chronicle 44* (3), 17-23. https://doi.org/10.5558/tfc44017-3

Blais, J.R. (1983). Trends in the frequency, extent, and severity of spruce budworm outbreaks in eastern Canada. *Canadian Journal of Forest Research 13* (4), 539-547. https://doi.org/10.1139/x83-079

Blais, J.R. (1985a). Epidemiology of the spruce budworm in western Ontario: A discussion. *The Forestry Chronicle 61* (6), 494-498. https://doi.org/10.5558/tfc61494-6

Blais, J.R. (1985b). *The ecology of the eastern spruce budworm: A review and discussion*. In: *Recent advances in spruce budworm research. Proceedings of the CANUSA Spruce Budworms Research Symposium, Bangor, Maine, 16-20 September 1984*. Sanders, C.J., Stark, R.W., Mullins, E.J., and Murphy, J. Canadian Forestry Service, Ottawa, ON.

Blarquez, O., Bremond, L., and Carcaillet, C. (2010). Holocene fires and a herb-dominated understorey track wetter climates in subalpine forests. *Journal of Ecology 98* (6), 1358-1368. https://doi.org/10.1111/j.1365-2745.2010.01721.x

Blarquez, O., Vannière, B., Marlon, J.R., Daniau, A-L., Power, M.J., Brewer, S., and Bartlein, P.J. (2014). paleofire: An R package to analyse sedimentary charcoal records from the Global Charcoal Database to reconstruct past biomass burning. *Computers and Geosciences 72*, 255-261. https://doi.org/10.1016/j.cageo.2014.07.020

Blarquez, O., Ali, A.A., Girardin, M.P., Grondin, P., Fréchette, B., Bergeron, Y., and Hély, C. (2015). Regional paleofire regimes affected by non-uniform climate, vegetation and human drivers. *Scientific Reports 5*, 13356. https://doi.org/10.1038/srep13356

Blarquez, O., and Aleman, J.C. (2016). Tree biomass reconstruction shows no lag in postglacial afforestation of eastern Canada. *Canadian Journal of Forest Research 46* (4), 485-498. https://doi.org/10.1139/cjfr-2015-0201

Bonan, G.B. (2008). Forests and climate change: forcings, feedbacks, and the climate benefits of forests. *Science 320* (5882), 1444-1449. https://doi.org/10.1126/science.1155121

Bond, G., Showers, W., Cheseby, M., Lotti, R., Almasi, P. deMenocal, P., Priore, P., Cullen, H., Hajdas, I., and Bonani, G. (1997). A pervasive millennial-scale cycle in north Atlantic Holocene and glacial climates. *Science 278* (5341), 1257-1266. https://doi.org/10.1126/science.278.5341.1257

Bond, G., Kromer, B., Beer, J., Muscheler, R., Evans, M.N., Showers, W., Hoffman, S., Lotti-Bond, R., Hajdas, I., and Bonani, G. (2001). Persistent solar influence on north Atlantic climate during the Holocene. *Science 294* (5549), 2130-2136

Bond, W.J., and Keeley, J.E. (2005). Fire as a global 'herbivore': the ecology and evolution of flammable ecosystems. *Trends in Ecology and Evolution 20* (7), 387-394. https://doi.org/10.1016/j.tree.2005.04.025

Bouchard, M., Kneeshaw, D., and Bergeron, Y. (2005). Mortality and stand renewal patterns following the last spruce budworm outbreak in mixed forests of western Quebec. *Forest Ecology and Management 204* (2-3), 297-313. https://doi.org/10.1016/j.foreco.2004.09.017

Bouchard, M., Kneeshaw, D., Bergeron, Y. (2006). Forest dynamics after successive spruce budworm outbreaks in mixedwood forests. *Ecology 87* (9): 2319-2329. https://doi.org/10.1890/0012-9658(2006)87[2319:FDASSB]2.0.CO;2

Bouchard, M., Kneeshaw, D., Bergeron, Y. (2007). Forest dynamics following spruce budworm outbreaks in the northern and southern mixedwoods of central Quebec. *Canadian Journal of Forest Research 37* (4), 763-772. https://doi.org/10.1139/X06-278

Bouchard, M., and Pothier, D. (2010). Spatiotemporal variability in tree and stand mortality caused by spruce budworm outbreaks in eastern Quebec. *Canadian Journal of Forest Research 40* (1), 86-94. https://doi.org/10.1139/X09-178

Boulanger, Y., and Arseneault, D. (2004). Spruce budworm outbreaks in eastern Québec over the last 450 years. *Canadian Journal of Forest Research 34* (5), 1035-1043. https://doi.org/10.1139/x03-269

Boulanger, Y., Arseneault, D., Morin, H., Jardon, Y., Bertrand, P., and Dagneau, C. (2012). Dendrochronological reconstruction of spruce budworm (*Choristoneura fumiferana*) outbreaks in southern Quebec for the last 400 years. *Canadian Journal of Forest Research 42* (7), 1264-1276. https://doi.org/10.1139/x2012-069

Boulanger, Y., Fabry, F., Kilambi, A., Pureswaran, D.S., Sturtevant, B.R., Saint-Amant, R. (2017). The use of weather surveillance radar and high-resolution three dimensional weather data to monitor a spruce budworm mass exodus flight. *Agricultural and Forest Meteorology 234-235*, 127-135. https://doi.org/10.1016/j.agrformet.2016.12.018

Brandt, J.P. (2009). The extent of the North American boreal zone. *Environmental Reviews 17*, 101-161. https://doi.org/10.1139/A09-004

Brandt, J.P., Flannigan, M.D., Maynard, D.G., Thompson, I.D., and Volney, W.J.A. (2013). An introduction to Canada's boreal zone: ecosystem processes, health, sustainability, and environmental issues. *Environmental Reviews 21* (4), 207-226. https://doi.org/10.1139/er-2013-0040

Broecker, W.S. (1997). Thermohaline circulation, the Achilles heel of our climate system: will man-made CO2 upset the current balance? *Science 278* (5343), 1582-1588. https://doi.org/10.1126/science.278.5343.1582

Broecker, W.S. (2003). Does the trigger for abrupt climate change reside in the ocean or in the atmosphere? *Science 300* (5625), 1519-1522. https://doi.org/10.1126/science.1083797

Buma, B., and Wessman, C.A. (2011). Disturbance interactions can impact resilience mechanisms of forests. *Ecosphere 2* (5), 1-13. https://doi.org/10.1890/ES11-00038.1

Buma, B., and Wessman, C.A. (2012). Differential species responses to compounded perturbations and implications for landscape heterogeneity and resilience. *Forest Ecology and Management 266*, 25-33. https://doi.org/10.1016/j.foreco.2011.10.040

Buma, B., and Wessman, C.A. (2013). Forest resilience, climate change, opportunities for adaptation: a specific case of a general problem. *Forest Ecology and Management 306*, 216-225. https://doi.org/10.1016/j.foreco.2013.06.044

Buma, B. (2015). Disturbance interactions: characterization, prediction, and the potential for cascading effects. *Ecosphere 6* (4), 1-15. https://doi.org/10.1890/ES15-00058.1

Buma, B., Harvey, B.J., Gavin, D.G., Kelly, R., Loboda, T., McNeil, B.E., Marlon, J.R., Meddens, A.J.H., Morris, J.L., Raffa, K.F., Shuman, B., Smithwick, E.A.H., and McLauchlan, K.K. (2019). The value of linking paleoecological and neoecological perspectives to understand spatially-explicit ecosystem resilience. *Landscape Ecology 34* (17-33), 17-33. https://doi.org/10.1007/s10980-018-0754-5

Buma, B., and Schultz, C. (2020). Disturbances as opportunities: learning from disturbance-response parallels in social and ecological systems to better adapt to climate change. *Journal of Applied Ecology 57* (6), 1113-1123. https://doi.org/10.1111/1365-2664.13606

Buma, B. (2021). Disturbance ecology and the problem of n=1: a proposed framework for unifying disturbance ecology studies to address theory across multiple ecological systems. *Methods in Ecology and Evolution 12* (12), 2276-2286. https://doi.org/10.1111/2041-210X.13702

Bunn, A. (2010). Statistical and visual crossdating in R using the dplR library. *Dendrochronologia 28* (4), 251-258. https://doi.org/10.1016/j.dendro.2009.12.001

Buras, A. (2017). A comment on the expressed population signal. *Dendrochronologia 44*, 130-132. https://doi.org/10.1016/j.dendro.2017.03.005

Burns, R.M., and Honkala, B.H. (dir). (1990). *Silvics of North America volume 1: conifers and volume 2: hardwoods*. United States Department of Agriculture Forest Service Agriculture Handbook 654

Burton, P.J., Jentsch, A., and Walker, L.R. (2020). The ecology of disturbance interactions. *BioScience 70* (10), 854-870. https://doi.org/10.1093/biosci/biaa088

Byrom, G.M. (1959). *Combustion of forest fuels*. In: *Forest fire: control and use*. McGraw-Hill, New York

Camarero, J.J., Tardif, J., Gazol, A., Conciatori, F. (2022). Pine processionary moth outbreaks cause longer growth legacies than drought and are linked to the North Atlantic Oscillation. *Science of the Total Environment 819*, 153041. https://doi.org/10.1016/j.scitotenv.2022.153041

Campbell, R., Smith, D.J., and Arsenault, A. (2006). Multicentury history of western spruce budworm outbreaks in interior Douglas-fir forests near Kamloops, British Columbia. *Canadian Journal of Forest Research 36* (7), 1758-1769. https://doi.org/10.1139/x06-069

Campbell, E., MacLean, D.A., and Bergeron, Y. (2008). The severity of budworm-caused growth reductions in balsam fir/spruce stands varies with the hardwood content of surrounding forest landscapes. *Forest Science 54* (2), 195-205. https://doi.org/10.1093/forestscience/54.2.195

Candau, J-N., Fleming, R.A., and Hopkin, A. (1998). Spatiotemporal patterns of large-scale defoliation caused by the spruce budworm in Ontario since 1941. *Canadian Journal of Forest Research 28* (11), 1733-1741. https://doi.org/10.1139/x98-164

Candau, J-N., Fleming, R.A., and Wang, X. (2018). Ecogregional patterns of spruce budworm-wildfire interactions in central Canada's forests. *Forests 9* (3), 137. https://doi.org/10.3390/f9030137

Cappucino, N., Lavertu, D., Bergeron, Y., and Régnière, J. (1998). Spruce budworm impact, abundance and parasitism rate in a patchy landscape. *Oecologia 114*, 236-242. https://doi.org/10.1007/s004420050441

Carcaillet, C., Bergeron, Y., and Richard, P.J.H., Féchette, B., Gauthier, S., and Prairie, Y.T. (2001a). Changes of fire frequency in the eastern Canadian boreal forests during the Holocene: does vegetation composition or climate trigger the fire regime? *Journal of Ecology 89* (6), 930-946. https://doi.org/10.1111/j.1365-2745.2001.00614.x

Carcaillet, C., Bouvier, M., Fréchette, B., Larouche, A.C., and Richard, P.J.H. (2001b). Comparison of pollen-slide and sieving methods in lacustrine charcoal analyses for local and regional fire history. *The Holocene 11* (4), 467-476. https://doi.org/10.1191/095968301678302904

Carcaillet, C., Ali, A.A., Blarquez, O., Genries, A., Mourier, B., and Bremond, L. (2009). Spatial variability of fire history in subalpine forests: From natural to cultural regimes. *Ecoscience 16* (1), 1-12. https://doi.org/10.2980/16-1-3189

Carroll, A.L, Taylor, S.W., Régnière, J., and Safranyik, L. (2004). *Effects of climate and climate change on the mountain pine beetle*. In: *Proceedings of the mountain pine beetle symposium: challenges and solutions, October 30-31, 2003, Kelowna, British Columbia, Canada*. T.L. Shore, J.E. Brooks, and J.E. Stone. Natural Resources Canada, Canadian Forest Service, Pacific Forestry Centre, Victoria, BC. Information Report BC-X-399

Cazelles, B., Chavez, M., Berteaux, D., Ménard, F., Vik, J.O., Jenouvrier, S., and Stenseth, N.C. (2008). Wavelet analysis of ecological time series. *Oecologia 156* (2), 287-304. https://doi.org/10.1007/s00442-008-0993-2

Chavardès, R.D., and Daniels, L.D. (2016). Altered mixed-severity fire regime has homogenized montane forests of Jasper National Park. *International Journal of Wildland fire 25* (4), 433-444. https://doi.org/10.1071/WF15048_CO

Chatfield, C. (1989). *The analysis of time series: An introduction*. 4th Ed. Chapman and Hall

Chen, C., Weiskittel, A., Bataineh, M., and MacLean, D.A. (2019). Modelling variation and temporal dynamics of individual tree defoliation caused by spruce budworm in Maine, US and New Brunswick, Canada. *Forestry 92* (1), 133-145. https://doi.org/10.1093/forestry/cpy037

Chicco, D., and Jurman, G. (2020). The advantages of the Matthews Correlation (MCC) over F1 score and accuracy in binary classification evaluation. *BMC Genomics 21*, 6. https://doi.org/10.1186/s12864-019-6413-7

Chicco, D., Totsch, N., Jurman, G. (2021a). The Matthews Correlation Coefficient (MCC) is more reliable than balanced accuracy, bookmaker informedness, and markness in two-class confusion matrix evaluation. *BioData Mining 14*, 13. https://doi.org/10.1186/s13040-021-00244-z

Chicco, D., Starovoitov, V, Jurman, G. (2021b). The benefits of the Matthews Correlation Coefficient (MCC) over the Diagnostic Odds Ratio (DOR) in binary classification assessment. *IEEE Access 9*, 47112-47124. https://doi.org/10.1109/ACCESS.2021.3068614

Chicco, D., Warrens, M.J., Jurman, G. (2021c). The Matthews Correlation Coefficient (MCC) is more informative than Cohen's Kappa and Brier Score in binary classification assessment. *IEEE Access 9*, 78368-78381. https://doi.org/10.1109/ACCESS.2021.3084050

Clark, J.S., and Royall, P.D. (1995). Particle-size evidence for source areas of charcoal accumulation in late Holocene sediments of eastern North American lakes. *Quaternary research 43* (1), 80-89. https://doi.org/10.1006/qres.1995.1008

Clark, J.S., Royall, P.D., and Chumbley, C. (1996). The role of fire during climate change in an eastern deciduous forest at Devil's Bathtub, New York. *Ecology 77* (7), 2148-2166. https://doi.org/10.2307/2265709

Clark, J.S., Lynch, J., Stocks, B.J., and Goldammer, J.G. (1998). Relationships between charcoal particles in air and sediments in west-central Siberia. *The Holocene 8* (1), 19-29. https://doi.org/10.1191/095968398672501165

Cohen, J. (1960). A coefficient of agreement for nominal scales. *Educational and Psychological Measurement 20* (1), 37-46. https://doi.org/10.1177/001316446002000104

Cohen, W.B., Yang, Z., and Kennedy, R. (2010). Detecting trends in forest disturbance and recovery using yearly Landsat time series: 2. TimeSync- tools for calibration and validation. *Remote Sensing of Environment 114* (12), 2911-2924. https://doi.org/10.1016/j.rse.2010.07.010

Cohn, G.M., Parsons, R.A., Heyerdahl, E.K., Gavin, D.G., and Flower, A. (2014). Simulated western spruce budworm defoliation reduces torching and crowning potential: a sensitivity analysis using a physics-based fire model. *International Journal of Wildland Fire 23* (5), 709-720. https://doi.org/10.1071/WF13074

Colford-Gilks, A.K., MacLean, D.A., Kershaw Jr., J.A., and Béland, M. (2012). Growth and mortality of balsam fir- and spruce-tolerant hardwood stands as influenced by stand characteristics and spruce budworm defoliation. *Forest Ecology and Management 280*, 82-92. https://doi.org/10.1016/j.foreco.2012.05.023

Colpron-Tremblay, J., and Lavoie, M. (2010). Long-term stand-scale dynamics of a boreal mixed forest in Québec, Canada. *Review of Palaeobotany and Palynology 161* (1-2): 43-58. https://doi.org/10.1016/j.revpalbo.2010.03.003

Conedera, M., Tinner, W., Neff, C., Meurer, M., Dickens, A.F., and Krebs, P. (2009). Reconstructing past fire regimes: methods, applications, and relevance to fire management and conservation. *Quaternary Science Reviews 28* (5-6), 555-576. https://doi.org/10.1016/j.quascirev.2008.11.005

Cooke, B.J., Nealis, V.G., and Régnière, J. (dir). (2007). *Insect defoliators as periodic disturbances in northern forest ecosystems*. In: *Plant disturbance ecology: the process and the response*. E.A., Johnson, and K., Miyanishi. Elsevier

Couillard, P-L., Payette, S., and Grondin, P. (2012). Recent impact of fire on high-altitude balsam fir forests in south-central Quebec. *Canadian Journal of Forest Research 42* (7), 1289-1305. https://doi.org/10.1139/x2012-081

Couillard, P-L., Payette, S., and Grondin, P. (2013). Long-term impact of fire on high-altitude balsam fir (Abies balsamea) forests in south-central Quebec deduced from soil charcoal. *Canadian Journal of Forest Research 43* (2), 188-199. https://doi.org/10.1139/cjfr-2012-0414

Couillard, P-L., Payette, S., Lavoie, M., and Frégeau, M. (2021). Precarious resilience of the boreal forest of eastern North American during the Holocene. *Forest Ecology and Management 485*, 118954. https://doi.org/10.1016/j.foreco.2021.118954

Cruz, M.G. (1999). *Modeling the initiation and spread and crown fires*. [M.Sc. Thesis. University of Montana. Missoula, Montana, USA]

Cruz, M.G., Alexander, M.E., and Wakimoto, R.H. (2003). Assessing canopy fuel stratum characteristics in crow fire prone fuel types of western North America. *International Journal of Wildland Fire 12* (1), 39-50 https://doi.org/10.1071/WF02024

Cruz, M.G., Alexander, M.E., and Wakimoto, R.H. (2004). Modeling the likelihood of crown fire occurrence in conifer forest stands. *Forest Science 50* (5), 640-658. https://doi.org/10.1093/forestscience/50.5.640

Cruz, M.G., Alexander, M.E., and Wakimoto, R.H. (2005). Development and testing of models for predicting crown fire rate of spread in conifer forest stands. *Canadian Journal of Forest Research 35* (7), 1626-1639. https://doi.org/10.1139/x05-085

Cudmore, T.J., Bjorklund, N., Carroll, A.L., and Lindgren, B.S. (2010). Climate change and range expansion of an aggressive bark beetle: evidence of higher beetle reproduction in naïve host tree populations. *Journal of Applied Ecology 47* (5), 1036-1043. https://doi.org/10.1111/j.1365-2664.2010.01848.x

Cullingham, C.I., Cooke, J.E.K., Dang, S., Davis, C.S., Cooke, B.J., and Coltman, D.W. (2011). Mountain pine beetle host-range expansion threatens the boreal forest. *Molecular Ecology 20* (10), 2157-2171. https://doi.org/10.1111/j.1365-294X.2011.05086.x

Dale, V.H., Joyce, L.A., McNulty, S., Neilson, R.P., Ayres, M.P., Flannigan, M.D., Hanson, P.J., Irland, L.C., Lugo, A.E., Peterson, C.J., Simberloff, D., Swanson, F.J., Stocks, B.J., and Wotton, B.M. (2001). Climate change and forest disturbances. *BioScience 51* (9), 723-734. https://doi.org/10.1641/0006-3568(2001)051[0723:CCAFD]2.0.CO;2

Dantas, V.L, Hirota, M., Oliveira, R.S., and Pausas, J.G. (2016). Disturbance maintains alternative biome states. *Ecology Letters 19* (1), 12-19. https://doi.org/10.1111/ele.12537

D'Aoust, V., Kneeshaw, D., and Bergeron, Y. (2004). Characterization of canopy openness before and after a spruce budworm outbreak in the southern boreal forest. *Canadian Journal of Forest Research 34* (2), 339-352. https://doi.org/10.1139/x03-278

Da Silva, A.C., Whalen, M.T., Hladil, J., Chadimova, L., Chen, D., Spassov, S., Boulvain, F., and Devleeschouwer, X. (2015). Magnetic susceptibility application: a window onto ancient environments and climatic variations: foreword. *Geological Society, London, Special Publications 414*, 1-13. https://doi.org/10.1144/SP414.12

Dearing, J.A., and Flower, R.J. (1982). The magnetic susceptibility of sediment material trapped in Lough Neagh, northern Ireland, and its erosional significance. *Limnology and Oceanography 27* (5), 969-975. https://doi.org/10.4319/lo.1982.27.5.0969

Dearing, J.A. (1999). *Environmental magnetic susceptibility: using the Bartington MS2 System* (2nd edition). Chi Publishing. Kenilworth.

De Grandpré, L., Kneeshaw, D.D., Perigon, S., Boucher, D. Marchand, M., Pureswaran, D., and Girardin, M.P. (2019). Adverse climatic periods precede and amplify defoliator-induced tree mortality in eastern boreal North America. *Journal of Ecology 107* (1), 452-467. https://doi.org/10.1111/1365-2745.13012

Deininger, M., McDermott, F., Mudelsee, M., Werner, M., Frank, N., and Mangini, A. (2017). Coherency of late Holocene European speleothem δ18O records linked to North Atlantic Ocean circulation. *Climate Dynamics 49*, 595-619. https://doi.org/10.1007/s00382-016-3360-8

Deslauriers, A., Caron, L., and Rossi, S. (2015). Carbon allocation during defoliation: Testing a defense-growth trade-off in balsam fir. *Frontiers in Plant Science 6,* 338. https://doi.org/10.3389/fpls.2015.00338

Drapeau, P., Leduc, A., Kneeshaw, D., and Deslauriers, A. (2024). Mémoire du Centre d'étude de la forêt présenté au Ministère des Ressources naturelles et des Forêts dans le cadre de la demarche de réflexion sur l'avenir de la forêt. [Mémoire, Centre d'études de la forêt]

Duschesne, L., Houle, D., Ouimet, R., Caldwell, L., Gloor, M., and Brienen, R. (2019). Large apparent growth increases in boreal forests inferred from tree-rings are an artefact of sampling biases. *Scientific Reports 9*, 6832. https://doi.org/10.1038/s41598-019-43243-1

Dymond, C.C., Neilson, E.T., Stinson, G., Porter, K., MacLean, D.A., Gray, D.R., Campagna, M., and Kurz, W.A. (2010). Future spruce budworm outbreak may create a carbon source in eastern Canadian forests. *Ecosystems 13*, 917-931. https://doi.org/10.1007/s10021-010-9364-z

Easterling, D.R., Meehl, G.A., Parmesan, C., Changnon, S.A., Karl, T.R., and Mearns, L.O. (2000). Climate extremes: observations, modelling and impacts. *Science 289* (5487), 2068-2074. https://doi.org/10.1126/science.289.5487.2068

Erbilgin, N., Ma, C., Whitehouse, C., Shan, B., Najar, A., Evenden, M. (2014). Chemical similarity between historical and novel host plants promotes range and host expansion of the mountain pine beetle in a naïve host ecosystem. *The New Phytologist 201* (3), 940-950. https://doi.org/10.1111/nph.12573

Ericsson, A., Larsson, S., and Tenow, O. (1980). Effects of early and late season defoliation on growth and carbohydrate dynamics in Scots Pine. *Journal of Applied Ecology 17* (3), 747-769. https://doi.org/10.2307/2402653

Esper, J., Büntgen, U., Frank, D.C., Nievergelt, D., and Liebhold, A. (2007). 1200 years of regular outbreaks in alpine insects. *Proceedings of the Royal Society B 274* (1610), 671-679. https://doi.org/10.1098/rspb.2006.0191

ESRI. 2015. ArcMap 10.4.1. Software. Environmental Systems Research Institute, Redlands, CA

Faegri, K., and Iversen, J. (1989). *Textbook of Pollen Analysis* (4th Edition). Chichester: John Wiley

Falk, D.A., Miller, C., McKenzie, D., and Black, A.E. (2007). Cross-scale analysis of fire regimes. *Ecosystems 10*, 809-823. https://doi.org/10.1007/s10021-007-9070-7

Fernández-Macho, J. (2012). Wavelet multiple correlation and cross-correlation: A multiscale analysis of Eurozone stock markets. *Physica A 391* (4), 1097-1104. https://doi.org/10.1016/j.physa.2011.11.002

Fernández-Macho, J. (2018). Time-localized wavelet multiple regression and correlation. *Physica A 493*, 1226-1238. https://doi.org/10.1016/j.physa.2017.11.050

Flannigan, M., Stocks, B., Turetsky, M., and Wotton, M. (2009). Impacts of climate change on fire activity and fire management in the circumboreal forest. *Global Change Biology 15* (3), 549-560. https://doi.org/10.1111/j.1365-2486.2008.01660.x

Flannigan, M., Cantin, A.S., de Groot, W.J., Wotton, M., Newbery, A., and Gowman, L.M. (2013). Global wildland fire season severity in the 21st century. *Forest Ecology and Management 294*, 54-61. https://doi.org/10.1016/j.foreco.2012.10.022

Fleming, R.A., Candau, J-N., McApline, R.S. (2002). Landscape-scale analysis of interactions between insect defoliation and forest fire in central Canada. *Climatic Change 55*, 251-272. https://doi.org/10.1023/A:1020299422491

Florescu, G., Brown, K.J., Carter, V.A., Kunes, P., Veski, S., and Feurdean, A. (2019). Holocene rapid climate changes and ice-rafting debris events reflected in high-resolution European charcoal records. *Quaternary Science Reviews 222*, 105877. https://doi.org/10.1016/j.quascirev.2019.105877

Frégeau, M., Payette, S., and Grondin, P. (2015). Fire history of the central boreal forest in eastern North America reveals stability since the mid-Holocene. *The Holocene 25* (12), 1912-1922. https://doi.org/10.1177/0959683615591361

Fulé, P.Z., Covington, W.W., and Moore, M.M. (1997). Determining reference conditions for ecosystem management of southwestern ponderosa pine forests. *Ecological Applications 7* (3), 895-908. https://doi.org/10.1890/1051-0761(1997)007[0895:DRCFEM]2.0.CO;2

Fuentealba, A., Pureswaran, D., Bauce, É., and Despland, E. (2017). How does synchrony with host plant affect the performance of an outbreaking insect defoliator? *Oecologia 184*, 847-857. https://doi.org/10.1007/s00442-017-3914-4

Gajewski, K. (2015). Quantitative reconstruction of Holocene temperatures across the Canadian Arctic and Greenland. *Global and Planetary Change 128*, 14-23. https://doi.org/10.1016/j.gloplacha.2015.02.003

Gavin, D.G., Hu, F.S., Lertzman, K., and Corbett, P. (2006). Weak climatic control of stand-scale fire history during the late Holocene. *Ecology 87* (7), 1722-1732. https://doi.org/10.1890/0012-9658(2006)87[1722:WCCOSF]2.0.CO;2

Gennaretti, F., Arseneault, D., and Bégin, Y. (2014a). Millennial disturbance-driven forest stand dynamics in the eastern Canadian taiga reconstructed from subfossil logs. *Journal of Ecology 102* (6), 1612-1622. https://doi.org/10.1111/1365-2745.12315

Gennaretti, F., Arseneault, D., Nicault, A., Perreault, L., and Bégin, Y. (2014b). Volcano-induced regime shifts in millennial tree-ring chronologies from northeastern North America. *Proceedings of the National Academy of Science 111* (28), 100077-10082. https://doi.org/10.1073/pnas.1324220111

Ghiradella, H. (dir). (1998). *Hairs, bristles, and scales*. In: *Microscopic Anatomy of Invertebrates*. Harrison, F.W. Wiley-Liss.

Girardin, M.P., Ali, A.A., Carcaillet, C., Blarquez, O., Hély, C., Terrier, A., Genries, A., and Bergeron, Y. (2013). Vegetation limits the impact of a warm climate on boreal wildfires. *The New Phytologist 199* (4), 1001-1011. https://doi.org/10.1111/nph.12322

Gouhier, T.C, Grinsted, A, Simk, V. (2021). *R package biwavelet: Conduct univariate and bivariate wavelet analyses* (Version 0.20.21). https://github.com/tgouhier/biwavelet

Gray, D.R., Régnière, J., Boulet, B. (2000). Analysis and use of historical patterns of spruce budworm defoliation to forecast outbreak patterns in Québec. *Forest Ecology and Management 127* (1-3), 217-231. https://doi.org/10.1016/S0378-1127(99)00134-6

Gray, D.R. (2008). The relationship between climate and outbreak characteristics of the spruce budworm in eastern Canada. *Climatic Change 87*, 361-383. https://doi.org/10.1007/s10584-007-9317-5

Greenbank, D.O., Schaefer, G.W., Rainey, R.C. (1980). Spruce budworm (Lepidoptera: Tortricidae) moth flight and dispersal: New understanding from canopy observations, radar, and aircraft. *Memoirs of the Entomological Society of Canada 112* (S110), 1-49. https://doi.org/10.4039/entm112110fv

Greene, G.A., and Daniels, L.D. (2017). Spatial interpolation and mean fire interval analyses quantify historical mixed-severity fire regimes. *International Journal of Wildland Fire 26* (2), 136-147. https://doi.org/10.1071/WF16084

Grinsted, A., Moore, J.C., and Jevrejeva, S. (2004). Application of the cross wavelet transform and wavelet coherence to geophysical time series. *Nonlinear Processes in Geophysics 11* (5/6), 561-566. https://doi.org/10.5194/npg-11-561-2004

Guay, R., Gagnon, R., and Morin, H. (1992). A new automatic and interactive tree ring measurement system based on a line scan camera. The *Forestry Chronicle 68* (1), 138-141. https://doi.org/10.5558/tfc68138-1

Guiterman, C.H, Lynch, A.M., and Axelson, J.N. (2020). dfoliatR: An R package for detection and analysis of insect defoliation signals in tree rings. *Dendrochronologia 63*, 125750. https://doi.org/10.1016/j.dendro.2020.125750

Halofsky, J.E., Peterson, D.L., and Harvey, B.J. (2020). Changing wildfire, changing forests: the effects of climate change on fire regimes and vegetation in the Pacific Northwest, USA. *Fire Ecology 16* (4), 1-26. https://doi.org/10.1186/s42408-019-0062-8

Harris, J.W.E., and Dawson, A.F. (1979). *Evaluation of aerial forest pest damage survey techniques in British Columbia*. Environment Canada, Canadian Forestry Service, Pacific Forest Research Centre, Victoria BC. BC-X-198.

Harrison, S.P., Prentice, I.C., Bloomfield, K.J., Dong, N., Forkel, M., Forrest, M., Ningthoujam, R.K., Pellegrini, A., Shen, Y., Baudena, M., Cardoso, A.W., Huss, J.C., Joshi, J., Oliveras, I., Pausas, J.G., and Simpson, K.J. (2021). Understanding and modelling wildfire regimes: an ecological perspective. *Environmental Research Letters 16*, 125008. https://doi.org/10.1088/1748-9326/ac39be

Hart, S.J., Veblen, T.T., Eisenhart, K.S., Jarvis, D., and Kulakowski, D. (2014). Drought induces spruce beetle (Dendroctonus rufipennis) outbreaks across northwestern Colorado. *Ecology 95* (4), 930-939. https://doi.org/10.1890/13-0230.1

Hart, S.J., Veblen, T.T., Schneider, D., and Molotch, N.P. (2017). Summer and winter drought drive the initiation and spread of spruce beetle outbreak. *Ecology 98* (10), 2698-2707. https://doi.org/10.1002/ecy.1963

He, T., and Lamont, B.B. (2018). Baptism by fire: the pivotal role of ancient conflagrations in evolution of the Earth's flora. *Natural Science Review 5* (2), 237-254. https://doi.org/10.1093/nsr/nwx041

Hély, C., Bergeron, Y., and Flannigan, M.D. (2000). Effects of stand composition on fire hazard in mixed-wood Canadian boreal forest. *Journal of Vegetation Science 11* (6), 813-824. https://doi.org/10.2307/3236551

Hély, C., Girardin, M.P., Ali, A.A., Carcaillet, C., Brewer, S., and Bergeron, Y. (2010). Eastern boreal North American wildfire risk of the past 7000 years: a model-data comparison. *Geophysical research letters 37* (14), L14709. https://doi.org/10.1029/2010GL043706

Hély, C., Chaste, E., Girardin, M.P., Remy, C.C., Blarquez, O., Bergeron, Y., and Ali, A.A. (2020). A Holocene perspective of vegetation controls on seasonal boreal wildfire sizes using numerical paleo-ecology. *Frontiers in Forests and Global Change 3*, 511901. https://doi.org/10.3389/ffgc.2020.511901

Hennebelle, A., Grondin, P., Aleman, J.C., Ali, A.A., Bergeron, Y., Borcard, D., and Blarquez, O. (2018). Using palecology to improve reference conditions for ecosystem-based management in western spruce-moss subdomain of Québec. *Forest Ecology and Management 430*, 157-165. https://doi.org/10.1016/j.foreco.2018.08.007

Hennigar, C.R., MacLean, D.A., Quiring, D.T., Kershaw Jr., J.A. (2008). Differences in spruce budworm defoliation among balsam fir, and white, red, and black spruce. *Forest Science 54* (2), 158-166. https://doi.org/10.1093/forestscience/54.2.158

Heyerdahl, E.K., Brubaker, L.B., and Agee, J.K. (2001). Spatial controls of historical fire regimes: a multiscale example from the interior west, USA. *Ecology 82* (3), 660-678. https://doi.org/10.1890/0012-9658(2001)082[0660:SCOHFR]2.0.CO;2

Heyerdahl, E.K., Lertzman, K., and Karpuk, S. (2007). Local-scale controls of a low-severity fire regime (1750-1950), southern British Columbia, Canada. *Écoscience 14* (1), 40-47. https://doi.org/10.2980/1195-6860(2007)14[40:LCOALF]2.0.CO;2

Hicke, J.E., Johnson, M.C., Hayes, J.L., and Preisler, H.K. (2012). Effects of bark beetles-caused tree mortality on wildfire. *Forest Ecology and Management 271*, 81-90. https://doi.org/10.1016/j.foreco.2012.02.005

Higuera, P.E., Sprugel, D.G., and Brubake, L.B. (2005). Reconstructing fire regimes with charcoal from small-hollow sediments: A calibration with tree-ring records of fire. *The Holocene 15* (2), 238-251. https://doi.org/10.1191/0959683605hl789rp

Higuera, P.E., Peters, M.E., Brubaker, L.B., and Gavin, D.G. (2007). Understanding the origin and analysis of sediment-charcoal records with a simulation model. *Quaternary Science Reviews 26* (13-14), 1790-1809. https://doi.org/10.1016/j.quascirev.2007.03.010

Higuera, P.E. (2009). *CharAnalysis 0.9: Diagnostic and analytical tools for sediment-charcoal analysis*. https://github.com/phiguera/CharAnalysis

Higuera, P.E., Gavin, D.G., Bartlein, P.J., and Hallet, D.J. (2010). Peak detection in sediment-charcoal records: Impacts of alternative data analysis methods on fire-history interpretations. *International Journal of Wildland Fire 19* (8), 996-1014. https://doi.org/10.1071/WF09134

Higuera, P.E., Whitlock, C., and Gage, J.A. 2011. Linking tree-ring and sediment-charcoal records to reconstruct fire occurrence and area burned in subalpine forests of Yellowstone National Park, USA. *The Holocene 21* (2), 327-341. https://doi.org/10.1177/0959683610374882

Holling, C.S. (1973). Resilience and stability of ecological systems. *Annual Review of Ecology and Systematics 4*, 1-23. https://doi.org/10.1146/annurev.es.04.110173.000245

Holmes, R.L. (1983). Computer-assisted quality control in tree-ring dating and measurement. *Tree-Ring Bulletin 43*, 69-78

Houndode, D.J., Krause, C., and Morin, H. (2021). Predicting balsam fir mortality in boreal stands affected by spruce budworm. *Forest Ecology and Management 496*, 119408. https://doi.org/10.1016/j.foreco.2021.119408

James, P.M.A., Robert, L-E., Wotton, B.M., Martell, D.L., and Fleming, R.A. (2017). Lagged cumulative spruce budworm defoliation affects the risk of fire ignition in Ontario, Canada. *Ecological Applications 27* (2), 532-544. https://doi.org/10.1002/eap.1463

Jasinski, J.P.P., and Payette, S. (2005). The creation of alternative stable states in the southern boreal forest, Québec. Canada. *Ecological Monographs 75* (4), 561-583. https://doi.org/10.1890/04-1621

Jardon, Y., Morin, H., and Dutilleul, P. (2003). Périodicité et synchronisme des épidémies de la tordeuse des bourgeons de l'épinette au Québec. *Canadian Journal of Forest Research 33* (10), 1947-1961. https://doi.org/10.1139/x03-108

Jepsen, J.U., Hagen, S.B., Ims, R.A., and Yoccoz, N.G. (2008). Climate change and outbreaks of the geometrids Operophtera brumata and Epirrita autumnata in subarctic birch forest: Evidence of a recent outbreak range expansion. *Journal of Animal Ecology 77* (2), 257-264. https://doi.org/10.1111/j.1365-2656.2007.01339.x

Jepsen, J.U, Kapari, L., Hagen, S.B., Schott, T., Vinstad, O.P.L., Nilssen, A.C., and Ims, R.A. (2011). Rapid northwards expansion of a forest insect pest attributed to spring phenology matching with sub-Arctic birch. *Global Change Biology 17* (6), 2071-2083. https://doi.org/10.1111/j.1365-2486.2010.02370.x

Johnson, E.A., Miyanishi, K., and Weir, J.M.H. (1998). Wildfires in the western Canadian boreal forest: landscape patterns and ecosystem management. *Journal of Vegetation Science 9* (4), 603-610. https://doi.org/10.2307/3237276

Jolly, W.M., Cochrane, M.A., Freeborn, P.H., Holden, Z.A., Brown, T.J., Williamson, G.J., and Bowman D.M.J.S. (2015). Climate-induced variations in global wildfire danger from 1979 to 2013. *Nature Communications 6*, 7537. https://doi.org/10.1038/ncomms8537

Juggens, S. (2020). *Rioja: Analysis of Quaternary Science Data*. https://cran.r-project.org/package=rioja

Khare, S., Drolet, G., Sylvain, J-D., Paré, M.C., and Rossi, S. (2019). Assessment of spatio-temporal patterns of black spruce bud phenology across Quebec based on MODIS-NDVI time series and field observations. *Remote Sensing 11* (23), 2745. https://doi.org/10.3390/rs11232745

Keane, R.E., Hessburg, P.E., Landres, P.B., and Swanson, F.J. (2009). The use of historical range and variability (HRV) in landscape management. *Forest Ecology and Management 258* (8), 1025-1037. https://doi.org/10.1016/j.foreco.2009.05.035

Keeley, J.E., Pausas, J.G., Rundel, P.W., Bond, W.J., and Bradstock, R.A. (2011). Fire as an evolutionary pressure shaping plant traits. *Trends in Plant Science 16* (8), 406-411. https://doi.org/10.1016/j.tplants.2011.04.002

Kefi, S., Holmgren, M., and Scheffer, M. (2016). When can positive interactions cause alternative stable states in ecosystems? *Functional Ecology 30* (1), 88-97. https://doi.org/10.1111/1365-2435.12601

Kettela, E.G. (1982). *Results of aerial surveys for current spruce budworm defoliation in New Brunswick and a review of the methodology*. Environment Canada, Canadian Forest Service, Maritimes Forest Research Centre, Fredericton, NB. Technical Note No. 66

Kleinman, J.S., Goode, J.D., Fries, A.C., and Hart, J.L. (2019). Ecological consequences of compound disturbances in forest ecosystems: a systematic review. *Ecosphere 10* (11), e02962. https://doi.org/10.1002/ecs2.2962

Kneeshaw, D.D., and Bergeron, Y. (1996). Ecological factors affecting the abundance of advance regeneration in Quebec's southwestern boreal forest. *Canadian Journal of Forest Research 26* (5), 888-898. https://doi.org/10.1139/x26-097

Kneeshaw, D.D., and Bergeron, Y. (1998). Canopy gap characteristics and tree replacement in the southeastern boreal forest. *Ecology 79* (3), 783-794. https://doi.org/10.1890/0012-9658(1998)079[0783:CGCATR]2.0.CO;2

Kneeshaw, D.D., and Bergeron, Y. (1999). Spatial and temporal patterns of seedling and sapling recruitment within canopy gaps caused by spruce budworm. *Écoscience 6* (2), 214-222. https://doi.org/10.1080/11956860.1999.11682522

Krause, C., and Morin, H. (1995). Changes in radial increment in stems and roots of balsam fir [*Abies balsamea* (L.) Mill.] after defoliation by spruce budworm. *The Forestry Chronicle 71* (6), 747-754. https://doi.org/10.5558/tfc71747-6

Krause, C., Gionest, F., Morin, H., and MacLean, D.A. (2003). Temporal relations between defoliation caused by spruce budworm (*Choristoneura fumiferana* Clem.) and growth of balsam fir (*Abies balsamea* (L.) Mill.). *Dendrochonologia 21* (1), 23-31. https://doi.org/10.1078/1125-7865-00037

Krause, C., Luszczynski, B., Morin, H., Rossi, S., and Plourde, P-Y. (2012). Timing of growth reductions in black spruce stem and branches during the 1970s spruce budworm outbreak. *Canadian Journal of Forest Research 42* (7), 1220-1227. https://doi.org/10.1139/x2012-048

Kurz, W.A., Shaw, C.H., Boisvenue, C., Stinson, G., Metsaranta, J., Leckie, D., Dyk, A., Smyth, C., and Neilson, E.T. (2013). Carbon in Canada's boreal forest- a synthesis. *Environmental Reviews 21* (4), 260-292. https://doi.org/10.1139/er-2013-0041

Labat D. (2005). Recent advances in wavelet analyses: Part 1. A review of concepts. *Journal of Hydrology 314* (1-4), 275-288. https://doi.org/10.1016/j.jhydrol.2005.04.003

Lafontaine-Boyer, K., and Gajewski, K. (2014). Vegetation dynamics in relation to late Holocene climate variability and disturbance, Outaouais, Québec, Canada. *The Holocene 24* (11), 1515-1526. https://doi.org/10.1177/0959683614544054

Lamont, B.B., Pausas, J.G., He, T., Witkowski, E.T.F., and Hanley, M.E. (2020). Fire as a selective agent for both serotiny and nonserotiny over space and time. *Critical Reviews in Plant Sciences 39* (2), 140-172. https://doi.org/10.1080/07352689.2020.1768465

Landres, P.B., Morgan, P., and Swanson, F.J. (1999). Overview of the use of natural variability concepts in managing ecological systems. *Ecological Applications 9* (4), 1179-1188. https://doi.org/10.1890/1051-0761(1999)009[1179:OOTUON]2.0.CO;2

Laroque, G.R., Bhatti, J., Hazlet, P., Arsenault, A., and Komarov, A. (2014). Special issue: Research advances in productivity, succession, management, and carbon and water cycles in the boreal forest. *Écoscience 21* (3-4), V-VIII. https://doi.org/10.2980/21-(3-4)-v-vii

Larroque, J., Johns, R., Canape, J., Morin, B., and James, P.M.A (2020). Spatial genetic structure at the leading edge of a spruce budworm outbreak: the role of dispersal in outbreak spread. *Forest Ecology and Management 461*, 117965. https://doi.org/10.1016/j.foreco.2020.117965

Lavoie, M., and Richard, P.J.H. (2000). Postglacial water-level changes of a small lake in southern Québec, Canada. *The Holocene 10* (5), 621-634. https://doi.org/10.1191/095968300672141865

Lavoie, M., Filion, L., and Robert, E.C. (2009). Boreal peatland margins as repository sites of long-term natural disturbance of balsam fir/spruce forests. *Quaternary Research 71* (3), 295-306. https://doi.org/10.1016/j.yqres.2009.01.005

Lavoie, J., Montoro Girona, M., and Morin, H. (2019). Vulnerability of conifer regeneration to spruce budworm outbreaks in the eastern Canadian boreal forest. *Forests 10* (10), 850. https://doi.org/10.3390/f10100850

Leckie, D.G., Teillet, P.M., Fedosejevs, G., and Ostaff, D.P. (1988). Reflectance characteristics of cumulative defoliation of balsam fir. *Canadian Journal of Forest Research 18* (8), 1008-1016. https://doi.org/10.1139/x88-154

Leclerc, M-AF., Daniels, L.D., and Carrol, A.L. (2021). Managing wildlife habitat: complex interactions with biotic and abiotic disturbances. *Frontiers in Ecology and Evolution 9*, 613371. https://doi.org/10.3389/fevo.2021.613371

Lemprière, T.C., Kurz, W.A., Hogg, E.H., Schmoll, C., Rampley, G.J., Yemshanov, D., McKenney, D.W., Gilsenan, R., Beatch, A., Blain, A., Bhatti, J.S., and Krcmar, E. (2013). Canadian boreal forests and climate change mitigation. *Environmental Letters 21* (4), 293-321. https://doi.org/10.1139/er-2013-0039

Li, Y-X., Yu, Z., and Kodama, K.P. (2007). Sensitive moisture response to Holocene millennial-scale climate variations in the Mid-Atlantic region, USA. *The Holocene 17* (1), 3-8. https://doi.org/10.1177/0959683606069386

Littell, J.S., Peterson, D.L., Riley, K.L., Liu, Y., and Luce, C.H. (2016). A review of the relationships between drought and forest fire in the United States. *Global Change Biology 22* (7), 2353-2369. https://doi.org/10.1111/gcb.13275

Loader, C. (2020). *locfit: Local regression, likelihood and density estimation*. R package version 1.5-9.4. https://CRAN.R-project.org/package=locfit

Long, C.J., Whitlock, C., Bartlein, P.J., and Millspaugh, S.H. (1998). A 900-year fire history from the Oregon Coast Range, based on a high-resolution charcoal study. *Canadian Journal of Forest Research 28* (5), 774-787. https://doi.org/10.1139/x98-051

Long, J.N. (2009). Emulating natural disturbance regimes as a basis for forest management: a North American view. *Forest Ecology and Management 257* (9), 1868-1873. https://doi.org/10.1016/j.foreco.2008.12.019

Lovett, G.M., Christenson, L.M., Groffman, P.M., Jones, C.G., Hart, J.E., and Mitchell, M.J. (2002). Insect defoliation and nitrogen cycling in forests. *BioScience 52* (4), 335-341. https://doi.org/10.1641/0006-3568(2002)052[0335:IDANCI]2.0.CO;2

Lynch, H.J., and Moorcroft, P.R. (2008). A spatiotemporal Ripley's K-function to analyze interactions between spruce budworm and fire in British Columbia, Canada. *Canadian Journal of Forest Research 38* (12), 3112-3119. https://doi.org/10.1139/X08-143

Lynch, A.M. (2012). *What tree-ring reconstruction tells us about conifer defoliator outbreaks*. In: *Insect outbreaks revisited*. Barbosa P., Letourneau, D.K., Agrawal, A.A., Blackwell Publishing Ltd.

MacKinnon, W.E., and MacLean, D.A. (2003). The influence of forest and stand conditions on spruce budworm defoliation in New Brunswick, Canada. *Forest Science 49* (5), 657-667. https://doi.org/10.1093/forestscience/49.5.657

Macias Fauria, M., and Johnson, E.A. (2008). Climate and wildfires in the North American boreal forest. *Philosophical Transactions of the Royal Society B 363* (1501), 2317-2329. https://doi.org/10.1098/rstb.2007.2202

Macias Fauria, M., Michaletz, S.T., and Johnson, E.A. (2010). Predicting climate change effects on wildfires requires linking processes across scales. *Climate Change 2* (1), 99-112. https://doi.org/10.1002/wcc.92

MacLean, D.A. (1980). Vulnerability of fir-spruce stands during uncontrolled spruce budworm outbreaks-A review and discussion. *Forestry Chronicle 56* (5), 213-221. https://doi.org/10.5558/tfc56213-5

MacLean, D.A. (1984). Effects of spruce budworm outbreaks on the productivity and stability of balsam fir forests. *Forestry Chronicle 60* (5), 273-279. https://doi.org/10.5558/tfc60273-5

MacLean, D.A., and Ostaff, D.P. (1989). Patterns of balsam fir mortality caused by an uncontrolled spruce budworm outbreak. *Canadian Journal of Forest Research 19* (9), 1087-1095. https://doi.org/10.1139/x89-165

MacLean, D.A., and MacKinnon, W.E. (1996). Accuracy of aerial sketch-mapping estimates of spruce budworm defoliation in New Brunswick. *Canadian Journal of Forest Research 26* (12), 2099-2108. https://doi.org/10.1139/x26-238

MacLean, D.A, Hunt, T.L., Eveleigh, E.S., and Morgan, M.G. (1996). The relation of balsam fir volume increment to cumulative spruce budworm defoliation. *The Forestry Chronicle 72* (5), 533-540. https://doi.org/10.5558/tfc72533-5

MacLean, D.A. (2016). Impacts of insect outbreaks on tree mortality, productivity, and stand development. *The Canadian Entomologist 148* (S1), S138-S159. https://doi.org/10.4039/tce.2015.24

Mageroy, M.H., Parent, G., Germanos, G., Giguère, I., Delvas, N., Maaroufi, H., Bauce, É., Bohlmann, J., and Mackay, J.J. (2014). Expression of the ß-glucosidase gene *Pgßglu-1* underpins natural resistance of white spruce against spruce budworm. *The Plant Journal 81* (1), 68-80. https://doi.org/10.1111/tpj.12699

Mallat, S. (1998). *A wavelet tour of signal processing*. Academic Press, San Diego

Mann, M.E. (2004). On smoothing potentially non-stationary time series. *Geophysical Research Letters 31* (7), L07214. https://doi.org/10.1029/2004GL019569

Mann, M.E. (2008). Smoothing of climate time series revisited. *Geophysical Research Letters 35* (16), L16708. https://doi.org/10.1029/2008GL034716

Mann, M.E., Zhang, Z., Rutherford, S., Bradley, R.S., Hughes, M.K., Shindell, D., Ammann, C., Faluvegi, G., and Ni, F. (2009). Global signatures and dynamical origins of the Little Ice Age and Medieval Climate Anomaly. *Science 326* (5957), 1256-1260. https://doi.org/10.1126/science.1177303

Marcott, S.A., Shakun, J.D., Clark, P.U., and Mix, A.C. (2013). A reconstruction of regional and global temperature for the past 11,300 years. *Science 339* (6124), 1198-1201. https://doi.org/10.1126/science.1228026

Marcoux, H.M., Gergel, S.E., and Daniels, L.D. (2013). Mixed-severity fire regimes: how well are they represented by existing fire-regime classification systems? *Canadian Journal of Forest Research 43* (7), 658-668. https://doi.org/10.1139/cjfr-2012-0449

Marcoux, H.M., Daniels, L.D., Gergel, S.E., Da Silva, E., Gedalof, Z., and Hessburg, P.F. (2015). Differentiating mixed- and high-severity fire regimes in mixed-conifer forests of the Canadian Cordillera. *Forest Ecology and Management 341*, 45-58. https://doi.org/10.1016/j.foreco.2014.12.027

Marsicek, J., Shuman, B.N., Bartlein, P.J., Shafer, S.L., and Brewer, S. (2018). Reconciling divergent trends and millennial variations in Holocene temperatures. *Nature 554*, 92-96. https://doi.org/10.1038/nature25464

Martin, M., Morin, H., and Fenton, N.J. (2019). Secondary disturbances of low and moderate severity drive the dynamics of eastern Canadian boreal old-growth forests. *Annals of Forest Science 76*, 108. https://doi.org/10.1007/s13595-019-0891-2

Martin, M., Krause, C., and Morin, H. (2020). Linking radial growth patterns and moderate-severity disturbance dynamics in boreal old-growth forests driven by recurrent insect outbreaks: a tale of opportunities, successes, and failures. *Ecology and Evolution 11* (1), 566-586. https://doi.org/10.1002/ece3.7080

Matthews, B.W. (1975). Comparison of the predicted and observed secondary structure of T4 phage lysozyme. *Biochimica et Biophysica Acta (BBA)- Protein Struct 405* (2), 442–451. https://doi.org/10.1016/0005-2795(75)90109-9

Mattson, W.J., and Addy, N.D. (1975). Phytophagous insects as regulators of forest primary production. *Science 190* (4214), 515-522. https://doi.org/10.1126/science.190.4214.515

Mayewski, P.A., Rohling, E.E., Stager, J.C., Karlen, W., Maasch, K.A., Meeker, L.D., Meyerson, E.A., Gasse, F., van Kreveld, S., Holmgren, K., Lee-Thorp, J., Rosqvist, G., Rack, F., Staubwasser, M., Schneider, R.R., and Steig, E.J. (2004). Holocene climate variability. *Quaternary Research 62* (3), 243-255. https://doi.org/10.1016/j.yqres.2004.07.001

McCullough, D.G., Werner, R.A., and Neumann, D. (1998). Fire and insects in northern and boreal forest ecosystems of North America. *Annual Review of Entomology 43*, 107-127

McDowell, N.G., Allen, C.D., Anderson-Teixeira, K., Aukema, B.H., Bond-Lamberty, B., Chini, L., Clark, J.S., Dietze, M., Grossiord, C., Hanbury-Brown, A., Hurtt, G.C., Jackson, R.B., Johnson, D.J., Kueppers, L., Lichstein, J.W., Ogle, K., Poulter, B., Pugh, T.A.M., Seidl, R., Turner, M.G., Uriarte, M., Walker, A.P., and Xu, C. (2020). Pervasive shifts in forest dynamics in a changing world. *Science 368* (6494), eaaz9463. https://doi.org/10.1126/science.aaz9463

McLauchlan, K.K., Higuera, P.E., Miesel, J., Rogers, B.M., Schweitzer, J., Shuman, J.K., Tepley, A.J., Varner, J.M., Veblen, T.T., Adalsteinsson, S.A., Blach, J.K., Baker, P., Batllori, E., Bigio, E., Brando, P., Cattau, M., Chipman, M.L., Coen, J., Crandall, R., Daniels, L., Enright, N., Gross, W.S., Harvey, B.J., Hatten, J.A., Hermann, S., Hewitt, R.E., Kobziar, L.N., Landesmann, J.B., Loranty, M.M., Maezumi, S.Y., Mearns, L., Moritz, M. Myers, J.A., Pausas, J.G., Pellegrini, A.F.A., Platt, W.J., Roozeboom, J., Safford, H., Santos, F., Scheller, R.M., Sherriff, R.L., Smith, K.G., Smith, M.D., and Watts, A.C. (2020). Fire as a fundamental ecological process: research advances and frontiers. *Journal of Ecology 108* (5), 2047-2069. https://doi.org/10.1111/1365-2745.13403

Méndez-Espinoza, C., Parent, G.J., Lenz, P., Rainville, A., Tremblay, L., Adams, G., McCartney, A., Bauce, É., and MacKay, J. (2018). Genetic control and evolutionary potential of a constitutive resistance mechanism against the spruce budworm (*Choristoneura fumiferana*) in white spruce (*Picea glauca*). *Heredity 121*, 142-154. https://doi.org/10.1038/s41437-018-0061-6

Meigs, G.W., Kennedy, R.E., and Cohen, W.B. (2011). A Landsat time series approach to characterize bark beetle and defoliator impacts on tree mortality and surface fuels in conifer forests. *Remote Sensing of Environment 115* (12), 3707-3718. https://doi.org/10.1016/j.rse.2011.09.009

Meigs, G.W., Campbell, J.L., Zald, H.S.J., Bailey, J.D., Shaw, D.C., and Kennedy, R.E. (2015). Does wildfire likelihood increase following insect outbreaks in conifer forests? *Ecosphere 6* (7), 118. https://doi.org/10.1890/ES15-00037.1

Meigs, G.W., Zald, H.S.J., Campbell, J.L., Keeton, W.S., and Kennedy, R.E. (2016). Do insect outbreaks reduce the severity of subsequent forest fires? *Environmental Research Letters 11* (4), 045008. http://dx.doi.org/10.1088/1748-9326/11/4/045008

MFFP (Ministère des forêts, de la faune et des parcs). (2021a). *Shapefiles of the aerial surveys done to assess the damage caused by the spruce budworm from 1967-present*. [Forest Inventory dataset]. Données ouvertes-Ministère des forêts, de la faune et des parcs. https://www.donneesquebec.ca/recherche/fr/dataset/donnees-sur-les-perturbations-naturelles-insecte-tordeuse-des-bourgeons-de-lepinette

MFFP (Ministère des forêts, de la faune et des parcs). (2021b). *Shapefiles of the forest inventory data including forest composition and previous disturbances*. [Forest Inventory dataset]. Données ouverte-Ministère des forêts, de la faune et des parcs. https://www.donneesquebec.ca/recherche/dataset/carte-ecoforestiere-avec-perturbations

Millar, C.I., and Stephenson, N.L. (2015). Temperate forest health in an era of emerging megadisturbance. *Science 349* (6250), 823-826. https://doi.org/10.1126/science.aaa9933

Millspaugh, S.H., and Whitlock, C. (1995). A 750-year fire history based on lake sediment records in central Yellowstone National Park, USA. *The Holocene 5* (3), 283-292. https://doi.org/10.1177/095968369500500303

Molinari, C., Lehsten, V., Blarquez, O., Carcaillet, C., Davis, B.A.S., Kaplan, J.O., Clear, J., and Bradshaw, R.H.W. (2018). The climate, the fuel and the land use: long-term regional variability of biomass burning in boreal forests. *Global Change Biology 24* (10), 4929-4945. https://doi.org/10.1111/gcb.14380

Morin, H., and Laprise, D. (1990). Histoire récente des épidémies de la Tordeuse des bourgeons de l'épinette au nord du lac-Saint-Jean (Québec): une analyse dendrochronologique. *Canadian Journal of Forest Research 20* (1), 1-8. https://doi.org/10.1139/x90-001

Morin, H. (1994). Dynamics of balsam fir forests in relation to spruce budworm outbreaks in the boreal zone of Québec. *Canadian Journal of Forest Research 24* (4), 730-741. https://doi.org/10.1139/x94-097

Montoro Girona M., Navarro L., and Morin H. (2018). A secret hidden in the sediments: Lepidoptera scales. *Frontiers in Ecology and Evolution 6* (2), 1-5 https://doi.org/10.3389/fevo.2018.00002

Muller, S.D., Richard, P.J.H., Guiot, J., de Beaulieu, J-L., and Fortin, D. (2003). Postglacial climate in the St. Lawrence lowlands, southern Québec: pollen and lake-level evidence. *Palaeogeography, Palaeoclimatology, Palaeoecology 193* (1): 51-72. https://doi.org/10.1016/S0031-0182(02)00710-1

Murdock, T.Q., Taylor, S.W., Flower, A., Mehlenbacher, A., Montenegro, A., Zwiers, F.W., Alfaro, R., and Spittlehouse, D.L. (2013). Pest outbreak distribution and forest management impacts in a changing climate in British Columbia. *Environmental Science & Policy 26*, 75-89. https://doi.org/10.1016/j.envsci.2012.07.026

Navarro, L., Harvey, A.E, and Morin, H. (2018a). Lepidoptera wing scales: a new paleocological indicator for reconstructing spruce budworm abundance. *Canadian Journal of Forest Research 48* (3), 302-308. https://doi.org/10.1139/cjfr-2017-0009

Navarro, L., Harvey, A.E, Ali, A.A., Bergeron, Y., and Morin, H. (2018b). A Holocene landscape dynamic multiproxy reconstruction: How do interactions between fire and insect outbreaks shape an ecosystem over long time scales? *PLoS ONE 13* (10), e0204316. https://doi.org/10.1371/journal.pone.0204316

Nealis, V.G., and Régnière, J. (2004). Insect-host relationships influencing disturbance by the spruce budworm in a boreal mixedwood forest. *Canadian Journal Forest Research 34* (9): 1870-1882. https://doi.org/10.1139/x04-061

Nealis, V.G. (2016). Comparative ecology of conifer-feeding spruce budworms (Lepidoptera: Tortricidae). *The Canadian Entomologist 148* (S1), S33-S57. https://doi.org/10.4039/tce.2015.15

Neil, K., and Gajewski, K. (2018). An 11,000-yr record of diatom assemblage responses to climate and terrestrial vegetation changes, southwestern Quebec. *Ecosphere 9* (11), e02505. https://doi.org/10.1002/ecs2.2505

North, M.P., and Keeton, W.S. (2008). (dir). *Emulating natural disturbance regimes: an emerging approach for sustainable forest management*. In: *Landscape Ecology: Sustainable Management of Forest Landscapes*. Lafortezza, R., Chen, J., Sanesi, G., Crow, T., Springer-Verlag Press.

Oliver, T.H., Heard, M.S., Isaac, N.J.B., Roy, D.B., Procter, D., Eigenbrod, F., Freckleton, R., Hector, A., Orme, C.D.L., Petchey, O.L., Proença, V., Raffaelli, D., Suttle, K.B., Mace, G.M. Martin-Lopez,

B., Woodcock, B.A., and Bullock, J.M. (2015). Biodiversity and resilience of ecosystem functions. *Trends in Ecology and Evolution 30* (11), 673-684. https://doi.org/10.1016/j.tree.2015.08.009

Oris, F., Asselin, H., Finsinger, W., Hély, C., Blarquez, O., Ferland, M-E., Bergeron, Y., and Ali, A.A. (2014). Long-term fire history in northern Québec: implications for the northern limit of commercial forests. *Journal of Applied Ecology 51* (3), 675-683. https://doi.org/10.1111/1365-2664.12240

Orme, L.C., Miettinen, A., Seidenkrantz, M-S., Tuominen, K., Pearce, C., Divine, D., Oksman, M., and Kuijpers, A. (2020). Mid to late-Holocene sea-surface temperature variability off north-eastern Newfoundland and its linkage to the North Atlantic Oscillation. *The Holocene 31* (1), 3-15. https://doi.org/10.1177/0959683620961488

Page, W.G., and Jenkins, M.J. (2007a). Mountain pine beetle-induced changes to selected lodgepole pine fuel complexes within the Intermountain region. *Forest Science 53* (4), 507-518. https://doi.org/10.1093/forestscience/53.4.507

Page, W., and Jenkins, M.J. (2007b). Predicted fire behavior in selected mountain pine beetle-infested lodgepole pine. *Forest Science 53* (6), 662-674. https://doi.org/10.1093/forestscience/53.6.662

Paine, R.T., Tegner, M.J., and Johnson, E.A. (1998). Compounded perturbations yield ecological surprises. *Ecosystems 1* (6), 535-545. https://doi.org/10.1007/s100219900049

Pàl, I., Buczko, K., Vincze, I., Finsinger, W., Braun, M., Biro, T, and Magyari, E.K. (2018). Terrestrial and aquatic ecosystem responses to early Holocene rapid climate change (RCC) events in the South Carpathian Mountains, Romania. *Quaternary International 477*, 79-93. https://doi.org/10.1016/j.quaint.2016.11.015

Paritsis, J., and Veblen, T.T. (2011). Dendroecological analysis of defoliator outbreaks on Nothofagus pumilio and their relation to climate variability in the Patagonian Andes. *Global Change Biology 17* (1), 239-253. https://doi.org/10.1111/j.1365-2486.2010.02255.x

Parmesan, C. (2006). Ecological and evolutionary responses to recent climate change. *Annual Review of Ecology, Evolution, and Systematics 37*, 637-669. https://doi.org/10.1146/annurev.ecolsys.37.091305.110100

Pausas, J.G. (2015). Evolutionary fire ecology: lessons learned from pines. *Trends in Plant Science 20* (5), 318-324. https://doi.org/10.1016/j.tplants.2015.03.001

Pausas, J.G., and Bond, W.J. (2019). Humboldt and the reinvention of nature. *Journal of Ecology 107* (3), 1031-1037. https://doi.org/10.1111/1365-2745.13109

Pausas, J.G., and Bond, W.J. (2020a). On the three major recycling pathways in terrestrial ecosystems. *Trends in Ecology & Evolution 35* (9), 767-775. https://doi.org/10.1016/j.tree.2020.04.004

Pausas, J.G., and Bond, W.J. (2020b). Alternative biome states in terrestrial ecosystems. *Trends in Plant Science 25* (3), 250-263. https://doi.org/10.1016/j.tplants.2019.11.003

Pausas, J.G., and Bond, W.J. (2022). Feedbacks in ecology and evolution. *Trends in Ecology & Evolution 37* (8), 637-644. https://doi.org/10.1016/j.tree.2022.03.008

Piene, H. (1989). Spruce budworm defoliation and growth loss in young balsam fir: Defoliation in space and unspaced stands and individual tree survival. *Canadian Journal of Forest Research 19* (10), 1211-1217. https://doi.org/10.1139/x89-185

Pothier, D., Elie, J-G., Auger, I., Mailly, D., and Gaudreault, M. (2012). Spruce budworm-caused mortality to balsam fir and black spruce in pure and mixed conifer stands. *Forest Science 58* (1), 24-33. https://doi.org/10.5849/forsci.10-110

Power, M.J., Marlon, J., Ortiz, N., Bartlein, P.J., Harrison, S.P., Mayle, F.E., Ballouche, A., Bradshaw, R.H.W., Carcaillet, C., Cordova, C., Mooney, S., Moreno, P.I., Prentice, I.C., Thonicke, K., Tinner, W., Whitlock, C., Zhang, Y., Zhao, Y., Ali, A.A., Anderson, R.S., Beer, R., Behling, H., Briles, C., Brown, K.J., Brunelle, A., Bush, M., Camill, P., Chu, G.Q., Clark, J., Colombaroli, D., Connor, S., Daniau, A-L., Daniels, M., Dodson, J., Doughty, E., Edwards, M.E., Finsinger, W., Foster, D., Frechette, J., Gaillard, M-J., Gavin, D.G., Gobet, E., Haberle, S., Hallet, D.J., Higuera, P., Hope, G., Horn, S., Inoue, J., Kaltenrieder, P., Kennedy, L., Kong, Z.C., Larsen, C., Long, C.J., Lynch, J., Lynch, E.A., McGlone, M., Meeks, S., Mensing, S., Meyer, G., Minckley, T., Mohr, J., Nelson, D.M., New, J., Newnham, R., Noti, R., Oswalk, W., Pierce, J., Richard, P.J.H., Rowe, C., Sanchez Goni, M.F., Shuman, B.N., Takahara, H., Toney, J. Turney, C., Urrego-Sanchez, D.H, Umbanhowar, C., Vandergoes, M., Vanniere, B., Vescovi, E., Walsh, M. Wang, X., Williams, N., Wilmshurst, J., and Zhang, J.H. (2008). Changes in fire regimes since the Last Glacial Maximum: an assessment based on global synthesis and analysis of charcoal data. *Climate Dynamics 30*, 887-907. https://doi.org/10.1007/s00382-007-0334-x

Price, D.T., Alfaro, R.I., Brown, K.J., Flannigan, M.D., Fleming, R.A., Hogg, E.H., Girardin, M.P., Lakusta, T., Johnston, M., McKenney, D.W., Pedlar, J.H., Stratton, T., Sturrock, R.N., Thompson, I.D., Trofymow, J.A., and Venier, L.A. (2013). Anticipating the consequences of climate change for Canada's boreal forest ecosystems. *Environmental Reviews 21* (4), 322-365. https://doi.org/10.1139/er-2013-0042

Pureswaran, D.S., De Grandpré, L., Paré, D., Taylor, A., Barrette, M., Morin, H., Régnière, J., and Kneeshaw, D.D. (2015). Climate-induced changes in host tree-insect phenology may drive ecological state-shift in boreal forests. *Ecology 96* (6), 1480-1491. https://doi.org/10.1890/13-2366.1

Pureswaran, D.S., Johns, R., Heard, S.B., and Quiring, D. (2016). Paradigms in eastern spruce budworm (Lepidopteran: Trotricidae) population ecology: a century of debate. *Environmental Entomology 45* (6), 1333-1342. https://doi.org/10.1093/ee/nvw103

Pureswaran, D.S., Roques, A, and Battisti, A. (2018). Forest insects and climate change. *Current Forestry Reports 4*, 35-50. https://doi.org/10.1007/s40725-018-0075-6

Pureswaran, D.S., Neau, M., Marchard, M., De Grandpré, L., and Kneeshaw, D. (2019). Phenological synchrony between eastern spruce budworm and its host trees increases with warmer temperatures in the boreal forest. *Ecology and Evolution 9* (1), 576-586. https://doi.org/10.1002/ece3.4779

R Core Team. (2021). *R: A language and environment for statistical computing*. R Foundation for Statistical Computing, Vienna, Austria. https://www.R-project.org/

Reams, G.A., Brann, T.B., and Halteman, W.A. (1988). A nonparametric survival model for balsam fir during a spruce budworm outbreak. *Canadian Journal of Forest Research 18*, 787-793. https://doi.org/10.1139/x88-120

Regent Instruments Inc. (2017). WinDendro: Tree ring and wood density image analysis system

Regent Instruments Inc. (2019). WinSEEDLE: Seed and needle morphology and count v. 2019a.

Régnière, J., and Nealis, V.G. (2007). Ecological mechanisms of population change during outbreaks of the spruce budworm. *Ecological Entomology 32* (5), 461-477. https://doi.org/10.1111/j.1365-2311.2007.00888.x

Régnière, J., St-Amant, R., Duval, P. (2012). Predicting insect distributions under climate change from physiological responses: spruce budworm as an example. *Biological Invasions 14*, 1571-1586. https://doi.org/10.1007/s10530-010-9918-1

Régnière, J., and Nealis, V.G. (2019). Density dependence of egg recruitment and moth dispersal in spruce budworms. *Forests 10* (8), 706. https://doi.org/10.3390/f10080706

Régnière, J., Delisle, J., Sturtevant, B.R., Garcia, M., and Saint-Amant, R. (2019a). Modeling migratory flight in the spruce budworm: temperature constraints. *Forests 10* (9), 802. https://doi.org/10.3390/f10090802

Régnière, J., Garcia, M., and Saint-Amant, R. (2019b). Modeling migratory flight in the spruce budworm: circadian rhythm. *Forests 10* (10), 877. https://doi.org/10.3390/f10100877

Renberg, I. (1991). The HON-Kajak sediment corer. *Journal of Paleolimnology 6*, 167-170. https://doi.org/10.1007/BF00153740

Renberg, I., and Hansson, H. (2008). The HTH sediment corer. *Journal of Paleolimnology 40*, 655-659. https://doi.org/10.1007/s10933-007-9188-9

Renssen, H., Seppä, H., Heiri, O., Roche, D.M., Goosse, H., and Fichefet, T. (2009). The spatial and temporal complexity of the Holocene thermal maximum. *Nature Geoscience 2*, 411-414. https://doi.org/10.1038/ngeo513

Renssen, H., Seppä H., Crosta, X., Goosse, H., and Roche, D.M. (2012). Global characterization of the Holocene Thermal Maximum. *Quaternary Science Reviews 48*, 7-19. https://doi.org/10.1016/j.quascirev.2012.05.022

Rhainds, M., Lavigne, D., Boulanger, Y., DeMerchant, I., Delisle, J., Motty, J., Rideout, T., and Labrecque, A. (2021). I know it when I see it: Incidence, timing and intensity of immigration in spruce budworm. *Agricultural and Forest Entomology 24* (2), 152-166. https://doi.org/10.1111/afe.12479

Richard, P.J.H. (1979). Contribution à l'histoire postglaciaire de la végétation au nord-est de la Jamésie, Nouveau-Québec. *Géographie physique et Quaternaire 33* (1), 93-112. https://doi.org/10.7202/1000324ar

Richard, P.J.H., Larouche, A., and Bouchard, M. (1982). Âge de la deglaciation finale et histoire postglaciaire de la vegetation dans la partie centrale du Nouveau-Québec. *Géographie physique et Quaternaire 36* (1-2), 63-90. https://doi.org/10.7202/032470ar

Richard, P.J.H. (1993). Origine et dynamique postglaciaire de la forêt mixte au Québec. *Review of Palaeobotany and Palynology 79* (1-2), 31-68. https://doi.org/10.1016/0034-6667(93)90037-U

Richard, P.J.H. (1995). Le couvert végétal du Québec-Labrador il y a 6000 ans BP: essai. *Géographie physique et Quaternaire 49* (1), 117-140. https://doi.org/10.7202/033033ar

Richards, A.G. (1947). Studies on arthropod cuticle. I. The distribution of chitin in lepidopterous scales, and its bearing on the interpretation of arthropod cuticle. *Annals of the Entomological Society of America 40* (2), 227-240. https://doi.org/10.1093/aesa/40.2.227

Riley, K.L., Williams, A.P., Urbanski, S.P., Calkin, D.E., Short, K.C., and O'Connor, C.D. (2019). Will landscape fire increase in the future? A systems approach to climate, fire, fuel and human drivers. *Current Pollution Reports 5*, 9-24. https://doi.org/10.1007/s40726-019-0103-6

Rodionov, S.N. (2004). A sequential algorithm for testing climate regime shifts. *Geophysical Research Letters 31* (9), L09204. https://doi.org/10.1029/2004GL019448

Rodionov, S., and Overland, J.E. (2005). Application of a sequential regime shift detection method to the Bering Sea ecosystem. *ICES Journal of Marine Science 62* (3), 328-332. https://doi.org/10.1016/j.icesjms.2005.01.013

Rodionov, S.N. (2006). Use of phrewhitening in climate regime shift detection. *Geophysical Research Letters 33* (12), L12707. https://doi.org/10.1029/2006GL025904

Rogers, B.M., Soja, A.J., Goulden, M.L., and Randerson, J.T. (2015). Influence of tree species on continental differences in boreal fires and climate feedbacks. *Nature Geoscience 8*, 228-234. https://doi.org/10.1038/ngeo2352

Rosenberger, D.W., Venette, R.C., Maddox, M.P., and Aukema, B.H. (2017). Colonization behaviors of mountain pine beetle on novel hosts: implications for range expansion into northeastern North America. *PloS ONE 12* (5), e0176269. https://doi.org/10.1371/journal.pone.0176269

Rother, M.T., Huffman, J.M., Harley, G.L., Platt, W.J., Jones, N., Robertson, K.M., and Orzell, S.L. (2018). Cambial phenology informs tree-ring analysis of fire seasonality in coastal plain pine savannas. *Fire Ecology 14*, 164-185. https://doi.org/10.4996/fireecology.140116418

Rothermel, R.C. (1983). *How to predict the spread and intensity of forest and range fires. United States Department of Agriculture Forest Service*. Intermountain Forest and Range Experiment Station Ogden, UT 84401. General Technical Report INT-143

Rowe, J.S. (1972). *Forest Regions of Canada*. Department of the Environment, Canadian Forestry Service, Publication No. 1300.

Royama, T. (1984). Population dynamics of the spruce budworm Choristoneura fumiferana. *Ecological Monographs 54* (4), 429-462. https://doi.org/10.2307/1942595

Royama, T., MacKinnon, W.E., Kettela, E.G., Carter, N.E., Hartling, L.K. (2005). Analysis of spruce budworm outbreak cycles in New Brunswick, Canada, since 1952. *Ecology 86* (5), 1212-1224. https://doi.org/10.1890/03-4077

Royama, T., Eveleigh, E.S., Morin, J.R.B., Pollock, S.J., McCarthy, P.C., McDougall, G.A., and Lucarotti C.J. (2017). Mechanisms underlying spruce budworm outbreak processes as elucidated by a 14-year study in New Brunswick, Canada. *Ecological Monographs 87* (4), 600-631. https://doi.org/10.1002/ecm.1270

Rullan-Silva, C.D., Olthoff, A.E., Delgado de la Mata, J.A., and Pajares-Alonso, J.A. (2013). Remote monitoring of forest insect defoliation. A review. *Forests Systems 22* (3), 377-391

Saucier, J-P., Bergeron, J-F., Grondin, P., and Robitaille, A. (1998). *Les régions écologiques du Québec méridional (3rd version) : un des éléments du système hiérarchique de classification écologique du territoire mis au point par le ministère des Ressources naturelles du Québec.*

Saucier, J-P., Robitaille, A., and Grondin, P. (2009). *Cadre bioclimatique du Québec*. In :*Manuel de foresterie.* (2nd edition). Ordre des ingénieurs forestiers du Québec, Éditions MultiMondes

Scheffer, M., Carpenter, S., Foley, J.A., Folke, C., and Walker, B. (2001). Catastrophic shifts in ecosystems. *Nature 413*, 591-596. https://doi.org/10.1038/35098000

Scheffer, M., Szabo, S., Gragnani, A., van Nes, E.H., Rinaldi, S., Kautsky, N., Norberg, J., Roijackers, R.M.M., and Franken, R.J.M. (2003). Floating plant dominance as a stable state. *Proceedings of the National Academy of Science 100* (7), 4040-4045. https://doi.org/10.1073/pnas.0737918100

Scheffer, M., and Carpenter, S.R. (2003). Catastrophic regime shifts in ecosystems: linking theory to observation. *Trends in Ecology and Evolution 18* (2), 648-656. https://doi.org/10.1016/j.tree.2003.09.002

Scheffer, M., and van Nes, E.H. (2007). Shallow lakes theory revisited: various alternative regimes driven by climate, nutrients, depth and lake size. *Hydrobiologia 584*, 455-466. https://doi.org/10.1007/978-1-4020-6399-2_41

Scheffer, M. Hirota, M., Holmgren, M., Van Nes, E.H., and Chapin III, F.S. (2012). Thresholds for boreal biome transitions. *Proceedings of the National Academy of Science 109* (52), 21384-21389. https://doi.org/10.1073/pnas.1219844110

SCIEM. (2015a). PAST5 (Personal Analysis System for Tree Ring Research) Version 5.0.576 software.

SCIEM. (2015b). PAST5 (Personal Analysis System for Tree Ring Research) software instruction manual. Vienna.

Senf, C., Seidl, R., and Hostert, P. (2017). Remote sensing of forest insect disturbances: current state and future directions. *International Journal of Applied Earth Observation and Geoinformation 60*, 49-60. https://doi.org/10.1016/j.jag.2017.04.004

Shuman, B.N., and Marsicek, J. (2016). The structure of Holocene climate change in mid-lattitude North America. *Quaternary Science Reviews 141*, 38-51. https://doi.org/10.1016/j.quascirev.2016.03.009

Simard, I., Morin, H., and Potelle, B. (2002). A new paleoecological approach to reconstruct long-term history of spruce budworm outbreaks. *Canadian Journal of Forest Research 32* (3), 428-438. https://doi.org/10.1139/x01-215

Simard, I., Morin, H., and Lavoie, C. (2006). A millennial-scale reconstruction of spruce budworm abundance in Saguenay, Québec, Canada. *The Holocene 16* (1), 31-37. https://doi.org/10.1191/0959683606hl904rp

Simard, I., Morin, H., and Krause, C. (2011). Long-term spruce budworm outbreak dynamics reconstructed from subfossil trees. *Journal of Quaternary Science 26* (7), 734-738. https://doi.org/10.1002/jqs.1492

Simard, M., Romme, W.H., Griffin, J.M., and Turner, M.G. (2011). Do mountain pine beetle outbreaks change the probability of active crown fire in lodgepole pine forests? *Ecological Monographs 81* (1), 3-24. https://doi.org/10.1890/10-1176.1

Simmons, M.J., Lee, T.D., Ducey, M.J., and Dodds, K.J. (2014). Invasion of winter moth in New England: Effects of defoliation and site quality on tree mortality. *Forests 5* (10), 2440-2463. https://doi.org/10.3390/f5102440

Smith, A.C., Wynn, P.M., Barker, P.A., Leng, M.J., Noble, S.R., and Tych, W. (2016). North Atlantic forcing of moisture delivery to Europe throughout the Holocene. *Scientific Reports 6*, 24745. https://doi.org/10.1038/srep24745

Springer, G.S., Rowe, H.D., Hardt, B., Edwards, R.L., and Cheng, H. (2008). Solar forcing of Holocene droughts in a stalagmite record from West Virginia and east-central North America. *Geophysical Research Letters 35* (17), L17703. https://doi.org/10.1029/2008GL034971

Stahl, A.T., Andrus, R., Hicke, J.A., Hudak, A.T., Bright, B.C., and Meddens, A.J.H. (2023). Automated attribution of forest disturbance types from remote sensing: a synthesis. *Remote Sensing of Environment 285*, 113416. https://doi.org/10.1016/j.rse.2022.113416

Stephens, S.L., Maier, L., Gonen, L., York, J.D., Collins, B.M., and Fry, D.L. (2018). Variation in fire scar phenology from mixed conifer trees in the Sierra Nevada. *Canadian Journal of Forest Research 48* (1), 101-104. https://doi.org/10.1139/cjfr-2017-0297

Stirnimann, L., Conversi, A., and Marini, S. (2019). Detection of regime shifts in the environment: testing 'STARS' using synthetic and observed time series. *ICES Journal of Marine Science 76* (7), 2286-2296. https://doi.org/10.1093/icesjms/fsz148

Stocks, B.J. (1987). Fire potential in the spruce budworm-damaged forests of Ontario. *The Forestry Chronicle 63* (1), 8-14. https://doi.org/10.5558/tfc63008-1

Stokes, M.A., and Smiley, T.L. (1968). *An introduction to tree-ring dating*. Chicago: University of Chicago Press

Sturtevant, B.R., Miranda, B.R., Shinneman, D.J., Gustafson, E.J., and Wolter, P.T. (2012). Comparing modern and presettlement forest dynamics of a subboreal wilderness: Does spruce budworm enhance fire risk? *Ecological Applications 22* (4), 1278-1296. https://doi.org/10.1890/11-0590.1

Sturz, H., and Robinson, J. (1986). *Anaerobic decomposition of chitin in fresh-water sediments*. In: *Chitin and nature and technology*. R. Muzzarelli, C. Jeuniaux, and GW Gooday. Springer, Boston.

Su, Q., MacLean, D.A., Needham, T.D. (1996). The influence of hardwood content on balsam fir defoliation by spruce budworm. *Canadian Journal of Forest Research 26* (9), 1620-1628. https://doi.org/10.1139/x26-182

Swetnam, T.W., Thompson, M.A., and Sutherland, E.K. (1985). *Using dendrochronology to measure radial growth of defoliated trees.* United States Department of Agricultural Handbook No. 639

Swetnam, T.W., and Lynch, A.M. (1989). Spruce budworm history in the southern Rocky Mountains. *Forest Science 35* (4), 962-986. https://doi.org/10.1093/forestscience/35.4.962

Swetnam, T.W., and Lynch, A.M. (1993). Multicentury, regional-scale patterns of western spruce budworm outbreaks. *Ecological Monographs 63* (4), 399-424. https://doi.org/10.2307/2937153

Swetnam, T.W., Allen, C.D., and Betancourt, J.L. (1999). Applied historical ecology: using the past to manage for the future. *Ecological Applications 9* (4), 1189-1206. https://doi.org/10.1890/1051-0761(1999)009[1189:AHEUTP]2.0.CO;2

Tai, A.R., and Carroll, A.L. (2022). In the pursuit of synchrony: northward shifts in western spruce budworm outbreaks in a warming environment. *Frontiers in Forests and Global Change 5*, 895579. https://doi.org/10.3389/ffgc.2022.895579

Thapa, B., Wolter, P.T., Sturtevant, B.R., and Townsend, P.A. (2022). Linking remote sensing and insect defoliation biology- a cross-system comparison. *Remote Sensing of Environment 281*, 113236. https://doi.org/10.1016/j.rse.2022.113236

Thompson, R., Battarbee, R.W., O'Sullivan, P.E., and Oldfield, F. (1975). Magnetic susceptibility of lake sediments. *Limnology and Oceanography 20* (5), 687-698. https://doi.org/10.4319/lo.1975.20.5.0687

Tikkanen, O-P., and Roininen, H. 2001. Spatial patterns of outbreaks of Operophtera brumata in eastern Fennoscandia and their effects on radial growth of trees. *Forest Ecology and Management 146*, 45-54. https://doi.org/10.1016/S0378-1127(00)00451-5

Törnqvist, T.E., and Hijma, M.P. (2012). Links between early Holocene ice-sheet decay, sea-level rise and abrupt climate change. *Nature Geoscience 115*, 601-606. https://doi.org/10.1038/ngeo1536

Torrence, C., and Compo, G.P. (1998). A practical guide to wavelet analysis. *Bulletin of the American Meteorological Society 79* (1), 61-78. https://doi.org/10.1175/1520-0477(1998)079%3C0061:APGTWA%3E2.0.CO;2

Tremblay, M-J., Rossi, S., and Morin, H. (2011). Growth dynamics of black spruce in stands located between the 51st and 52nd parallels in the boreal forest of Quebec, Canada. *Canadian Journal of Forest Research 41* (9), 1769-1778. https://doi.org/10.1139/x11-094

Tremblay, E. (2022). *Quantification de la relation entre la défoliation des peuplements forestiers causée par la tordeuse des bourgeons de l'épinette (Choristoneura fumiferana Clem.) et les écailles du papillon de la tordeuse des bourgeons de l'épinette retrouvées dans les sédiments lacustres annuels boréaux*. [M. Sc. Thesis, Université du Québec à Chicoutimi, Faculté des sciences fondamentales. Chicoutimi, QC, Canada]

van Nes, E.H., Rip, W.J., and Scheffer, M. (2007). A theory for cyclic shifts between alternative states in shallow lakes. *Ecosystems 10*, 17-28. https://doi.org/10.1007/s10021-006-0176-0

Van Wagner, C.E. (1967). *Seasonal variation in moisture content of eastern Canadian tree foliage and the possible effect on crown fires*. Department of Forestry and Rural Development Forestry Branch Departmental Publication no. 1204

Van Wagner, C.E. (1977). Conditions for the start and spread of crown fire. *Canadian Journal of Forest Research 7* (1), 23-34. https://doi.org/10.1139/x77-004

Viau, A.E., Gajewski K., Fines, P., Atkinson, D.E., and Sawada, M.C. (2002). Widespread evidence of 1500 yr climate variability in North America during the past 14000 yr. *Geology 30* (5), 455-458. https://doi.org/10.1130/0091-7613(2002)030%3C0455:WEOYCV%3E2.0.CO;2

Viau, A.E., Gajewski, K., Sawada, M.C., and Fines, P. (2006). Millennial-scale temperature variations in North America during the Holocene. *Journal of Geophysical Research 111* (D9), D09102. https://doi.org/10.1029/2005JD006031

Viau, A.E., and Gajewski, K. (2009). Reconstructing millennial-scale, regional paleoclimates of boreal Canada during the Holocene. *Journal of Climate 22* (2), 316-330. https://doi.org/10.1175/2008JCLI2342.1

Viau, A.E., Ladd, M. and Gajewski, K. (2012). The climate of North America during the past 2000 years reconstructed from pollen data. *Global and Planetary Change 84-85*, 75-83. https://doi.org/10.1016/j.gloplacha.2011.09.010

Volney, W.J.A., and Fleming, R.A. (2007). Spruce budworm (*Choristoneura spp*.) biotype reactions to forest and climate characteristics. *Global Change Biology 13* (8), 1630-1643. https://doi.org/10.1111/j.1365-2486.2007.01402.x

Walker, M.J.C., Berkelhammer, M., Bjorck, S., Cwynar, L.C., Fisher, D.A., Long, A.J., Lowe, J.J., Newnham, R.M., Rasmussen, S.O., and Weiss, H. (2012). Formal subdivision of the Holocene series/Epoch: a discussion paper by a working group of INTIMATE (Integration of ice-core, marine and terrestrial records) and the Subcommission on Quaternary Stratigraphy (International Commission on Stratigraphy). *Journal of Quaternary Science 27* (7), 649-659. https://doi.org/10.1002/jqs.2565

Wanner, H., Beer, J., Bütikofer, J., Crowley, TJ., Cubasch, U., Fluckiger, J., Goosse, H., Grosjean, M., Joos, F., Kaplan, JO., Kuttel, M., Muller, SA., Prentice, IC., Solomina, O., Stocker, TF., Tarasov, P., Wagner, M., and Widmann, M. (2008). Mid- to late Holocene climate change: an overview. *Quaternary Science Reviews 27* (19-20), 1791-1828. https://doi.org/10.1016/j.quascirev.2008.06.013

Wanner, H., Solomina, O., Grosjean, M., Ritz, S.P., and Jetel, M. (2011). Structure and origin of Holocene cold events. *Quaternary Science Reviews 30* (21-22), 3109-3123. https://doi.org/10.1016/j.quascirev.2011.07.010

Wanner, H., Mercolli, L., Grosjean, M., and Ritz, S.P. (2015). Holocene climate variability and change; a data-based review. *Journal of the Geological Society 172* (2), 254-263. https://doi.org/10.1144/jgs2013-101

Waito, J., Girardin, M.P., Tardif, J.C., Conciatori, F., Bergeron, Y., and Ali, A.A. (2018). Recent fire activity in the boreal eastern interior of North America is below that of the past 2000 yr. *Ecosphere 9* (6), e02287.10.1002/ecs2.2287. https://doi.org/10.1002/ecs2.2287

Warrens, M.J. (2008). On the equivalence of Cohen's Kappa and the Hubert-Arabie Adjusted Rand Index. *Journal of Classification 25*, 177-183. https://doi.org/10.1007/s00357-008-9023-7

Warrens, M.J. (2010). Cohen's Kappa can always be increased and decreased by combining categories. *Statistical Methodology 7* (6), 673-677. https://doi.org/10.1016/j.stamet.2010.05.003

Warrens, M.J. (2014). New interpretations of Cohen's Kappa. *Journal of Mathematics 2014*, Article ID 203907, 1-9. https://doi.org/10.1155/2014/203907

Warrens, M.J. (2015). Five ways to look at Cohen's Kappa. *Journal of Psychology and Psychotherapy 5*, 197. https://doi.org/10.4172/2161-0487.1000197

Watt, G.A., Fleming, R.A., Smith, S.M., and Fortin, M-J. (2018). Spruce budworm (*Choristoneura fumiferana* Clem.) defoliation promotes vertical fuel continuity in Ontario's boreal mixedwood forest. *Forests 9* (5), 256. https://doi.org/10.3390/f9050256

Watt, G.A., Stocks, B.J., Fleming, R.A., and Smith, S.M. (2020). Stand breakdown and surface fuel accumulation due to spruce budworm (*Choristoneura fumiferana*) defoliation in the boreal mixedwood forest of central Canada. *Canadian Journal of Forest Research 50* (6), 533-541. https://doi.org/10.1139/cjfr-2019-0076

Weed, A.S., Ayres, M.P., and Hicke, J.A. (2013). Consequences of climate change for biotic disturbance in North American forests. *Ecological Monographs 83* (4), 441-470. https://doi.org/10.1890/13-0160.1

Westerling, A.L., Gershunov, A., Brown, T.J., Cayan, D.R., and Dettinger, M.D. (2003). Climate and wildfire in the western United States. *Bulletin of the American Meteorological Society 84* (5), 595-604. https://doi.org/10.1175/BAMS-84-5-595

Westerling, A.L. Hidalgo, H.G., Cayan, D.R., and Swetnam, T.W. (2006). Warming and earlier spring increase western U.S. forest wildfire activity. *Science 313* (5789), 940-943. https://doi.org/10.1126/science.1128834

Westerling, A.L. Turner, M.G., Smithwick, E.A.H., Romme, W.H., and Ryan, M.G. (2011). Continued warming could transform Greater Yellow stone fire regimes by mid-21st century. *Proceedings of the National Academy of Sciences of the United States of America 108* (32), 13165-13170. https://doi.org/10.1073/pnas.1110199108

Whitlock, C., Marlon, J., Briles, C., Brunelle, A., Long, C., and Bartlein, P. (2008). Long-term relations among fire, fuel, and climate in the north-western WS based on lake-sediment studies. *International Journal of Wildland Fire 17* (1), 72-83. https://doi.org/10.1071/WF07025

Wigley, T.M.L., Briffa, K.R., and Jones, P.D. (1984). On the average value of correlated time series, with applications in Dendroclimatology and Hydrometeorology. *Journal of Applied Meteorology and Climatology 23* (2), 201-213. https://doi.org/10.1175/1520-0450(1984)023%3C0201:OTAVOC%3E2.0.CO;2

Willard, D.A., Bernhardt, C.E., Korejwo, D.A., and Meyers, S.R. (2005). Impacts of millennial-scale Holocene climate variability on eastern North American terrestrial ecosystems: pollen-based climatic reconstruction. *Global and Planetary Change 47* (1), 17-35. https://doi.org/10.1016/j.gloplacha.2004.11.017

Wood, S.N. (dir). (2017). *Generalized Additive Models: An introduction with R* (2nd ed.). Chapman and Hall/CRC

Woolford, D.G., Dean, C.B., Martell, D.L., Cao, J., and Wotton, B.M. (2014). Lightning-caused forest fire risk in Northwestern Ontario, Canada, is increasing and associated with anomalies in fire weather. *Environmetrics 25* (6), 496-416. https://doi.org/10.1002/env.2278

Wotton, B.M., Nock, C.A., and Flannigan, M.D. (2010). Forest fire occurrence and climate change in Canada. *International Journal of Wildland Fire 19* (3), 253-271. https://doi.org/10.1071/WF09002

Wotton, B.M., Flannigan, M.D., and Marshall, G.A. (2017). Potential climate change impacts on fire intensity and key wildfire suppression thresholds in Canada. *Environmental Research Letters 12* (9), 095003. https://doi.org/10.1088/1748-9326/aa7e6e

Wright Jr., H.E., Mann, D.H., and Glaser, P.H. (1984). Piston corers for peat and lake sediments. *Ecology 65* (2), 657-659. https://doi.org/10.2307/1941430

Zald, H.S.J., Ohmann, J.L., Roberts, H.M., Gregory, M.J., Henderson, E.B., McGaughey, R.J., and Braaten, J. (2014). Influence of lidar, Landsat imagery, disturbance history, plot location accuracy, and plot size on accuracy of imputation maps of forest composition and structure. *Remote Sensing of Environement 143*, 26-38. https://doi.org/10.1016/j.rse.2013.12.013

Zhang, Y., Renssen, H., and Seppä, H. (2016). Effects of melting ice sheets and orbital forcing on the early Holocene warming in the extratropical Northern Hemisphere. *Climate of the Past 12* (5), 1119-1135. https://doi.org/10.5194/cp-12-1119-2016

Zhang, Y., Renssen, H., Seppä, H., and Valdes, P.J. (2017). Holocene temperature evolution in the Northern Hemisphere high latitudes- Model-data comparisons. *Quaternary Science Reviews 173*, 101-113. https://doi.org/10.1016/j.quascirev.2017.07.018

Zhang, Y., Woodcock, C.E., Chen, S., Wang, J.A., Sulla-Menashe, D., Zuo, Z., Olofsson, P., Wang, Y., and Friedl, M.A. (2022). Mapping causal agents of disturbance in boreal and arctic ecosystems of North America using time series of Landsat data. *Remote Sensing of Environment 272*, 112935. https://doi.org/10.1016/j.rse.2022.112935

Zysno, P.V. (1997). The modification of the Phi-coefficient reducing its dependence on the marginal distributions. *Methods of Psychological Research Online 2*, 41-52